Mineral stress response of *Vitis* cell wall transcriptome: Identification, characterization and expression of genes from key families involved in wall biosynthesis and modification

TESE APRESENTADA PARA OBTENÇÃO DO GRAU DE DOUTOR EM ENGENHARIA AGRONÓMICA

JÚRI:

Presidente: Maria Wanda Sarujine Viegas Professora Catedrática Instituto Superior de Agronomia Universidade de Lisboa

Vogais: Doutor José Luis Acebes Arranz Professor Titular Universidade de León, Espanha;

Doutor Manuel António Coimbra Rodrigues da Silva Professora Associado com agregação Universidade de Aveiro;

Doutora Sara de Barros Queiroz Amâncio Professora Associada com Agregação Instituto Superior de Agronomia Universidade de Lisboa;

Doutora Sílvia Vieira de Almeida Coimbra Professora Auxiliar Faculdade de Ciências Universidade do Porto;

Doutora Maria Leonor Mota Morais Cecílio Professora Auxiliar Instituto Superior de Agronomia Universidade de Lisboa

JOÃO CARLOS MARTINS FERNANDES

LISBOA

2015

Agradecimentos

À Professora Sara Amâncio, pela sugestão do tema e orientação do trabalho, pela constante disponibilidade, pela partilha do seu profundo conhecimento, pela sincera amizade um muito obrigado com o mais profundo reconhecimento.

Ao Doutor Luís Goulão pela ajuda, orientação e valiosas discussões que tanto ajudaram a valorizar este trabalho.

Ao Doutor José Luís Acebes pela simpatia com que me recebeu no seu laboratório em León, pela ajuda constante e incansável e pela paixão que sempre demonstrou pela ciência. Um muito obrigado com o mais profundo reconhecimento.

À Prof. Leonor Morais e Engenheira Vera Inácio pela ajuda nos procedimentos de fixação do material. À Engenheira Teresa Quilhó e ao seu laboratório pela ajuda na preparação dos cortes para microscopia.

A todos os colegas do Departamento de Botânica e Engenharia Biológica (DBEB/LEAF) pela ajuda dispensada em diversas ocasiões, pela permanente disponibilidade e pela amizade de todos.

A todos os colegas do Laboratório de Fisiologia Vegetal da Universidade de León, em especial à Doutora Penélope García-Angulo, pelo carinho e ajuda com que me receberam, fazendo-me sentir em casa.

À bolsa concedida pela FCT (SFRH/BD/64047/2009), sem o qual este trabalho não seria possível.

A todos aqueles que contribuíram para aquilo que sou hoje, Bem Hajam.

Abstract

Grapevine (*Vitis vinifera* L.) is one of the most economically important fruit crops in the world. Abiotic stresses are likely to affect the plant development, yield and ultimately the quality of economic products. The cell wall (CW) is a dynamic structure that determines plant form, growth and response to environmental conditions. To investigate *V. vinifera* CW adaptative response to restrictions in major nutrients, essential to plant growth and development, N, P and S were excluded from *V. vinifera* callus and shoots growing substrates. Water stress on berry skin CW was studied in non-irrigated versus irrigated plants of two varieties. Specific CW components, namelly cellulose, were impacted in callus, shoots and berries subjected to abiotic stress. To overcome this, *V. vinifera* CWs suffered compositional changes and reorganization of deposition of several CW components, in particular the degree and pattern of pectin methyl-esterification, arabinan and XyG, which together promote stiffening of the CW. Moreover, polysaccharides of callus grown under mineral deficiency, mainly N, were more tightly bound in the CW. Under mineral stress the expression of genes from CW candidate enzyme families was affected for example downregulation of GH9C, XTHs with predicted hydrolytic activity and PMEs were observed. In shoots probed with CW-epitope monoclonal antibodies an increase in pectins with a low degree of methyl-esterification able to dimerise association through calcium ions was observed. CWs grown under N deficiency were enriched in 1,5-arabinan rhamnogalacturonan-I (RG-I) side chains. The impact on CW was dependent on the mineral stress, nitrogen leading to more pronounced responses, supporting the primary role of this major nutrient in plant development and metabolism. Water shortage affected berry skin by stiffening the CW, probably due to alterations in *PG*s, *XTH* and *PME* expression and pectin methyl-esterification in a variety dependent way.

Keywords: *Arabinan; Cellulose; Mineral Stress; Pectin; V. vinifera; Water Stress; Xyloglucan*

Resumo

A videira (*Vitis vinifera* L.) é uma das mais importantes culturas frutícolas no mundo. Os stresses abióticos afetam o desenvolvimento das plantas bem como o seu rendimento e em última análise a qualidade do seu produto final. A parede celular (PC) é uma estrutura dinâmica que influencia a forma, o crescimento e a resposta da planta aos estímulos ambientais. Para investigar os efeitos provocados pelo stresse mineral na regulação das alterações sofridas pela PC, azoto (N), fósforo (P) e enxofre (S) foram retirados do meio onde callus e estacas de *V. vinifera* foram colocados a crescer. O stress hídrico, na PC da pelicula do bago, foi avaliado em plantas irrigadas e não irrigadas. Callus, rebentos e bagos sujeitos a stress abiótico vêem as suas PC afetadas em diversos dos seus componentes, principalmente celulose. Para fazer face a esta situação a PC de *V. vinifera* sofre uma reorganização dos seus componentes, em particular o grau e o padrão de esterificação das pectinas, o teor de arabinose e xiloglucana, o que leva a um reforço da parede. Para além disto os polissacáridos dos callus e dos bagos encontram-se mais agregados na PC. O stresse mineral provocou uma diminuição na expressão dos genes de famílias de enzimas associadas à PC, principalmente GH9C, XTHs (com actividade hidrolítica) e PMEs. Rebentos analisados com imunolocalização com anticorpos monoclonais mostraram um aumento das pectinas com um baixo grau de metilesterificação, com potencial formação de associações diméricas através de pontes de cálcio e um possível enriquecimento em 1,5-arabinanas das cadeias laterais de ramnogalaturonanas-I em resposta `a carência de N e P. Mostrou-se que o efeito sobre a PC depende do tipo de stresse mineral, sendo o N o que leva a respostas mais intensas, suportando o seu papel como macro nutriente essencial para o desenvolvimento e metabolismo. Os efeitos do stresse hídrico, embora dependendo da variedade afetaram a película dos bagos através de um reforço da PC, provavelmente devido a alterações na expressão de membros de PGs, XTHs e PMEs e do grau de metilesterificação das pectinas.

Palavras-chave: *Arabinose, Celulose, Pectinas; V. vinifera; Stress Hidríco; Stresse Mineral; Xiloglucana*

Resumo alargado

A videira (*Vitis vinifera* L.) é uma das mais importantes culturas frutícolas no mundo. Cerca de 80% das uvas cultivadas são usadas para vinho mas esta espécie pode também ser usada para uva de mesa ou para a produção de passas.

A Parede Celular (PC) das plantas é uma estrutura dinâmica e complexa capaz de modificar os seus constituintes e as suas ligações para satisfazer os requisitos específicos da célula, em resposta a vários estímulos exteriores. O stresse abiótico pode conduzir a situações que são desfavoráveis ao crescimento das plantas. O stresse mineral e hídrico pode conduzir a tais condições que prejudiquem o crescimento, rendimento e, em última análise, a qualidade do produto final. A importância do stresse abiótico no desenvolvimento das plantas e a sua influência na síntese e a modificação dos componentes da PC merecem particular atenção. Este trabalho pretendeu caracterizar a resposta da PC da videira ao stress abiótico, em particular o stress mineral e hídrico. Para estudar o efeito do stresse mineral, N, P e S foram retirados dos substratos de crescimento de callus e entrenós de *V. vinifera*. O efeito do stresse hídrico na PC da pelicula dos bagos foi analisado em duas variedades de videira, Touriga Nacional (TN) e Trincadeira (TR), irrigadas e não irrigadas.

Plantas modelo estudadas em condições controladas são uma ferramenta importante para aferir situações de stresse. Callus de *V. vinifera*, como sistema desdiferenciado e homogéneo, permite obter um modelo simples e elegante para aferir o efeito dos stresses abióticos. Uma vez que o principal objetivo era compreender a resposta da PC a um determinado estímulo exterior, este sistema permitiu uma reduzida interferência de outros fatores. No entanto, tecidos diferenciados, como é o caso dos entrenós, podem apresentar comportamentos diferentes dos tecidos desdiferenciados. Por serem mais complexos, oferecem vantagens para o estudo da organização e modificação dos polímeros da PC.

O objetivo inicial de identificar as modificações ocorridas na PC devido ao stresse mineral por carência de azoto (-N), fósforo (-P) e enxofre (-S) foi conseguido utilizando a técnica de Espetroscopia de Infravermelho por Transformadas de

Fourier (FT-IR) em callus sob stresse mineral. Modificações na biossíntese ou disposição das microfibrilas de celulose, glicanas de ligação à parede, pectinas e quantidade de proteínas estruturais foram os principais componentes alterados indicados por esta técnica. Uma análise mais pormenorizada das alterações ocorridas na biossíntese de alguns componentes da PC em resposta ao stresse abiótico revelaram uma redução significativa na quantidade de celulose e ao mesmo tempo um aumento da arabinose principalmente em resposta à carência de N e P. A forma e dimensão das células dos callus e dos entrenós sofreu também alterações devido ao stresse mineral. O stresse hídrico provocou igualmente redução do conteúdo de celulose da PC de películas do bago, principalmente em Trincadeira na maturação. O aumento dos níveis de polímeros ricos em arabinose fortemente ligada à PC, detetados em callus e na película do bago pode indicar um aumento da substituição das cadeias laterais de ramnogalaturonanas-I por resíduos de arabinose. O mesmo foi confirmado pela ligação do anticorpo LM13, especifico para (1-5)-α-L-arabinanas lineares, em PCs de entrenós de videira. Isto leva-nos a concluir que a redução de celulose pode ser uma resposta geral ao stresse abiótico que é compensado por um aumento dos polímeros ricos em arabinose na PC.

A diminuição do teor de celulose na PC levou-nos a estudar os genes envolvidos na sua síntese, conhecidos como celulose sintases (CesA). A taxa de transcrição dos CesA não explica a redução na quantidade de celulose, uma vez que a sua expressão não foi globalmente alterada pelo stresse. Sabemos que a transcrição de CesA não é suficiente para a síntese correta da celulose, sendo necessária a coadjuvação de genes de outras famílias. Estão nesse caso as glicosil-hidrolases da família 9 (GH9), principalmente as classes A e C. Os elementos da classe A desta família interagem com a celulose para que haja a sua correta ligação à parede. Os callus de *V. vinifera* que se desenvolveram na ausência de minerais não demonstraram alterações na expressão de genes desta classe. No entanto a expressão de genes da classe C das GH9 foi fortemente afetada. Foi demonstrado recentemente que os genes GH9C estão envolvidos na regulação do grau de cristalização da celulose. A forte repressão de VvGH9C2 na ausência de azoto e enxofre leva-nos a concluir que este poderá ter um efeito na redução da celulose.

Em situações adversas as plantas dispõem de mecanismos compensatórios para reforçar a PC quando a biossíntese ou deposição dos seus componentes é afetada. Sob influência de stresse mineral, principalmente –N, a PC compensa a diminuição da celulose através da redução do grau de metil-esterificação das suas pectinas, sobretudo contígua e em cadeias longas de homogalacturonana (HG). Este resultado foi confirmado pelo uso do anticorpo PAM1 em callus e entrenós de estacas que se desenvolveram em –N quando comparado com o controlo. A formação das longas cadeias de HG de-esterificadas possibilitou a formação de pontes de cálcio, confirmadas através do uso do anticorpo 2F4. Foi proposto que, sob a influência do stress mineral, este padrão de de-esterificação conduz a um reforço da PC, conferindo-lhe uma maior rigidez sem alterar as suas características elásticas. A diminuição geral do grau de metil-esterificação das pectinas, observado na ausência de minerais, não pode ser explicado pelos níveis gerais de expressão dos genes que codificam para as Pectinas Metilesterases (PME). A maioria destes genes apresentaram uma redução da sua taxa de transcrição, tanto nos tecidos de callus como na pelicula dos bagos. A exceção foi os genes de PMEs com pI básico. Estas PMEs são aquelas que formam longas cadeias de HG de-esterificado, o que promove a formação de ligações entres pectinas por pontes de Ca^{2+} e deste modo reforça a PC. As alterações nos constituintes da parede podem conduzir a alterações das suas propriedades biofísicas. Usando testes de extensiometria em hipocótilos de pepino, foi possível provar que a deformação causada na PC do hipocótilo não resultou da ação de expansinas (EXPA) mas talvez seja promovida por outras enzimas principalmente GH9s e XTHs. Os extratos salinos obtidos a partir de callus em –N e –P induziram um aumento da deformação plástica nos hipocótilos do pepino. Ao mesmo tempo foi observada uma diminuição da atividade de endo-glicosil hidrolase em –N. Este facto levou-nos a concluir que as modificações irreversíveis ocorridas na parede se deveram, pelo menos em parte, a fenómenos mecânicos em complemento com atividade enzimática, possibilitando-nos concluir que a deficiência de azoto alterou mais as propriedades mecânicas da parede.

O stresse hídrico influenciou a composição e os atributos sensoriais dos bagos de videira. Os resultados globais permitiram uma clara separação entre as duas

variedades estudadas e também entre os dois regimes hídricos. O stresse hídrico induziu o aumento de antocianinas nos bagos das duas variedades, e tal como já descrito como resposta geral a um stresse abiótico, uma redução da quantidade de celulose e aumento de polímeros ricos em arabinose na PC da película do bago. Como resposta ao stresse hídrico houve uma diminuição na taxa de transcrição da maioria dos genes ligados à síntese e modificação da PC cuja expressão foi quantificada. Os resultados apontam para um aumento da rigidez da parede através da alteração da estrutura das pectinas em resposta à ausência de água.

Globalmente os resultados apontaram para diferentes estratégias levadas a cabo pelos modelos de videira para fazer face a situações adversas, levando a um alteração na composição, estrutura e rearranjo da PC dependendo da severidade do stresse. Os modelos de *V. vinifera* sujeitos a stresse abiótico sofreram uma redução da quantidade de celulose. Para superar esta situação a PC sofreu uma reorganização de vários dos seus compostos, em particular no grau de esterificação das pectinas, na quantidade dos polímeros contendo arabinose e na xiloglucana, o que promoveu um reforço da parede. No seu conjunto os resultados contribuíram para o esclarecimento dos processos de reorganização da PC em situações de stresse abiótico.

Index

Figure List

Table List

General abbreviations

CesA	Cellulose synthase
CW	Cell Wall
EXP	Expansin
GalA	Galacturonic acid
GH9A	Glycosyl hydrolase family 9A
GH9C	Glycosyl hydrolase family 9C
HG	Homogalacturonan
-N	Absence of nitrogen
-P	Absence of phosphorous
PG	Polygalacturonase
PL	Pectate lyases
PME	Pectin methylesterase
PMEI	Pectin methylesterases inhibitor
RG–I	Rhamnogalacturonan–I
-S	Absence of sulfur
XTH	Xyloglucan transglycosylase/hydrolase
XyG	Xyloglucan

Chapter 1

General Introdution

1. General introduction

1.1. Plant Cell Wall

The plant cell wall (CW) is a complex and heterogeneous structure of polysaccharides, glycoproteins and enzymes, which surrounds the protoplasts. The deposition and modification of CW material plays an essential role during plant growth (Reiter 2002), determining the cell size and shape, also providing protection against stresses, both biotic and abiotic (Seifert and Blaukopf 2010) enabling cells to adapt to different physiological and environmental situations (Braidwood et al. 2014). Two other important functions are assigned to CW: as an important source of biologically active signaling molecules, which regulate cell-to-cell interactions and as carbohydrate storage reserve (Wolf et al. 2012).

1.2. Plant Cell Wall composition and structure

Remarkable progress has been made in the elucidation of CW structure and architectural organization (Cosgrove and Jarvis 2012). However, no agreement has been reached regarding a clear-cut model of the CW.

Two types of CW can be distinguished: i) the primary wall, present in growing cells which needs to be strong to withstand the tensile forces arising from turgor pressure and also extensible to allow wall stress relaxation which enables physical enlargement of the cell (Hamant and Traas 2010) and ii) the secondary wall which results from the deposition of new polymers after the arrest of cell growth, conferring mechanical stability in some cell types like xylem and sclerenchyma cells. Both primary and secondary CWs contain cellulose and hemicelluloses. The main difference is that primary walls polysaccharide matrix is embedded in pectins and structural proteins while secondary walls contain little protein or pectin but normally incorporate lignin (McCann and Carpita 2008). Despite this, the involvement of pectin in the secondary wall was proposed since the controlled and localized modifications of these polysaccharides define cell properties and architecture, contributing to different biophysical characteristics (Bourquin et al. 2002; Goulao et al. 2011). Cellulose is synthesized at the plasma

membrane and deposited directly into the wall (Doblin et al. 2003), the other components are made in the Golgi and delivered into the wall by secretory vesicles (Carpita and McCann 2000). The secondary CW results from lignin deposition within the cellulose microfibrils and matrix polymers. Lignin, is the second most abundant plant organic compound, after cellulose. The main building blocks of lignin are the hydroxycinnamyl alcohols, mostly the monolignols *p*-hydroxyphenyl (H), guaiacyl (G) and syringil (S) units forming a branched and complex heteropolymer (Vanholme et al. 2010).

The relative amount of each unit varies between species, tissues and environmental conditions (Bonawitz and Chapple 2010). In angiosperms, lignin is almost exclusively composed by G and S subunits. Enzymes of the lignin biosynthetic pathway are thought to be active at the cytosolic side of the endoplasmic reticulum (Ro et al. 2001; Bassard et al. 2012).

1.2.1. Primary Cell Wall

The primary CW of dicotyledonous and non-commelinoid monocot species, known as Type-I CW, (Carpita and Gibeaut 1993) is composed of approximately 90% w/w polysaccharides (McNeil et al. 1984) mainly: cellulose, matrix cross-linked glycans (hemicelluloses) and pectic polysaccharides Primary walls are comprised of 15–40 % cellulose, 30–50 % pectins and 20–30 % hemicelluloses, predominantly xyloglucans (XyGs), on a dry weight basis (Cosgrove and Jarvis 2012). Also present in Type-I CW are structural glycoproteins, phenolic esters, minerals, and enzymes that can modify its physical and chemical properties.

Cellulose is a paracrystalline structure of β-(1→4)-D-glucan chains, which are synthesized individually and can crystallize into cellulose microfibrils through inter- and intramolecular hydrogen bonds and Van der Waals forces. Because cellulose is the main load-bearing polymer of the CW, the length, angle, and crystallinity of cellulose microfibrils are important determinants for the physical characteristics of the CW (Wolf et al. 2012). The cellulose synthase (CesA) complex (CSC), which produces cellulose, was originally described in cotton (Pear et al. 1996). When a fracture plane was generated between two sides of the plasma membrane, a rosette structure with six fold symmetry was observed

by transmission electron microscopy and found to be associated with plasma membrane impressions that may have resulted from cellulose microfibrils (Mueller and Brown 1980). Attempts to measure the size of cellulose microfibrils and to correlate with the number of glucan chains have yielded estimates of 12–36 glucan chains per microfibril (Delmer 1999). Thus, if 36 CesA subunits comprise the sixfold symmetry of the CSC, then a single CSC could synthesize up to 36 glucan chains (reviewed in McFarlane et al. 2014). However, recent studies provide evidence for an alternative structure. The predicted cross-sectional area of a 36-chain microfibril is too large to agree with recent experimental data (Jarvis 2013). Analysis of cellulose using both wide-angled X-ray scattering (WAXS) and small angle neutron scattering (SANS) to look at microfibril size, coupled with NMR and FT-IR techniques to measure the surface ratio exposed to internal chains, concluded that cellulose microfibrils are most likely formed with 24-chain (Fernandes at al 2011). The number of CesA genes is very similar between plant species (Fernandes et al. 2015). In *Arabidopsis* both *CesA1* and *CesA3* are necessary for plant growth and development, as knockout mutants were lethal (Persson et al. 2007). Milder defects in either of these genes resulted in a drastic reduction in cellulose synthesis and a wide array of cellulose-deficient phenotypes, including dwarfism, cell swelling and lignification (Scheible et al. 2001; Caño-Delgado et al. 2003; Somerville 2006). Mutations in the other primary CW CesA genes (*CesA2*, *-5*, *-6*, and *-9*; refereed as CesA6-like genes) resulted in milder phenotypes in single-knockout mutants (Desprez et al. 2007; Persson et al. 2007), meaning genetic redundancy between these CesA6 -like genes. This led to a model in which CesA1 and CesA3 form a complex with any CesA6-like protein (McFarlane et al. 2014).

Apart from CesA proteins, cellulose biosynthesis requires the cooperation of other proteins. Mutations in the KORRIGAN (KOR) gene encoding a putative β-1,4-endo-glucanase (GH9) from class A (Urbanowicz et al. 2007a) lead to lateral organ swelling, reduction in cellulose and altered pectin amounts (Nicol et al. 1998; Zuo et al. 2000; Sato et al. 2001). Along with KOR a role for a poplar class C β-1,4-endo-glucanase (GH9C) member in modulating cellulose crystallinity and its involvement in cell growth was recently demonstrated using reverse genetic approaches (Glass et al. 2015).

Cellulose microfibrils are the load-bearing fibers of CW. Cross-linking glycans, also referred as hemicellulose polysaccharides can bind to cellulose (Cosgrove 2005). Hemicellulose polysaccharides are diverse and include XyG, xylans and manans (Liepman et al. 2007). XyG is the major hemicellulose in the primary wall. The cellulose-XyG network is generally considered the major load-bearing element within the primary wall (Carpita and McCann 2000). Xyloglucan endotransglycosylases/hydrolases (XTHs) are responsible for the cleavage and/or rearrangement of the XyG backbones (Eklöf and Brumer 2010). XTH genes encode proteins that can potentially have two distinct catalytic activities, with a different effect on the XyG polymers. Acting as a transglycosylase (XET), a dual biochemical mode of action occurs: the integration of newly secreted XyG chains into an existing wall-bound XyG restructuring existing CW material by catalyzing the transglycosylation between previously wall bound XyG molecules, what results in the non-hydrolytic cleavage and ligation of XyG chains or acting as hydrolase (XEH), hydrolyzing XyG molecules, depending on the nature of the XyG donor and acceptor substrates (Fry et al. 1992; Nishitani and Tominaga 1992; Rose et al. 2002). Most XTHs have XET activity, whereas only some XTHs use water as the acceptor substrate, resulting in XEH activity (Rose et al. 2002; Nishitani and Vissenberg 2007). It has been reported that spatial distribution of XTH expression and XET activities are closely correlated with both cell elongation (Fry 1992; Catala et al. 1997; Vissenberg et al. 2000; Ji et al. 2003) and non-elongation zones (Vissenberg et al. 2001; Takeda et al. 2002), even during secondary wall formation (Antosiewicz et al. 1997; Bourquin et al. 2002; Matsui et al. 2005; Goulao et al. 2011). Recent studies proposed XyG as a minor component of the CW, closely intertwined with cellulose at limited sites, promoting selective targets for CW loosening, the so called “biomechanical hotspots” theory was proposed recently (Park and Cosgrove 2012; 2015).

Pectins are complex polysaccharides that consist of 1,4-linked α-D-galactosyluronic acid (GalA) residues containing linear chains, assembled through substitutions with variable degrees of ramifications by single sugars or complex side-chains (Voragen et al. 1995; Ridley et al. 2001). GalA forms the backbone of three polysaccharide domains that are thought to be present in all pectin species: homogalacturonan (HG), rhamnogalacturonan-I (RG-I),

rhamnogalacturonan-II (RG-II) (Caffall and Mohnen 2009). Pectin structure can be significantly altered by the activity of enzymes. These modifications have crucial roles in various growth and development processes in plants. Catalysis of specific hydrolysis of the methyl ester bond at C-6 of a GalA residue in the linear HG domain of pectin is the result of pectin methylesterase (PME) activity, leading to alterations in the degree and pattern of methyl esterification (Jolie et al. 2010). The pattern and extent of pectin deesterification is controlled by the interaction of pectin methylesterases (PMEs) and their specific inhibitors (PMEI) (Bellincampi et al. 2004; Di Matteo et al. 2005; Juge 2006; Jolie et al. 2010) and therefore, PMEs and PMEIs can change the biophysical properties to the CW. Depending on the specific pattern and degree of methyl esterification, pectins can aggregate into hydrated calcium-linked gel structures, that increase wall stiffness and reduce creep (Willats et al. 2001), or make pectins more susceptible to depolymerisation by polygalacturonases (PGs) contributing to CW loosening (Brummell and Harpster 2001; Wakabayashi et al. 2003).

HGs are polymers formed by α-1,4-linked linear chains of more than 100-200 GalA residues (Thibault et al. 1993; Zhan et al. 1998; Willats et al. 2001) and can account for more than 60-65% of the total plant pectins. HG, synthesized in the Golgi apparatus is deposited into the CW with a degree of methyl-esterification up to 70-80% of the GalA residues at the C-6 carboxyl and/or acetylated at the O-2 or O-3 position (Willats et al. 2001). Methyl-esterification is tightly regulated and depends on development phase and tissue. When stretches of 10 or more consecutive un-methyl-esterified residues occur, the un-methylated GalA residues may be cross-linked with Ca^{2+} to form stable gels with other pectic molecules. The hypothesized *in vivo* structure of the HG–calcium complex named “egg-box” (Liners et al. 1989), may induce gelling phase in plant CW. These cross-links together with RG-II- boron diester bonds are thought to indirectly affect the cellulose-XyG network by influencing the wall porosity (Peaucelle et al. 2012). Pectins are, as presented, a very dynamic class of polymers which due to their hydrophilic character may ease microfibrils motions as CW expands, reducing the direct cellulose–cellulose contacts (Park and Cosgrove 2015). Instead of XyG, pectic monosaccharides (most likely from RG-I side chains galactan and arabinan rich (Zykwinska et al. 2007; 2008) may be associated to

the cellulose (Cosgrove 2014). Pectins can then serve as mechanical tethers between microfibrils (Wang et al. 2012; Peaucelle et al. 2012). The occurrence of pectic polysaccharides micro-domains means the localization of precise areas with distinct properties as the result of different, localized demethylation mechanism which may lead to stiffening or loosening of the wall (reviewed by Goulao 2010).

Along with HG an acidic pectic domain consisting of 100 repeats of the disaccharide α-1,2-L-rhamnose-α-1,4-linked GalA known as RG-I has been isolated from several plants (Willats et al. 2001). The backbone holds a variable number of repeats, and three types of neutral sugar side-groups are attached to the 4-position of approximately 20-80% of the rhamnose backbone units, depending on the source of the polysaccharide (Albersheim et al. 1996). These side-chains can derive from single or polymeric substitutions and are mainly composed of α-1,5-L-arabinans, β-1,4-D-galactans and arabinogalactans, where arabinose is usually terminal and galactose links can be connected through C-4, C-3 or C-6. Its abundance is developmentally and differentially regulated (Caffall and Mohnen 2009). RG-I is the major branched, heterogeneous and hydrated component of the middle lamella and primary CWs.

Despite the name RG-II is not structurally related to RG-I. RG-II consists of molecules with stretches of HG backbone approximately 7-9 α-1,4-D-GalA residues long, substituted with clusters of four highly complex and conserved side chains containing different types of sugars, in more than 20 different linkages (Voragen et al. 2009). Its structure consists of self-associated dimers cross-linked by single borate di-esters (Kobayashi et al. 1999; Ishii et al. 1999) and stabilized by the presence of calcium (O'Neill et al. 2004). The main pectin domains, HG, RG-I and RG-II, are covalently cross linked forming the pectic matrix. Despite the unclear nature of the covalent arrangements, the pectic matrix functions as a complex macromolecule (Ridley et al. 2001; Vincken et al. 2003; Coenen et al. 2007). Vincken et al. (2003) and Coenen et al. (2007) proposed a representation of the pectin network in which RG-I supplies the main backbone to which HG, RG-II and the other less abundant pectic domains are covalently cross-linked to form side-chains of the same molecule.

In CW remodelling, expansins (EXP), are considered the major contributors of loosening (McQueen-Mason et al. 1992), acting by reversibly weakening interactions or disrupting hydrogen bonds between cellulose microfibrils and matrix-linked glycans (McQueen-Mason and Cosgrove 1995; Cosgrove 2000; Whitney et al. 2000; Wang et al. 2013). α-expansins (EXPA) are the foremost promoters in controlling cell extensibility in dicots (Cosgrove 1999; 2000). As reviewed by Choi et al. (2006), genetic modification indicated that EXPAs are involved in cell enlargement and fruit softening and have other effects on plant growth and development.

1.2.2. Secondary Cell Wall

When the cell stops dividing and expanding, lignin is deposited in the CW within the cellulose microfibrils and matrix carbohydrates, establishing chemical bonds with non-cellulosic carbohydrates, forming a thick secondary CW. Generally, secondary CWs consist of three layers: the outer (S1), the middle (S2), and the inner (S3) (Pinelo et al. 2006; Donaldson 2001). The formation of secondary walls occurs mainly in xylem vessels, structural fibers, seed pods and seed integument (Cadot et al. 2006; Bonawitz et al. 2010). The process starts in the middle lamella and the primary wall (initiation of S1 formation). When the polysaccharide matrix of the S2 layer is completed, lignification proceeds through the secondary wall (Boerjan et al. 2003), in particular at the final stage of xylem differentiation (Vanholme et al. 2008). As so, lignin deposition is developmentally programmed assuring structural integrity and waterproofing the CW, enabling water and solutes transport through the vascular system efficiently. Biotic and abiotic stress conditions can also induce lignin biosynthesis (Boerjan et al. 2003; Vanholme et al. 2010).

Lignin, is the second most abundant plant organic compound (Vanholme et al. 2008). Dehydrogenated monolignols can form dimmers through covalent bonds between the central carbon of the monolignol tail β-β type (Bonawitz et al. 2010), or between the β carbon and C atoms of the aromatic ring. After a new dehydrogenation of the dimer, another covalent bond can be established by a polymerization progressing one unit at a time. Molecular species other than the canonical monolignols can be integrated in the lignin polymer, explaining the

plasticity of the polymerization process and the variability of the final polymer (Vanholme et al. 2008; Bonawitz et al. 2010). The majority of lignin in angiosperms, such as in grapevine, is composed by G and S subunits. In poplar, a woody plant, the linear lignin length is between 13 and 20 units (Stewart et al. 2009), but the length of lignin chain in grapevine is not reported.

1.3. *Vitis vinifera* – the species object of study

1.3.1. The paramount economic value of grapevine

The genus *Vitis* is the only genus of the *Vitaceae* family that produces edible fruits (Bouquet 2011). Grapevine, *Vitis vinifera* L., is the only species naturally found in the Eurasian area, and the two subspecies *V. vinifera* subsp. *vinifera* and *V. vinifera* subsp. *sylvestris* are domesticated from wild forms. *V. vinifera* represents one of the most important crops from an economic point-of-view partly due to the high value of the fruit predominantly resultin from its importance for winemaking (Giribaldi et al. 2010).

Due to its economic importance and its position as a model species for perennial fruit crops, *V. vinifera*, has benefited from efforts to develop genomic tools and data. The genomes sequencing of the heterozygous variety Pinot Noir and a near homozygous Pinot Noir derived inbred (Jaillon et al. 2007; Velasco et al. 2007) reveled the importance of grapevine as model species. Consequently, the bioinformatics resources for the grapevine species has expanded in the past few years focusing post-genomics era applications (Grimplet et al. 2012).

1.3.2. The berry skin Cell Wall

1.3.2.1. Composition

The majority of studies on CW composition are performed on grape berries, with no studies in *V. vinifera* dedifferentiated systems, such as callus cultures. The berry skin of *V. vinifera* is constituted by a typical Type-I CW, consisting of approximately 90% polysaccharides and less than 10% protein fraction. Cellulose and polygalacturonans are the major constituents accounting for ca. 30-40% by weight of the polysaccharide component of the walls (Nunan et al. 1997; Vidal et

al. 2001) but may display varietal differences in the relative abundance of the two polysaccharides. Berry skins from “Traminer” and “Sauvignon Blanc” consist of thick-walled epidermal and hypodermal cells (Hardie et al. 1996). In the skin, 50% of the CW material is made of polysaccharides (Lecas and Brillouet 1994) with similar composition to mesocarp walls (Saulnier and Brillouet 1989; Nunan et al. 1997). Polysaccharides like XyG, arabinan, galactan, xylan and mannan account for 30%, while acidic pectin substances (of which ca. 62% are methyl esterified) account for 20%. The remaining part is composed of 15% insoluble proanthocyanidins, <5% structural proteins (Lecas and Brillouet 1994) and lignin (Bindon et al. 2010).

The pectic fraction is composed of 65% HG, 10% RG-I, 2% RG-II and 23% neutral side chains (Saulnier and Thibault 1987; Nunan et al. 1997; Vidal et al. 2001). The contribution of arabinans and RG-I, is about 4-6% by weight of the pectic polysaccharides (Nunan et al. 1997). When compared with other fruits, *V. vinifera* berries contain higher amounts of HG and RG-I, (Hilz et al. 2007). The majority of the grape berry walls (by weight) are originated from the skin but only 25% of the total fresh berry weight comes of them (Vidal et al. 2001; Doco et al. 2003). The relative molar distribution (mol %) of the different polysaccharides in the red wine grape skins was estimated to be 57-62 HG, 6-14 cellulose, 10-11 XyG, 7 mol %, 4.5-5 RG-I, 3.5-4 RG-II, 3 mol % AG, and 0.5-1 mannans (Arnous and Meyer 2009).

The major hemicellulosic polysaccharide is XyG, accounting 8-12% of the total wall polysaccharide fraction (Nunan et al. 1997; Doco et al. 2003), the remaining part are mannans, heteroxylans, arabinans, galactans and arabinogalactans, in smaller amounts (Lecas and Brillouet 1994; Nunan et al. 1997; Doco et al. 2003). In grapes the amount of XyG is lower than the typical XyG content of dicot walls despite its similar structures (Doco et al. 2003).

Phenolic compounds are mainly present in the skin and seeds. The skin CW of *V. vinifera* contain about 15% tannins (Pinelo et al. 2006). Bidon et al. (2010) report 54% of proanthocyanidins (PA) in the skin fraction of the total extractable PA. Interestingly, a different interaction pattern occurs between flesh and skin CW material and PA, with eventual effects on PA extraction and winemaking (Bidon et al. 2010).

1.3.2.2. Skin Cell Wall and berry ripening

During fruit softening a number of modifications occur within the CW of different tissues. During the first growth phase of development, berry enlargement occurs in all of the tissues, however, in the transition period between veraison and the second growth phase, only the exocarp expands. Then, in the second growth phase only the mesocarp undergoes cell expansion.

Most of the skin CW modification occurs post veraison, as the skin begins to soften. The rearrangement that CW undergoes during softening of the tissues leads to further cellular growth of the mesocarp with the influx of water and sugars typically seen during the second growth phase. Throughout maturation of the berry, thinning of the CW material occurs, although there is a debate whether total CW decreases during this period. Some reported that in varieties like “Monastrell” and “Cabernet Sauvignon” total CW decreased (Ortega-Regules et al. 2008) but in others, like Syrah, no change were observed (Vicens et al. 2009). A degradation of the middle lamella in the hypodermis cells has also been noticed to aide with the cell expansion within the mesocarp (Huang et al. 2005). Although there have been decreases of CW material witnessed in the mesocarp of the “Gordo” variety (Nunan et al. 1998)

Despite drastic softening of the skin, Vicens et al. (2009) reported only moderate changes within CW composition. Over the period of ripening, and as the berry reaches maturity, the content of the water-soluble sugar fraction roughly doubles within the berry skin CW from 3 to 8% of total sugar content (Vicens et al. 2009). However in the mesocarp, the levels of the water-soluble fractions are higher with an increase of 10 to 23% (Nunan et al. 1998) being probably variety dependent. In addition, the content of insoluble pectins also decreases (Huang et al. 2005). This occurs in parallel with the decrease in insoluble galactose levels within the CW (Ortega-Regules et al. 2008; Vicens et al. 2009), mainly attributed to the degradation and solublisation of AG-I sidechains, as soluble arabinose levels increase whereas rhamnose levels remain constant. Enzymatic activity also suggests the solubilisation of sidechains, with α-galactosidase and β-galactosidase activities increasing dramatically as the berry softens (Nunan et al. 2001). Moreover, this is in conjunction with a decrease in the calcium bridge

bound pectins, also attributed to loosening of the CW (Huang et al. 2005). The calcium ions may be translocated into the cytoplasm of the cells as they are required for the cell to function. This is possibly due to localized pH decreases within the CW, with the acidification being the cause of the cleaving of the bridges. Additionally there is an increase in pectin methylesterase activity catalyzing the hydrolysis of the methylester groups in the pectins of the CW (Nunan et al. 2001). Both mechanisms lead to an increase in CW loosening with weaker interactions between the polysaccharides. However the rate of decrease of methyl and acetyl-esterification is variety specific, with dramatic changes witnessed in Cabernet Sauvignon, Monastrell and Merlot, with little change in Syrah (Ortega-Regules et al. 2008). As stated, pectins are probably the CW components that change most noticeably during fruit softening (Paniagua et al. 2014).

Cellulose degradation throughout ripening is not a clear cut event. Several studies have shown that cellulose levels did not decrease throughout maturity (Nunan et al. 1998; Ortega-Regules et al. 2008), whereas others have shown a decrease in cellulose and hemicellulose levels in the skin (Ishimaru and Kobayashi 2002), suggesting different regulatory mechanisms. Acidification can also cleave the hydrogen bonds between XyG and cellulose microfibils (Huang et al. 2005). This could suggest that the XyG are exposed to enzymatic activity, or more likely that it is an unwinding of the matrix structure, resulting in more fluid model, in accordance with the new proposed model of “biomechanical hotspots” proposed by Park and Cosgrove (2012; 2015) in which wall extensibility is less dependent on the viscoelasticity of the matrix polymers but depending more of the selective separation between microfibrils at limited CW sites.

The berry skin CWs have also an important role in wine making, since it forms a hydrophobic barrier to the diffusion of phenols, controling extractability (Ortega-Regules et al. 2006; Hanlin et al. 2010). Most phenolic compounds are nearly absent in the grape berry flesh, and mainly located in the skin and seeds, and can be released during the wine making process (Pinelo et al. 2006). Tannins accumulate in the berry during the first growth period and decline during phase III of growth (Kennedy et al. 2001). The retention of phenols by the CW depends on the composition, structure and molecular weight of the phenol molecule and of CW physical traits (Bindon et al. 2010; Hanlin et al. 2010), therefore CW

porosity, structure, chemical composition, can influence the aggregation between polysaccharides and phenolic substances. Anthocyanin extraction from the grape skin and diffusion into must and wine depends on anthocyanin content but also on the capacity of the berry skin to yield the pigment as a consequence of CW degradation. When phenolic ripeness is attained, the pectin-rich middle lamella between cells is degraded and the CWs are perforated and allow extraction and diffusion (Ortega-Regules et al. 2006). Río Segade et al. (2008) proposed the interesting concept of *phenolic ripeness* associated to anthocyanin content and extractability.

1.3.2.3. Berry and skin Cell Wall biomechanical characteristics

Plant cell growth is the result of CW extensibility and the turgor pressure exerted on the wall (Peaucelle et al. 2012). Wall relaxation and cell expansion can occur without changes in CW strength depending on changes on the load-bearing bonds (Peaucelle et al. 2012). In light of recent observations, reconsideration of the tethered network model is needed. Recent findings by Dick-Perez et al. (2011) using NMR, suggest that only a small portion of the XyG is bound to cellulose. Using extensometer assays on cucumber CWs it was shown that creep is not solely caused by Expansins (EXPAs), but also promoted by β-1,4-endo-glucanases and XTHs (Park and Cosgrove 2012) suggesting a new model for CW architecture.

The enological potential of *V. vinifera* depends on berry characteristics (Rolle et al. 2011). These characteristics are influence by environmental conditions (Hall and Jones 2009). Texture analysis studies on winegrapes begun in the 1980s, to describe changes in mechanical properties during ripening (Lee and Bourne, 1980) due to the numerous physiological and biochemical changes that berries undergo that induce texture modifications (Ribèreau-Gayon et al. 2003). The berry soluble solid content can influence the characteristics of the berry skin, like puncture force, however this may not apply to all grape varieties (Letaief et al. 2008). Abiotic stresses, like water or mineral, can induce different behaviors in grape mechanical parameters in particular in berry skin thickness (Porro et al. 2010). Several studies observed the behavior of the berry skin break force during maturation. From veraison to ripening an increase in berry skin hardness and

thickness as observed. Normal CW expansion is not result of wall constitutive properties but from continuous action by the cell or by wall-associated proteins (Park and Cosgrove 2012).

1.3.3. *Vitis vinifera callus* and shoots as experimental models to determine the Cell Wall response to mineral stress

Plant model systems analyzed in controlled experimental conditions, such as callus, are useful tools to assess limiting nutrient situations, due to their homogeneity and absence of complex structure. Therefore callus is a simple way to study stress induced conditions without interference of complex metabolisms. But plant differentiated tissues can exhibit a different behaviour as compared to unorganized tissues. For instance, specific CW composition and structure can be localized in a small number and type of cells (Freshour et al. 1996), which provide the cell with the ability to respond to abiotic stresses, e.g. osmotic stress (Iraki et al. 1989) or chemical stress (Shedletzky et al. 1992; Mélida et al. 2009). Plant mineral deficiency, in particular nitrogen (N), phosphorus (P), potassium (K) and sulphur (S), strongly affect plant metabolism, reducing plant growth and crop yield as well as the nutritional and organoleptic quality of the agronomic product (Amtmann et al. 2009; Fernandes et al. 2009; Tschoep et al. 2009). Due to their involvement in primary metabolic pathways, N, P and S are major regulators of plant growth and development, influencing amino acid and nucleotide biosynthesis, protein phosphorylation or disulfide bonds between cysteine, causing changes at biochemical and physiological levels with effects in anatomical and developmental patterns. Despite the diversity in plant species a generic “stress–induced” response to abiotic stresses can be revealed through the inhibition of cell elongation, localized stimulation of cell division and alterations in cell differentiation status (Potters et al. 2007; Patakas 2012). Mineral nutrient deficiency arrests the production or expansion of meristematic cells and then growth rates of plant organs. (Volenec and Nelson 1983; McDonald 1989; Palmer et al. 1996) via a decrease in CW plasticity (Taylor et al. 1993; Snir and Neumann 1997). It has been proposed that nutrient stress induced CW rearrangements with reductions in roots hydraulic conductivity (Radin and Boyer 1982; Radin and Eidenbock 1984; Chapin et al. 1988), modifying xylem tension

to overcome the stress (Chazen et al. 1995). These features are determined by the dynamic regulatory properties of the CW. However, despite the importance of mineral nutrition in plant development, its influence on the synthesis and modifications of the CW is not fully documented. To address these limitations *V. vinifera* callus and shoots were used to study CW response to mineral depletion, respectively as unorganized and organized tissues.

1.4. *Vitis vinifera* as its own molecular model

The sequencing and public availability of the *V. vinifera* genome (Jailon et al. 2007; Velasco et al. 2007) enables the study of individual pathways, profiling of the expression pattern of isoforms in each tissue, developmental phase and response to the different stresses. One way of tackling the pathways of a given physiological event is to understand the regulation of the transcription of related genes. Genomic resources for *V. vinifera* have proliferated rapidly within last years, allowing large-scale mRNA expression profiling studies of gene expression during grapevine development (Grimplet el al. 2009; Zenoni et al. 2010). Proteomic studies also received great attention, either on berry metabolism (Sarry et al. 2004; Giribaldi et al. 2007), abiotic stress resistence (Castro et al. 2005; Vincent et al. 2007; Jellouli et al. 2008) or both (Grimplet et al. 2009). Global transcriptomic studies involving nutrient depleted plants revealed differential regulation of CW–related genes and proteins in various species (Takahashi et al. 2001; Guo et al. 2008), emphasizing the CW role in survival response mechanisms.

The role of CW synthesis and modifying enzymes and coding genes has been investigated through quantification of enzyme activity and gene expression in a variety of plants including *V. vinifera*. Besides, the biological function of those enzymes has been disclosed by CW characterization of genotypes impaired or overexpressing specific members of CW-related gene families ins several plant species (e.g. Osato et al. 2006; Peaucelle et al. 2008; Miedes et al. 2010).

The initial studies associated with the CW used enzyme activity and gene expression based on “candidate gene” approaches in grapes. Up-regulation of genes involved in the cellulose-hemicellulose network, such as EXPA and XTH,

at veraison, coincident with de-polymerization of XyG (Nunan et al. 2001; Ishimaru et al. 2002; 2007) was observed. In grape berry, the expression of GH9 genes seems to be confined to the initial growth stages and was not detected during ripening (Nunan et al. 2001), which contrasts with the majority of fruit species, except for apple (Goulao et al. 2007; 2008). In skin, the transcription profiles of CW-modifying enzymes have high levels of expression in period of rapid berry growth and cellular expansion and low expression levels during growth arrest (Schlosser et al. 2008). The involvement of these gene families is confirmed with large-scale transcriptomics. Among these are included pectin modifying enzymes (PME, PG and PL) and enzymes that modify the cellulose-hemicellulosic network (EXP and XTH). However, moving from "candidate gene" approaches to "large scale high throughput" transcriptomics in the grape berry, allowed the identification of members of CW-related enzymes previously overlooked such as PMEIs or CesA (Deluc et al. 2007). Using the Affymetrix *Vitis* GeneChip genome array, Pilati et al. (2007) identify 10 members of the XTH family that were modulated during development, four of them strongly up-regulated during ripening. Moreover, comprehensive comparisons of gene expression between pulp, skin and seed tissues are now facilitated (Grimplet et al. 2007).

1.5. Objectives

The main aim of the present work was to investigate the response of the CW to the depletion of individual major nutrients, nitrogen, phosphorus and sulfur in *V. vinifera*. Callus was used as a homogeneous and dedifferentiated system and plant differentiated tissues, namely shoots, were used as a complex experimental system to address the CW response to mineral stress in organized tissues. In grapevine, the berry is the economic product. Mineral stress is not common in field conditions and berry production in pot plants is difficult to obtain in acceptable physiological conditions. However, global climate changes are exacerbating problems associated with water deficit and high evapotranspiration rates that are likely to affect berry development, yield and ultimately wine quality. The CW can influence the extractability of several components in the berry.

Consequently the effect of water stress on berry skin CW was studied in non-irrigation versus irrigation plants.

To retrieve the major candidate events occurring in the CW in response to mineral depletion an integrated approach employing complementary methodologies, in particular, Fourier–Transform Infrared (FT–IR) spectroscopy coupled with chemometrics was followed. With these candidate events in mind and to gain insight on the molecular regulation underlying CW specific composition and arrangement, comprehensive *in silico* data mining was undertaken to retrieve sequences for all identified members of *V. vinifera* candidate CW-modifying multigenic families and their expression was quantified in callus under mineral stress. Using grapevine shoot internodes organized tissues as an experimental model and to investigate *in situ* CW responses and specifically component rearrangement in response to the depletion of individual major nutrients, immunolocalization assays were performed, which allowed investigation of specific *V. vinifera* CW responses to individual mineral depletion. Finally, berry yield, chemical characteristics and mechanical properties as well as berry skin CW composition and expression of key candidate genes associated with berry development and ripening were investigated. The combined use of these methodologies allowed drafting a map of *V. vinifera* CW responses to different forms of abiotic stress, namely water and mineral deficit.

References

Albersheim P, Darvill AG, O'Neill MA, Schols HA, Voragen AGJ In Pectins and pectinases, Visser, J.; Voragen, A.G.J., Eds., Elsevier Science B.V.: Amsterdam, 1996; pp 47–56.

Amtmann A, Armengaud P (2009) Effects of N, P, K and S on metabolism: new knowledge gained from multi–level analysis. Curr Opin Plant Biol 12:275–83. doi: 10.1016/j.pbi.2009.04.014.

Antosiewicz DM, Purugganan MM, Polisensky DH, Braam J (1997) Cellular localization of *Arabidopsis* xyloglucan endotransglycosylase-related proteins during development and after wind stimulation. Plant Physiol 115:1319–1328.

Arnous A, Meyer A (2009) Grape skins (*Vitis vinifera* L.) catalyze the in vitro enzymatic hydroxylation of p-coumaric acid to caffeic acid. Biotech Lett 31:1953-1960. doi: 10.1007/s10529-009-0103-5.

Bassard JE, Richert L, Geerinck J, Renault H, Duval F, Ullmann P, Schmitt M, Meyer E, Mutterer J, Boerjan W, De Jaeger G, Mely Y, Goossens A, Werck-Reichhart D (2012) Protein-protein and protein-membrane associations in the lignin pathway. Plant Cell 24:4465-82. doi: 10.1105/tpc.112.102566.

Bellincampi D, Camardella L, Delcour JA, Desseaux V, D'Ovidio R, Durand A, Elliot G, Gebruers K, Giovane A, Juge N, Sorensen JF, Svensson B, Vairo D (2004) Potential physiological role of plant glycosidase inhibitors. BBA Proteins Proteomics 1696:265–274. doi: 10.1016/j.bbapap.2003.10.011.

Bindon KA, Smith PA, Kennedy JA (2010) Interaction between grape-derived proanthocyanidins and cell wall material. 1. effect on proanthocyanidin composition and molecular mass. J Agr Food Chem 58:2520-2528. doi: 10.1021/jf9037453.

Boerjan W, Ralph J, Baucher M (2003) Lignin biosynthesis. Annu Rev Plant Biol 54:519-546. doi: 10.1146/annurev.arplant.54.031902.134938.

Bonawitz ND, Chapple C (2010) The genetics of lignin biosynthesis: connecting genotype to phenotype. Annu Rev Genet 44:337-63. doi: 10.1146/annurev-genet-102209-163508.

Bouquet A (2011). Grapevines and Viticulture. In Genetics, Genomics, and Breeding of Grapes. Adam-Blondon, A.-F., Martinez-Zapater. J.-M. and C. Kole (eds). Science Publishers, CRC Press, pp. 1-29.

Bourquin V, Nishikubo N, Abe H, Brumer H, Denman S, Eklund M, Christiernin M, Teeri TT, Sundberg B, Mellerowicz EJ (2002) Xyloglucan endotransglycosylases have a function during the formation of secondary cell walls of vascular tissues. Plant Cell 14:3073–3088.

Braidwood L, Breuer C, Sugimoto K (2014) My body is a cage: mechanisms and modulation of plant cell growth. New Phytol 201:388–402. doi: 10.1111/nph.12473.

Brummell DA, Harpster MH (2001) Cell wall metabolism in fruit softening and quality and its manipulation in transgenic plants. Plant Mol Biol 47:311–340. doi: 10.1023/A:1010656104304.

Cadot Y, Miñana-Castelló MT, Chevalier M (2006) Anatomical, histological, and histochemical changes in grape seeds from *Vitis vinifera* L. cv Cabernet franc during fruit development. J Agric Food Chem 54:9206-9215. doi: 10.1021/jf061326f.

Caffall KH, Mohnen D (2009) The structure, function, and biosynthesis of plant cell wall pectic polysaccharides. Carbohydr. Res. 344:1879–1900. doi: 10.1016/j.carres.2009.05.021.

Caño-Delgado A, Penfield S, Smith C, Catley M, Bevan M (2003) Reduced cellulose synthesis invokes lignification and defense responses in *Arabidopsis thaliana*. Plant J 34:351-62. doi: 10.1046/j.1365-313X.2003.01729.x.

Carpita NC, Gibeaut DM (1993) Structural models of primary cell walls in flowering plants: consistency of molecular structure with the physical properties of the walls during growth. Plant J 3:1-30. doi: 10.1111/j.1365-313X.1993.tb00007.x.

Carpita N, McCann M (2000) The cell wall. In Biochemistry and Molecular Biology of Plants (Buchanan BB, Gruissem W, Jones RL, eds). Rockville, MD: American Society of Plant Physiologists, pp. 52–108.

Castro AJ, Carapito C, Zorn N, Magné C, Leize E, et al. (2005) Proteomic analysis of grapevine (*Vitis vinifera* L.) tissues subjected to herbicide stress. J Exp Bot 56:2783–2795. doi: 10.1093/jxb/eri271.

Catalá C, Rose JKC, Bennett A (1997) Auxin regulation and spatial localization of an endo-1,4-β-D-glucanase and a xyloglucan endotransglycosylase in expanding tomato hypocotyls. Plant J 12:417-426. doi: 10.1046/j.1365-313X.1997.12020417.x.

Chapin ES, Walter CHS, Clarkson DT (1988) Growth response of barley and tomato to nitrogen stress and its control by abscisic acid, water relations and photosynthesis. Planta 173:352–366.

Chazen O, Hartung W, Neumann PM (1995) The different effects of PEG 6000 and NaCl on leaf development are associated with differential inhibition of root water transport. Plant Cell Environ 18:727–735.

Choi D, Cho HT, Lee Y (2006) Expansins: expanding importance in plant growth and development. Physiol Plantarum 126:511-518. doi: 10.1111/j.1399-3054.2006.00612.x.

Coenen GJ, Bakx EJ, Verhoef RP, Schols HA, Voragen AGJ (2007) Identification of the connecting linkage between homo- or xylogalacturonan and rhamnogalacturonan type I. Carbohydrate Polym 70:224-235. doi:10.1016/j.carbpol.2007.04.007.

Cosgrove DJ (1999) Enzymes and other agents that enhance cell wall extensibility. Annu Rev Plant Physiol Plant Mol Biol 50:391–417. doi: 10.1146/annurev.arplant.50.1.391.

Cosgrove DJ (2000) Loosening of plant cell walls by expansins. Nature 407:321–326. doi: 10.1038/35030000.

Cosgrove DJ (2005) Growth of the plant cell wall. Nat Rev Mol Cell Biol 6:850–861. doi:10.1038/nrm1746.

Cosgrove DJ, Jarvis MC (2012) Comparative structure and biomechanics of plant primary and secondary cell walls. Front Plant Sci 3:204. doi: 10.3389/fpls.2012.00204.

Delmer DP (1999) Cellulose biosynthesis: exciting times for a difficult field of study. Annu Rev Plant Physiol Plant Mol. Biol 50:245–276.

Deluc LG, Grimplet J, Wheatley MD, Tillett RL, Quilici DR, Osborne C, Schooley DA, Schlauch KA, Cushman JC, Cramer GR (2007) Transcriptomic and metabolite analyses of Cabernet Sauvignon grape berry development. BMC Genom 8:429. doi:10.1186/1471-2164-8-429.

Desprez T, Juraniec M, Crowell EF, Jouy H, Pochylova Z, Parcy F, Höfte H, Gonneau M, Vernhettes S (2007) Organization of cellulose synthase complexes involved in primary cell wall synthesis in *Arabidopsis thaliana*. Proc Natl Acad Sci USA 104:15572–15577. doi: 10.1073/pnas.0706569104.

Di Matteo A, Giovane A, Raiola A, Camardella L, Bonivento D, De Lorenzo G, Cervone F, Bellincampi D, Tsernoglou D (2005) Structural basis for the interaction between pectin methylesterase and a specific inhibitor protein. Plant Cell 17:849-858. doi: 10.1105/tpc.104.028886.

Dick-Perez M, Zhang Y, Hayes J, Salazar A, Zabotina OA, Hong M (2011) Structure and interactions of plant cell-wall polysaccharides by two- and three-dimensional magicangle-spinning solid-state NMR. Biochemistry 50: 989-1000. doi: 10.1021/bi101795q.

Doblin MS, Pettolino F, Bacic A (2010) Plant cell walls: the skeleton of the plant world. Funct Plant Biol 37:357–381. doi: http://dx.doi.org/10.1071/FP09279

Doco T, Williams P, Pauly M, O'Neill MA, Pellerin P (2003) Polysaccharides from grape berry cell walls. Part II. Structural characterization of the xyloglucan polysaccharides. Carbohydrate Polym 53:253-261. doi:10.1016/S0144-8617(03)00072-9.

Donaldson LA (2001) Lignification and lignin topochemistry - an ultrastructural view. Phytochemistry 57:859-873. doi:10.1016/S0031-9422(01)00049-8.

Eklöf JM, Brumer H (2010) The XTH gene family: an update on enzyme structure, function, and phylogeny in xyloglucan remodeling. Plant Physiol 153:456–466. doi: 10.1104/pp.110.156844.

Fernandes AN, Thomas LH, Altaner CM, Callow P, Forsyth VT, Apperley DC, Kennedy CJ, Jarvis MC (2011) Nanostructure of cellulose microfibrils in spruce wood. Proc Natl Acad Sci USA 108:1195–1203. doi: 10.1073/pnas.1108942108

Fernandes J, Tavares S, Amâncio S (2009) Identification and exprexssion of cytokinin signaling and meristem identity genes in sulfur deficient grapevine (*Vitis vinifera* L.). Plant Signal Behav 4:1128–1135.

Freshour G, Clay RP, Fuller MS, Albersheim P, Darvill AG, Hahn MG (1996) Developmental and tissue–specific structural alterations of the cell–wall polysaccharides of *Arabidopsis thaliana* roots. Plant Physiol 110:1413-1429.

Fry SC, Smith RC, Renwick KF, Martin DJ, Hodge SK, Matthews KJ (1992) Xyloglucan endotransglycosylase, a new wall-loosening enzyme-activity from plants. Biochem J 282:821-828.

Giribaldi M, Perugini I, Sauvage F-X, Schubert A (2007) Analysis of protein changes during grape berry ripening by 2-DE and Maldi-Tof. Proteomics 7:3154–3170. doi: 10.1002/pmic.200600974.

Giribaldi M, Giuffrida MG (2010) Heard it through the grapevine: proteomic perspective on grape and wine. J Proteomics 73:1647-55. doi: 10.1016/j.jprot.2010.05.002.

Glass M, Barkwill S, Unda F, Mansfield SD (2015) Endo-β-1,4-glucanases impact plant cell wall development by influencing cellulose crystallization. J Integr Plant Biol 57:396-410. doi: 10.1111/jipb.12353.

Goulao LF, Santos J, de Sousa I, Oliveira CM (2007) Patterns of enzymatic activity of cell wall-modifying enzymes during growth and ripening of apples. Postharvest Biol Technol 43:307-318. doi:10.1016/j.postharvbio.2006.10.002.

Goulao LF, Cosgrove DJ, Oliveira CM (2008) Cloning, characterisation and expression analyses of cDNA clones encoding cell wall-modifying enzymes isolated from ripe apples. Postharvest Biol Technol 48:37-51.

Goulao LF (2010) Pectin de–esterification and fruit softening: revisiting a classical hypothesis. Stewart Postharvest Rev 6:1-12.

Goulao LF, Vieira-Silva S, Jackson PA (2011) Association of hemicellulose- and pectin-modifying gene expression with Eucalyptus globulus secondary growth. Plant Physiol Biochem 49:873-381. doi: 10.1016/j.plaphy.2011.02.020.

Guo W, Zhang L, Zhao J, Liao H, Zhuang C, Yan X (2008) Identification of temporally and spatially phosphate–starvation responsive genes in Glycine max. Plant Sci 175:574–584. doi:10.1016/j.plantsci.2008.06.007.

Grimplet J, Deluc L, Tillett R, Wheatley M, Schlauch K, Cramer G, Cushman J (2007) Tissue-specific mRNA expression profiling in grape berry tissues. BMC Genom 8:187. doi:10.1186/1471-2164-8-187.

Grimplet J, Van Hemert J, Carbonell-Bejerano P, Díaz-Riquelme J, Dickerson J, Fennell A, Pezzotti M, Martínez-Zapater JM (2012) Comparative analysis of grapevine whole-genome gene predictions, functional annotation, categorization and integration of the predicted gene sequences. BMC Res Notes 5:213. doi: 10.1186/1756-0500-5-213.

Hall A, Jones G.V. (2009) Effect of potential atmospheric warming on temperature-based indices describing Australian winegrape growing conditions. Aust J Grape Wine Res 15:97–119. doi: 10.1111/j.1755-0238.2008.00035.x

Hamant O, Traas J (2010) The mechanics behind plant development. New Phytol 185:369–385. doi: 10.1111/j.1469-8137.2009.03100.x.

Hanlin RL, Hrmova M, Harbertson JF, Downey MO (2010) Condensed tannin and grape cell wall interactions and their impact on tannin extractability into wine. Aust J Grape Wine Res 16:173-188. doi: 10.1111/j.1755-0238.2009.00068.x.

Hardie WJ, O'Brien TP, Jaudzems VG (1996) Morphology, anatomy and development of the pericarp after anthesis in grape, *Vitis vinifera* L. Aust J Grape Wine Res 2:97-142. doi: 10.1111/j.1755-0238.1996.tb00101.x.

Hilz H (2007) Characterisation of cell wall polysaccharides in bilberries and black currants. PhD Thesis, U. Wageningeng: Wageningen, NL; pp. 158

Huang X-M, Huang H-B, Wang H-C (2005) Cell walls of loosening skin in post-veraison grape berries lose structural polysaccharides and calcium while accumulate structural proteins. Sci Hortic 104:249-263.

Iraki NM, Bressan RA, Hasegawa PM, Carpita NC (1989) Alteration of the physical and chemical structure of the primary cell wall of growth–limited plant cells adapted to osmotic stress. Plant Physiol 91:39–47.

Ishii T, Matsunaga T, Pellerin P, O'Neill MA, Darvill A, Albersheim P (1999) The plant cell wall polysaccharide rhamnogalacturonan II self-assembles into a covalently cross-linked dimer. J Biol Chem 274:13098-13104.

Ishimaru M, Kobayashi S (2002) Expression of a xyloglucan endo-transglycosylase gene is closely related to grape berry softening. Plant Sci 162:621-628.

Ishimaru M, Smith DL, Gross KC, Kobayashi S (2007) Expression of three expansin genes during development and maturation of Kyoho grape berries. J Plant Physiol 164:1675-1682.

Jaillon O, Aury J-M, Noel B, Policriti A, Clepet C, Casagrande A, Choisne N, Aubourg S, Vitulo N, Jubin C, et al. (2007) The grapevine genome sequence

suggests ancestral hexaploidization in major angiosperm phyla. Nature 449:463-467.

Jarvis MC (2013) Cellulose Biosynthesis: Counting the Chains. Plant Physiol 163:1485–1486.

Jellouli N, Jouira BH, Skouri H, Ghorbel A, Gourgouri A, et al. (2008) Proteomic analysis of Tunisian grapevine cultivar Razegui under salt stress. J Plant Physiol 165:471–481.

Jolie RP, Duvetter T, Van Loey AM, Hendrickx ME (2010) Pectin methylesterase and its proteinaceous inhibitor: a review. Carbohydr Res 345:2583-95. doi: 10.1016/j.carres.2010.10.002.

Juge N (2006) Plant protein inhibitors of cell wall degrading enzymes. Trends Plant Sci 11: 359–367. doi: 10.1016/j.tplants.2006.05.006.

Kennedy JA, Hayasaka Y, Vidal S, Waters EJ, Jones GP (2001) Composition of grape skin proanthocyanidins at different stages of berry development. J Agric Food Chem 49:5348-5355.

Kobayashi M, Nakagawa H, Asaka T, Matoh T (1999) Borate-rhamnogalacturonan II bonding reinforced by Ca^{2+} retains pectic polysaccharides in higher-plant cell walls. Plant Physiol 119:199-204.

Lecas M, Brillouet JM (1994) Cell-Wall composition of grape berry skins. Phytochemistry 35:1241-1243.

Lee CY and Bourne M (1980) Changes in grape firmness during maturation. J Texture Stud 11:163–171.

Letaief H, Rolle L, Zeppa G, Gerbi V (2008) Assessment of grape skin hardness by a puncture test. J Sci Food Agric 88:1567–1575.

Liepman AH, Cavalier DM, Lerouxel O, Keegstra K (2007) Cell wall structure, biosynthesis and assembly. In Plant Cell Separation and Adhesion, Roberts J.A. and Gonzalez-Carranza Z, eds (Oxford: Blackwell Publishing), pp. 8-39

Liners F, Letesson J–J, Didembourg C, Van Cutsem P (1989). Monoclonal antibodies against pectin. Recognition of a conformation induced by calcium. Plant Physiol 91:1419-1424.

Matsui A, Yokoyama R, Seki M, Ito T, Shinozaki K, Takahashi T, Komeda Y, Nishitani K (2005) AtXTH27 plays an essential role in cell wall modification during the development of tracheary elements. Plant J 42:525-534. doi: 10.1111/j.1365-313X.2005.02395.x.

McCann MC, Carpita NC (2008) Designing the deconstruction of plant cell walls. Curr Opin Plant Biol 11:314-20. doi: 10.1016/j.pbi.2008.04.001.

McFarlane HE, Döring A, Persson S (2014) The cell biology of cellulose synthesis. Annu Rev Plant Biol 65:69-94. doi: 10.1146/annurev-arplant-050213-040240.

McDonald AJS (1989) Nitrate availability and shoot area development in small willow (Salix vinimalis). Plant Cell Environ 12:417–424.

McNeil M, Darvill AG, Fry SC, Albersheim P (1984) Structure and function of the primary cell walls of plants. Annu Rev Biochem 53:652-683.

Miedes E, Herbers K, Sonnewald U, Lorences EP (2010) Overexpression of a cell wall enzyme reduces xyloglucan depolymerization and softening of transgenic tomato fruits. J Agric Food Chem 58:5708–5713. doi: 10.1021/jf100242z.

Mueller SC, Brown RM Jr (1980) Evidence for an intramembrane component associated with a cellulose microfibril-synthesizing complex in higher plants. J Cell Biol 84:315-26.

McQueen-Mason S, Durachko DM, Cosgrove DJ (1992) Two endogenous proteins that induce cell wall extension in plants. Plant Cell 4:1425-33. doi: http://dx.doi.org/10.1105/tpc.4.11.1425.

McQueen-Mason SJ, Cosgrove DJ (1995) Expansin mode of action on cell walls. Analysis of wall hydrolysis, stress relaxation and binding. Plant Physiol 107:87-100. doi: http://dx.doi.org/10.1104/pp.107.1.87.

Mélida H, García–Angulo P, Alonso–Simón A, Encina A, Alvarez J, Acebes JL (2009) Novel type II cell wall architecture in dichlobenil–habituated maize calluses. Planta 229:617–631.

Nicol F, His I, Jauneau A, Vernhettes S, Canut H, and Höfte H (1998) A plasma membrane-bound putative endo-1,4-beta-D-glucanase is required for normal wall

assembly and cell elongation in *Arabidopsis*. EMBO J 17:5563–5576. doi: 10.1093/emboj/17.19.5563.

Nishitani KT, Tominaga R (1992) Endo-xyloglucan transferase, a novel class of glycosyltransferase that catalyses transfer of a segment of xyloglucan molecule to another xyloglucan molecule. J Biol Chem 267:21058–21064.

Nishitani K, Vissenberg K (2007) Roles of the XTH family in the expanding cell. In: Verbelen JP, Vissenberg K, Eds. The expanding cell. Plant Cell Monographs. Vol. 5. Berlin: Springer. p. 89-116.

Nunan KJ, Sims IM, Bacic A, Robinson SP, Fincher GB (1997) Isolation and characterization of cell walls from the mesocarp of mature grape berries (*Vitis vinifera*). Planta 203:93-100.

Nunan KJ, Sims IM, Bacic A, Robinson SP, Fincher GB (1998) Changes in cell wall composition during ripening of grape berries. Plant Physiol 118:783–792.

Nunan K, Davies C, Robinson S, Fincher G (2001) Expression patterns of cell wall-modifying enzymes during grape berry development. Planta 214:257-264.

O'Neill MA, Ishi T, Albersheim P, Darvill AG (2004) Rhamnogalacturonan II: structure and function of a borate cross-linked cell wall pectic polysaccharide. Annu Rev Plant Biol 55:109-39.

Ortega-Regules A, Ros-García JM, Bautista-Ortín AB, López-Roca JM, Gómez-Plaza E (2008) Changes in skin cell wall composition during the maturation of four premium wine grape varieties. J Sci Food Agric 88:420–428.

Osato Y, Yokoyama R, Nishitani K (2006) A principal role for AtXTH18 in *Arabidopsis thaliana* root growth – a functional analysis using RNAi plants. J Plant Res 119:153–162. doi: 10.1007/s10265-006-0262-6

Palmer SJ, Berridge DM, McDonald AJS, Davies WJ (1996) Control of leaf expansion in sunflower (Helianthus annuus L.) by nitrogen nutrition. J Exp Bot 47:359–368.

Paniagua C, Posé S, Morris VJ, Kirby AR, Quesada MA, Mercado JÁ (2014) Fruit softening and pectin disassembly: an overview of nanostructural pectin modifications assessed by atomic force microscopy. Ann Bot 114:1375-83. doi: 10.1093/aob/mcu149.

Park YB, Cosgrove DJ (2012) A revised architecture of primary cell walls based on biomechanical changes induced by substrate-specific endoglucanases. Plant Physiol 158:1933-1943. doi: 10.1104/pp.111.192880

Park YB, Cosgrove DJ (2015) Xyloglucan and its interactions with other components of the growing cell wall. Plant Cell Physiol 56:180-94. doi: 10.1093/pcp/pcu204.

Patakas A (2012) Abiotic stress–induced morphological and anatomical changes in plants. in Ahmad P and. Prasad M.N.V (Eds.), Abiotic stress responses in plants metabolism, productivity and sustainability New York, Springer pp. 21–40.

Pear JR, Kawagoe Y, Schreckengost WE, Delmer DP, Stalker DM (1996) Higher plants contain homologs of the bacterial celA gene enconding the catalytic subunit of cellulose synthase. Proc Natl Acad USA 93:12637-12642.

Peaucelle A, Louvet R, Johansen JN, Hofte H, Laufs P, Pelloux J, Mouille G (2008) *Arabidopsis* phyllotaxis is controlled by the methyl-esterification status of cell-wall pectins. Curr Biol 18:1943-1948. doi: 10.1016/j.cub.2008.10.065.

Peaucelle A, Braybrook S, Hofte H (2012) Cell wall mechanics and growth control in plants: the role of pectins revisited. Front Plant Sci 3:121. doi: 10.3389/fpls.2012.00121.

Persson S, Paredez A, Carroll A, Palsdottir H, Doblin M, Poindexter P, Khitrov N, Auer M, Somerville CR (2007) Genetic evidence for three unique components in primary cell-wall cellulose synthase complexes in *Arabidopsis*. Proc Natl Acad Sci USA 104:15566-71. doi: 10.1073/pnas.0706592104.

Pilati S, Perazzolli M, Malossini A, Cestaro A, Dematte L, Fontana P, Dal Ri A, Viola R, Velasco R, Moser C (2007) Genome-wide transcriptional analysis of grapevine berry ripening reveals a set of genes similarly modulated during three seasons and the occurrence of an oxidative burst at vèraison. BMC Genom 8:428. doi:10.1186/1471-2164-8-428.

Pinelo M, Arnous A, Meyer AS (2006) Upgrading of grape skins: Significance of plant cell-wall structural components and extraction techniques for phenol release. Trends Food Sci Technol 17:579-590. doi:10.1016/j.tifs.2006.05.003

Porro D, Ramponi M, Tomasi T, Rolle L, Poni S (2010) Nutritional implications of water stress in grapevine and modifications of mechanical properties of berries. Acta Hort 868:73–80.

Potters G, Pasternak TP, Guisez Y, Palme KJ, Jansen MA (2007) Stress–induced morphogenic responses: growing out of trouble? Trends Plant Sci 12:98-105. doi:10.1016/j.tplants.2007.01.004.

Radin JW, Boyer JS (1982) Control of leaf expansion by nitrogen nutrition in sunfiower plants: Role of hydraulic conductivity and turgor. Plant Physiol 69:771–775. doi: http://dx.doi.org/10.1104/pp.69.4.771.

Radin JW, Eidenbock MP (1984) Hydraulic conductance as a factor limiting leaf expansion of phosphorus deficient cotton plants. Plant Physiol 75:372–377. doi: http://dx.doi.org/10.1104/pp.75.2.372

Reiter WD (2002) Biosynthesis and properties of the plant cell wall. Curr Opin Plant Biol 5:536-42. doi:10.1016/S1369-5266(02)00306-0.

Ribéreau-Gayon P, Glories Y, Maujean A, Dubourdieu D (2003) Compuestos fenólicos en Tratado de Enología. In Química del vino. Estabilización y tratamientos. Vol. 2. Ed. Hemisferio Sur, Buenos Aires.

Ridley BL, O'Neill MA, Mohnen D (2001) Pectins: structure, biosynthesis, and oligogalacturonide-related signaling. Phytochem 57:929-967. doi:10.1016/S0031-9422(01)00113-3.

Río Segade S, Vázquez ES, Orriols I, Giacosa S, Rolle L (2011) Possible use of texture characteristics of winegrapes as markers for zoning and their relationship with anthocyanin extractability index. Int J Food Sci Technol 46:386–394. doi: 10.1111/j.1365-2621.2010.02489.x.

Ro DK, Mah N, Ellis BE, Douglas CJ (2001) Functional characterization and subcellular localization of poplar (*Populus trichocarpa* × *Populus deltoides*) cinnamate 4-hydroxylase. Plant Physiol 126:317–329. doi: http://dx.doi.org/10.1104/pp.126.1.317.

Rolle L, Giacosa S, Gerbi V, Novello V (2011) Comparative study of texture properties, color characteristics, and chemical composition of ten white table-grape varieties. Am J Enol Vitic 62:49-56. doi: 10.5344/ajev.2010.10029.

Rose JKC, Braam J, Fry SC, Nishitani K (2002) The XTH family of enzymes involved in xyloglucan endotransglucosylation and endohydrolysis: Current perspectives and a new unifying nomenclature. Plant Cell Physiol 43:1421-1435. doi: 10.1093/pcp/pcf171.

Sarry J-E, Sommerer N, Sauvage F-X, Bergoin A, Rossignol M, et al. (2004) Grape berry biochemistry revisited upon proteomic analysis of the mesocarp. Proteomics 4:201–215. DOI 10.1002/pmic.200300499.

Sato S, Kato T, Kakegawa K, Ishii T, Liu YG, Awano T, Takabe K, Nishiyama Y, Kuga S, Sato S, Nakamura Y, Tabata S, Shibata D (2001) Role of the putative membrane–bound endo-1,4–beta–glucanase KORRIGAN in cell elongation and cellulose synthesis in *Arabidopsis thaliana*. Plant Cell Physiol 42:251–63.

Saulnier L, Brillouet JM (1989) An arabinogalactan protein from the pulp of grape berries. Carbohyd Res 188:137-144.

Saulnier L, Thibault J-F (1987) Enzymic degradation of isolated pectic substances and cell wall from pulp of grape berries. Carbohydrate Polym 7:345-360.

Scheible W-R, Eshed R, Richmond T, Delmer D, Somerville C (2001). Modifications of cellulose synthase confer resistance to isoxaben and thiazolidinone herbicides in *Arabidopsis* Ixr1 mutants. Proc Natl Acad Sci USA 98:10079–10084. doi: 10.1073/pnas.191361598.

Schlosser J, Olsson N, Weis M, Reid K, Peng F, Lund S, Bowen P (2008) Cellular expansion and gene expression in the developing grape (*Vitis vinifera* L.). Protoplasma 232:255-265. doi: 10.1007/s00709-008-0280-9.

Seifert GJ, Blaukopf C (2010) Irritable walls: the plant extracellular matrix and signaling. Plant Physiol 153: 467–478. doi: http://dx.doi.org/10.1104/pp.110.153940.

Shedletzky E, Shmuel M, Trainin T, Kalman S, Delmer D (1992) Cell wall structure in cells adapted to growth on the cellulose–synthesis inhibitor 2,6–Dichlorobenzonitrile : A comparison between Two Dicotyledonous Plants and a Graminaceous Monocot. Plant Physiol 100:120-130.

Snir N, Neumann PM (1997) Mineral nutrient supply, cell wall adjustment and the control of leaf growth. Plant Cell Environ 20:239–246.

Somerville C (2006) Cellulose synthesis in higher plants. Annu Rev Cell Dev Biol 22:53–78. doi: 10.1146/annurev.cellbio.22.022206.160206.

Stewart JJ, Akiyama T, Chapple C, Ralph J, Mansfield SD (2009) The effects on lignin structure of overexpression of ferulate 5-hydroxylase in hybrid poplar. Plant Physiol 150:621-35. doi: http://dx.doi.org/10.1104/pp.109.137059.

Takahashi H, Braby CE, Grossman AR (2001) Sulfur economy and cell wall biosynthesis during sulfur limitation of *Chlamydomonas reinhardtii*. Plant Physiol 127:665–673. doi: http://dx.doi.org/10.1104/pp.010257.

Takeda T, Furuta Y, Awano T, Mizuno K, Mitsuishi Y, Hayashi T (2002) Suppression and acceleration of cell elongation by integration of xyloglucans in pea stem segments. Proc Natl Acad Sci USA 99:9055-60. doi: 10.1073/pnas.132080299.

Taylor G, McDonald AJS, Stadenberg I, Ereer Smith PH (1993) Nitrate supply and the biophysics of leaf growth in Salix viminalis. J Exp Bot 44:155- 64.

Thibault J-F, Renard CMGC, Axelos MAV, Roger P, Crépeau M-J (1993) Studies of the length of homogalacturonic regions in pectins by acid hydrolysis Carbohydrate Res 238:271-286.

Tschoep H, Gibon Y, Carillo P, Armengaud P, Szecowka M, Nunes–Nesi A, Fernie AR, Koehl K, Stitt M (2009) Adjustment of growth and central metabolism to a mild but sustained nitrogen limitation in *Arabidopsis*. Plant Cell Environ 32:300–318. doi: 10.1111/j.1365-3040.2008.01921.x.

Urbanowicz BR, Bennett AB, del Campillo E, Catalá C, Hayashi T, Henrissat B, Höfte H, McQueen-Mason SJ, Patterson SE, Shoseyov O, Teeri TT, Rose JK (2007) Structural organization and a standardized nomenclature for plant endo-1,4-beta-glucanases (cellulases) of glycosyl hydrolase family 9. Plant Physiol 144:1693-6. doi: http://dx.doi.org/10.1104/pp.107.102574.

Vanholme R, Morreel K, Ralph J, Boerjan W (2008) Lignin engineering. Curr Op Plant Biol 11:278-285. doi:10.1016/j.pbi.2008.03.005.

Vanholme R, Demedts B, Morreel K, Ralph J, Boerjan W (2010) Lignin Biosynthesis and Structure. Plant Physiol 153:895-905. doi: http://dx.doi.org/10.1104/pp.110.155119.

Vicens A, Fournand D, Williams P, Sidhoum L, Moutounet M, Doco T (2009) Changes in polysaccharide and protein composition of cell walls in grape berry skin (Cv. Shiraz) during ripening and over-ripening. J Agr Food Chem 57:2955-2960. doi: 10.1021/jf803416w.

Vincent D, Ergul A, Bohlman MC, Tattersall EA, Tillett RL, et al. (2007) Proteomic analysis reveals differences between *Vitis vinifera* L. cv. Chardonnay and cv. Cabernet Sauvignon and their responses to water deficit and salinity. J Exp Bot 58:1873–1892. doi: 10.1093/jxb/erm012.

Vidal S, Williams P, O'Neill MA, Pellerin P (2001) Polysaccharides from grape berry cell walls. Part I: tissue distribution and structural characterization of the pectic polysaccharides. Carbohydrate Polym 45:315-323. doi:10.1016/S0144-8617(00)00285-X.

Vincken J, Schols HA, Oomen RJ, McCann MC, Ulvskov P, Voragen AG, Visser RG (2003) If homogalacturonan were a side chain of rhamnogalacturonan I. implications for cell wall architecture. Plant Physiol 132:1781-1789.

Vissenberg K, Martinez-Vilchez IM, Verbelen J-P, Miller JG, Fry SC (2000) In vivo co-localization of xyloglucan endotransglycosylase activity and its donor substrate in the elongation zone of *Arabidopsis* roots. P Cell 12:1229-1238.

Vissenberg K, Fry SC, Verbelen J-P (2001) Root hair initiation is coupled to a highly localized increase of xyloglucan endotransglycoslyase action in *Arabidopsis* roots. Plant Physiol127:1125-1135.

Velasco R, Zharkikh A, et al. (2007) A high quality draft consensus sequence of the genome of a heterozygous grapevine variety. PLoS One 2: e1326. doi: 10.1371/journal.pone.0001326.

Volonec JJ, Nelson CJ (1983) Responses of tall fescue leaf meristems to N fertilization and harvest frequency. Crop Science 23: 720-724.

Voragen AGJ, Pilnik W, Thibault J-F, Axelos MAV, Renard CMGC (1995) Pectins. In Food polysaccharides and their applications, Stephen, A.M., Ed.; Marcel Dekker: New York, pp 287–339.

Voragen A, Coenen G-J, Verhoef R, Schols H (2009) Pectin, a versatile polysaccharide present in plant cell walls. Struct Chem 20:263-275.

Wakabayashi K, Soga K, Kamisaka S, Hoson T (2003) Modification of cell wall architecture of wheat coleoptiles grown under hypergravity conditions. Biol Sci Space 17:228-9.

Wang T, Zabotina O, Hong M (2012) Pectin–cellulose interactions in the *Arabidopsis* primary cell wall from two-dimensional magic-angle-spinning solid-state nuclear magnetic resonance. Biochemistry 51:9846–9856. doi: 10.1021/bi3015532.

Wang T, Park YB, Caporini MA, Rosay M, Zhong L, Cosgrove DJ, Hong M (2013) Sensitivity-enhanced solid-state NMR detection of expansin's target in plant cell walls. Proc Natl Acad Sci USA 110:16444–16449. doi: 10.1073/pnas.1316290110.

Willats WG, McCartney L, Mackie W, Knox JP (2001) Pectin: cell biology and prospects for functional analysis. Plant Mol Biol 47:9–27.

Whitney SEC, Gidley MJ, McQueen-Mason SJ (2000) Probing expansin action using cellulose/hemicellulose composites. Plant J 22:327–334. doi: 10.1046/j.1365-313x.2000.00742.x.

Wolf S, Hématy K, Höfte H (2012) Growth control and cell wall signaling in plants. Annu Rev Plant Biol 63:381-407. doi: 10.1146/annurev-arplant-042811-105449.

Zenoni S, Ferrarini A, Giacomelli E, Xumerle L, Fasoli M, Malerba G, Bellin D, Pezzotti M, Delledonne M (2010) Characterization of transcriptional complexity during berry development in *Vitis vinifera* using RNA-Seq. Plant Physiol 152:1787-95. doi: 10.1104/pp.109.149716.

Zhang DP, Li M, Wang Y (1997) Ultrastructural changes in the mesocarp cells of grape berry during its development. Acta Botanica Sinica 39:389–396.

Zuo J, Niu QW, Nishizawa N, Wu Y, Kost B, Chua NH (2000) KORRIGAN, an *Arabidopsis* endo-1,4-beta-glucanase, localizes to the cell plate by polarized targeting and is essential for cytokinesis. Plant Cell 12:1137-52.

Zykwinska A, Thibault J-F, Ralet M-C (2007) Organization of pectic arabinan and galactan side chains in association with cellulose microfibrils in primary cell walls and related models envisaged. J Expl Bot 58:1795–1802. doi: 10.1093/jxb/erm037.

Zykwinska A, Thibault JF, Ralet MC (2008) Competitive binding of pectin and xyloglucan with primary cell wall cellulose. Carbohydr Polym 74:957–961. doi:10.1016/j.carbpol.2008.05.004.

Chapter 2

Mineral stress affects the cell wall composition and structure of grapevine (*Vitis vinifera* L.) *callus*

João C. Fernandes[1], Penélope García–Angulo[2], Luis F. Goulao[3], José L. Acebes[2] and Sara Amâncio[1]

[1] DRAT/CBAA, Instituto Superior de Agronomia, Universidade Técnica de Lisboa, Tapada da Ajuda, 1349–017 Lisbon, Portugal.

[2] Departamento de Biología Vegetal. Área de Fisiología Vegetal, Universidad de León, E–24071, León, Spain

[3] Eco–Bio/BIOTROP – Instituto de Investigacao Cientifica Tropical (IICT, IP), Av. da Republica, 2784–505 Oeiras, Portugal.

Published in Plant Science (2013, 205–206:111–120. doi: 10.1016/j.plantsci.2013.01.013)

2. Mineral stress affects the cell wall composition and structure of grapevine (*Vitis vinifera* L.) *callus*

João C. Fernandes, Penélope García–Angulo, Luis F. Goulao, José L. Acebes and Sara Amâncio

Abstract

Grapevine (*Vitis vinifera* L.) is one of the most economically important fruit crops in the world. Deficit in nitrogen, phosphorus and sulfur nutrition impairs essential metabolic pathways. The influence of mineral stress in the composition of the plant cell wall (CW) has received residual attention. Using grapevine callus as a model system, 6-weeks deficiency of those elements caused a significant decrease in growth. Callus CWs were analyzed by Fourier transform infrared spectroscopy (FT-IR), by quantification of CW components and by immunolocalization of CW epitopes with monoclonal antibodies. PCA analysis of FT-IR data suggested changes in the main components of the CW in response to individual mineral stress. Decreased cellulose, modifications in pectin methyl esterification and increase of structural proteins were among the events disclosed by FT-IR analysis. Chemical analyses supported some of the assumptions and further disclosed an increase in lignin content under nitrogen deficiency, suggesting a compensation of cellulose by lignin. Moreover, polysaccharides of callus under mineral deficiency showed to be more tightly bonded to the CW, probably due to a more extensive cross-linking of the cellulose-hemicellulose network. Our work showed that mineral stress impacts the CW at different extents according to the withdrawn mineral element, and that the modifications in a given CW component are compensated by the synthesis and/or alternative linking between polymers. The overall results here described for the first time pinpoint the CW of *Vitis* callus different strategies to overcome mineral stress, depending on how essential they are to cell growth and plant development.

Keywords: *Cellulose; FT-IR; Lignin; Mineral Stress; Pectin*

Abbreviations

2.4–D	2,4–dichlorophenoxy–acetic acid
CDTA	Cyclohexane–*trans*-1.2–diamine–*N*,*N*,*N′*,*N′*–tetraacetic acid sodium salt
CW	Cell Wall
FT–IR	Fourier–Transform Infrared
GC	Gas chromatography
HRP	Horseradish peroxidase
-N	Nitrogen deficient callus
-P	Phophorus deficient callus
PBS	Phosphate buffered saline
PCA	Principal Component analysis
PVP–40T	Polyvinylpyrrolidon
RG–I	Rhamnogalacturonan–I
-S	Sulfur deficient callus
SD	Standard deviation
TFA	Trifluoroacetic acid

2.1. Introduction

The structural and mechanical support of plants is provided by cell walls (CW), which are load–bearing, extensible viscoelastic structures that surround the cells, acting as an “exoskeleton". The CW plays a vital role in the regulation of the rate and direction of growth and the morphology of plant cells and organs (Fry 1986; Brett and Waldron 1996). The plant CW is a dynamic complex with further functions such as control of the diffusion through the apoplast, signaling, regulation of cell–to–cell interactions, reserve storage of carbohydrates, or protection against biotic (Vorwerk et al. 2004) and abiotic stress agents (Zhong and Ye 2007).

In the primary CW, cellulose is the main load–bearing polysaccharide which interlinks with cross–linking matrix glycans, predominantly xyloglucan in dicots (Carpita and Gibeaut, 1993), to form an extensive framework that provides most of the tensile strength to the CW matrix. This network is embedded in a surrounding phase constituted by pectic polysaccharides, forming hydrophilic gels that determine the regulation of the hydration status and ion transport, the definition of the porosity, stiffness and control of the wall permeability (Willats et al. 2001). These features are, in turn, defined by the chemical structure of pectic polysaccharides, particularly the branching degree and pattern, the decoration with neutral sugars and the degree and pattern of acetyl– and methyl–esterification, which can lead to either stiffening or loosening of the CW (reviewed in Goulao 2010). The occurrence of micro–domains inside the pectic polysaccharides means the localization of precise areas with distinct properties, providing a highly fine–tuned regulation of the wall properties to cope with the cell functioning. In addition to polysaccharides, a third network composed by structural glycoproteins contributes to the biophysical properties of the primary CW and cell adhesion (Showalter 1993; Cosgrove 1997). In some tissues, after cell growth has ceased, a secondary CW is formed with higher cellulose content and a different organization of its deposition. After cellulose, lignin is the second most abundant plant polymer in vascular plants (Boerjan et al. 2003). In secondary CWs, lignin is deposited within the cellulose microfibrils establishing covalent bonds with carbohydrates, providing additional strength and rigidity that, along evolution, allowed plants to grow upward (Vanholme et al. 2008).

The most consensual dicot primary CW model has been the “tethered network”, a representation in which hemicellulose polymers link cellulose through hydrogen bonds to create a load bearing tether, inserted in an amorphous cement-like pectin matrix (reviewed in Cosgrove 2001). However, recent results disclosed the presence of covalent linkages between rhamnogalacturonan–I (RG–I)–arabinan side–chains and cellulose microfibrils (Zykwinska et al. 2005; 2007a,b) and covalent linkages between xyloglucan and pectins (Abdel–Massih et al. 2003; Cumming et al. 2005; Popper and Fry 2005; Marcus et al 2008) *in muro*, providing structural links between two major CW domains. Moreover, since not all of the cellulose microfibril surfaces are covered with xyloglucans and not all xyloglucans are adsorbed to cellulose (Bootten et al. 2004; Hanus and Mazeau 2008; Park and Cosgrove 2012), the existence of such other linkages within the CW is expected to maintain its structure.

During development, the fine structure of the plant CW matrix is extensively modified. The amount and composition of specific molecules and their arrangements differs among plants, organs, cell types and even in different micro–domains of the wall of a given individual cell (Freshour et al. 1996).

Localized changes in CW composition and structure also provide the cell with a notable ability to tolerate abiotic stresses, such as osmotic (Iraki et al. 1989) and chemical (Shedletzky et al. 1992; Mélida et al. 2009).

Deficiencies in mineral nutrition, particularly nitrogen (N), phosphorus (P), potassium (K) and sulfur (S), which are required in relatively large amounts by the plant, strongly affect the plant metabolism with subsequent impact on the plant growth, crop yield and in both nutritional and organoleptic quality of the agronomic product (Amtmann et al. 2009; Fernandes et al. 2009; Tschoep et al. 2009). Essential nutrients are major regulators of plant growth and development due to their involvement in primary metabolic pathways e.g. amino acid and nucleotide biosynthesis, protein phosphorylation or disulfide bonds between cysteine.

Plant development and anatomy are impacted by abiotic stresses and a common “stress–induced” set of responses have been reported: prompting of localized cell division, arrestment of cell elongation, and modifications in cell differentiation status (Patakas 2012; Potters et al. 2007).

Limited mineral nutrient availability has been reported to affect organ growth rates, through inhibition of the production of new cells and/or cell expansion (Palmer et al. 1996) via reduction of CW plasticity (Taylor et al. 1993; Snir and Neumann 1997). It has been proposed that known nutrient–induced stress act by modifying xylem tension which then signals the onset of CW rearrangements in growing tissues (Radin and Eidenbock 1984; Chapin et al. 1988). These components are determined by the dynamic regulatory properties of the CW. Nevertheless, and even though the importance of mineral nutrition in plant development has been widely recognized, only residual attention has been given to its influence on the CW dynamics. More recently, global transcriptomic studies involving nutrient depleted plants revealed differential regulation of CW–related genes and proteins in various species (Takahashi et al. 2001; Guo et al. 2008), emphasizing the CW role in survival response mechanisms.

Despite the grapevine (*Vitis vinifera* L.) economic value and scientific relevance as a model species, there is little information about the CW structure and polysaccharide composition in this species. Investigation has been mainly focused to the economic important organ, the fruit, both berry pulp and skin reviewed in Goulao et al. (2012).

The aim of the present work was to investigate the adaptive response of the CW to mineral depletion of individual major nutrients, nitrogen, phosphorus and sulfur, using *Vitis callus* as experimental model. Here, an integrated approach employing complementary methodologies was followed. Fourier–Transform Infrared (FT–IR) spectroscopy coupled with chemometrics was used to detect changes in CW polymers and putative cross–links (Alonso–Simón et al. 2004; Mouille et al. 2003) to retrieve the major candidate events occurring in the CW in response to the imposed conditions. Candidate events were further tested by chemical methods and immunochemical staining using monoclonal antibodies (Knox 2008) and through the determination of monosaccharide composition of fractionated CWs. The combined use of these methodologies allowed drafting a map of CW responses to specific changes in the mineral health in *Vitis callus*.

2.2. Material and methods

2.2.1. Cell culture and mineral stress imposition

Vitis vinifera cv Touriga Nacional *callus* tissue was maintained in the dark at 25ºC, as described in Jackson et al. (2001). Four and a half grams *of callus* tissue were used as initial explant in medium containing MS basal salts (Murashige and Skoog 1962, DuchefaBiochemie, Haarlem, NL) supplemented with 2.5 µM 2.4–D (2,4–dichlorophenoxy–acetic acid); 1 µM kinetin; 5 g l^{-1} PVP–40T; 20 g l^{-1}, sucrose; 2 g l^{-1} Gelrite®, pH 5.7. The *callus* were sub-cultured every three weeks. Four treatments were applied: full nutrients (control), nitrogen deficiency (–N), phosphorus deficiency (–P) and sulfur deficiency (–S). Commercial MS was used to obtain control samples while modified MS media in which nitrates, phosphates and sulfates were substituted for chlorides were considered –N, –P and –S respectively. *Callus* were sub–cultured to the respective medium after three weeks of growing. After each culture cycle in the respective treatment medium each sample, corresponding to 10 petri dishes (9cm Ø) containing four *callus* was collected to monitor growth. Based on the results obtained, six weeks grown *callus* (2X3 weeks) samples were used for CW analyses.

2.2.2. Cell wall isolation

Twenty gram *callus* samples were homogenized in liquid nitrogen using a mortar and pestle, washed with cold 100 mM potassium phosphate buffer pH 7.0 (2X), and treated overnight with 2.5 U ml^{-1} VI α–amylase from hog pancreas (Sigma–Aldrich Co., St. Louis) at 37ºC. The suspensions were centrifuged and the pellet was sequentially washed with distilled water (3X), acetone (3X), methanol:chloroform (1:1; v/v) (3X), diethylether (2X), and then air–dried (Talmadge et al. 1973).

2.2.3. FT–IR spectroscopy and multivariate analysis

FT-IR analysis was performed according to the methodology described in Alonso–Simón et al. (2004). Tablets for FT–IR spectroscopy were prepared in a Graseby–Specac Press, using 2 mg of total CW samples mixed with potassium

bromide (KBr) (1:100 w/w) from a minimum of 11 biological replicates per treatment. Spectra were obtained on a Perkin–Elmer System 2000 FT–IR at a resolution of 1 cm^{-1}. In order to tackle CW structure modifications, a window between 800 and 1800 cm^{-1}, which contains information of polysaccharide characteristic linkages, was selected for analysis. Normalization and baseline–correction were made using the Perkin–Elmer IR Data manager software and the data exported to Microsoft Excel for area normalization. Principal component analysis (PCA), using Pearson coefficient for distance estimation, was performed with a maximum of four principal components using the Statistica 6.0 software package (StatSoft, Inc., USA)

2.2.4. Cellulose quantification

Cellulose was quantified by the Updegraff (1969) method, using the hydrolytic conditions described by Saeman et al. (1963) and quantifying the glucose released by the anthrone method (Dische 1962).

2.2.5. Lignin quantification

Klason lignin was determined using the method described by Hatfield et al. (1994). Briefly, 60 mg of CW material was solubilized in 2 ml of 72% H_2S0_4 at 30°C for 60 min. The solution was diluted to 2.48% H_2S0_4 prior to secondary hydrolysis by autoclaving at 115°C for 60 min. The non–hydrolyzed residue was collected by filtration and dried at 60ºC. The results are expressed as µg lignin $(mg\ CW)^{-1}$.

2.2.6. Quantification of pectin methyl–esterification

The extent of esterification of pectins was assessed by quantification of the released methanol using the method described by Wood and Siddiqui (1971). To each 10 mg CW sample, 0.75 ml distillated water and 0.25 ml 1.5M NaOH were added. The samples were incubated at room temperature for 30 min, chilled on ice and added with 0.25 ml 4.5M H_2SO_4. After centrifugation, 0.5 ml of the supernatant was mixed with 0.5 ml 0.5M H_2SO_4, chilled on ice and 0.2 ml 2%

$KMnO_4$ (w/v) were added. The samples were allowed to stand in an ice bath for 15 min and added with 0.2 ml 0.5M sodium arsenite in 0.06M H_2SO_4. The samples were thoroughly mixed and left for 1 hour at room temperature. Finally, 2 ml acetylacetone–ammonium acetate reagent was added, tubes were vortexed, closed and heated to 59 ºC for 15 min. After cooling to room temperature, absorbance was read at 412 nm and the results were expressed as ml CH_3OH $(mg\ CW)^{-1}$, using methanol as standard.

2.2.7. Cell wall fractionation

CW fractionation was done according to Selvendran and O'Neill (1987) with minor modifications. Dried CW were extracted at room temperature with 50 mM cyclohexane–*trans*-1.2–diamine–*N*,*N*,*N′*,*N′*–tetraacetic acid sodium salt (CDTA) adjusted to pH 6.5 with KOH, for 8 h (2X), collected by centrifugation, washed with distilled water and the combined supernatants referred to as the CDTA–soluble fraction. The residue was incubated for 18 h with 0.1M KOH containing 20 mM $NaBH_4$ centrifuged and the pellet washed with distilled water. The combined alkali and water supernatants were adjusted to pH 5.0 with acetic acid. This fraction was referred to as the 0.1M KOH–soluble fraction. Then, the residue was incubated for 18 h in 6 M KOH containing 20 mM $NaBH_4$, processed as described for the 0.1M KOH–soluble fraction, to obtain the 6M KOH–soluble fraction. All fractions were dialyzed against distilled water with a dialysis membrane of 12-14KDa cut-off and lyophilized

2.2.8. Total sugar and monosaccharide quantification

Total sugars and uronic acids were determined using the phenol–sulfuric acid assay (Dubois et al. 1956) and the m–hydroxydiphenyl assay (Blumenkrantz and Asboe–Hansen 1973) respectively, using glucose and galacturonic acid as standards. Neutral sugars were quantified as described by Albersheim et al. (1967). Lyophilized samples of each CW fraction were hydrolysed with 2N Trifluoroacetic acid (TFA) at 121ºC for 1 hour and the sugars were derivatized to alditol acetates and analyzed by Gas Chromatography (GC) analysis using a Supelco SP–2330 30m x 0.25mm x 0.20µm Capillary Column in a Perkin Elmer

Autosystem gas chromatograph fitted with a flame–ionization detector. Helium (2ml min^{-1}) was used as the carrier gas. Sugar quantification was carried out after determination of each sugar response factor using pure rhamnose, fucose, arabinose, xylose, mannose, galactose and glucose as standards. Inositol was used as internal standard.

2.2.9. Immunodot blot assays

Immunodot assays, 1µl aliquots from CDTA–, 0.1M KOH– and 6M KOH–soluble fractions in three replicated dilution series (1:5 dilutions) as described by García–Angulo et al. (2006) were spotted onto a nitrocellulose membrane (Scheicher & Schull, Dassel, Germany). The membranes were blocked for 2h with 0.1M Phosphate buffered saline (PBS) containing 4% fat–free milk powder and each primary antibody (2F4, LM1, LM5 and LM6) at a 1:5 dilution. After washing with PBS, the membranes were incubated for 1h with a 1:1000 dilution of an anti–rat IgG1 secondary antibody linked to horseradish peroxidase (HRP). For signal detection, the membranes were incubated with 25 ml of deionized water, 5 ml methanol containing 10 mg ml^{-1} 4–chloro-1–naphtol and 30 µl 6% (v/v) H_2O_2, and photographed with a digital camera.

2.2.10. Statistical analysis

Data is presented as mean values ± standard deviation (SD). The results were statistically evaluated by variance analysis (ANOVA) and Bonferroni test as post hoc tests with a p=0.05 significance, to compare the treatment effect. The SigmaPlot (Systat Software Inc.) statistical package was used in the analyses.

2.3. Results

2.3.1. Effect of mineral stress on callus growth

Our main aim was to analyze the effect of nitrogen, phosphorus or sulfur nutrient depletion in grapevine CW composition and structure. The effect of the imposed individual mineral stresses on the functioning of the biological experimental system used was firstly assessed by measuring the growth of *callus* along time.

The absolute growth of *Vitis callus* in full MS culture medium (control) and in modified MS media without nitrogen (–N), phosphorous (–P) or sulfate (–S) along two cycles of 3–weeks each is showed in Fig. 2.1.

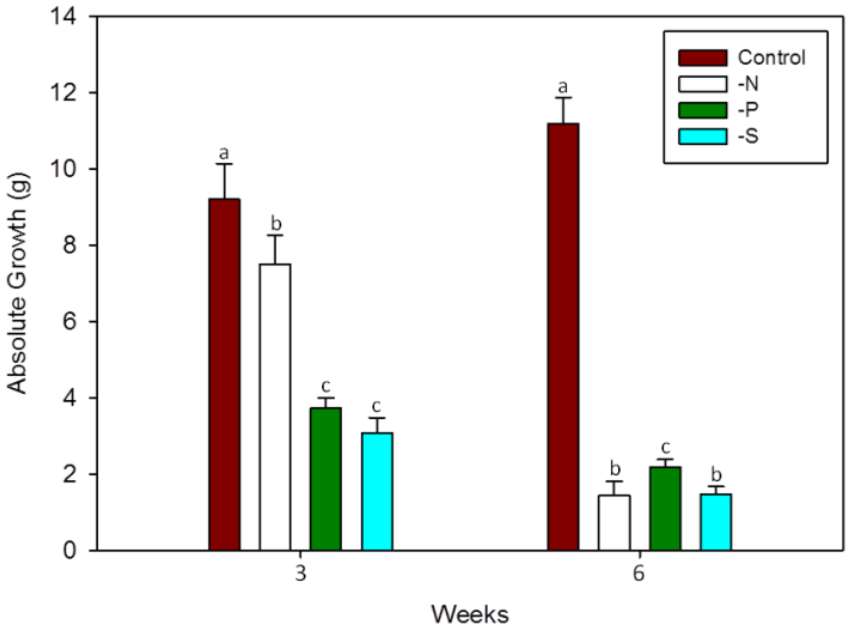

Fig. 2.1 Absolute growth (AG) of *Vitis* callus growing under nitrogen deficient (-N), phosphorus deficient (-P), sulfur deficient (-S) and with full nutrients (Control) for three and 6 weeks. Bars represent means of the AG of *Vitis* callus from 10 petri dish ± SD. In each graph, different letters indicate significant differences at p=0.05 significance.

After withdrawing of nutrients, the absolute growth of the callus was significantly affected in both cycles when compared to the control. During the first three weeks, phosphorus and sulfur depleted media affected growth in a more pronounced way than under nitrogen absence. After a second growing cycle under nutrient depletion, a more severe reduction in growth was noticed in all individual stresses, with a reduction in growth of ca. 80% in comparison with the control. This time scale (2 cycles of three weeks) was selected to produce template material to be used in the subsequent analyses.

2.3.2. FT–IR spectroscopy determination

Putative changes in CW relative composition during nutrient deprivation were monitored by FT-IR spectroscopy by analysis of at least 11 FT-IR CW spectra per treatment.

For a clear analysis of the FT-IR spectra a multivariate analysis (Principal Component Analysis; PCA) was performed (Fig. 2.2). Principal components 1 and 2 (PC1 and PC2), which explain 71.9% of the total variation, were useful to separate the samples. PC1 clearly differentiates the control samples from treatments –N and –P, while PC2 separates the samples according to each individual mineral stress. Samples from the –S treatment also tend to be discriminated from the control, considering their distribution across the gradient from the negative to the positive areas of the PC1 and PC2 axes (Fig. 2.2A). PC1 loading factor plot (Fig. 2.2B) showed several negative peaks associated with cellulose, such as 1160 cm^{-1}, assigned to the C–O and C–C vibration (Wilson et al. 2000), 1120 cm-1, associated with the glycosidic C–O–C vibration (Kačuráková et al. 2000) or 988 cm^{-1}, associated with bonds shared by cello–triose, –tetraose and –pentose (Sekkal et al. 1995), indicating that samples located in the negative part of PC1 (all control and some –S samples) should have a higher content of cellulose. In the same samples, an alteration in the esterification patterns of pectins is also suggested, as reveled by the contribution of the 950 cm^{-1} peak (Coimbra et al. 1999), indicating that the absence of nutrients alters pectin biochemistry. PC2 loading factor plot (Fig. 2.2B) showed negative peaks associated with xyloglucan (1041 cm^{-1}, related to β–glucan) (Kačuráková et al. 2000) and with proteins (1650 cm^{-1}, related to C=O amide I linkage). This evidence points to decreased concentrations of these CW components upon –N and –P conditions. PC2 positive peaks were also observed, mainly related to phenolic compounds (1630 and 1430 cm^{-1}) (Séné et al. 1994), suggesting an increase of these components in CW under some mineral stresses. Other positive peaks were also observed, mainly at 840, 1295, 1565 and 1700 cm^{-1}, for factor 1 and 885, 1180, 1250 and 1390 cm^{-1} for factor 2, but no information is available about the nature of the linkages and wall components associated with these peaks. It should be noted that –N and, in a minor extent, –P callus samples tend to cluster more compactly in the plots, while control

samples appear as a more dispersed group (Fig. 2.2A) suggesting lower variability in samples exposed to higher stresses.

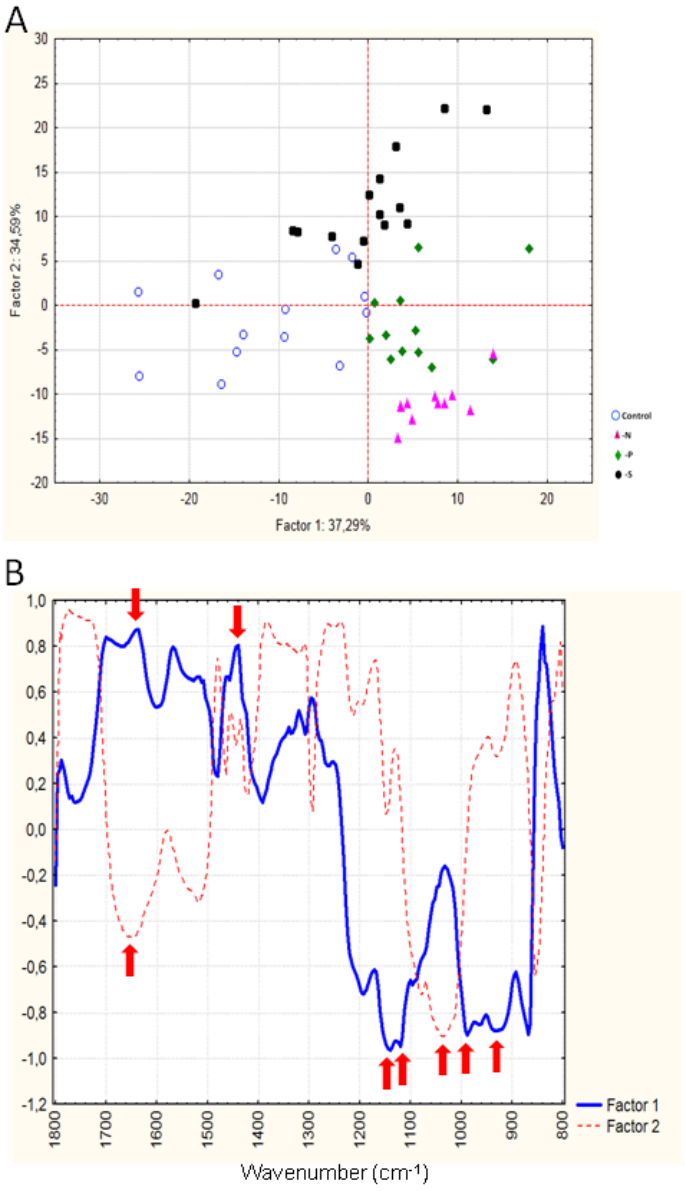

Fig. 2.2 Principal Component Analysis (PCA) of all callus spectra. A) Plot of the first and second PCs based on the FTIR spectra obtained from 6 weeks callus grown in the absence of nitrogen (–N), phosphurus (–P), sulfur (–S) and under full nutrients (control); B) Loading factor plot for PC1 (——) and PC2 (----) explaining PCA clustering. Arrows point meaningful wavenumbers

To acquire additional information on the significance of spectral differences between the control and the mineral stressed callus, a subtraction of the spectra was also performed (Fig. 2.3). Using this approach, the differences in -N spectra observed were more striking as negative peaks in wavenumbers 1033 cm^{-1} characteristic of cellulose, related to deformations of C–OH groups (Kačuráková

et al. 2000) and 1650 cm^{-1}, assigned to proteins, as stated above. These negative peaks points to a minor amount of cellulose and proteins in –N condition. They were accompanied by positive peaks at 950 and 1740 cm^{-1}, both related to a higher amount of pectins. These trends were not maintained in –P or –S conditions. In –S, alterations in cellulose assigned to the vibrations associated with the CH2 group, as revealed by the 1265 cm^{-1} wavenumber peak (Sekkal et al. 1995), were also observed (Fig. 2.3). A positive peak at 1180 cm^{-1} was also observed in all cases but it has not been associated with any known wall component or group linkage. A clear difference in the absorbance peaks for cellulose between the three treatments was observed in agreement with the PC1 separations (Fig. 2.2A). The overall results pinpoint cellulose and pectins as major candidates to be affected by mineral stress, what prompted us to a more detailed investigation.

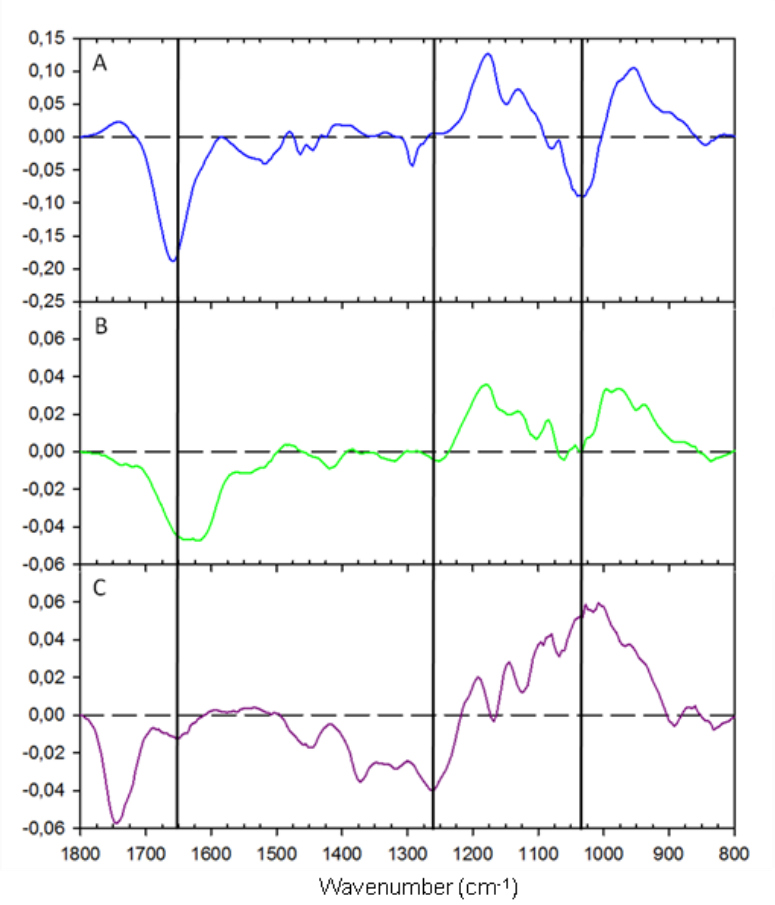

Fig. 2.3 Difference between normalized and baseline-corrected FT-IR spectra of CW obtain from callus in the absence of nitrogen (A), phosphurus (B) and sulfur (C) relative to control. Vertical lines represent wavenumbers with known significance (n>11)

2.3.3. Cellulose and lignin content

Cellulose is the main constituent of the CW. Figure 4a shows the variation in cellulose amount in response to mineral stress imposition. A significant reduction in cellulose was observed at the extent of ca. 43% in the absence of nitrogen and, to a less extent of ca. 12%, in the absence of phosphorus (Fig. 2.4A), when compared to the control. Sulfur depletion did not affect significantly the synthesis or deposition of cellulose. Although lignin Klason levels were small compared with cellulose or other cell wall components, lignin quantification in control and stressed calluses reveled an increase of ca. 36% relative to the control when nitrogen is removed from the growing medium (Fig. 2.4B). The absence of phosphorus and sulfur did not affect the amount of lignin in the CW of *Vitis* callus after 6 weeks growth.

2.3.4. Degree of pectin methyl–esterification

To further examine the putative modifications in pectin esterification suggested by FT-IR analysis, the extent of pectin methyl esterification was determined by quantification of the released methanol. The decrease in the methanol released observed in samples from callus growing under absence of nitrogen in the culture medium, indicates a lower degree of methyl esterification in comparison with the control (Fig. 2.4C), confirming the FT-IR results for this stress. Neither phosphorus nor sulfur absence affected the total degree of pectin esterification.

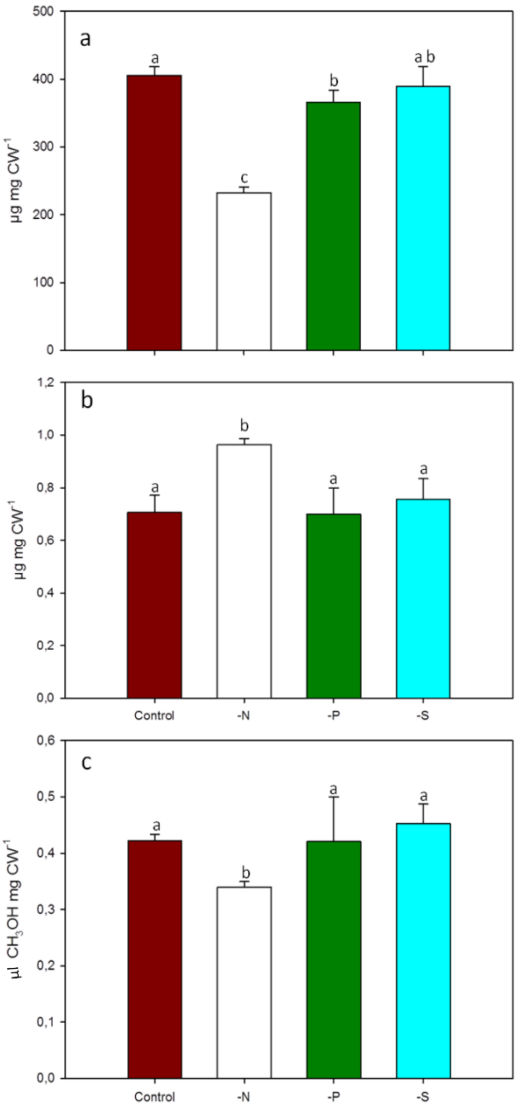

Fig. 2.4 a) Cellulose content, b) Lignin content and c) Total methyl–esterification degree of 6 weeks CW callus grown in nitrogen deficient (–N), phosphorus deficient (–P), sulfur deficient (–S) and full nutrient media (control). Bars represent means of 6 *Vitis callus* ± SD Different letters indicate significant differences at *p*=0.05 significance

2.3.5. Immunodot-blot of cell wall polysaccharide specific antibodies

The results of immunodot assays are presented in Figure 2.5. The abundance of pectins with a degree of esterification up to 40% was tested by immunodetection using 2F4 monoclonal antibody (Liners et al. 1989). As expected, labeling was only detected in the CDTA and, to a less extent, in the 0.1M KOH-soluble fraction. A stronger signal was detected under –N and –S conditions (Fig. 2.5). The LM1 antibody, specific to an extensin epitope (Smallwood et al. 1995), showed a higher labeling under stress conditions in all soluble fractions, indicating that

mineral stress increases the deposition of this structural protein. This is more striking in –N and –S conditions, the former more tightly attached to the CW. LM5 and LM6 antibodies recognize 1,4-β-galactan and 1,5-α-arabinan epitopes, respectively (Jones et al. 1997; Willats et al. 1998). Under –N, the amount of 1,5-α-arabinan and 1,4-β-galactan decreases relative to the control in the CDTA-soluble fraction. A reduction of labeling was observed in the 0.1M KOH-soluble fraction in all stresses for both antibodies. Conversely, an increase in 1,5-α-arabinan is suggested to occur under –S conditions, both in weakly and tightly CW attached polysaccharides (CDTA- and 6M KOH-soluble fractions, respectively).

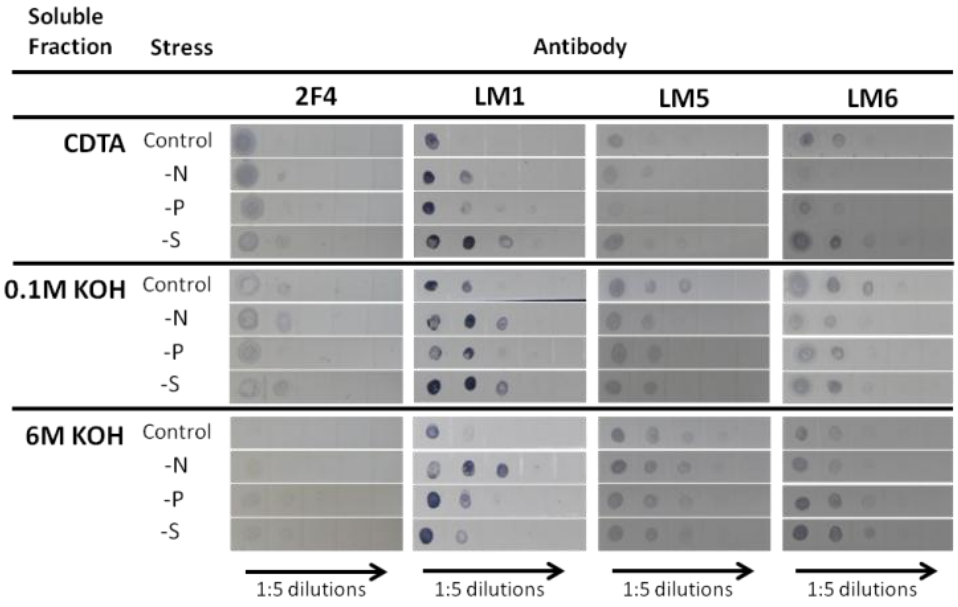

Fig. 2.5 Immunodot assays of CW-soluble fractions from callus grown in nitrogen deficient (–N), phosphorus deficient (–P), sulfur deficient (–S) and full nutrients (Control), probed with monoclonal antibodies with specificity for homogalacturonan with a degree of methyl esterification up to 40% (2F4), for extensin hydroxyproline–rich glycoproteins (LM1), for 1,4-β-galactan (LM5) and 1,5-α-arabinan (LM6). In each row the antibody was used to probe samples at a 1:5 sequential dilution

2.3.6. Sugar analysis in CW fractions

CW fractionation showed that the majority of polysaccharides were extracted from the CW by the strong alkaline treatment (Fig. 2.6). All mineral stress treatments decreased the amount of polysaccharides solubilized in CDTA and 0.1M KOH. Conversely in 6M KOH-soluble fractions, they were more abundantly detected in the –N and –P treatments (Fig. 2.6).

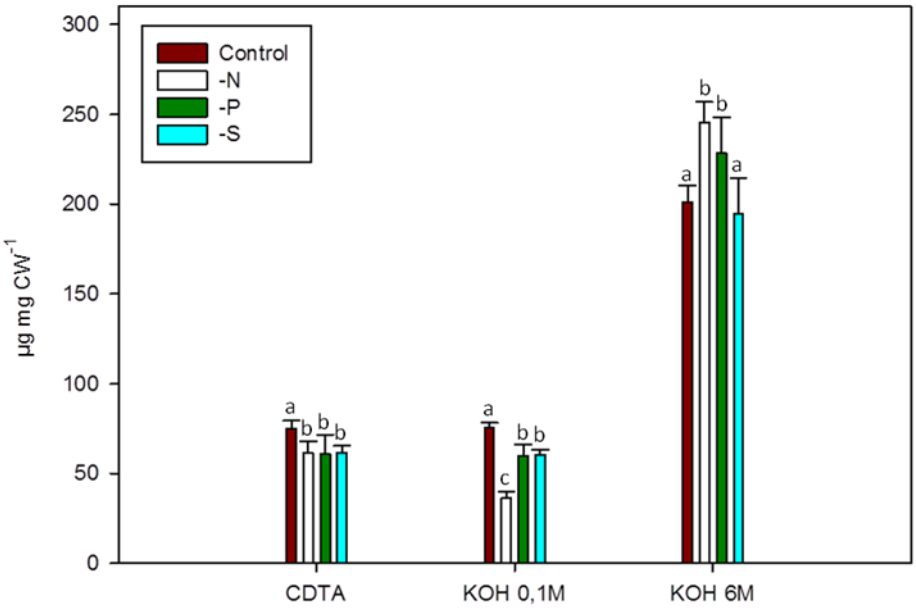

Fig. 2.6 Total sugars quantified in CW fractions obtained from callus grown for 6 weeks in the absence of nitrogen (–N), phosphorus (–P), sulfur (–S) and in full nutrient media (Control) Units are µg of glucose (mg CW)$^{-1}$ Bars represent means of *Vitis* callus ± SD. In each sub-graph, different letters indicate significant differences at p=0.05

As expected, the majority of pectins (quantified as uronic acids, UA) were extracted by the CDTA and 0.1M KOH (Fig. 2.7A and B). GC analysis of CW fractions showed that the more significant neutral monosaccharide present in all fractions was arabinose followed by galactose, xylose and glucose (Fig. 2.7A, B and C). The amount of uronic acids decreased in alkaline soluble fractions upon the three mineral stress treatments imposed (Fig. 2.7B and C).

Arabinose-containing polysaccharides responded to –N by decreasing its amount in weak alkaline–soluble fraction but increasing significantly in 6M KOH-soluble one. A different trend was observed for xylose- and galactose-containing polysaccharides, with a decrease in both alkaline–soluble fractions. Regarding xylose, an increase in the 6M KOH-soluble fraction was noticed in the –S treatment. Finally, glucose-containing polysaccharides showed increased extraction by both alkaline solutions from –P CWs.

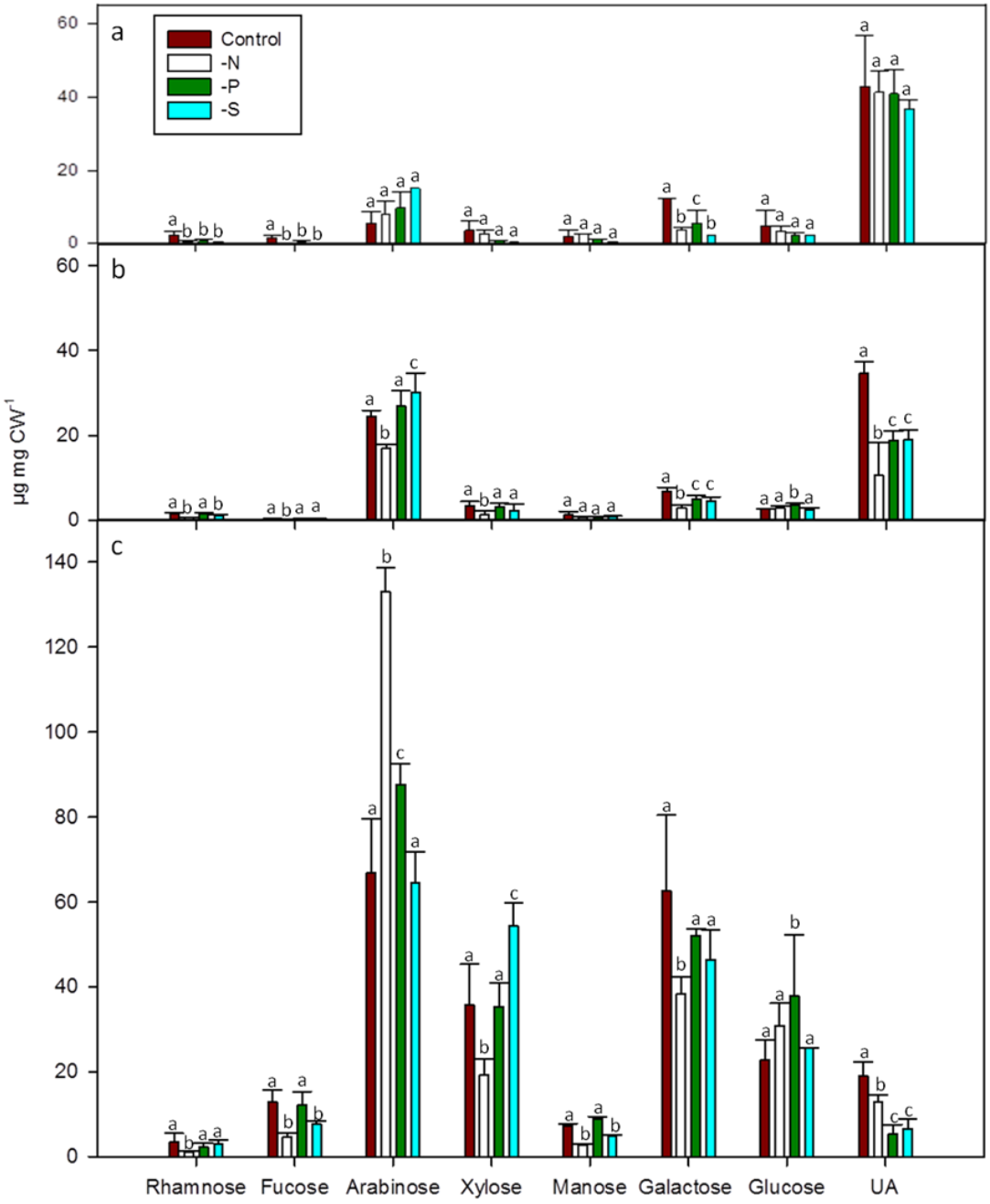

Fig. 2.7 Monosaccharide composition of CW CDTA-soluble fraction (A), 0.1M KOH-soluble fraction (B) and 6M KOH-soluble fraction (C) obtained by GC analysis of callus grown in nitrogen deficient (–N), phosphorus deficient (–P), sulfur deficient (–S) and full nutrients (Control) media. Units are µg of each monosaccharide and galacturonic acid equivalents for uronic acids (UA) (mg CW)$^{-1}$. Different letters indicate significant differences at p=0.05

The increase in neutral sugars observed in the 6M KOH soluble fraction, under nitrogen starvation (Fig. 2.7C), is only due to the increase in arabinose, since all other monosaccharides decreased or maintain the same levels relative to control when nitrogen is withdrawn from the culture media.

2.4. Discussion

Plant model systems analyzed in controlled experimental conditions are useful tools to assess limiting nutrient situations. Using the model described, we observed that during the first three weeks of development, callus growth was impaired by the absence of phosphates and sulfates (Fig. 2.1). Callus from plates depleted in nitrates was less affected, probably due to previous nitrogen accumulation, since the nitrate concentration in the MS medium is much higher than those of phosphate or sulfate. By the sixth week, in the second culture cycle, the callus growth was drastically reduced to levels significantly lower than those observed at –P and similar to –S (Fig. 2.1). The collective results confirm the essential role of these elements and validate the experiment model employed to access the effect of mineral nutrition in CW constituents and dynamics. Previous studies also report the effect of mineral depletion on growth (Wu et al. 2003; Tschoep et al. 2009), including of *Vitis* callus (Fernandes et al. 2009).

Our goal was to address changes in CW composition triggered by mineral deficiency. FT-IR proved to be a readily-employed and efficient method for simultaneously identifying a broad range of structural differences in CWs (Alonso–Simón et al. 2004). The overall FT-IR results suggest changes in all of the main components of the CW as candidate events, such as modifications in the biosynthesis or rearrangements of cellulose microfibrils and of matrix linked glycans, in pectin biochemistry and in the amounts of structural proteins (Fig. 2.2B and Fig. 2.3). Moreover, PCA analysis (Fig. 2.2A) showed that CW is differentially affected, according to the specific stress imposed. These results prompted us to pursue a more detailed biochemical analysis of the stressed material.

The statistically significant reduction in cellulose content observed under –N and –P (Fig. 2.4A) could compromise the CW integrity and, probably, the viability of the cells to survive. Due to the paramount importance of the CW in survival and environment adaptation, plants are equipped with compensatory alternative mechanisms to reinforce their CWs when the biosynthesis or deposition of a given component is impaired (Pilling and Höfte 2003; Wolf et al. 2012). Our results agree with such model. In fact, CWs from callus growing in medium exhausted in nitrates respond to low levels of cellulose (Fig. 2.4A) by slightly

increasing their lignin content (Fig. 2.4B) and reducing their degree of pectin methyl esterification (Fig. 2.4C). If occurring in long stretches of the galacturonic acid chains as suggested by immunodot detection with the 2F4 antibody (Fig. 2.5), it could lead to reinforce the wall via the formation of calcium bridges, eg "egg–box" structures (Jarvis 1984) and supramolecular pectic gels, both important in controlling the porosity and mechanical properties of CW and maintenance of intercellular adhesion (Knox 1992; Carpita and Gibeaut 1993). Moreover, an expected looser cellulose network prods arabinan-containing polysaccharides to become more cross–linked to the cellulose-hemicellulose network (Fig. 2.7B and C), providing the wall with additional mechanical support and instigates the formation of extensin networks (Fig. 2.5). Likewise, the lower cellulose quantified in –P callus is accompanied by an increase in neutral sugars enriched in arabinose polysaccharides (Fig. 2.7B) including 1,5-α-arabinans (Fig. 2.5) detected in polysaccharides tightly bonded to the CW (Fig. 2.6).

Alterations in the biosynthesis of individual CW constituents can affect the synthesis and/or deposition of othe CW polymers. In fact, changes in the cellulose content are known to be compensated by an increase in lignin polymers. It was demonstrated that cinnamoyl-CoA reductase (CCR) down-regulation in transgenic tobacco (*Nicotiana tabacum* L.) lines lead to a 24.7% reduction of its Klason lignin with a concomitant increase of 15% in cellulose content (Prashant et al. 2011). Similarly, different works report that high nitrate availability reduces the lignin in the CW (Entry et al. 1998; Blodgett et al. 2005; Pitre et al. 2007), so the opposite trend is expected to happen. In fact, a mutation in *CesA3*, one of the genes encoding cellulose synthases, was proved to lead to CW reinforcement through lignin synthesis (Caño–Delgado et al. 2003). It has also been suggested that, under conditions where cellulose synthesis is inhibited, compensation with a higher quantity of hemicellulosic polysaccharides occurs (Potters et al. 2007). Several other lines of evidence have demonstrated alterations in the CW architecture of the *kor1-1 Arabidopsis* mutant (Nicol et al. 1998; Sato et al. 2001), in which a deficiency in an endo-1,4-β-glucanase that is not directly implicated in pectin metabolism, induces a 150% increase of pectins in the primary CW (His et al. 2001). Moreover, other cellulose synthase *Arabidopsis* mutant, *MUR10/CesA7*, showed an increase in pectic arabinan contents in response to

impaired cellulose biosynthesis (Bosca et al. 2006). On the other hand, augmented arabinose levels may indicate a higher substitution by arabinosyl residues in the rhamnogalacturonan–I (RGI) side chains of pectic polysaccharides. RGI arabinosyl side chains can work as plasticizers in CWs that undergo large physical remodeling under abiotic stresses such as extreme water deficient conditions (Harholt et al. 2010). Ulvskov et al. (2005) analyzed the mechanical properties of the CW of potato (*Solanum tuberosum*) tubers from wild-type and transformed plants with decreased contents of arabinan and certified that the force needed to induce failure of the CW decreased in transgenic tubers.

Absence of sulfates in the media impaired callus growth in levels similar to those observed under nitrate deficiency (Fig. 2.1), but no significant reduction in cellulose was noticed (Fig. 2.4A). Nonetheless, among the assays conducted in our work, increases in weakly and tightly bonded extensins (Fig. 2.5) and increases in arabinose- and xylose- containing polysaccharides in alkali-soluble fractions (Fig. 2.7B and C) were detected, unveiling CW modifications. Extensins are abundant constituents of the primary CW (Showalter 1993), known to increase in response to several stresses (Showalter et al. 1992; Hirsinger et al. 1997; Ueda et al. 2007). These structural proteins have been implicated in the control of CW extension and strengthening by the formation of peroxidase-mediated intermolecular cross-links (Jackson et al. 2001).

In summary, grapevine calluses submitted to individual mineral stresses are impaired on specific CW components or suffer reorganization of their deposition. Our results highlight that *V. vinifera* callus followed different strategies to overcome the adverse effects induced in the CW by the imposed mineral stress according to the severity perceived and its primary biological role, confirming previous assumptions that plants have evolved fine–tuned mechanisms to turn on different pathways related with specific wall components, in response to different stimulus.

Acknowledgements The research was funded by Fundação para a Ciência e Tecnologia (FCT) grant SFRH/BD/64047/2009 to JCF and CBAA (PestOE/AGR/UI0240/2011).

References

Abdel–Massih RM, Baydoun EA–H, Brett CT (2003) In vitro biosynthesis of 1,4–β–galactan attached to a pectin–xyloglucan complex in pea. Planta 216:502–511

Albersheim P, Nevins PD, English PD, Karr A (1967) A method for the analysis of sugar in plant cell wall polysaccharides by gas liquid chromatography. Carbohydr Res 5:340–345

Alonso–Simón A, Encina AE, García–Angulo P, Álvarez JM, Acebes JL (2004) FTIR spectroscopy monitoring of cell wall modifications during the habituation of bean (Phaseolus vulgaris L.) callus cultures to dichlobenil. Plant Sci 167:1273-1281

Amtmann A, Armengaud P (2009) Effects of N, P, K and S on metabolism: new knowledge gained from multi–level analysis. Curr Opin Plant Biol 12:275–83

Blodgett JT, Herms DA; Bonello P (2005) Effects of fertilization on red pine defense chemistry and resistance to *Sphaeropsis sapinea.* For Ecol Manag 208:373 382

Blumenkrantz N, Asboe–Hansen G (1973) New method for quantitative determination of uronic acids. Anal Biochem 54:484–489

Boerjan W, Ralph J, Baucher M (1993) Lignin biosynthesis. Annu Rev Plant Biol 54:519-46

Bootten TJ, Harris PJ, Melton LD, Newman RH (2004) Solid–state ^{13C}NMR spectroscopy shows that the xyloglucans in the primary cell walls of mung bean (*Vigna radiata L.*) occur in different domains: a new model for xyloglucan–cellulose interactions in the cell wall. J of Exp Bot 55:571–583

Bosca S, Barton CJ, Taylor NG, Ryden P, Neumetzler L, Pauly M, Roberts K, Seifert GJ (2006) Interactions between MUR10/CesA7–dependent secondary cellulose biosynthesis and primary cell wall structure. Plant Physiol 142:1353-1363

Brett C, Waldron K. Physiology and Biochemistry of Plant Cell Walls. Chapman & Hall, London 1996

Caño–Delgado A, Penfield S, Smith C, Catley M, Bevan M (2003) Reduced cellulose synthesis invokes lignification and defense responses in *Arabidopsis thaliana*. Plant J 34:351–362

Carpita NC, Gibeaut DM (1993) Structural models of primary cell walls in flowering plants: consistency of molecular structure with the physical properties of the walls during growth. Plant J 3:1–30

Chapin ES, Walter CHS, Clarkson DT (1988) Growth response of barley and tomato to nitrogen stress and its control by abscisic acid, water relations and photosynthesis. Planta 173:352–366.

Coimbra MA, Barros A, Rutledge DN, Delgadillo I (1999) FTIR spectroscopy as a tool for the analysis of olive pulp cell–wall polysaccharide extracts. Carbohydr Res 317:145-154

Cosgrove DJ (2001) Wall structure and wall loosening. A look backwards and forwards. Plant Physiol 125:131-134

Cosgrove DJ (1997) Assembly and enlargement of the primary cell wall in plants. Annu Rev Cell Dev Biol 13:171-201

Cumming CM, Rizkallah HD, McKendrick KA, Abdel–Massih RM, Baydoun EA–H, Brett CT (2005) Biosynthesis and cell–wall deposition of a pectin–xyloglucan complex in pea. Planta 222:546–555

Dische Z (1962) General color reactions. In: Whistler, R. L.; Wolfran, M. L. Carbohydrate chemistry. p. 477–512 New York: Academic.

Dubois M, Gilles KA, Hamilton JK, Rebers PA, Smith F (1956) Colorimetric method for determination of sugars and related substances. Anal Chem 28:350–356

Entry JA, Runion GB, Prior SA, Mitchell RJ, Rogers HH (1998) Influence of CO_2 enrichment and nitrogen fertilization on tissue chemistry and carbon allocation in longleaf pine seedlings. Plant Soil 200:3-11

Fernandes J, Tavares S, Amâncio S (2009) Identification and exprexssion of cytokinin signaling and meristem identity genes in sulfur deficient grapevine (*Vitis vinifera L.*). Plant Signal Behav 4:1128–1135

Freshour G, Clay RP, Fuller MS, Albersheim P, Darvill AG, Hahn MG (1996) Developmental and tissue–specific structural alterations of the cell–wall polysaccharides of *Arabidopsis thaliana* roots. Plant Physiol 110:1413-1429

Fry SC (1986) Cross–linking of matrix polymers in the growing cell walls of angiosperms. Ann Rev Plant Physiol 37:165-186

García–Angulo P, Willats WGT, Encina AE, Alonso–Simon A, Alvarez JM, Acebes JL (2006) Immunocytochemical characterization of the cell wall of bean cell suspenion cutures during habituation and dehabituation to doclobenil. Physiol Plant 127:87–99

Goulao LF (2010) Pectin de–esterification and fruit softening: revisiting a classical hypothesis. Stewart Postharvest Rev 6:1-12

Goulao LF, Fernandes JC, Lopes P, Amâncio S (2012) Tackling the Cell Wall of the Grape Berry, *In* Hernâni Gerós, M Manuela Chaves, Serge Delrot (Eds) Bentham eBooks, pp. 172-193, eISBN: 978-1-60805-360-5

Guo W, Zhang L, Zhao J, Liao H, Zhuang C, Yan X (2008) Identification of temporally and spatially phosphate–starvation responsive genes in Glycine max. Plant Sci 175:574–584

Harholt J, Suttangkakul A, Vibe Scheller H (2010) Biosynthesis of pectin. Plant Physiol 153:384–395

Hanus J, Mazeau K (2006) The xyloglucan–cellulose assembly at the atomic scale. Biopolymers 81:59–73

Hatfield RD, Jung HG, Ralph J, Buxton DR, Weimer PJ (1994) A comparison of the insoluble residues produced by the Klason lignin and acid detergent lignin procedures. J Sci Food Agric 65:51−58

Hirsinger C, Parmentier Y, Durr A, Fleck J, Jamet E (1997) Characterization of a tobacco extensin gene and regulation of its gene family in healthy plants and under various stress conditions. Plant Mol Biol 33:279–89

His I, Driouich A, Nicol F, Jauneau A, Höfte H (2001) Altered pectin composition in primary cell walls of korrigan , a dwarf mutant of *Arabidopsis* deficient in a membrane–bound endo-1,4–β–glucanase. Planta 212:348–358

Iraki NM, Bressan RA, Hasegawa PM, Carpita NC (1989) Alteration of the physical and chemical structure of the primary cell wall of growth–limited plant cells adapted to osmotic stress. Plant Physiol 91:39–47

Jackson P, Galinha C, Pereira C, Fortunato A, Soares N, Amâncio S, Pinto Ricardo C (2001) Rapid deposition of extensin during the elicitation of grapevine callus cultures is specifically catalysed by a 40 kDa peroxidase. Plant Physiol 127:1065-1076.

Jarvis MC (1984) Structure and properties of pectin gels in plant cell walls. Plant Cell Environ 7:153-164

Jones L, Seymour GB, Knox JP (1997) Localization of pectic galactan in tomato cell walls using a monoclonal antibody specific to (1[–>]4)–[beta]–D–Galactan. Plant Physiol 113:1405-1412.

Kačuráková M, Capek P, Sasinková V et al (2000) FT–IR study of plant cell wall model compounds: pectic polysaccharides and hemicelluloses. Carbohydr Polym 43:195–203

Knox JP (1992) Cell adhesion, cell separation and plant morphogenesis. The Plant J 2:137-141.

Knox J (2008) Revealing the structural and functional diversity of plant cell walls. Curr Opin Plant Biol 11: 308–313

Liners F, Letesson J–J, Didembourg C, Van Cutsem P (1989) Monoclonal antibodies against pectin. Recognition of a conformation induced by calcium. Plant Physiol 91:1419-1424

Marcus SE, Verhertbruggen Y, Hervé C, Ordaz–Ortiz JJ, Farkas V, Pedersen HL, Willats WGT, Knox JP (2008) Pectic homogalacturonan masks abundant sets of xyloglucan epitopes in plant cell walls. BMC Plant Biol 8:60

Mélida H, García–Angulo P, Alonso–Simón A, Encina A, Alvarez J, Acebes JL (2009) Novel type II cell wall architecture in dichlobenil–habituated maize calluses. Planta 229:617–631

Mouille G, Robin S, Lecomte M, Pagant S, Hofte H (2003) Classification and identification of *Arabidopsis* cell wall mutants using Fourier–transform infrared (FT–IR) microspectroscopy. Plant J 35:393–404

Murashige T, Skoog F (1962) A revised medium for rapid growth and bioassays with tobacco tissue. Physiol Plant 15:493–497.

Nicol F, His I, Jauneau A, Vernhettes S, Canut H, Höfte H (1998) A plasma membrane–bound putative endo-1, 4–β–D–glucanase is required for normal wall assembly and cell elongation in *Arabidopsis*. EMBO J 17:5563–5576

Palmer SJ, Berridge DM, McDonald AJS, Davies WJ (1996) Control of leaf expansion in sunflower (Helianthus annuus L.) by nitrogen nutrition. J Exp Bot 47:359–368.

Park YB, Cosgrove DJ (2012) A revised architecture of primary cell walls based on biomechanical changes induced by substrate-specific endoglucanases. Plant Physiol 158:1933-1943.

Patakas A (2012) Abiotic stress–induced morphological and anatomical changes in plants. in Ahmad P and. Prasad M.N.V (Eds.), Abiotic stress responses in plants metabolism, productivity and sustainability (pp. 21–40) New York, Springer

Pilling E, Höfte H (2003) Feedback from the wall. Curr Opin Plant Biol 6:611–616

Pitre FE, Pollet B, Lafarguette F, Cooke JE, MacKay JJ, Lapierre C (2007) Effects of increased nitrogen supply on the lignification of poplar wood. J Agric Food Chem 55:10306-10314

Potters G, Pasternak TP, Guisez Y, Palme KJ, Jansen MA (2007) Stress–induced morphogenic responses: growing out of trouble? Trends Plant Sci 12:98-105

Prashant S, Srilakshmi Sunita M, Pramod S, Gupta RK, Anil Kumar S, Rao Karumanchi S, Rawal SK, Kavi Kishor PB (2011) Down–regulation of Leucaena leucocephala cinnamoyl CoA reductase (LlCCR) gene induces significant changes in phenotype, soluble phenolic pools and lignin in transgenic tobacco. Plant Cell Rep 30:2215–2231

Popper ZA, Fry SC (2005) Widespread occurrence of a covalent linkage between xyloglucan and acidic polysaccharides in suspension–cultured angiosperm cells. Ann Bot 96:91–99

Radin JW, Boyer JS (1982) Control of leaf expansion by nitrogen nutrition in sunfiower plants: Role of hydraulic conductivity and turgor. Plant Physiol 69:771–775

Radin JW, Eidenbock MP (1984) Hydraulic conductance as a factor limiting leaf expansion of phosphorus deficient cotton plants. Plant Physiol 75:372–377

Saeman JF, Moore WE, Millet MA (1963) Sugar units present. Hydrolysis and quantitativepaper chromatography. *In* Methods in CarbohydrateChemistry, Vol. 3, Cellulose (R.L. Whistler, ed.) pp. 54–69. Academic Press, New York.

Sato S, Kato T, Kakegawa K, Ishii T, Liu YG, Awano T, Takabe K, Nishiyama Y, Kuga S, Sato S, Nakamura Y, Tabata S, Shibata D (2001) Role of the putative membrane–bound endo-1,4–beta–glucanase KORRIGAN in cell elongation and cellulose synthesis in *Arabidopsis thaliana*. Plant Cell Physiol 42:251–63

Selvendran RR, O'Neill MA (1987) Isolation and analysis of cell walls from plant material. Methods Biochem Anal 32:25-153

Sekkal M, Dincq V, Legrand P, Huvenne JP (1995) Investigation of the linkages in several oligosaccharides using FT–IR and FT Raman spectroscopies. J Mol Struct 349:349–352

Séné CFB, McCann MC, Wilson RH, Grinter R (1994) Fourier-transform Raman and Fourier-transform infrared spectroscopy an investigation of five higher plant cell walls and their components. Plant Physiol 106:1623-1631

Shedletzky E, Shmuel M, Trainin T, Kalman S, Delmer D (1992) Cell wall structure in cells adapted to growth on the cellulose–synthesis inhibitor 2,6–Dichlorobenzonitrile : A comparison between Two Dicotyledonous Plants and a Graminaceous Monocot. Plant Physiol 100:120-130

Showalter AM, Butt AD, Kim S (1992) Molecular details of tomato extensin and glycine–rich protein gene expression. Plant Mol Biol 19:205-15

Showalter AM (1993) Structure and function of plant cell wall proteins. Plant Cell 5:9–23

Smallwood M, Martin H, Knox JP (1995) An epitope of rice threonine– and hydroxyproline–rich glycoprotein is common to cell wall and hydrophobic plasma–membrane glycoproteins. Planta 196:510–22

Snir N, Neumann PM (1997) Mineral nutrient supply, cell wall adjustment and the control of leaf growth. Plant Cell Environ 20:239–246

Talmadge KW, Keegstra K, Bauer WD, Albersheim P (1973) The structure of plant cell walls I. The macromolecular components of the walls of suspension–cultured sycamore cells with a detailed analysis of the pectic polysaccharides. Plant Physiol 51:158-173

Taylor G, McDonald AJS, Stadenberg I, Ereer Smith PH (1993) Nitrate supply and the biophysics of leaf growth in Salix viminalis. J Exp Bot 44:155-64

Takahashi H, Braby CE, Grossman AR (2001) Sulfur economy and cell wall biosynthesis during sulfur limitation of *Chlamydomonas reinhardtii*. Plant Physiol 127:665–673

Tschoep H, Gibon Y, Carillo P, Armengaud P, Szecowka M, Nunes–Nesi A, Fernie AR, Koehl K, Stitt M (2009) Adjustment of growth and central metabolism to a mild but sustained nitrogen limitation in *Arabidopsis*. Plant Cell Environ 32:300–318

Ueda A, Yamamoto–Yamane Y, Takabe T (2007) Salt stress enhances proline utilization in the apical region of barley roots. Biochem Biophys Res Commun 355:61–6

Ulvskov P, Wium H, Bruce D, Jorgensen B, Qvist KB, Skjot M, Hepworth D, Borkhardt B, Sorensen SO (2005) Biophysical consequences of remodeling the neutral side chains of rhamnogalacturonan I in tubers of transgenic potatoes. Planta 220:609–620

Updegraff DM (1969) Semi–micro determination of cellulose in biological materials. Anal Biochem 32:420–424

Vanholme R, Morreel K, Ralph J, Boerjan W. (2008) Lignin engineering. Curr Opin Plant Biol 11:278–285

Vorwerk S, Somerville S, Somerville C (2004) The role of plant cell wall polysaccharide composition in disease resistance. Trends Plant Sci 9:203–209

Willats WG, Marcus SE, Knox JP (1998) Generation of monoclonal antibody specific to (1—>5)–alpha–L–arabinan. Carbohydr Res 308:149–52

Willats WG, McCartney L, Mackie W, Knox JP (2001) Pectin: cell biology and prospects for functional analysis. Plant Mol Biol 47:9–27

Wilson RH, Smith AC, Kačuráková M et al (2000) The mechanical properties and molecular dynamics of plant cell wall polysaccharides studied by Fourier–transform infrared spectroscopy. Plant Physiol 124:397–405

Wolf S, Hématy K, Höfte H (2012) Growth control and cell wall signaling in plants. Annual Review of Plant Biology 63:381–407

Wood PJ, Siddiqui IR (1971) Determination of methanol and its application to measurement of pectin methyl ester content and pectin methylesterase activity. Anal Biochem 39:418–428

Wu P, Ma L, Hou X, Wang M, Wu Y, Liu F, Deng XW (2003) Phosphate starvation triggers distinct alterations of genome expression in *Arabidopsis* roots and leaves. Plant Physiol 132:1260-1271

Zhong R, Ye Z–H (2007) Regulation of cell wall biosynthesis. Curr Opin Plant Biol 10:564–572

Zykwinska A, Ralet MC, Garnier C, Thibault JF (2005) Evidence for in vitro binding of pectic side chains to cellulose. Plant Physiol 139:397–407

Zykwinska A, Gaillard C, Buléon A, Pontoire B, Garnier C, Thibault JF, Ralet MC (2007a) Assessment of in vitro binding of isolated pectic domains to cellulose by adsorption isotherms, electron microscopy and X–ray diffraction methods. Biomacromolecules 8:223–232

Zykwinska A, Thibault JF, Ralet MC (2007b) Organization of pectic arabinan and galactan side chains in association with cellulose microfibrils in primary cell walls and related models envisaged. J Exp Bot 58:1795–80

Chapter 3

Regulation of cell wall remodeling in grapevine (*Vitis vinifera* L.) callus under individual mineral stress conditions

João C. Fernandes[1], Luis F. Goulao[2] and Sara Amâncio[1]

[1] *DRAT/LEAF, Instituto Superior de Agronomia, Universidade de Lisboa, Tapada da Ajuda, 1349-017 Lisbon, Portugal.*

[2] *BioTrop, Instituto de Investigação Científica Tropical (IICT, IP), Pólo Mendes Ferrão - Tapada da Ajuda, 1349-017 Lisbon, Portugal.*

Published in Journal of Plant Physiology (2016, 190:95-105. doi: 10.1016/j.jplph.2015.10.007)

3. Regulation of cell wall remodeling in grapevine (*Vitis vinifera* L.) callus under individual mineral stress conditions

João C. Fernandes, Luis F. Goulao and Sara Amâncio

Abstract

Cell wall (CW) is a dynamic structure that determines the plant form, growth and response to environmental conditions. *V. vinifera* callus grown under nitrogen (–N), phosphorous (–P) and sulfur (–S) deficiency were used as a model system to address the influence of mineral stress in CW remodeling. Callus cells morphology was altered, mostly under –N, resulting in changes in cell length and width compared with the control. CW composition ascertained with specific staining and immuno-detection showed a decrease in cellulose and altered pattern of pectin methylesterification. Under mineral stress genes expression from candidate families disclosed mainly a downregulation of a glycosyl hydrolase family 9C (GH9C), xyloglucan transglycosylase/hydrolases (XTHs) with predicted hydrolytic activity and pectin methylesterases (PMEs). Conversely, upregulation of PMEs inhibitors (PMEIs) was observed. While methylesterification patterns can be associated to PME/PMEI gene expression, the lower cellulose content cannot be attributed to altered cellulose synthase (CesA) gene expression suggesting the involvement of other gene families. Salt extracts from –N and –P callus tissues increased plastic deformation in cucumber hypocotyls while no effect was observed with –S extracts. The lower endo-acting glycosyl hydrolase activity of –N callus extracts pinpoints a more expressive impact of –N on CW-remodeling.

Keywords: *Cell wall polymers, Endoglucanase activity, Gene expression, Nutrient deficiency, Pectin deesterification*

Abbreviations

2,4–D	2,4–dichlorophenoxy–acetic acid
CesA	Cellulose synthase
CMC	Carboxymethylcellulose
CW	Cell wall
EXP	Expansin
EXPA	*α*-expansin
GalA	Galacturonic acid
GH9A	Glycosyl hydrolase family 9A
GH9C	Glycosyl hydrolase family 9C
HG	Homogalacturonan
KOR	*KORRIGAN*
-N	Absence of nitrogen
-P	Absence of phosphorous
PBS	Phosphate buffered saline
PG	Polygalacturonase
PL	Pectate lyases
PME	Pectin methylesterase
PMEI	Pectin methylesterases inhibitor
PVP–40T	Polyvinylpyrrolidone
-S	Absence of sulfur
XEH	Endo-hydrolase activity from xyloglucan transglycosylase/hydrolases
XTH	Xyloglucan transglycosylase/hydrolase
XyG	Xyloglucan

3.1. Introduction

The primary plant cell wall (CW) is a dynamic structure formed by a complex of inextensible cellulose microfibrils bonded to a network of coextensive glycans embedded in a pectin-rich gel matrix that includes structural glycoproteins, phenolic compounds and enzymes. CW plays a vital role in controlling the cell shape and, consequently, its morphology (Doblin et al. 2010; Cosgrove and Jarvis 2012). Well-orchestrated CW alterations resulting from synthesis, disassembly, solubilization and rearrangements of its structural components and linkages, are the basis of cell expansion and growth. Moreover, CWs represent one of the first levels of communication between the plant and surrounding environment, playing a decisive role in adaptation to biotic and abiotic pressures (Landrein and Hamant 2013; Malinovsky et al. 2014; Tenhaken 2015). CW changes relate to events such as localized cell division, arrestment of cell elongation and alterations in differentiation status, resulting in constraints that impact changes in anatomy and development (Potters et al. 2007; Braidwood et al. 2014).

The molecular regulation underlying CW dynamic behavior outcomes paradoxal effects in the contribution provided to the cell mechanical properties. Growing cells expand by CW loosening while, at the same time, enough strength is kept to retain the integrity and withstand high turgor forces. The control of CW loosening has been postulated to occur, at least in part, due to modifications in the cellulose-xyloglucan (XyG) network linkages (McQueen-Mason and Cosgrove, 1995; Cosgrove 2000; Whitney et al. 2000), was proved by Van Sandt et al. (2007). Recently Park and Cosgrove (2012, 2015) proposed that XyG is restricted to a minor component of the CW, closely intertwined with cellulose at limited sites, promoting selective targets for CW loosening, the so called “biomechanical hotspots” theory. Other modifications in the same network as well as in the pectin structure can, conversely, result in CW stiffening and suppression of cell elongation (Takeda et al. 2002), also contributing to CW integrity and rigidity. In fact, hydrolysis of methyl ester bonds at GalA residues, leading to alterations in linear homogalacturonan (HG) domains, degree and pattern of pectin methyl esterification, significantly impacts CW biophysical properties (Peaucelle et al. 2008; 2011; Jolie et al. 2010).

The role of CW synthesis and modification has been investigated through quantification of related enzymes activity and gene expression and the enzyme biological function has been disclosed in genotypes impaired or overexpressing specific gene members (e.g. Osato et al. 2006; Peaucelle et al. 2008; Miedes et al. 2010).

In knocked-out cellulose synthase (CesA) *Arabidopsis thaliana* mutants an effective reduction in cellulose content was observed together with moderate abnormal growth (Desprez 2007; Handakumbura et al. 2013) confirming other results on CesAs requirement for cellulose synthesis (Somerville 2006; Endler and Persson 2011). Nonetheless, CesA activity is insufficient to guarantee the correct formation of the network suggesting that the coordinated participation of other components is needed for cellulose synthesis, assemblage or deposition (Takahashi et al. 2009). Mutations impairing the expression of KORRIGAN (KOR), a class A β-1,4-endo-glucanase (GH9A) (Urbanowicz et al. 2007a), demonstrate the requirement of KOR for the correct assemblage in elongating cells (Nicol et al. 1998) since they show a significant reduction in cellulose content even when the expression of all CesA members was normal. This reduction was apparently compensated with increased pectin amounts and altered composition, particularly an increased glucose content (Sato et al. 2001). Recently Vain et al (2014) showed that KOR is an integral part of the CesA complex. A role for a poplar class C β-1,4-endo-glucanase (GH9C) member in modulating cellulose crystallinity and its involvement in cell growth was recently demonstrated using reverse genetic approaches (Glass et al. 2015).

Regarding CW remodeling, expansins (EXP), proteins with the ability to cause loosening in *in vitro* assays (McQueen-Mason et al. 1992), are considered the major contributors, acting by reversible weakening interactions or disrupting hydrogen bonds between cellulose microfibrils and matrix-linked glycans (McQueen-Mason and Cosgrove 1995; Cosgrove 2000; Whitney et al. 2000; Wang et al. 2013). Among the expansin superfamily, α-expansins (EXPA) are the foremost promoters in controlling cell extensibility in dicots (Cosgrove 1999; 2000). As reviewed by Choi et al. (2006), genetic modification allowed associating EXPAs to cell enlargement and fruit softening among other effects on plant growth and development. Other members of CW enzyme families were further

demonstrated to cause CW extensibility under *in vitro* conditions, namely some xyloglucan endotransglycosylases/hydrolases (XTHs) (Van Sandt et al. 2007) and endoglucanases (GHs) (Yuan and Cosgrove 2001; Park and Cosgrove 2012). Tomato hypocotyls over-expressing or suppressed in a specific XTH produced respectively increased and decreased levels of soluble XET activity, and a positive correlation with CW extensibility and organ growth was observed (Miedes et al. 2010). With a specific *Arabidopsis* RNAi-silenced XTH Osato et al. (2006) obtained a small but significant reduction in primary root cell elongation recently confirmed in Wilson et al. (2015) using multi-omics analysis. Similarly, also in *Arabidopsis*, the down-regulation of a specific class C β-1,4-endo-glucanase (GH9C) led to weakening of the CW during root hair formation and growth (del Campillo et al. 2012). The regulation, pattern and extent of pectin de-esterification is controlled by the activity of particular members of pectin methylesterases (PMEs) (reviewed by Goulao 2010) and their interaction with specific inhibitors (PMEI) (Bellincampi et al. 2004; Di Matteo et al. 2005; Juge 2006; Jolie et al. 2010) and therefore, are among the main enzymes to impact changes in biophysical properties of the CW. It is proposed that depending on the specific pattern and degree of methylesterification, pectins can aggregate into hydrated calcium-linked gel structures, that increase wall stiffness and reduce creep (Willats et al. 2001), or make pectins more susceptible to depolymerisation by polygalacturonases (PGs) and pectate lyases (PLs) hydrolysis contributing to CW relaxation (Brummell and Harpster 2001; Wakabayashi et al. 2003). In Arabidopsis mutants over-expressing a PME or a PMEI, Peaucelle et al. (2008; 2011) observed respectively, decreased and increased pectin methylesterification, suggesting CW loosening is generated by PME activity. This assumption was confirmed in other works using *Arabidopsis* mutants impaired in PME activity with evidence of inhibition of cell elongation (Derbyshire et al. 2007) and reduction in the degree of methylesterification (Hongo et al. 2012). Models of CW architecture are supported by evidences for the presence of covalent bonds between pectin chains and cellulose microfibrils (Zykwinska et al. 2005; 2007; Park and Cosgrove 2015) or matrix-linked glycans (Popper and Fry 2005; Marcus et al. 2008) disclosing important ties in CW biochemistry and an under-looked role played by PMEs and PMEIs in CW mechanical properties. Furthermore, under conditions that drastically compromise the CW integrity, plant

cells are known to trigger compensatory alternative mechanisms to its reinforcement via biosynthesis of new material or establishment of new linkages (Pilling and Hofte 2003; Wolf et al. 2012), adding additional complexity to the fine-tuned process of CW responses to development-impacting stimuli.

Using *Vitis vinifera* callus as a model experimental system we recently showed that individual mineral deprivation leads to CW structural modifications (Fernandes et al. 2013), in particular a decrease in cellulose compensated by an increase in lignin content, and modifications in pectin methyl esterification. This suggests a specific level of control to produce a complex fine-tuned sensing mechanism to maintain CW integrity. Plant CW-modifying enzymes are present in large multigenic families (Lerouxel et al. 2006; Farrokhi et al. 2006), involving more than 2000 genes (Carpita et al. 2001) with distinct patterns of expression among cells and tissues.

To extend our previous results on the CW specific composition and arrangement modifications in response to individual mineral deprivation at molecular regulation level, a comprehensive in silico data mining was undertaken to retrieve the sequence of all identified members of *V. vinifera* candidate CW-modifying multigenic families and the expression of amplified sequences in callus was quantified. The potential loosening activity of salt extracts from callus growing under mineral deficiency was addressed and an extensometer-based experimental approach was used to evaluate in vivo mechanical modifications on dicot CW specimens.

3.2. Material and methods

3.2.1. Callus culture and mineral stress imposition

Callus tissues established from *Vitis vinifera* cv. Touriga Nacional leaves were obtained as described in Jackson et al. (2001). Four explants with *circa* 4.5 g total weight per 9cm Ø Petri dish were growing in MS basal salts medium (Murashige and Skoog 1962) (DuchefaBiochemie, Haarlem, NL) supplemented with 2.5 µM 2.4–D (2,4–dichlorophenoxy–acetic acid); 1 µM kinetin; 5 g l^{-1} PVP–40T; 20 g l^{-1}, sucrose; 2 g l^{-1} Gelrite®, pH 5.7, at 25 ºC, in the dark. Following the experimental conditions described in Fernandes et al. (2013) callus tissue was sub-cultured

every three weeks, for a total of 9 weeks. To obtain the samples under imposed mineral deficiency (mineral stresses), four treatments were applied: i) MS complete medium (control), and ii) nitrogen (–N), iii) phosphorus (–P), iv) sulfur (–S) deficient media, in which nitrates, phosphates and sulfates were replaced by chlorides. After each three weeks culture cycle in each treatment medium, samples corresponding to three Petri dishes were collected to monitor growth. Based on the results obtained, callus grown for 6 weeks (2×3 weeks) were used immediately for microscopy studies or stored at -80ºC for subsequent extraction of protein salt extracts or RNA.

3.2.2. Histological staining

Samples of callus tissue were gently disaggregated in PBS buffer and incubated with 2-3 drops of 0.1% (w/v) Calcofluor White fluorescent brightener (Sigma, St. Louis, MO) for cellulose detection. The material was then transferred to a microscope slide with a cover slip and visualized with a Leitz Laborlux S Fluorescence Microscope under UV light. Images were acquired with a Zeiss AxioCam digital camera. Pectic polysaccharides were stained according to the same procedure, but in this case, Calcofluor was replaced by 2-3 drops of 1% (w/v) Toluidine Blue and the slides were observed under light microscopy. Cells were measured using the Carl Zeiss Vision AxioVision Viewer 4.

3.2.3. Immunolocalization with monoclonal antibodies

Callus were gently disaggregated and equilibrated in 5% dry milk/PBS for 30 min at RT and then incubated overnight at 4°C with a 10-fold dilution of 2F4 or PAM1 antibodies (Liners et al. 1989; Willats et al. 1999) diluted in 5% non-fat dry milk/PBS. After extensive washing with PBS, a 30-fold dilution of the secondary antibody (anti-mouse IgG and anti-rat IgG (Sigma), respectively) was applied to the sections and left to incubate for 60 min in the dark. For negative controls the primary antibodies were omitted. The slides were then washed with PBS and briefly incubated with 1% (w/v) Calcofluor White in distilled water, rinsed and mounted on a microscope slide. Sections were observed with a Leitz Laborlux S Fluorescence Microscope and images were acquired using a Zeiss AxioCam

digital camera. The Images were superimposed and analysed using the ImageJ 1.48 package (http://imagej.nih.gov/ij/). Average number of blue pixels (Calcofluor) and green pixels (PAM1 and 2F4) were quantified.

3.2.4. Gene expression analyses

3.2.4.1. Database mining and sequence retrieval of *V. vinifera* CW-related genes

Sequences from members of the CesA, EXPA, XTH, EGase from here on referred as GH9 (http://www.cazy.org), PME and PMEI families were retrieved by multiple database searches for *V. vinifera* and three other model species with sequenced genomes, namely tale cress (*Arabidopsis thaliana*), rice (*Oryza sativa*) and poplar (*Populus trichocarpa*). The NCBI (http://www.ncbi.nlm.nih.gov/) and Genoscope 12X (http://www.genoscope.cns.fr/spip/) databases were used for *Vitis vinifera* gene searches while TAIR (http://www.arabidopsis.org/index.jsp), OryGenesDG (http://orygenesdb.cirad.fr/cgi-bin/gbrowse/odb_japonica/?name=Os_1:1..10000) and Phytozome (http://www.phytozome.net/poplar) were mined for *Arabidopsis*, *Oryza* and *Populus*, respectively. In each case, after identification of the amino acid sequence, the same database was mined for each hit to retrieve the full-length cDNA sequence of the predicted corresponding gene. *V. vinifera* sequences were named according to their similarity with *Arabidopsis* orthologous. After prediction (SignalP 4.0; Petersen et al. 2011) and removal of signal peptides from the amino acid sequences, alignments were performed using MUSCLE software (Edgar 2004a; 2004b) and curated by Gblocks software (Talavera and Castresana 2007). The dendrograms were constructed using PhyML (Guindon 2010), and viewed using TreeDyn software (Chevenet et al. 2006). Putative biological activity was inferred from amino acid sequences using InterProScan 5 (http://www.ebi.ac.uk/Tools/pfa/iprscan5/; Quevillon et al. 2005. Tertiary structure- models were predicted using the alignment-based modelling tools SWISS-MODEL (http://swissmodel.expasy.org/; Arnold et al. 2006) and SwisspdbViewer DeepView 4.0 (http://www.expasy.org/spdbv/; Guex and Peitsch 1997).

3.2.4.2. RNA extraction and cDNA synthesis

Total RNA was extracted from *V. vinifera* callus using the method described by Reid et al. (2006). RNA samples were further treated with RNase-free DNase I (Qiagen) according to the manufacturer protocol. Quantification was carried out in a Synergy HT Multiplate Reader, with Gene5 software, using a Take3™ Multi-Volume Plate (Bio-Tek Instruments Inc. Winooski, USA). For reverse transcription, the RevertAid reverse transcriptase priming with oligo-d(T) kit was used (Thermo Scientific) according to the manufacturer's recommendations.

3.2.4.3. Quantification of gene expression by quantitative Real-Time PCR (RT-qPCR)

For each *V. vinifera* cDNA sequence retrieved, a set of specific primers were designed (Supplementary Table 3.1) and used to amplify callus grapevine cDNA resulting from the transcription of 2 µg of total RNA, using conventional PCR and gel agarose electrophoresis. When amplification was observed, confirming the expression in callus tissues, the transcripts were quantified by real-time PCR (RT-qPCR), performed in 20 µL reaction volumes composed of cDNA derived from 2 µg RNA, 0.5 µM gene-specific primers (Supplementary Table 3.1) in SsoFast™ EvaGreen® Supermixes (Bio-Rad, Hercules, CA) using a iQ5 Real-Time Thermal Cycler (BioRad, Hercules, CA). Reactions conditions for cycling were: 95ºC for 3 min followed by 40 cycles of 95ºC for 10 sec, 61ºC for 25 sec and 72ºC for 30 sec. Melting curves were generated in each case to confirm the amplification of single products and absence of primer dimerization. Each analysis was performed in triplicate reactions of three biologic replicates. The corresponding quantification cycles (C_q) were determined by the iQ5 optical system software (Bio-Rad, Hercules, CA) and exported to a MS Excel spreadsheet (Microsoft Inc., CA) for further analysis. Cq values of each gene of interest were normalized with respect to actin (Act) and translation initiation factor eIF-3 subunit 4 (TIF) Cqs (Coito et al. 2012). Relative gene expression values in the absence of a given nutrient (–N, –P, –S) are presented as $\log_2$ fold-change values in relation with the

control conditions (C). Heat Map was performed with Pearson correlations using the MeV software (Saeed et al. 2003).

3.2.5. Evaluation of callus salt extract potential to induce CW extensibility

3.2.5.1. Preparation of salt extracts

Samples of 20 g (FW) *V. vinifera* callus tissues growing under each experimental condition were cut into small pieces and washed with 20 mM NaOAc pH 4.5 buffer. The washed callus samples were filtered by vacuum and the flowthroughs were discarded. Twenty milliliters of a 20mM NaOAc; 1M KCl pH 4.5 solution were then added to the callus were incubated for 30 min at 4ºC, filtered and each solution was concentrated to 1 ml using Amicon Ultra Ultracell 3K columns (Millipore) as per the manufacturer's recommendations and desalinized with PD-10 desalting columns (cut-off 5 kDA) (GE, Fairfield, USA). Protein in each callus-derived extract was quantified using the Bradford method (1976) with BSA as standard. The same extracts were evaluated for ability to induce extensible deformation in cucumber hypocotyl sections, taken as model for dicot CW specimens, and tested for β-1,4-endo-glucanase activity.

3.2.5.2. Extensibility assays

Cucumber seeds were sown at 25ºC, in the dark and germinated hypocotyl apical zones (3 cm) were cut and stored at -20ºC. Prior to the analyses, the hypocotyls cuticles were abraded using carborundum powder and samples were boiled for 15 sec. to inactivate endogenous enzymes. The hypocotyls were then assayed clapped to tension grips in a TA-XT Texture Analyser (Stable Micro Systems Ltd, UK), using a custom made clamping reservoir filled with 50 mM NaOAc pH 4.5 buffer. A 20g load tensile force was applied with a 1.5 mm test length between clamps and, after a 20 min period of extension for equilibration, the buffer was replaced by each saline extract solution being tested and assayed for additional 15 min. The force was then removed during 10 min and reapplied for additional 20 min, to allow calculation of total, plastic and elastic extensibilities (Cosgrove 1993). Total extensibility was calculated as the maximum hypocotyl length at constant load. Plastic extensibility was calculated as the minimum value reached

after force removal. Elastic extensibility is the difference between the Total and Plastic extensibility (Richmond et al. 1980). Each experiment was performed using at least 6 independent samples for each treatment.

3.2.6. β-1,4-endo-glucanase activity

Endo-acting glycosyl hydrolase activity was measured by the change in viscosity of a carboxymethylcellulose (CMC) (medium viscosity, Sigma) solution (Durbin and Lewis 1988). One hundred µl of each salt extract, at a concentration of 3 µg μl^{-1}, was added to 350 ml of a 1.5% (w/v) CMC solution in 20 mM phosphate buffer pH 6.0, incubated for 6h at 37ºC. Viscosity was determined by measuring the time taken for the movement of the mixture through the 0 and the 0.05 ml marks of a 0.1 mL glass pipette fixed in a vertical position using a stopwatch. Readings were taken at time 0, 2 h and 6 h in triplicates. Activity is reported as the decrease in viscosity (%) with respect to time zero.

3.2.7. Statistical analysis

All data is presented as mean values ± standard deviation (SD) of an appropriate number of replicates in each assay. The results were statistically evaluated by variance analysis (ANOVA) and post hoc Bonferroni test with a $p<0.05$ to compare the significance of each treatment effect. The SigmaPlot (Systat Software Inc.) statistical package was used.

3.3. Results

3.3.1. Callus growth in –N, -P and –S and full MS medium

The effect of the imposed individual mineral stresses on the *Vitis* callus was assessed by measuring the callus growth along time. After withdrawing of nutrients, the relative growth of the callus was significantly affected in the three cycles when compared to the control (Supplementary Fig. 3.1). After the first cycle, –N callus was the most affected; at the end of the second cycle the three mineral stresses severely affected callus growth impairing their viability thereafter. So, six-week-old callus were selected for subsequent analyses.

3.3.2. Cell morphology in response to mineral deficiencies

A first indication of the effect of stress imposition in the callus was gained through measurement of cell anatomical parameters. Except for sulfur, the absence of individual minerals produced changes in the morphology of *V. vinifera* callus cells (Table 3.1). Noticeably, the deprivation of each mineral effected different alterations to the cell morphology. Under nitrogen starvation the cells were longer but had a similar width, when compared with the control. On the other hand, under phosphorus depletion the cells were longer and wider than the control, although still shorter than under –N conditions (Table 3.1).

Table 3.1 Length and width of *V. vinifera* callus cells measured after two three weeks growth cycles in MS medium (control), and in the absence of nitrogen (–N), phosphorus (–P) and sulfur (–S). Values are the mean ± SD of 20 random cells. Different letters in each row indicate significant differences at $p<0.05$.

	Control	**–N**	**–P**	**–S**
Length (µm)	121.0^{a} ± 12.1	228.7^{b} ± 38.9	147.9^{c} ± 19.1	130.5^{a} ± 13.3
Width (µm)	48.6^{a} ± 3.5	47.2^{a} ± 2.7	49.4^{b} ± 2.0	48.1^{a} ± 3.2

3.3.3. In situ localization of callus CW polymers and epitopes

Calcofluor White was used to detect CW matrix polysaccharide as it readily binds to cellulose. The absence of minerals in the medium resulted, in all callus tissues, in a reduced intensity of Calcofluor labeling. This reduction was more pronounced in samples produced under nitrogen starvation (Fig. 3.1; Supplementary Table 3.2). Toluidine Blue binds to carboxylated polysaccharides such as pectins, producing a reddish purple staining. As observed in Fig. 3.1, in the absence of nitrogen a more intense staining occurs. Immunolocalization with monoclonal antibodies targeted to specific CW epitopes is a useful tool to analyse *in vivo* detailed localization of CW components and was employed to ascribe putative modifications in the CW composition in response to the imposed stresses, targeting differences in methyl esterification patterns. The combined use of CW-

epitope antibodies and histological dyes enabled us to gain more detailed information regarding differences in the pectic composition. The results show that, under –N and –S conditions, an increase in 2F4 labelling, an antibody that recognizes the dimeric association of pectic chains through calcium ions, is observed in the whole cell, being more prominent in the middle lamella (Fig. 3.1; arrows). On the other hand, PAM1, which recognizes epitopes of long un-esterified blocks of GalA residues, did not bind to the boundaries of the cell in –P and –S callus tissues, while it was clearly noticeable in these specific regions in cells of callus growing under full nutrients and under nitrogen deprivation conditions (Fig. 3.1, arrows).

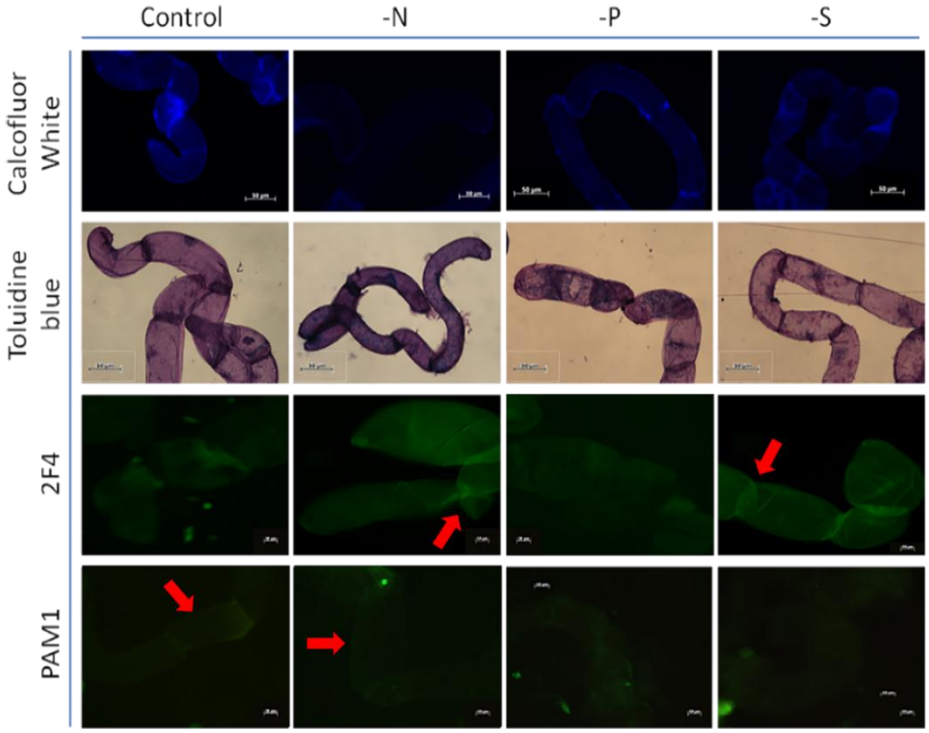

Fig. 3.1 Histological staining for cellulose and pectic polysaccharides and immunolocalization of 2F4 and PAM1 reactive homogalacturonan epitopes in callus grown under control and -N, -P and -S conditions. Immunolocalization samples were also stained with Calcofluor White to reveal anatomical details. 2F4 and PAM1 signals are shown in green. No label as observed when primary antibodies were omitted from control sections (not shown). The photos taken for Calcofluor White, 2F4 and PAM1 have the same exposition time for all treatments. Bar scale for histological observations represents 50 µm (and) and 10 µm for immunolocalization of 2F4 and PAM1.

3.3.4. Changes in gene expression of CW-related families

3.3.4.1. In silico analyses

The initial approach was to evaluate the relationship of CW synthesis and modification candidate gene families between *V. vinifera* and annotated genes in other flowering plants. *In silico* analysis showed that, in general, the *V. vinifera* genome has a similar number of members compared with *Arabidopsis*, *Oryza* and *Populus* for CW-related gene families that act on cellulose-hemicellulose complexes (Table 3.2). Noticeably, fewer PMEs were identified from *V. vinifera* and *O. sativa* than the other two species used for comparison. On the other hand, the number of PMEIs varied according to each individual species, being lower in *A. thaliana* (6 members) and higher in *O. sativa* (13 members). It should be however noted that database mining did not differentiate true PMEI from invertase inhibitors. A higher number of EXPAs was retrieved from the *O. sativa* genome.

Table 3.2 Number of genes related to primary CW biosynthesis and modification retrieved *in silico* from the higher plant sequenced species *Vitis vinifera*, *Oryza sativa*, *Populus trichocarpa* and *Arabidopsis thaliana* genomes.

	Vitis vinifera	*Arabidopsis thaliana*	*Oryza sativa*	*Populus trichocarpa*
CesA	**10**	10	10	18
Expansin superfamily	**30**	36	56	36
XTH	**33**	33	29	24
GH9	**21**	25	24	31
PME	**36**	66	37	84
PMEI	**11**	6	13	10

The dendrograms built with amino acid sequences, reveals that, in general, *V. vinifera* CW-related sequences cluster with orthologs from monocot, dicot and woody model species in most families (Supplementary Fig. 3.2, 3.3 and 3.4). Noticeably, in the XTH family, some clusters are enriched with *V. vinifera* sequences, suggesting specification with respect to evolution or a possible correlation with substrate specificity.

Since XTH genes encode proteins that can have two distinct catalytic activities, sequence alignments and structural *in silico* analysis were performed to distinguish putative xyloglucan endotransglucosylases (XET) from xyloglucan endohydrolases (XEH) (Supplementary Fig. 3.5). The XTH identity was confirmed by the presence in all *V. vinifera* sequences of the conserved catalytic motif (W/R)-(D/N)-E-(I/L/F/V)-D-(F/I/L/M)-E-(F/L)-(L/M)-G, as previously described by Eklöf and Brumer (2010) and XET or XEH putative activities were assigned based on the presence/absence of two insertions, (Y/N)-P-G and R-(I/L)-I-G-R (Supplementary Fig. 3.6) in the amino acid sequence (Eklöf and Brumer 2010). Based on these structural differences, two isoforms, VvXTH31 (XP_002275862) and VvXTH32 (XP_002269285), were identified. Despite the insertions, the structural similarity between XET and XEH was very high, as indicated by the superimposition of their backbones (Supplementary Fig. 3.5). The main difference occurs between species, especially in the C-terminus in which an α-helix is observed both in *Tropaeolum majus* and *Arabidopsis* but is absent in *V. vinifera*.

Likewise, PMEIs share structural properties with other invertase inhibitors and its classification was proposed to be possible based on the conformation features of an extension that precedes a four-helix bundle core (Scognamiglio et al. 2003). We notice a high similarity between *V. vinifera* and *Arabidopsis* PMEI, which show highly similar extension (Supplementary Fig. 3.7).

3.3.4.2. Changes in expression of key genes involved in the biosynthesis and modification of CW under mineral stress

One way of investigating the pathways of a given physiological event is to understand the transcription of related genes. Thus, isoforms of several gene families (Supplementary Table 3.1) were chosen based on their putative role in the synthesis and modification of CW after nutrient starvation. Fifty out of the 131 genes investigated (38.2%) were expressed in the callus tissue and their expression level was quantified by RT-qPCR as shown in Figs. 3.3 and 3.4 and more detail in Supplementary Table 3.3.

Although a similar number of genes had been up- and down- regulated in response to individual mineral stress imposition, the majority of them were downregulated in all treatments (Fig. 3.2). Seven showed up-regulation in all stress conditions (*VvCesA2*, *VvEXP8*, *VvXTH8*, *VvXTH10*, *VvPMEI2*, *VvPMEI3* and *VvPMEI4*) (Fig. 2a), while 16 were down-regulated in all treatments (*VvCesA4*, *VvXTH32*, *VvGH9A1*, *VvGH9C2*, *VvXTH2*, *VvEXP5*, *VvEXP3*, *VvEXP11*, *VvXTH15*, *VvPME1.17*, *VvPME1.18*, *VvPME1.19*, *VvPME2.4*, *VvPME2.7*, *VvPME2.14*, *VvPME2.20*) (Fig. 3.2b). The number of genes with detected altered expression was always higher in –N, followed by –P and lower in –S callus samples which, as showed by hierarchical clustering (Fig. 3.3) indicates that samples from –N callus tissues have more uncorrelated transcription patterns than the samples obtained under the other two conditions.

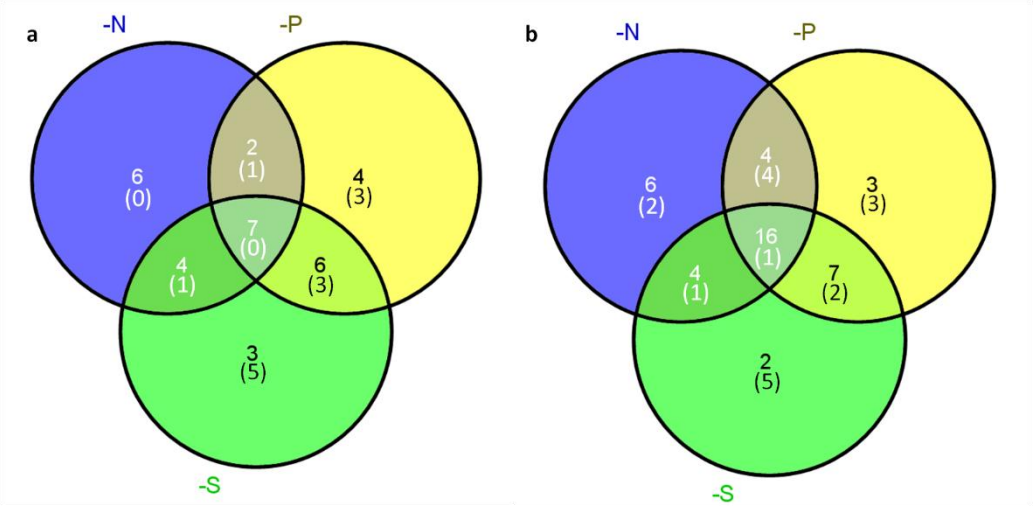

Fig. 3.2 Venn diagram summarizing the number of unique and common genes showing different trends of gene expression, up- (a) or down-regulated (b), in response to each individual mineral stress imposed (-N, -P and –S), when compared to control conditions. In brakets is the number of genes with more than two fold change. The Venn diagram was drawn using the Venny Tool (Oliveros 2007).

Concerning the genes studied that can be putatively associated with cellulose biosynthesis, the results indicated the up-regulation of one CesA gene in response to nitrogen (*VvCesA3*) and phosphorus (*VvCesA8*) deficiencies in the growing medium, and three members in response to sulfur (*VvCesA1-3*) deprivation. Conversely, the transcription of *VvCesA6* was 3-fold repressed under –S conditions. GH9A, which are orthologous to KORRIGAN genes, was not differentially expressed in response to the mineral stress imposition but a

severe reduction of 4.45 and 5.25 fold-change in the class C, *VvGH9C2*, transcript amounts was observed in samples growing under nitrogen and sulfur deficiency, respectively (Fig. 3.3).

EXPA gene expression was similarly regulated in response to nitrogen and phosphorus deficiencies, as illustrated by the down-regulation, in both cases, of two isoforms, *VvEXP6* and *VvEXP11* (Supplementary Table 3.3). Transcription impairment of those members was particularly severe in –P conditions (Fig. 3.3). Noticeably, VvEXP6 transcripts showed a 2-fold increase under -S starvation and the absence of this mineral in the growing medium repressed the transcription of three other EXPA family members (*VvEXPA5*, *VvEXPA19* and *VvEXPA20*).

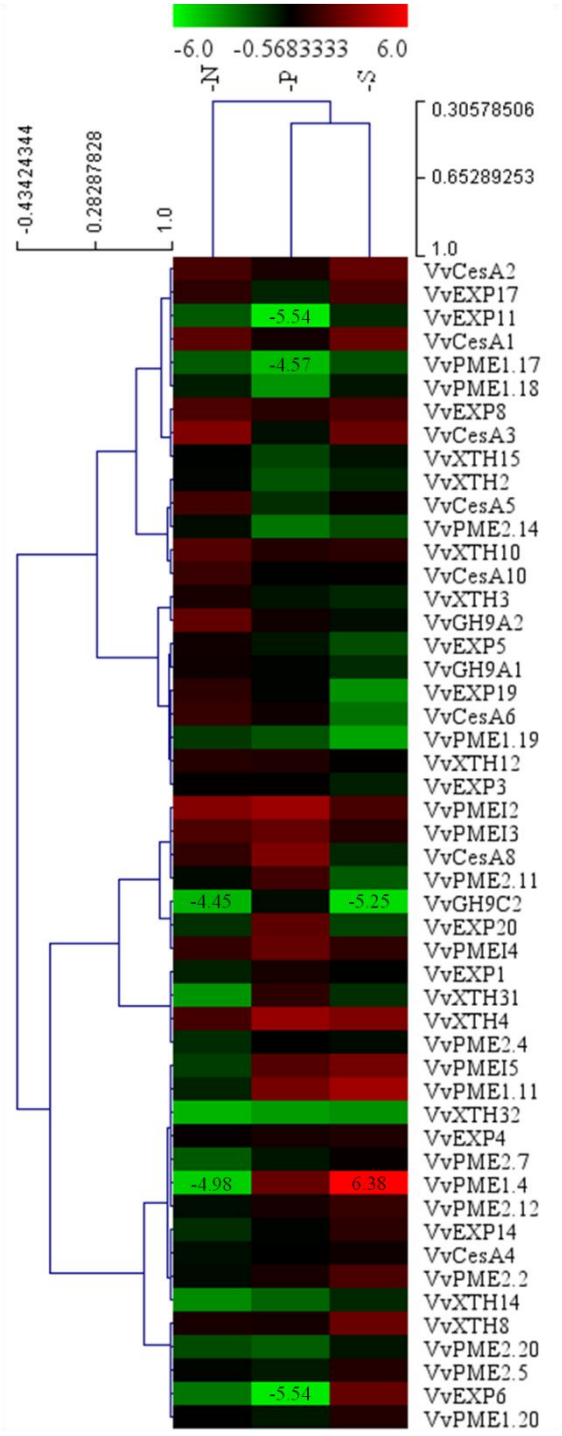

Fig. 3.3 Differentially expressed genes transcribed in callus under mineral stress imposition with respect to callus grown under complete medium. Hierarchical clustering was performed on 50 CW-modifying-encoding genes from candidate families showing express in callus tissues. Gene dendrogram (left) and condition dendrogram (top) were obtained using Pearson's uncentered distance metric calculated from all $\log_2$ transcription ratios (mineral stress /control). Color scale from green to red indicates $\log_2$ transcription ratios from 6-fold under transcription to 6-fold over transcription). The exact value of relative expression is given when a striking fold change of 4 was observed, although in this paper we discuss differences in gene expression when the fold change at least doubles. Each gene is identified by the code provided in Supplementary Table 3.1.

Out of the 10 XTH members expressed in callus tissue, two (*VvXTH31* and *VvXTH32*) were predicted to have hydrolase activity (Supplementary Fig. 3.6). The quantified gene expression of *VvXTH32* was significantly compromised in response to all stress conditions (Fig. 3.3). Moreover, *VvXTH31* was also strongly repressed under nitrogen deficiency (Supplementary Table 3.3). The remaining XTHs were differently regulated according to the specific experimental condition. Under nitrogen deficiency only *VvXTH14* was differently expressed, showing a 3.5 fold down-regulation. Under –P, which was the condition that affected more XTHs, this member was also repressed, together with *VvXTH2* and *VvXTH15* while *VvXTH4* showed a clear up regulation. On the contrary, under –S conditions no significant XTH down-regulation was detected, with two genes (*VvXTH4* and *VvXTH8*) up-regulated (Supplementary Table 3.3).

More PME genes were down-regulation under mineral starvation than up-regulated. The latter situation was observed for two members, *VvPME1.4* and *VvPME1.1*, in both –P and, to a higher extent, –S conditions. About 1/3 of the PME genes quantified were down-regulated in each experimental condition. Some displayed the same pattern in response to more than one stress, namely *VvPME1.19* and *VvPME2.14* under –P and –S, and *VvPME2.20* under –N and –P. *VvPME1.17* was down-regulated in response to all stresses. Highlighted is the response of *VvPME1.4* which was severely impaired under –N (5-fold down regulation) and strongly induced under sulfur starvation (6-fold up-regulation) (Fig. 3.3). Interestingly, under mineral depletion, PMEI gene expression was generally up-regulated, although a different member was affected according to each individual mineral stress under –N and –S conditions and phosphorus starvation significantly impacted three out of the four PMEIs expressing in *V. vinifera* callus tissues. Collectively PME down-regulation results suggest a reduction in enzymatic de-esterification potential under imposed mineral stress.

3.3.5. Loosening activity from callus extracts

The occurrence of different amounts and relative proportions of the protein mixture that acts on the CW to alter its structural properties can be addressed by measuring the changes in extension that are able to induce. Salt extracts from the four experimental samples were added to cucumber hypocotyls, used as model dicot CW specimens, in an extensometer assay and a significant increase in the total deformation was observed when the –N and –P extracts were used (Fig. 3.4). The effect was more evident in extracts isolated from –N callus even though the total quantity of extractable proteins had been lower than in the other conditions (Fig. 3.4. Inset). The higher total deformation observed is the direct result of an increase of the plastic deformation since the elastic deformation was not significantly affected by any of the mineral stresses. Endoglucanase activity was estimated through a viscosity test where the higher the decrease in CMC substrate viscosity after incubation with acting enzyme solutions, the higher the enzymatic activity. After two hours incubation, the extracts prepared from –N callus showed significantly lower activity than all the other treatments, while in those obtained from –S and –P higher activities were measured as compared to the control (Fig. 3.5).

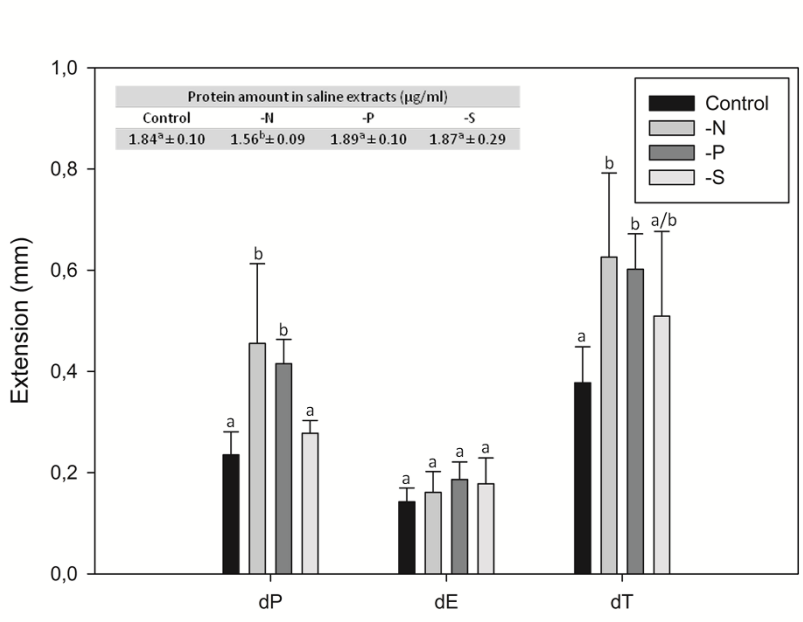

Fig. 3.4 Plastic (dP), Elastic (dE) and Total (dT) deformation of cucumber hypocotyls when saline extracts from callus grown under nitrogen (-N), phosphorus (-P), sulfur (-S) depletion and control were applied. Inner table represents the protein quantification for the salt extracts from -N, -P, -S and control ± SD. The same amount of soluble protein, in each treatment, was used in all tests Different letters indicate significant differences at $p<0.05$.

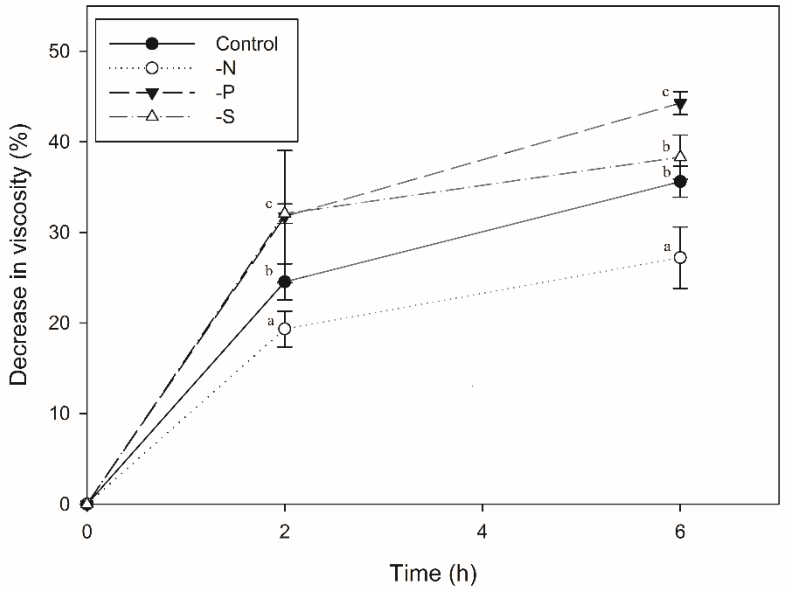

Fig. 3.5 β-1,4-endo-glucanase activity of salt extracts from callus grown under nitrogen (-N), phosphorus (-P), sulfur (-S) depletion and control. Activity is given as the decrease in viscosity (%) with respect to time zero. The same amount of soluble protein, in each treatment, was used in all tests Different letters indicate significant differences at $p<0.05$.

3.4. Discussion

Taking advantage of the optimized experimental callus model system, insights on the regulation underlying the effects of limiting nutrient supply to cell development through CW dynamics were gained. Previous work based on FT-IR spectroscopy and biochemical quantification of CW components reported changes in the amount or rearrangements of cellulose and matrix linked glycans, in the levels of pectin methyl-esterification and in the strength the polysaccharides association to the CW as the main effects induced by N, P and S mineral deprivation (Fernandes et al. 2013).

Confirming biochemical changes observed (Fernandes et al. 2013), under mineral stress a reduction in cellulose and an increase in pectin contents were perceived via Calcofluor and toluidine blue labeling, respectively. Similarly, higher labelling by the antibody identifying dimeric associations of pectic chains through calcium ions, 2F4, was detected in –N callus, supporting the evidence of a lower

degree of methyl-esterification, and the promotion of conditions favorable to the formation of calcium bridges (Pelloux et al. 2007).

CW-biosynthesis and modification associated genes are present in large multigenic families with related overlapping functions which may lead to compensatory mechanisms for the transcription changes of most of these genes (Giovannoni 2004). Making use of the sequenced *V. vinifera* genome availability (Jaillon et al. 2007; Velasco et al. 2007), a comprehensive *in silico* analysis was conducted to, in a first step, compare the size of the gene families with other plant model species. Then, the transcription pattern of genes encoding CW synthase, hydrolase, trans-glycosylase, expansin and esterase enzymes which, based on their known modes of action and combined activity may result in the observed changes, were examined. This approach was complemented with the evaluation of salt extracts loosening-promoting activity on dicot CW specimens (Fig. 3.4 and Fig. 3.5).

Most of the *V. vinifera* CW-related gene families include a similar number of members to *A. thaliana*, *O. sativa* and *P. trichocarpa*. Moreover, the dendrogram analysis of *V. vinifera* CW-related amino acid sequences, showed clustering with orthologues from those in model species (Supplementary Fig. 3.2; 3.3; 3.4), as previously observed by Baumann et al. (2007), suggesting conservation of CW biosynthesis and modification mechanisms throughout Angiosperm evolution.

Gene expression of key candidate genes above a $\log_2$ +/- 2-fold change relative to the control showed that responsive members were detected in all families (Fig. 3.2 and Supplementary Table 3.3). Despite the impact of nitrogen starvation, leading to more dramatic developmental and morphological modifications in callus tissues (Fernandes et al. 2013; Supplementary Fig. 3.1), a lower number of genes with significant expression alteration, was observed. (Fig. 3.3 and Supplementary Table 3.3). Lower levels of cellulose were detected under –N and –P (Fernandes et al. 2013; Fig.2), which lead us to investigate the gene expression of families associated with cellulose biosynthesis. *CesA*s are present in multigenic families with at least 10 members in *A. thaliana*, 10 in *O. sativa* (Richmond and Somerville 2000), and at least 18 in *P. trichocarpa* (Suzuki et al. 2006). Except for *VvCesA6* under –S conditions, all other significantly

affected genes showed an increased (ca. 2-3 log_2 fold-change) transcript accumulation, not explaining the reduction in the observed cellulose content. In *Arabidopsis*, three distinct CesA proteins are required to produce cellulose (Desprez et al. 2007). If *VvCesA6* is the counterpart of *AtCesA6*, it can be assumed that the callus primary CW in our experimental system may be affected in a similar way to the *irregular xylem* (*irx*) mutant lines which harbor lesions in AtCesAs 4, 7, and 8 (Taylor et al. 2003). Accepting the hypothesis of non-redundancy, in the lack of one protein the assembly of the complex is impaired without formation of the cellulose microfiber (Desprez et al. 2007). Strikingly, *VviCesA* down-regulation was observed only under –S conditions, which is the only tested mineral that does not impact a reduction in cellulose content (Fernandes et al. 2013).

Nevertheless, CesA activity is not sufficient to produce cellulose, which requires the combined action with members from other gene families. Among those, the sub-classes A and C of the GH9 family is also known to interact in cellulose biosynthesis. Regarding class A, a mutant (KORRIGAN) impaired in GH9 gene expression has a dwarf phenotype and changes in the cellulose-XyG network, demonstrating that these gene members are essential for correct cellulose formation (Nicol et al. 1998). *V. vinifera* callus tissue growing under mineral stress did not show significant modifications in the expression of these gene members. On the other hand, class C GH9 harbor a cellulose binding module (CBM) rigidly attached to the C-terminus of the catalytic domain (Urbanowicz et al. 2007b), and its role in cellulose biochemistry was recently demonstrated in *P. trichocarpa*. In this species, a specific member, *PtGH9C2*, was shown to be involved in regulating the degree of cellulose crystallinity (Glass et al. 2015). As proposed by Fujita et al. (2011) this property regulates the rate of expansion of the primary CW by restricting the number of cross-links with hemicelluloses (Lai-Kee-Him et al. 2002). *PtGH9C2* may play a role in cessation of primary growth, thereby resulting in impaired or enhanced growth of poplar lines overexpressing or RNAi suppressed, respectively (Glass et al. 2015). Under mineral stress the only GH9C that expressed in callus tissues, *VvGH9C2*, was severely down-regulated under –N and, surprisingly, under –S conditions, showing an invariant expression pattern under –P (Fig. 3.1; Fig. 3.3 and

Supplementary Table 3.3). The observed reduction in endoglucanase activity under –N (Fig. 3.5) could cause the inhibition of microfibril crystallization and consequent increase cellulose-XyG cross-linking to reinforce the wall (Fujita et al. 2011).

Under –P and –S, specific XTH and PME family members were up-regulated, while others were repressed. This observation can be related to the opposite effects in CW modifications that, as previously discussed, particular members of both families can exert (Osato et al. 2006). Regarding XTHs, the enzymes encoded by this gene family can hold distinct activities, xyloglucan endotransglucosylase (XET), xyloglucan endohydrolase (XEH) or both, often to produce paradoxal effects on the CW (Eklöf and Brumer 2010). Hence the assignment of each *V. vinifera* XTH to a putative activity was conducted based on sequence analyses (Eklöf and Brumer 2010). As expected, and in accordance with Johansson et al. (2004) in *Populus*, key active-sites revealed subtle differences restricted to two loops outside the substrate-binding cleft, attributed to two insertions in XTH enzymes proposed to display XEH activity (Eklöf and Brumer 2010). Two *V. vinifera* XTH proteins displayed an insertion of those motifs, making them strong candidates as XEHs (Supplementary Fig. 3.6). The number of *V. vinifera* of XTH-XEH members is similar to the one in the *A. thaliana* genome (Baumann et al. 2007) and, in the present study, these genes were repressed under all mineral stresses, often at high levels. Recent studies reported by Kaewthai et al. (2013) demonstrate that these enzymes have no significant effect on growth patterns or developmental phenotypes, which may suggest their action as key enzymes in a XyG-recycling pathway where an excess of non-reducing ends leads to a reinforced XyG network (Sampedro et al. 2010; 2012). On the other hand, XTH genes may function redundantly (Matsui et al. 2005), with the repression of one member compensated by the up-transcription of others.

PME genes also belong to a multigene family (Markovic and Janecek 2004). Some members carry an N-terminal PRO region extension, which precedes a conserved domain similar to the PMEI domain (Jolie et al. 2010). Depending on the absence or presence of this PRO region, PMEs are classified into two subfamilies: type II/group 1 and type I/group 2 respectively (Micheli

2001). After the integration into the CW, PMEs can randomly or linearly de-esterify the HG chain. (Markovic and Kohn 1984). Random PME de-esterification activates the polygalacturonase activity promoting the CW loosening while linear PME de-esterification can promote Ca^{2+}-linked gel structures and stiffen the CW (Micheli 2001). It is often mentioned that plant PMEs with a basic pI, which represents most isoforms, act in a block-wise fashion, while plant PMEs with an acidic pI act in a nonblock-wise fashion (Bosch and Hepler 2005) making these families strong candidates to act in compensatory mechanisms within the same function. Hence, the lower global degree (Fernandes et al. 2013) and pattern (Fig. 3.1) of methyl-esterification observed under some mineral starvation conditions cannot be directly explained by the PME gene expression levels. In fact most PME genes were down-regulated and all PMEI genes were up-regulated with the exception of the basic PME1.4 and PME1.11 under -P and -S. From these findings we hypothesize that under mineral stresses the basic PMEs produces long linear stretches of unesterified HG chains promoting the formation of Ca^{2+}-linked gel structures and, in this way, stiffening the CW. As a whole, the results of gene expression changes in response to the individual mineral stresses are in accordance with previous evidence suggests that response and eventual adaptation are specific to each stress.

After incubation of protein salt extracts with heat inactivated cucumber hypocotyl under conditions that promote extensibility, increases in plastic deformation was observed with extracts from -N and -P callus (Fig. 3.4). Plastic deformation, meaning an irreversible increase in length after removal of an applied stretching force, is a necessary condition for the wall-loosening reactions involved in growth (Hohl and Schopfer 1992). Expansins and XTHs are CW-loosening agents that regulate CW expansion and cell enlargement through elastic deformation (Cosgrove, 2000; Miedes et al 2013). The general down-regulation of α-expansin and most XTHs genes in V. vinifera callus tissues observed in response to mineral stress are in line with the results obtained in extensibility tests, where no alteration in the elastic component of the deformations was observed.

Considering the gene expression results discussed above, it may be speculated that the lower proportion of hydrolytic enzymes present in the protein

extracts obtained under mineral stress conditions had a less effect on the cucumber hypocotyl CWs polysaccharides. This feature may promote irreversible modifications in the physical properties due to mechanical, non-enzymatic effects. In fact under nitrogen deprivation, *XTH*-XEH, *GH9C* and *PME* expression in callus were among the genes most dramatically down-regulated, along with the reduced activity of endoglucanase under –N, suggesting that the putative encoding enzymes are present at lower levels in the extracts applied to the inactivated dicot CW samples.

The use of ssNMR CW analyses unraveled that less than 8% of cellulose surface is in contact with XyG (Bootten et al. 2004; Dick-Perez et al. 2011), with pectins filling the gaps. Pectins are presented as very dynamic polymers which due to their hydrophilic character may ease microfibrils motions as CW expands, reducing the direct cellulose–cellulose contacts (Park and Cosgrove 2015). Instead of XyG, pectic monosaccharides (most likely from RG-I side chains galactan and arabinan rich (Zykwinska et al. 2007; 2008)) may be associated to the cellulose (Cosgrove 2014). Pectins can then serve as mechanical tethers between microfibrils (Wang et al. 2012; Peaucelle et al. 2012). Using the same system we had previously observed an increase in arabinose under –N conditions leading to CW reinforcement although still allowing significant plastic deformation (Fig. 3.4). These results agree with the presence of “biomechanical hotspots” as proposed by Park and Cosgrove (2012; 2015) in which wall extensibility is less dependent on the viscoelasticity of the matrix polymers depending more of the selective separation between microfibrils at limited CW sites.

The role of hydrolytic enzymes in CW loosening was formerly envisioned as the prime players in the expansion process (Farkas and Maclachlan 1988; McDougall and Fry 1990). Although it is not clearly acknowledged that they break glycosidic bonds of crystalline cellulose (Vissenberg et al. 2001; Cosgrove 2005), it is recognized that their activity could contribute to the loosening of the CW, making it more pliable for expansion (Cosgrove, 2005). Park and Cosgrove (2012) reported that β-1,4-endo-glucanases may induce plastic deformation. This assumption agrees with our observations on the increase in endoglucanase activity and the increase in plastic deformation under –P.

The results taken as a whole support the hypothesis that different mineral stresses impact different responses in the CW-related mechanisms that underlie development, with nitrogen effecting those responses more dramatically and sulfur leading to less pronounced responses. This may be due to the vital role of nitrogen in plant metabolism. In fact, as key element in protein synthesis, nitrogen depletion can redirect the metabolism preventing protein compensation by other members of the same family.

Acknowledgments

The research was funded by Fundação para a Ciência e a Tecnologia (FCT) project PTDC/AGR-GPL/099624/2008, CBAA (PestOE/AGR/UI0240/2011) and Grant SFRH/BD/64047/2009 to JCF.

References

Arnold K, Bordoli L, Kopp J, Schwede T (2006) The SWISS-MODEL Workspace: A web-based environment for protein structure homology modelling. Bioinformatics 22:195-201. doi: 10.1093/bioinformatics/bti770

Baumann MJ, Eklof JM, Michel G, Kallas AM, Teeri TT, Czjzek M, Brumer H III (2007) Structural evidence for the evolution of xyloglucanase activity from xyloglucan endo-transglycosylases: biological implications for cell wall metabolism. Plant Cell 19:1947–1963. doi: 10.1105/tpc.107

Bellincampi D, Camardella L, Delcour JA, Desseaux V, D'Ovidio R, Durand A, Elliot G, Gebruers K, Giovane A, Juge N, Sorensen JF, Svensson B, Vairo D (2004) Potential physiological role of plant glycosidase inhibitors. BBA Proteins Proteomics 1696:265–274. doi: 10.1016/j.bbapap.2003.10.011

Bootten TJ, Harris PJ, Melton LD, Newman RH (2004) Solid-state 13C-NMR spectroscopy shows that the xyloglucans in the primary cell walls of mung bean (*Vigna radiata* L.) occur in different domains: a new model for xyloglucan-cellulose interactions in the cell wall. J Exp Bot 55: 571-583. doi: 10.1093/jxb/erh065

Bosch M, Hepler PK (2005) Pectin methylesterases and pectin dynamics in pollen tubes. Plant Cell 17:3219-3226. doi: 10.1105/tpc.105.037473

Bradford MM (1976) A rapid and sensitive method for the quantitation of microgram quantities of protein utilizing the principle of protein-dye binding. Anal Biochem 72: 248–254

Braidwood L, Breuer C, Sugimoto K (2014) My body is a cage: mechanisms and modulation of plant cell growth. New Phytol 201:388–402. doi: 10.1111/nph.12473

Brummell DA, Harpster MH (2001) Cell wall metabolism in fruit softening and quality and its manipulation in transgenic plants. Plant Mol Biol 47:311–340. doi: 10.1023/A:1010656104304

del Campillo E, Gaddam S, Mettle-Amuah D, Heneks J (2012) A tale of two tissues: AtGH9C1 is an endo-β-1,4-glucanase involved in root hair and endosperm development in *Arabidopsis*. PLoS One 7: e49363. doi: 10.1371/journal.pone.0049363.

Carpita N, Tierney M, Campbell M (2001). Molecular biology of the plant cell wall: searching for the genes that define structure, architecture and dynamics. Plant Mol Biol 47:1-5. doi: 10.1023/A:1010603527077

Chevenet F, Brun C, Banuls AL, Jacq B, Chisten R (2006) TreeDyn: towards dynamic graphics and annotations for analyses of trees. BMC Bioinformatics 7:439. doi:10.1186/1471-2105-7-439

Choi D, Cho HT, Lee Y (2006) Expansins: expanding importance in plant growth and development. Physiol Plantarum 126:511-518. doi: 10.1111/j.1399-3054.2006.00612.x

Coito JL, Rocheta M, Carvalho L, Amâncio S (2012) Microarray-based uncovering reference genes for quantitative real time PCR in grapevine under abiotic stress. BMC Res Notes 5:220. doi: 10.1186/1756-0500-5-220.

Cosgrove DJ (1993) How do plant cell walls extend? Plant Physiol 102:1-6.

Cosgrove DJ (1999) Enzymes and other agents that enhance cell wall extensibility. Annu Rev Plant Physiol Plant Mol Biol 50:391–417. doi: 10.1146/annurev.arplant.50.1.391

Cosgrove DJ (2000) Loosening of plant cell walls by expansins. Nature 407:321–326. doi: 10.1038/35030000

Cosgrove DJ (2005) Growth of the plant cell wall. Nat Rev Mol Cell Biol 6:850–861

Cosgrove DJ, Jarvis MC (2012) Comparative structure and biomechanics of plant primary and secondary cell walls. Front Plant Sci 3:204. doi: 10.3389/fpls.2012.00204

Cosgrove DJ (2014) Re-constructing our models of cellulose and primary cell wall assembly. Curr Opin Plant Biol 22:122-31. doi:10.1016/j.pbi.2014.11.001

Derbyshire P, McCann MC, Roberts K (2007) Restricted cell elongation in *Arabidopsis* hypocotyls is associated with a reduced average pectin esterification level. BMC Plant Biol 7:31. doi:10.1186/1471-2229-7-31

Desprez T, Juraniec M, Crowell EF, Jouy H, Pochylova Z, Parcy F, Höfte H, Gonneau M, Vernhettes S (2007) Organization of cellulose synthase complexes involved in primary cell wall synthesis in *Arabidopsis* thaliana. Proc Natl Acad Sci USA 104:15572–15577. doi: 10.1073/pnas.0706569104

Di Matteo A, Giovane A, Raiola A, Camardella L, Bonivento D, De Lorenzo G, Cervone F, Bellincampi D, Tsernoglou D (2005) Structural basis for the interaction between pectin methylesterase and a specific inhibitor protein. Plant Cell 17:849-858. doi: 10.1105/tpc.104.028886

Dick-Perez M, Zhang Y, Hayes J, Salazar A, Zabotina OA, Hong M (2011) Structure and interactions of plant cell-wall polysaccharides by two- and three-dimensional magicangle-spinning solid-state NMR. Biochemistry 50: 989-1000. doi: 10.1021/bi101795q

Doblin MS, Pettolino F, Bacic A (2010) Plant cell walls: the skeleton of the plant world. Funct Plant Biol 37:357–381. doi: http://dx.doi.org/10.1071/FP09279

Durbin ML, Lewis LN (1988) Cellulases in *Phaseolus vulgaris*. Methods Enzymol. 160:342–351. doi: 10.1016/0076-6879(88)60137-6

Edgar R (2004a) MUSCLE: a multiple sequence alignment method with reduced time and space complexity. BMC Bioinformatics 5:113. doi:10.1186/1471-2105-5-113

Edgar RC (2004b) MUSCLE: multiple sequence alignment with high accuracy and high throughput. Nucleic Acids Res 32:1792–1797. doi: 10.1093/nar/gkh340

Endler A, Persson S (2011) Cellulose synthases and synthesis in *Arabidopsis*. Mol Plant 4:199-211. doi: 10.1093/mp/ssq079

Eklöf JM, Brumer H (2010) The XTH gene family: an update on enzyme structure, function, and phylogeny in xyloglucan remodeling. Plant Physiol 153:456–466. doi: 10.1104/pp.110.156844

Farrokhi N, Burton RA, Brownfield L, Hrmova M, Wilson SM, Bacic A, Fincher GB (2006) Plant cell wall biosynthesis: genetic, biochemical and functional genomics approaches to the identification of key genes. Plant Biotechnol J 4:145–167. doi: 10.1111/j.1467-7652.2005.00169.x

Farkas V, Maclachlan G (1988) Stimulation of pea 1,4-β-glucanase activity by oligosaccharides derived from xyloglucan. Carbohydr Res 184:213-219.

Fernandes JC, García-Angulo P, Goulao LF, Acebes JL, Amâncio S (2013) Mineral stress affects the cell wall composition of grapevine (*Vitis vinifera* L.) callus. Plant Sci 205-206:111-120. doi: 10.1016/j.plantsci.2013.01.013.

Fujita M, Himmelspach R, Hocart CH, Williamson RE, Mansfield SD, Wasteneys GO (2011) Cortical microtubules optimize cell-wall crystallinity to drive unidirectional growth in *Arabidopsis*. Plant J 66:915–928. doi: 10.1111/j.1365-313X.2011.04552.x.

Giovannoni JJ (2004) Genetic regulation of fruit development and ripening. Plant Cell 16 Suppl:S170-80. doi: 10.1105/tpc.019158

Glass M, Barkwill S, Unda F, Mansfield SD (2015) Endo-β-1,4-glucanases impact plant cell wall development by influencing cellulose crystallization. J Integr Plant Biol 57:396-410. doi: 10.1111/jipb.12353.

Goulao LF (2010) Pectin de-esterification and fruit softening: revisiting a classical hypothesis. Stewart Postharvest Rev 1: 1-12. doi: 10.2212/spr.2010.1.7

Guex, N, Peitsch, MC (1997) SWISS-MODEL and the Swiss-PdbViewer: An environment for comparative protein modeling. Electrophoresis 18:2714-2723. doi: 10.1002/elps.1150181505

Guindon S, Dufayard J-F, Lefort V, Anisimova M, Hordijk W, et al. (2010) New algorithms and methods to estimate maximum-likelihood phylogenies: assessing the performance of PhyML 3.0. Syst Biol 59:307–321. doi: 10.1093/sysbio/syq010

Handakumbura PP, Matos DA, Osmont KS, Harrington MJ, Heo K,Kafle K, Kim SH, Baskin TI, Hazen SP (2013) Perturbation of *Brachypodium distachyon CELLULOSE SYNTHASE A4*or *7* results in abnormal cell walls. BMC Plant Biol 13:131. doi: 10.1186/1471-2229-13-131

Hohl M, Schopfer P (1992) Physical extensibility of maize coleoptile cell walls: apparent plastic extensibility is due to elastic hysteresis. Planta 187:498-504. doi: 10.1007/BF00199968

Hongo S, Sato K, Yokoyama R, Nishitani K (2012) Demethylesterification of the primary wall by PECTIN METHYLESTERASE35 provides mechanical support to the *Arabidopsis* stem. Plant Cell 24:2624-34. doi: 10.1105/tpc.112.099325

Jaillon O, Aury JM, Noel B, Policriti A, Clepet C, Casagrande A, Choisne N, Aubourg S, Vitulo N, Jubin C et al. (2007) The grapevine genome sequence suggests ancestral hexaploidization in major angiosperm phyla. Nature 449:463-467. doi:10.1038/nature06148

Jackson P, Galinha C, Pereira C, Fortunato A, Soares N, Amâncio S, Pinto Ricardo C (2001) Rapid deposition of extensin during the elicitation of grapevine callus cultures is specifically catalysed by a 40 kDa peroxidase. Plant Physiol 127:1065-1076. doi: http://dx.doi.org/10.1104/pp.01019

Johansson P, Brumer H 3rd, Baumann MJ, Kallas AM, Henriksson H, Denman SE, Teeri TT, Jones TA (2004) Crystal structures of a poplar xyloglucan endotransglycosylase reveal details of transglycosylation acceptor binding. Plant Cell 16:874-86. doi: 10.1105/tpc.020065

Jolie RP, Duvetter T, Van Loey AM, Hendrickx ME (2010) Pectin methylesterase and its proteinaceous inhibitor: a review. Carbohydr Res 345:2583-95. doi: 10.1016/j.carres.2010.10.002

Juge N (2006) Plant protein inhibitors of cell wall degrading enzymes. Trends Plant Sci 11: 359–367. doi: 10.1016/j.tplants.2006.05.006

Kaewthai N, Gendre D, Eklöf JM, Ibatullin FM, Ezcurra I, Bhalerao RP, Brumer H (2013) Group III-A XTH genes of *Arabidopsis* encode predominant xyloglucan endohydrolases that are dispensable for normal growth. Plant Physiol 161:440-454. doi: 10.1104/pp.112.207308

Lai-Kee-Him J, Chanzy H, Muller M, Putaux J, Imai T, Bulone V (2002) In vitro versus in vivo cellulose microfibrils from plant primary wall synthases: Structural differences. J Biol Chem 277:36931–36939. doi: 10.1074/jbc.M203530200

Landrein B, Hamant O (2013) How mechanical stress controls microtubule behavior and morphogenesis in plants: history, experiments and revisited theories. Plant J 75:324–338. doi: 10.1111/tpj.12188

Lerouxel O, Cavalier DM, Liepman AH, Keegstra K (2006) Biosynthesis of plant cell wall polysaccharides - a complex process. Curr Opin Plant Biol 9:621-630. doi: 10.1016/j.pbi.2006.09.009

Liners F, Letesson JJ, Didembourg C, Van Cutsem P (1989) Monoclonal Antibodies against Pectin: Recognition of a Conformation Induced by Calcium. Plant Physiol 91:1419-1424. doi: http://dx.doi.org/10.1104/pp.91.4.1419

Malinovsky FG, Fangel JU, Willats WGT (2014) The role of the cell wall in plant immunity. Front Plant Sci 5: 178. doi: 10.3389/fpls.2014.00178

Markovic O, Janecek S (2004) Pectin methylesterases: Sequence-structural features and phylogenetic relationships. Carbohydr. Res 339:2281–2295. doi: 10.1016/j.carres.2004.06.023

Markovic O, Kohn R (1984) Mode of pectin deesterification in *Trichodrema reesei* pectinesterese. Experientia 5:842-843.

Marcus SE, Verhertbruggen Y, Hervé C, Ordaz–Ortiz JJ, Farkas V, Pedersen HL, Willats WGT, Knox JP (2008) Pectic homogalacturonan masks abundant sets of xyloglucan epitopes in plant cell walls. BMC Plant Biol 8:60. doi: 10.1186/1471-2229-8-60

Matsui A, Yokoyama R, Seki M, Ito T, Shinozaki K, Takahashi T, Komeda Y, Nishitani K (2005) AtXTH27 plays an essential role in cell wall modification during the development of tracheary elements. Plant J 42:525-534. doi: 10.1111/j.1365-313X.2005.02395.x

McDougall GJ, Fry SC (1990) Xyloglucan oligosaccharides promote growth and activate cellulase. Evidence for a role of cellulase in cell expansion. Plant Physiol 93:1042-1048. doi: http://dx.doi.org/10.1104/pp.93.3.1042

McQueen-Mason S, Durachko DM, Cosgrove DJ (1992) Two endogenous proteins that induce cell wall extension in plants. Plant Cell 4:1425-33. doi: http://dx.doi.org/10.1105/tpc.4.11.1425

McQueen-Mason SJ, Cosgrove DJ (1995) Expansin mode of action on cell walls. Analysis of wall hydrolysis, stress relaxation and binding. Plant Physiol 107:87-100. doi: http://dx.doi.org/10.1104/pp.107.1.87

Micheli F (2001) Pectin methylesterases: cell wall enzymes with important roles in plant physiology. Trends Plant Sci 6:414-419. doi: 10.1016/S1360-1385(01)02045-3

Miedes E, Herbers K, Sonnewald U and Lorences EP (2010) Overexpression of a cell wall enzyme reduces xyloglucan depolymerization and softening of transgenic tomato fruits. J Agric Food Chem 58:5708–5713. doi: 10.1021/jf100242z

Murashige T, Skoog F (1962) A revised medium for rapid growth and bioassays with tobacco tissue. Physiol Plant 15:493–497. doi: 10.1111/j.1399-3054.1962.tb08052.x

Nicol F, His I, Jauneau A, Vernhettes S, Canut H, and Höfte H (1998) A plasma membrane-bound putative endo-1,4-beta-D-glucanase is required for normal wall assembly and cell elongation in *Arabidopsis*. EMBO J 17:5563–5576. doi: 10.1093/emboj/17.19.5563

Oliveros JC (2007) VENNY. An interactive tool for comparing lists with Venn Diagrams. http://bioinfogp.cnb.csic.es/tools/venny/index.html.

Osato Y, Yokoyama R, Nishitani K (2006) A principal role for AtXTH18 in *Arabidopsis thaliana* root growth – a functional analysis using RNAi plants. J Plant Res 119:153–162. doi: 10.1007/s10265-006-0262-6

Park YB, Cosgrove DJ (2012) A revised architecture of primary cell walls based on biomechanical changes induced by substrate-specific endoglucanases. Plant Physiol 158:1933-1943. doi: 10.1104/pp.111.192880

Park YB, Cosgrove DJ (2015) Xyloglucan and its interactions with other components of the growing cell wall. Plant Cell Physiol 56:180-94. doi: 10.1093/pcp/pcu204

Peaucelle A, Louvet R, Johansen JN, Hofte H, Laufs P, Pelloux J, Mouille G (2008) *Arabidopsis* phyllotaxis is controlled by the methyl-esterification status of cell-wall pectins. Curr Biol 18:1943-1948. doi: 10.1016/j.cub.2008.10.065

Peaucelle A, Braybrook SA, Le Guillou L, Bron E, Kuhlemeier C, Höfte H (2011) Pectin-induced changes in cell wall mechanics underlie organ initiation in *Arabidopsis*. Curr Biol 21:1720-1726. doi: 10.1016/j.cub.2011.08.057

Peaucelle A, Braybrook S, Hofte H (2012) Cell wall mechanics and growth control in plants: the role of pectins revisited. Front Plant Sci 3:121. doi: 10.3389/fpls.2012.00121

Pelloux J, Rustérucci C, Mellerowicz EJ (2007) New insights into pectin methylesterase structure and function. Trends Plant Sci 12:267-277. doi: 10.1016/j.tplants.2007.04.001

Petersen TN, Brunak S, von Heijne G, Nielsen H (2011) SignalP 4.0: discriminating signal peptides from transmembrane regions. Nature Methods 8:785-786. doi: 10.1038/nmeth.1701

Pilling E, Höfte H (2003) Feedback from the wall. Curr Opin Plant Biol 6:611-6. doi: 10.1016/j.pbi.2003.09.004

Popper ZA, Fry SC (2005) Widespread occurrence of a covalent linkage between xyloglucan and acidic polysaccharides in suspension-cultured angiosperm cells. Ann Bot 96:91-9. doi: 10.1093/aob/mci153

Potters G, Pasternak TP, Guisez Y, Palme KJ, Jansen MAK (2007) Stress-induced morphogenic responses: growing out of trouble? Trends Plant Sci 12:98–105. doi: 10.1016/j.tplants.2007.01.004

Quevillon E, Silventoinen V, Pillai S, Harte N, Mulder N, Apweiler R, Lopez R (2005) InterProScan: protein domains identifier. Nucleic Acids Res 33 (Web Server issue): W116-20. doi: 10.1093/nar/gki442

Reid KE, Olsson N, Schlosser J, Peng F, Lund ST (2006) An optimized grapevine RNA isolation procedure and statistical determination of reference genes for real-

time RT-PCR during berry development. BMC Plant Biol 6:27. doi:10.1186/1471-2229-6-27

Richmond PA, Métraux JP, Taiz L (1980) Cell expansion patterns and directionality of wall mechanical properties in nitella. Plant Physiol 65:211-7. doi: http://dx.doi.org/10.1104/pp.65.2.211

Richmond TA, Somerville CR (2000) The cellulose synthase superfamily. Plant Physiol 124:495–498. doi: http://dx.doi.org/10.1104/pp.124.2.495

Saeed AI, Sharov V, White J, Li J, Liang W, Bhagabati N, Braisted J, Klapa M, Currier T, Thiagarajan M, Sturn A, Snuffin M, Rezantsev A, Popov D, Ryltsov A, Kostukovich E, Borisovsky I, Liu Z, Vinsavich A, Trush V, Quackenbush J (2003) TM4: a free, open-source system for microarray data management and analysis. Biotechniques 34:374-8

Sampedro J, Pardo B, Gianzo C, Guitián E, Revilla G, Zarra I (2010) Lack of α-xylosidase activity in *Arabidopsis* alters xyloglucan composition and results in growth defects. Plant Physiol 154:1105–1115. doi: 10.1104/pp.110.163212

Sampedro J, Gianzo C, Iglesias N, Guitián E, Revilla G, Zarra I (2012). AtBGAL10 is the main xyloglucan β-galactosidase in *Arabidopsis*, and its absence results in unusual xyloglucan subunits and growth defects. Plant Physiol 158:1146–1157. doi: 10.1104/pp.111.192195

Sato S, Kato T, Kakegawa K. *et al.* (2001) Role of the putative membrane-bound endo-1,4-beta-glucanase KORRIGAN in cell elongation and cellulose synthesis in *Arabidopsis thaliana*. Plant Cell Physiol 42:251–263. doi: 10.1093/pcp/pce045

Scognamiglio MA, Ciardiello MA, Tamburrini M, Carratore V, Rausch T, Camardella L (2003) The plant invertase inhibitor shares structural properties and disulfide bridges arrangement with the pectin methylesterase inhibitor. J Protein Chem 22:363-9

Shpigel E, Roiz L, Goren R, Shoseyov O (1998) Bacterial cellulose-binding domain modulates in vitro elongation of different plant cells. Plant Physiol 117:1185–1194. doi: http://dx.doi.org/10.1104/pp.117.4.1185

Somerville C (2006) Cellulose synthesis in higher plants. Annu Rev Cell Dev Biol 22:53–78. doi: 10.1146/annurev.cellbio.22.022206.160206

Suzuki S, Li L, Sun YH, Chiang VL (2006) The cellulose synthase gene superfamily and biochemical functions of xylem-specific cellulose synthase-like genes in *Populus trichocarpa*. Plant Physiol 142:1233-45. doi: http://dx.doi.org/10.1104/pp.106.086678

Takahashi J, Rudsander UJ, Hedenström M, Banasiak A, Harholt J, Amelot N, Immerzeel P, Ryden P, Endo S, Ibatullin FM, Brumer H, del Campillo E, Master ER, Scheller HV, Sundberg B, Teeri TT, Mellerowicz EJ (2009) KORRIGAN1 and its aspen homolog PttCel9A1 decrease cellulose crystallinity in *Arabidopsis* stems. Plant Cell Physiol 50:1099-115. doi: 10.1093/pcp/pcp062

Talavera G, Castresana J (2007) Improvement of Phylogenies after Removing Divergent and Ambiguously Aligned Blocks from Protein Sequence Alignments. Systematic Biol 56:564–577. doi: 10.1080/10635150701472164

Takeda T, Furuta Y, Awano T, Mizuno K, Mitsuishi Y, Hayashi T (2002) Suppression and acceleration of cell elongation by integration of xyloglucans in pea stem segments. Proc Natl Acad Sci USA 99:9055-60. doi: 10.1073/pnas.132080299

Taylor NG, Howells RM, Huttly AK, Vickers K, Turner SR (2003) Interactions among three distinct CesA proteins essential for cellulose synthesis. Proc Natl Acad Sci USA 100:1450–1455. doi: 10.1073/pnas.0337628100

Tenhaken R (2015) Cell wall remodeling under abiotic stress. Front Plant Sci 5:771. doi: 10.3389/fpls.2014.00771

Urbanowicz BR, Bennett AB, del Campillo E, Catalá C, Hayashi T, Henrissat B, Höfte H, McQueen-Mason SJ, Patterson SE, Shoseyov O, Teeri TT, Rose JK (2007a) Structural organization and a standardized nomenclature for plant endo-1,4-beta-glucanases (cellulases) of glycosyl hydrolase family 9. Plant Physiol 144:1693-6. doi: http://dx.doi.org/10.1104/pp.107.102574

Urbanowicz BR, Catalá C, Irwin D, Wilson DB, Ripoll DR, Rose JKC (2007b) A tomato endo-*β*-1,4-glucanase, SlCel9C1, represents a distinct subclass with a new family of carbohydrate binding modules (CBM49). J Biol Chem 282**:**12066–12074. doi: 10.1074/jbc.M607925200

Van Sandt VS, Suslov D, Verbelen JP, Vissenberg K (2007) Xyloglucan endotransglucosylase activity loosens a plant cell wall. Ann Bo 100:1467-1473. doi: 10.1093/aob/mcm248

Velasco R, Zharkikh A, et al. (2007) A high quality draft consensus sequence of the genome of a heterozygous grapevine variety. PLoS One 2: e1326. doi: 10.1371/journal.pone.0001326

Vissenberg K, Fry SC, Verbelen J-P (2001) Root hair initiation is coupled to a highly localized increase of xyloglucan endotransglycoslyase action in *Arabidopsis* roots. Plant Physiol 127:1125–1135. doi: http://dx.doi.org/10.1104/pp.010295

Wang T, Zabotina O, Hong M (2012) Pectin–cellulose interactions in the *Arabidopsis* primary cell wall from two-dimensional magic-angle-spinning solid-state nuclear magnetic resonance. Biochemistry 51:9846–9856. doi: 10.1021/bi3015532

Wang T, Park YB, Caporini MA, Rosay M, Zhong L, Cosgrove DJ, Hong M (2013) Sensitivity-enhanced solid-state NMR detection of expansin's target in plant cell walls. Proc Natl Acad Sci USA 110:16444–16449. doi: 10.1073/pnas.1316290110

Wakabayashi K, Soga K, Kamisaka S, Hoson T (2003) Modification of cell wall architecture of wheat coleoptiles grown under hypergravity conditions. Biol Sci Space 17: 228-9.

Willats WG, Gilmartin PM, Mikkelsen JD, Knox JP (1999) Cell wall antibodies without immunization: generation and use of de-esterified homogalacturonan block-specific antibodies from a naive phage display library. Plant J 18:57-65. doi: 10.1046/j.1365-313X.1999.00427.x

Willats WGT, Orfila C, Limberg G, Buchholt HC, van Alebeek GJWM, Voragen AGJ, Marcus SE, Christensen TMIE, Mikkelsen JD, Murray BS, Knox JP (2001) Modulation of the degree and pattern of methyl-esterification of pectic homogalacturonan in plant cell walls. Implications for pectin methyl esterase action, matrix properties, and cell adhesion. J Biol Chem 276:19404–19413. doi: 10.1074/jbc.M011242200

Whitney SEC, Gidley MJ, McQueen-Mason SJ (2000) Probing expansin action using cellulose/hemicellulose composites. Plant J 22:327–334. doi: 10.1046/j.1365-313x.2000.00742.x

Wolf S, Mravec J, Greiner S, Mouille G, Höfte H (2012) Plant cell wall homeostasis is mediated by brassinosteroid feedback signaling. Curr Biol 22:1732-7. doi: 10.1016/j.cub.2012.07.036.

Yuan S, Wu Y, Cosgrove DJ (2001) A fungal endoglucanase with plant cell wall extension activity. Plant Physiol 127:324-333. doi: http://dx.doi.org/10.1104/pp.127.1.324

Zykwinska A, Ralet MC, Garnier C, Thibault JF (2005) Evidence for in vitro binding of pectic side chains to cellulose. Plant Physiol 139:397-407. doi: http://dx.doi.org/10.1104/pp.105.065912

Zykwinska A, Thibault J-F, Ralet M-C (2007) Organization of pectic arabinan and galactan side chains in association with cellulose microfibrils in primary cell walls and related models envisaged. J Expl Bot 58:1795–1802. doi: 10.1093/jxb/erm037

Zykwinska A, Thibault JF, Ralet MC (2008) Competitive binding of pectin and xyloglucan with primary cell wall cellulose. Carbohydr Polym 74:957–961. doi:10.1016/j.carbpol.2008.05.004

Chapter 4

Immunolocalization of cell wall polymers in grapevine (*Vitis vinifera* L.) internodes under nitrogen, phosphorus or sulfur deficiency

João C. Fernandes[1], Luis F. Goulao[2] and Sara Amâncio[1]

[1] *DRAT/LEAF, Instituto Superior de Agronomia, Universidade de Lisboa, Tapada da Ajuda, 1349-017 Lisbon, Portugal.*

[2] *BioTrop, Instituto de Investigação Científica Tropical (IICT, IP), Pólo Mendes Ferrão - Tapada da Ajuda, 1349-017 Lisbon, Portugal.*

Under review in Journal of Plant Research

4. Immunolocalization of cell wall polymers in grapevine (*Vitis vinifera*) internodes under nitrogen, phosphorus or sulfur deficiency

Fernandes JC, Goulao LF, Amâncio S

Abstract

The impact on cell wall (CW) of the deficiency in nitrogen (-N), phosphorus (-P) or sulphur (-S), known to impair essential metabolic pathways, was investigated in the economically important fruit species *Vitis vinifera* L. Using cuttings as an experimental model a reduction in total internode number and altered xylem shape was observed. Under –N an increased internode length was also seen. CW composition, visualised after staining with Calcofluor white, and Toluidine blue and Ruthenium red, showed decreased cellulose in all stresses and increased pectin content in recently formed internodes under –N compared to the control. Using CW-epitope specific monoclonal antibodies (mAbs), lower amounts of extensins incorporated in the wall were also observed under –N and –P conditions. Conversely, increased pectins with a low degree of methyl-esterification and richer in 1,5-arabinan rhamnogalacturonan-I (RG-I) side chains were observed under –N and –P in mature internodes which, in the former condition, were able to form dimeric association through calcium ions. Higher xyloglucan content in older internodes was also observed under –N. The results suggest that impairments of specific CW components led to changes in the deposition of other polymers to promote stiffening of the CW. The unchanged extensin amount observed under –S may contribute to attenuating the effects on the CW integrity caused by this stress. Our work showed that, in organized *V. vinifera* tissues, modifications in a given CW component can be compensated by synthesis of different polymers and/or alternative linking between polymers. The results also pinpoint different strategies at the CW level to overcome mineral stress depending on how essential they are to cell growth and plant development.

Keywords: *Cell wall epitopes, Cellulose, Mineral stress, Pectin, Xyloglucan.*

Abbreviations

CBM	Carbohydrate binding module
CW	Cell wall
EXT	Extensin
GH9C	Glycosyl hydrolase family 9C
HG	Homogalacturonan
I-1	Top internode
I-4	Fourth internode
–N	Absence of nitrogen
mAbs	Monoclonal antibodies
–P	Absence of phosphorous
PBS	Phosphate buffered saline
RG-I and –II	Rhamnogalacturonans I and II
–S	Absence of sulfur
XyG	Xyloglucan

4.1. Introduction

The plant capacity for upright growth and penetration into the soil comes from the high organ mechanical robustness conferred by semi-rigid and cemented together cell walls (CW). CWs also provide plants with the necessary strength and plasticity to resist adverse environmental conditions.

The properties, structural integrity, and simultaneous strength and flexibility of the plant CW depends on changes in composition and complex arrangement of its polymers throughout growth and differentiation processes (Braidwood et al. 2014). Two types of CW differing in function and composition can be formed. Primary CWs surround dividing cells allowing extensibility during organ growth, while after growth ceases a thicker secondary wall may be deposited (Lee et al. 2011). The frontier between the two types of CW is not clear cut, but rather a continuum, when based on structure and architecture (Knox 2008; Albersheim et al. 2010).

Several polysaccharides compose the CW. Primary walls are comprised of 15–40 % cellulose, 30–50 % pectins and 20–30 % hemicelluloses, predominantly xyloglucans (XyGs), on a dry weight basis (Cosgrove and Jarvis 2012). Together with these major polymers, lower amounts of structural glycoproteins, phenolic esters, ionically and covalently bound minerals and enzymes are present (Cosgrove and Jarvis 2012). Cellulose forms long, rigid crystalline microfibrils of 1,4-linked β-D-glucose residues that provide the major load-bearing role of CW (Cosgrove 2005; Brashline et al. 2014). The hemicellulose class consists of several types of branched polysaccharides that include XyGs, xylans, mannans, and mixed-linkage glucans (Scheller and Ulvskov 2010). Hemicelluloses are structurally homologous to cellulose since their backbones are composed of 1,4-linked β-D-hexosyl residues. This property suggested coating and tethering to cellulose microfibrils to form a load-bearing network (Cosgrove 2000). However, the capacity of XyG–cellulose binding to confer sufficient strength to withstand the tensile forces in the CW has been challenged (Thompson 2005). Moreover, *Arabidopsis* mutants defective in XyG displayed only moderate growth impairment (Cavalier et al. 2008; Zabotina et al. 2012). A model in which XyG is restricted within the CW and intertwined with cellulose only at limited sites forming selective targets for CW loosening, the so called “biomechanical hotspots” theory,

was recently proposed (Park and Cosgrove 2012; 2015). Three classes of pectic polysaccharides containing 1,4-linked α-D-galacturonic acid have been characterized: linear homogalacturonans (HGs), branched rhamnogalacturonans (RG-I and –II) and substituted galacturonans. Pectic polysaccharides are particular targets for enzymatic modulation through methyl or acetyl de-esterification of HG chains that can dramatically influence CW properties and assembly, affecting cell adhesion porosity and hydration (Lionetti et al. 2007; Pelloux et al. 2007; Peaucelle et al. 2008). Recently a role for enzymatic modulation of pectin polymer size in CW expansion was demonstrated (Xiao et al. 2014).

These new findings have been challenging CW architecture models. It was recently hypothesized that linkages between pectins and xylans may control mechanical properties in the XyG-deficient walls (Park and Cosgrove 2012; Zabotina et al. 2012). As cellulose-XyG hydrogen bonds are the major targets for expansin action and CW extensibility, the reduction of their frequency makes these walls mechanically weaker and simultaneously less extensible. Evidence for covalent linkages between side-chains of specific pectin polysaccharides and cellulose microfibrils (Zykwinska et al. 2007) and XyG molecules (Popper and Fry 2008) have been reported, further supporting these assumptions.

Although present in lower amounts in the CW of vascular plants, extensins (EXT), a family of structural hydroxyproline-rich glycoproteins (HRGPs) (Showalter 1993), were demonstrated to have a key role during cell expansion and growth (Cannon et al. 2008; Ringli 2010; Lamport et al. 2011) and to be required for normal wall architecture and function in development, particularly during polarized cell expansion (Velasquez et al. 2011, 2012). Despite the high number of proteins with EXT domains found in plants (Lamport et al. 2011), little is known about their function and how this protein diversity is coordinated during plant development (Hijazi et al. 2014).

Although knowledge on the biochemical structure of cellulose, hemicelluloses and pectins is largely available, the organization and interactions between these components and other molecules in the CW is poorly known and the type and extent of CW changes that are associated with the plants capacity to interact with the environment and cope with abiotic stresses has been insufficiently

investigated. A great variety of CWs have been described at the molecular level. Impacting the overall dynamics and modulating development does not require dramatic restructuring of the entire CW. Changes in composition and structure are often occur specifically localized to a small number and type of cells. The sensitivity and resolution of chemical quantification methods neither provide accurate measurement nor information about alterations in the architecture of CW polymers. Immunohistochemical techniques enable localization of CW epitopes *in situ* within complex tissues, overcoming this limitation. In the last two decades, over 150 molecular probes targeting at the cellular level have been developed (Knox 2008; Moller et al. 2008; Pattathil et al. 2010; Ralet et al. 2010). The distribution of carbohydrate epitopes in plant CWs can be selectively recognized by several monoclonal antibodies (mAbs) and carbohydrate binding modules (CBMs) (Lee et al. 2011), allowing direct *in muro* visualization. Following immunolocalization approaches, several detailed aspects of CW heterogeneity including the importance of specific pectin methylation patterns on cell adhesion (Willats et al. 2001; Ordaz-Ortiz et al. 2009), or localized changes in precise CW polymers in response to abiotic stresses (Liu et al. 2014; Muszynska et al. 2014) have been disclosed. The knowledge acquired hastens our ability to relate CW structures to cell biological events and integration of this information into the emerging understanding of polymer functions (Knox 2008).

Using *V. vinifera* callus developing under depletion of major nutrients, nitrogen, phosphorus and sulfur, we previously reported reorganization of specific CW components in response to individual nutrient deprivation. Decreased cellulose, modifications in pectin methyl-esterification, increase of structural proteins and tighter association of polysaccharides were observed in the CW, although to different degrees according to the specific stress imposed (Fernandes et al. 2013). Under nitrogen and, to a lower extent, under phosphorus deficiency, we hypothesize that cellulose reduction could be counterbalanced by modifications in matrix polymers to maintain tissue integrity. However, callus are plant dedifferentiated tissues, so may behave differently to organized tissues. The aim of the present work was to investigate CW responses, specifically components rearrangement, to the depletion of the same individual major nutrients, using grapevine shoot internodes organized tissues as experimental model. For that

purpose immunolocalization assays were performed to investigate *V. vinifera* CW responses to specific mineral depletion.

4.2. Material and methods

4.2.1. Plant material and stress imposition

Grapevine (*V. vinifera* L.) cv. Trincadeira pruned wood cuttings were treated with fungicide (2 % w/v, Benlate) and stored at 4 °C for two months. Rooting and shoot elongation took place in 30 % nutrient solution (Knight and Knigth 2001) in the dark, at 25 ± 2 °C. When shoots had developed four internodes they were transferred to 3L pots filled with vermiculite in greenhouse under an irradiance of 200 µmol m^{-2} s^{-1}, 16h photoperiod, day/night temperature of 25 ± 2/23 ± 2 °C and relative humidity of ca. 60 %. Four experimental conditions were set up: weekly watering with full nutrient solution (control), nitrogen deficiency (–N), phosphorus deficiency (–P) and sulfur deficiency (–S) (Supplementary Table. 4.1). Shoot internode number and length of the fourth internode from the top (I-4) were recorded weekly for 8 weeks. I-4 and the top internode (I-1) were collected at the 6^{th} week for histological staining and immunohistochemical analysis.

4.2.2. Cross sectioning

Internode samples of about 1 cm in length were vacuum infiltrated and fixed overnight in 4 % (v/v) paraformaldehyde solution in 1 x sodium phosphate buffer (pH 7.4) and dehydrated in a graded ethanol series. Absolute ethanol was substituted by an ethanol:limonen (1:1) solution (Histo-Clear II; National Diagnostics) for 1 hour and replaced 3 times by 100 % Histo-clear for 1 hour each. The samples were then infiltrated with 50 % paraffin (Histosec, Merck) 50 % Histo-clear solution overnight at 58 °C and spacing in 100 % Histosec for 2 days, replaced twice a day. Embedded tissues were casted with Histosec. Five µm thick sections were prepared using a Meditome M530 (Medite) micrometer and collected on poly-L-lysine coated microscope slides. Paraffin removal was accomplished as described by Nic-Can et al. (2013).

4.2.3. Histological staining

Sections were stained with aqueous 1 % (w/v) toluidine blue or 0.05% (w/v) ruthenium red dye (Sigma, St. Louis, MO) for 5 min, rinsed twice with distilled water for 30 min, mounted in water and observed under light microscopy. Similar sample sections were stained with 0.1 % (w/v) Calcofluor White fluorescent brightener (Sigma, St. Louis, MO). Images were observed under a Leitz Laborlux S epifluorescence microscope with the objectives Leitz Phaco 1 10X and Leitz Fluoreszenz 63x and for Calcofluor stained sections, with filters 365/445 Nm. Images were acquired with a Zeiss AxioCam digital camera and analyzed using the ImageJ 1.48 package (http://imagej.nih.gov/ij/).

4.2.4. Immunolocalization analysis

Immunolocalization assays were performed using PAM1, 2F4, LM6, LM13, LM15 and LM1 mAbs which target polymer and recognition region are presented in Table 1. De-paraffinated and rehydrated sections were blocked with 5 % (w/v) non-fat milk in 0.1 M phosphate-buffered saline (PBS, pH 7.2) for 30 min at room temperature. The sections were then incubated with each of the primary antibodies under appropriate dilutions (1:250 for 2F4, 1:10 for LM6, LM13, LM15 and LM1, 1:5 for PAM1) in blocking solution overnight at 4 °C. 2F4, LM6, LM13, LM15 and LM1 hybridized sections were rinsed and incubated with secondary anti-rat or anti-mouse IgG/FITC (Sigma-Aldrich, St Louis, MO, USA) diluted 1:30 in blocking solution for 4 h at room temperature in the dark. For PAM1 detection, the Anti-HIS (Sigma-Aldrich, St Louis, MO, USA) was used as secondary antibody for 2 h at 1:100 dilution followed by incubation with a tertiary antibody anti-mouse/FITC (1:50) for additional 2 h. The sections were then rinsed with PBS and briefly incubated in 1 % (w/v) Calcofluor white and further rinsed. Finally, sections were mounted with glycerol/PBS-based anti-fade solution (SlowFade Antifade Kit; Life Technologies) according to the manufacture recommendations. Images were observed under a Leitz Laborlux S epifluorescence microscope with the objective Leitz Phaco 1 10X and Leitz Fluoreszenz 63x and filters 470/525 and acquired using a Zeiss AxioCam digital camera. Single layer or simultaneously visualized images were analyzed using the ImageJ 1.48 package (http://imagej.nih.gov/ij/). Negative controls for each mAb (Supplementary Fig.

4.2), where primary antibodies were omitted confirmed the absence of unspecific labelling (Coimbra, 2007).

Table 4.1 Used mAbs, target polymers and recognition region.

mAbs	Target polymer	Epitope	Reference
PAM1	Unesterified homogalacturonan	30 contiguous unmethy esterified galacturonic acid	Willats et al. 1999
2F4	Homogalacturonan	Pectic chains linked by calcium ions	Liners et al. 1989
LM6	Pectic arabinans	(1-5)-α-L-arabinans	Willats et al. 1998
LM13	Pectic arabinans	Linear (1-5)-α-L-arabinans	Moller et al. 2008
LM15	Xyloglucan	XXXG motif	Marcus et al. 2008
LM1	Hydroxyproline-rich glycoproteins (HRGPs)	Extensin glycans	Smallwood et al. 1995

4.2.5. Data analysis

Data is presented as mean values ± standard deviation (SD) of an appropriate number of replicates for each assay. The results were statistically evaluated by variance analysis (ANOVA) and post hoc Bonferroni test with a $p<0.01$ significance level, to compare the significance of each treatment effect. The SigmaPlot (Systat Software Inc.) statistical package was used.

4.3. Results

4.3.1. Growth under mineral deficiency

Growth parameters were recorded to assess the effect of the imposed conditions on the cutting development, for validating the grapevine cuttings as experimental model. As observed in Fig. 4.1, individual mineral stress (–N, –P, –S) altered the normal growth of *V. vinifera* cuttings. Mineral depletion significantly reduced the number of internodes from the 4th week (Fig. 4.1a), with a more pronounced effect

under –N and –P. The length of the fourth internode (I-4) was also affected by –N conditions, which contributed to a significant increase when compared to the other conditions (Fig.4.1b).

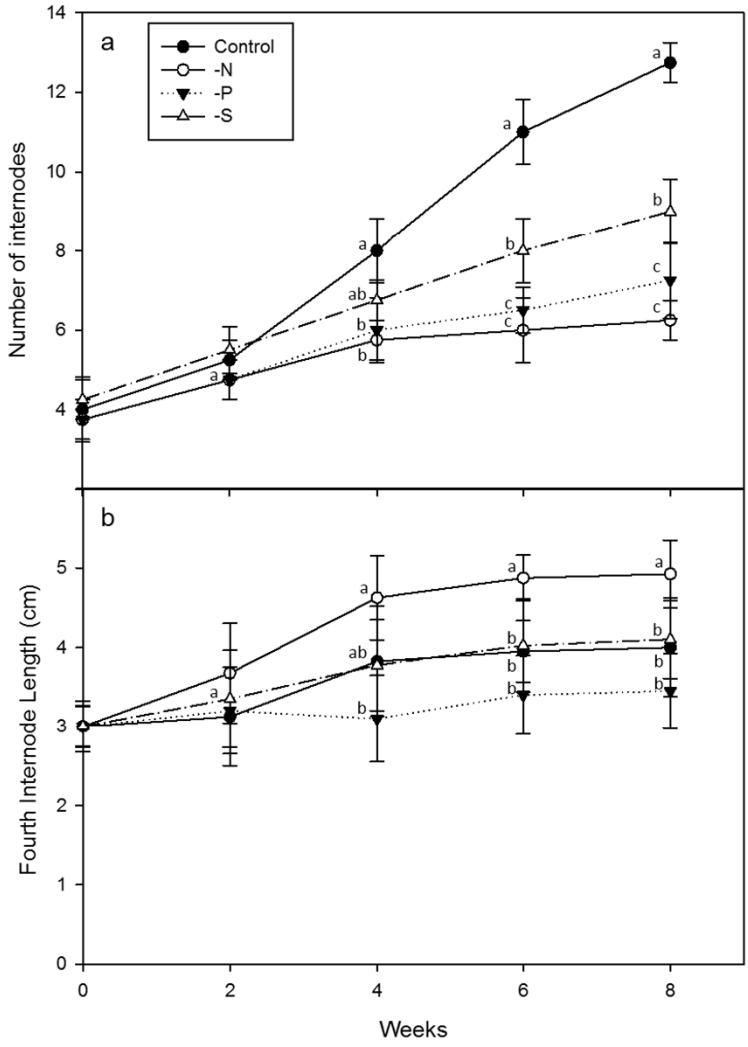

Fig. 4.1 Average number of shoot internodes (a) and length of the fourth internode (b) of *V. vinifera* cuttings grown under complete nutrient medium (control), and in the absence of nitrogen (–N), phosphorus (–P) and sulfur (–S). Values are the mean ± SD of at least 3 measurements. Different letters in each time point indicate statistically significant differences at $p<0.01$.

4.3.2. Internode anatomy

The top (I-1) and fourth (I-4) internodes show the expected arrangement of shoot tissues and, in I-4, secondary structures were already present (Fig. 4.2). Mineral stress affected xylem anatomy in a nutrient-dependent way (Table 4.2). Noticeably, –N and –S did not produce effects on the form and area of I-1 and I-

4, respectively. In I-1, xylem vessels produced under phosphorus and sulfur starvation were more elliptical than in the control while in I-4, the absence of nitrogen also altered the shape of the xylem to a more elliptical shape. Concerning xylem area, under –P and –S, an increased was observed in the recently formed internodes while in I-4 the absence of nitrogen and phosphorus significantly reduced it, when compared to the control (Table 4.2).

Table 4.2 Measured xylem vessel diameter ratio and area of *V. vinifera* shoots top (I-1) and fourth (I-4) internode after six weeks growth in complete nutrient solution (control) and in the absence of nitrogen (–N), phosphorus (–P) and sulfur (–S). Values are the mean ± SD of 20 random measurements. Different letters in each row indicate statistically significant differences at $p<0.01$.

		Control	–N	–P	–S
Xylem vessel diameter ratio	I-1	$1.18^{b} \pm 0.12$	$1.20^{b} \pm 0.16$	$1.30^{a} \pm 0.17$	$1.38^{a} \pm 0.19$
	I-4	$1.18^{b} \pm 0.18$	$1.37^{a} \pm 0.21$	$1.24^{a} \pm 0.09$	$1.21^{ab} \pm 0.18$
Xylem vessel area (μm^2)	I-1	$519.94^{c} \pm 119.80$	$439.94^{c} \pm 107.43$	$696.80^{b} \pm 91.76$	$1549.98^{a} \pm 224.45$
	I-4	$2668.20^{a} \pm 631.32$	$1262.64^{b} \pm 236.57$	$1632.55^{b} \pm 192.77$	$3205.90^{a} \pm 486.79$

These structural differences promoted by the absence of specific nutrients were reflected also in the integrity of the older tissues. While in I-1 all tissues are structurally visible, in I-4, some structures were damaged during sectioning, namely the pith, the vascular bundles and the cortical parenchyma (Fig. 4.2, arrows), suggesting a more pronounced structural weakening in tissues developed under mineral deficiency (Fig. 4.2).

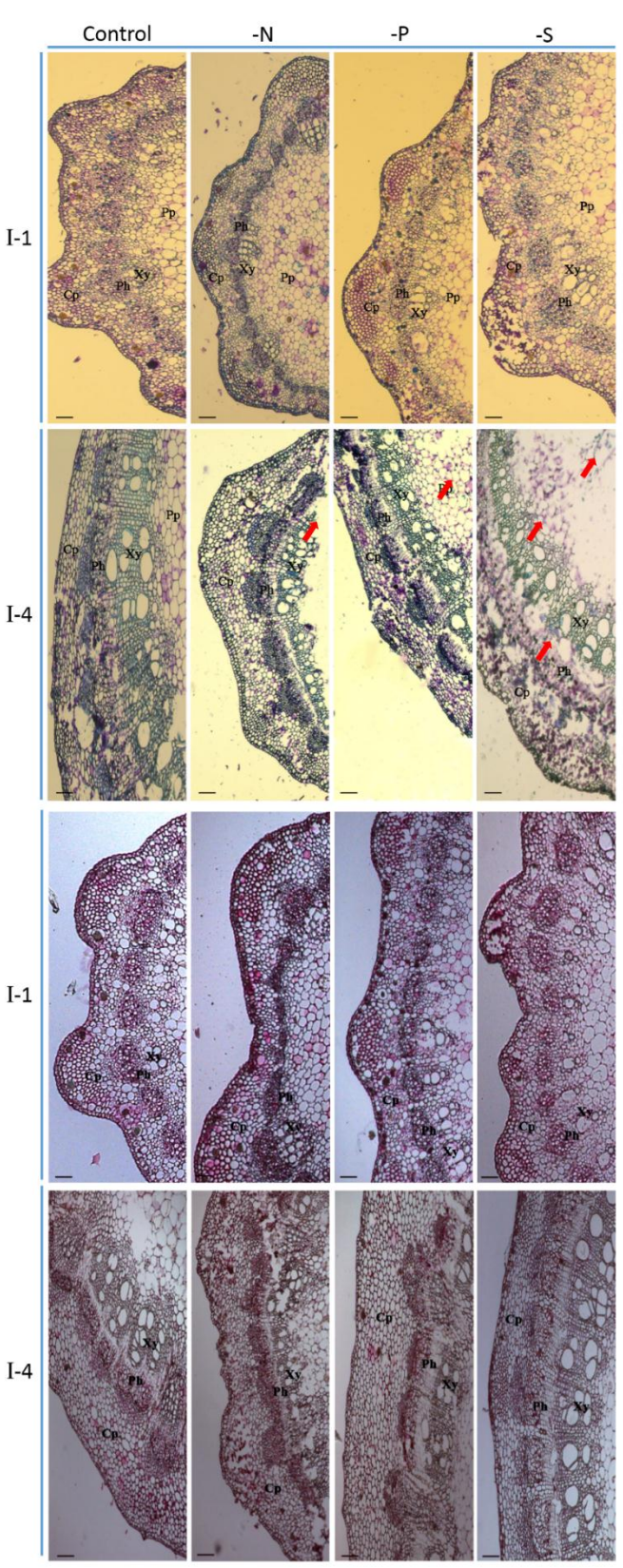

Fig. 4.2 Toluidine blue and ruthenium red histological staining of V. vinifera top (I-1) and fourth (I-4) internode sections obtained after six weeks growth under control and –N, –P and –S conditions. Images were acquired under the same exposition time for all treatments. Arrows indicate structures with compromised integrity. Xy = Xylem; Ph = Phloem; Cp = Cortical parenchyma; Pp = Pith parenchyma. Bar scale = 50 µm.

4.3.3. Histological staining

Toluidine blue binds to acidic cell components including carboxylated polysaccharides such as pectins, producing a reddish purple staining while ruthenium red is a selective for acid pectin monomers. As observed in Fig. 4.3, in the absence of nitrogen the phloem cells are more intensely stained, both in I-1 and I-4 with both dyes. In I-1 under –P, a reduction of the toluidine blue staining was observed in the same region while in –S phloem cells a reduction of the ruthenium staining was observed. Toluidine blue also binds to lignin, producing a characteristic blue staining. The absence of nitrogen led to an increased blue staining in the I-1 xylem cells, suggesting increased lignin content. Calcofluor white readily binds to cellulose and other ß-linked glucans. The absence of minerals in the nutrient solution resulted, in both internodes, in a reduced intensity of calcofluor staining (Table 4.3). This reduction was more pronounced in samples developing under nitrogen starvation. A reduction in the Calcofluor white staining between I-1 and I-4 under –N and –P conditions was also observed, in an opposite trend to the observations in control cuttings (Fig. 4.3; Table 4.3).

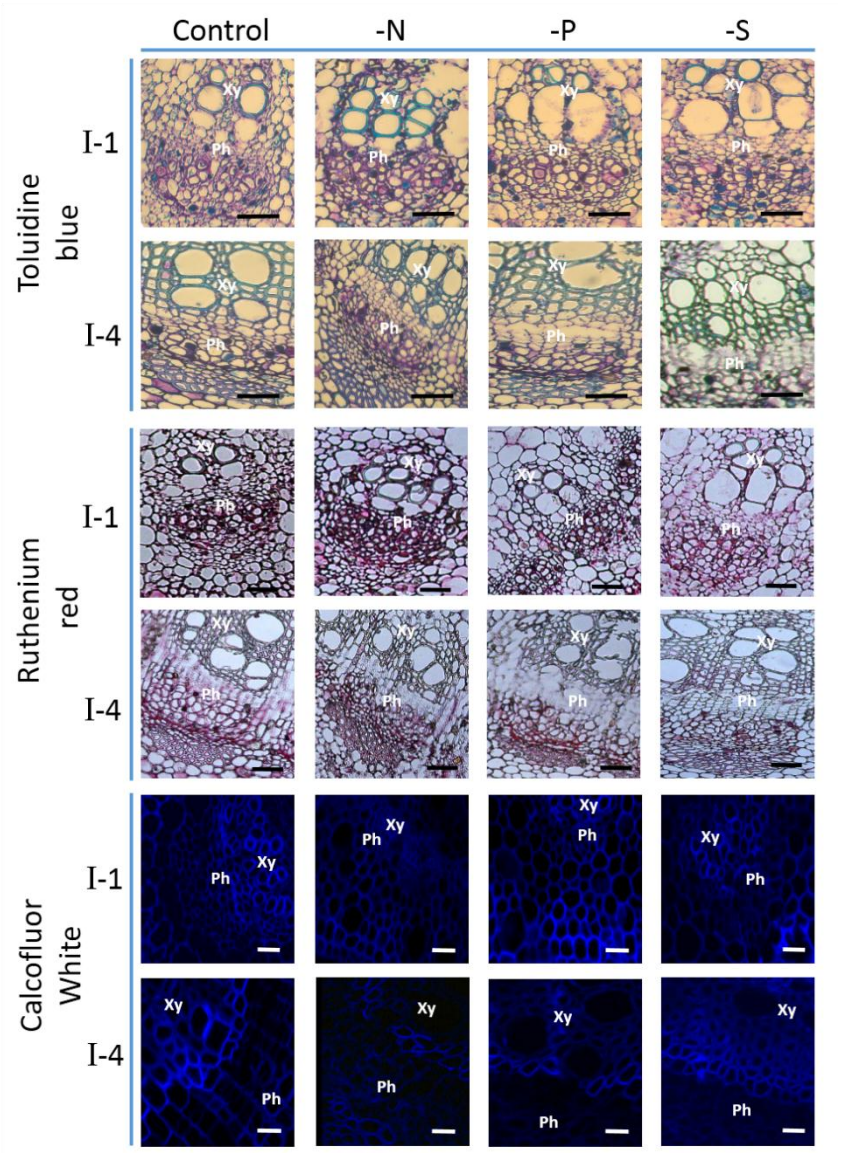

Fig. 4.3 Histological staining of pectic polysaccharides and lignin (Toluidine blue), pectic polysaccharides (ruthenium red) and cellulose (Calcofluor white) of the *V. vinifera* top (I-1) and fourth (I-4) internodes after six weeks growth under control and –N, –P and –S conditions. Images were acquired under the same exposition time for all treatments. Xy = Xylem; Ph = Phloem. Bar scale = 20 µm

4.3.4. In situ localization of CW epitopes

To get insight on how the structural arrangement of CW polymers is modified under mineral stress conditions, a set of mAbs specific to selected epitopes was used to probe *V. vinifera* internode cross sections. PAM1, specific to long stretches of unesterified HG, was used to investigate the extent to which each mineral stress affected the distribution of those stretches in pectins. Except under –S, the amount of low methyl-esterified pectins increased in the cortical parenchyma of both internodes, compared to the control (Fig. 4.4; Table 3).

These long stretches of unesterified HGs are known to be able to dimerise. This biochemical event was investigated by observing the labeling pattern of the 2F4 antibody. The signal pattern was altered only under –N, although in opposite trends in both internodes investigated. While younger material showed a decreased labelling, an increase relative to controls was observed in I-4 (Fig. 4.4; Table 4.3). Recognition of these low methyl-esterified pectins by both PAM1 and 2F4 antibodies was restricted to cell corners (Fig. 4.4, arrows). LM6 was used to probe (1-5)-α-L-arabinans. In the present experimental system pectic arabinan is mainly present in I-1 xylem cells. In –N I-1 an increase of pectic arabinans was observed while under phosphorus depletion, an increased labeling was observed in the cortical parenchyma. In the I-4 internode the labeling of LM6 increased under –S (Fig. 4.5 Table 4.3; Supplementary Fig. 4.1). LM13 binds preferentially to long oligoarabinosides from RG-I side branches. Although a low intensity in the CWs from I-1 was observed, under nutrient starvation, the signal was increased with a similar degree for all conditions (Fig. 4.5; Table 4.3; Supplementary Fig. 4.2). Conversely, in I-4, specific labelling was significantly stronger that in I-1 and increased in result of –N and –P, but not –S conditions. Specific CW signal was only detected in the xylem (Fig. 4.4 arrow; Table 4.3; Supplementary Fig. 4.1).

Table 4.3 Number of pixels quantified in the images of *V. vinifera* section of the top (I-1) and fourth (I-4) internodes developed under each individual mineral stress (–N, –P and –S) and control conditions after hybridization using 2F4, PAM1, LM6, LM13, LM15 and LM1 antibodies and Calcofluor labelling . Data are presented as mean ± SD of the number of pixels from 50 individual specifically labelled spots after subtracting the number of pixels obtained in equivalent spots of the in negative controls (Supplementary Fig 4.1). Different letters in the same row indicate significant differences at $p < 0.01$.

		Control	–N	–-P	–S
Calcofluor white	I-1	$161.30^{a} \pm 13.13$	$115.80^{c} \pm 15.09$	$130.45^{b} \pm 11.12$	$127.10^{bc} \pm 7.20$
	I-4	$194.40^{a} \pm 20.68$	$97.60^{c} \pm 11.27$	$108.35^{bc} \pm 18.71$	$123.30^{b} \pm 25.32$
PAM1	I-1	$31.50^{b} \pm 4.72$	$91.75^{a} \pm 7.64$	$86.45^{a} \pm 7.27$	$23.55^{c} \pm 5.93$
	I-4	$23.90^{c} \pm 4.14$	$89.60^{a} \pm 9.97$	$45.45^{b} \pm 6.43$	$20.90^{c} \pm 3.14$
2F4	I-1	$40.75^{ab} \pm 6.66$	$15.40^{c} \pm 2.08$	$35.35^{b} \pm 3.95$	$50.90^{a} \pm 4.08$
	I-4	$28.00^{b} \pm 3.49$	$51.95^{a} \pm 4.83$	$31.10^{b} \pm 4.37$	$26.65^{b} \pm 3.63$
LM6	I-1	$140.05^{d} \pm 9.16$	$174.35^{b} \pm 7.61$	$151.05^{c} \pm 4.28$	$195.70^{a} \pm 7.88$
	I-4	$110.60^{b} \pm 4.86$	$110.25^{b} \pm 7.39$	$79.35^{c} \pm 7.23$	$137.2^{a} \pm 5.48$
LM13	I-1	$2.05^{b} \pm 3.83$	$17.85^{a} \pm 5.74$	$19.15^{a} \pm 6.00$	$17.00^{a} \pm 5.70$
	I-4	$136.45^{c} \pm 10.36$	$157.35^{a} \pm 11.37$	$145.25^{b} \pm 8.95$	$137.70^{bc} \pm 9.87$
LM15	I-1	$129.20^{c} \pm 7.78$	$211.10^{a} \pm 13.23$	$171.70^{b} \pm 8.54$	$148.80^{c} \pm 10.63$
	I-4	$45.75^{b} \pm 6.70$	$75.95^{a} \pm 8.12$	$46.65^{b} \pm 7.83$	$41.40^{b} \pm 5.92$
LM1	I-1	$16.65^{a} \pm 3.54$	$15.75^{a} \pm 4.11$	$16.05^{a} \pm 4.14$	$16.15^{a} \pm 4.28$
	I-4	$145.45^{a} \pm 9.66$	$136.20^{b} \pm 6.87$	$125.65^{c} \pm 8.99$	$143.45^{a} \pm 7.66$

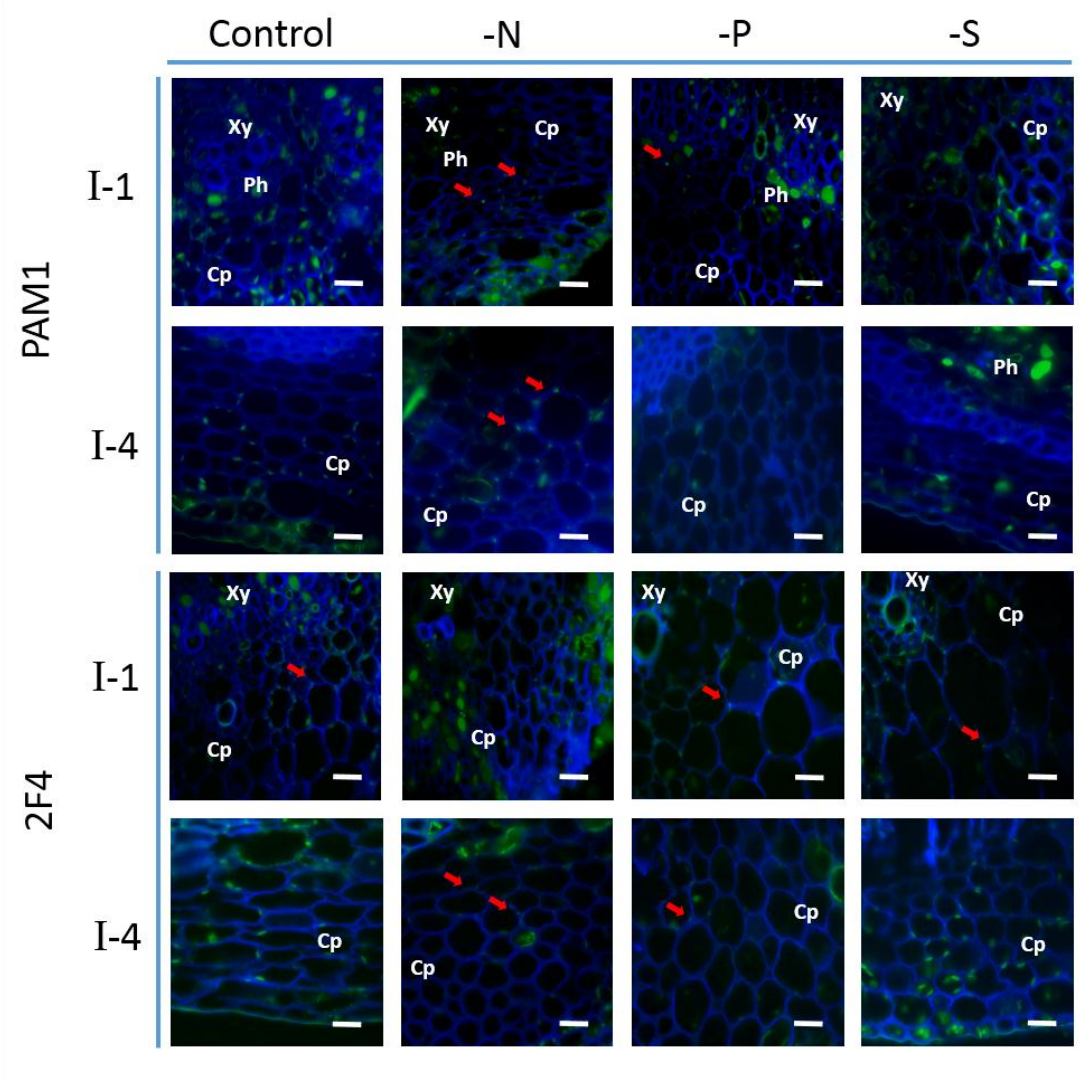

Fig. 4.4 In situ localization of 2F4, PAM1 reactive homogalacturonan epitopes of *V. vinifera* top (I-1) and fourth (I-4) internodes after six weeks growth in complete nutrient medium (control) and in the absence o of nitrogen (–N), phosphorus (–P) and sulfur (–S). Samples were also stained with Calcofluor white to reveal anatomical details. 2F4 and PAM1 signals are shown in green. Arrows highlight regions where specific labeling occurs. No label localized on the CW was observed when primary antibodies were omitted from control sections (Supplementary Fig 4.1). Images were taken under the same exposition time for all treatments. Xy = Xylem; Ph = Phloem; Cp = Cortical parenchyma. Bar = 20 µm.

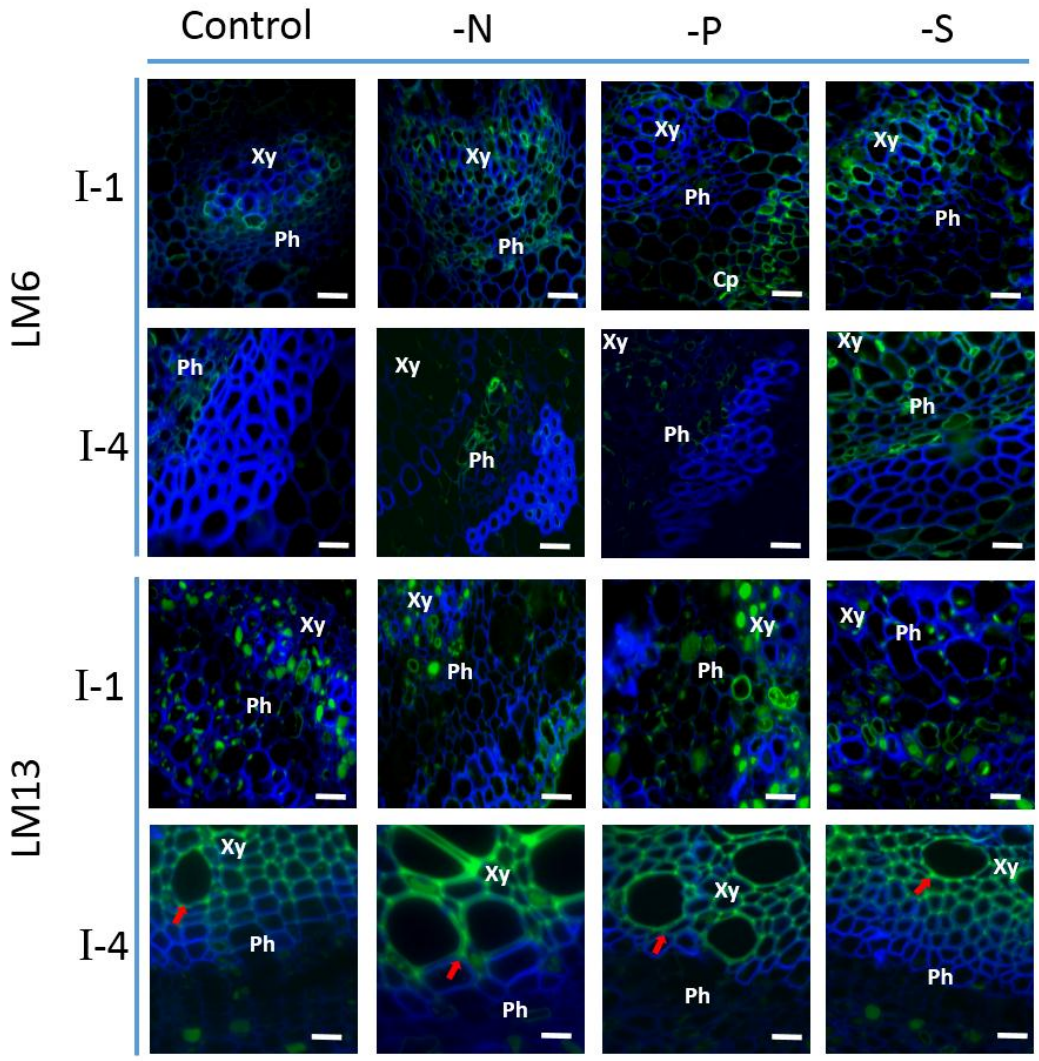

Fig. 4.5 In situ localization of LM6 and LM13, reactive pectic arabinans epitopes of *V. vinifera* top (I-1) and fourth (I-4) internodes after six weeks growth in complete nutrient medium (control) and in the absence of nitrogen (–N), phosphorus (–P) and sulfur (–S). Samples were also stained with Calcofluor white to reveal anatomical details. LM6 and LM13 signals are shown in green. Arrows highlight regions where specific labeling occurs. No label localized on the CW was observed when primary antibodies were omitted from control sections (Supplementary Fig 4.1). Images were taken under the same exposition time for all treatments. *Xy* = Xylem; *Ph* = Phloem; *Cp* = Cortical parenchyma. Bar scale = 20 µm.

The LM15 antibody was used to probe XyG, the major hemicellulose present in primary CWs of dicots. As observed in Fig. 4.6, in recently formed internodes LM15-labelling was restricted to the phloem and to some xylem cells. In I-4, LM15 labeling intensity was significantly lower than in I-1 for all conditions and additionally detected in the parenchyma cells but generally absent from xylem cells.

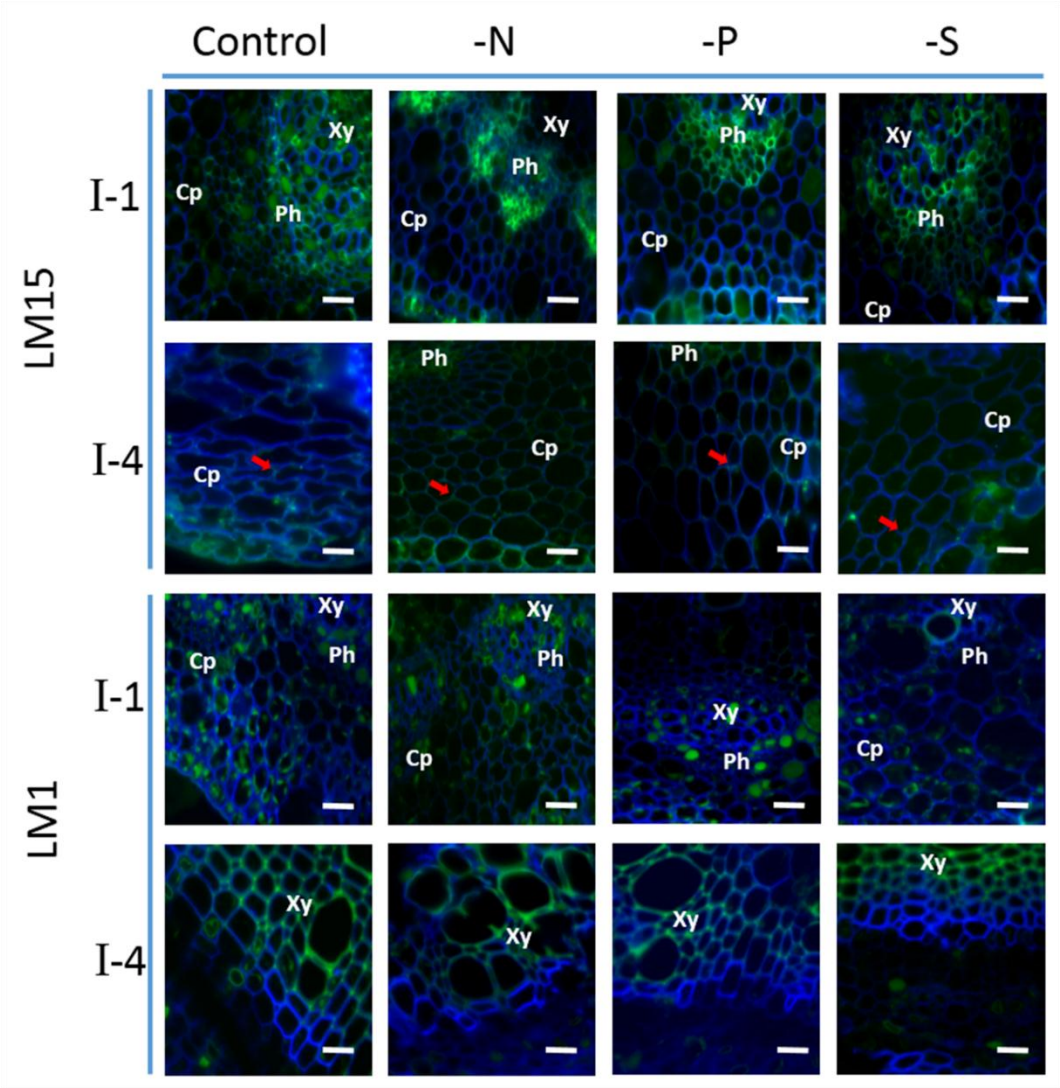

Fig. 4.6 In situ localization of LM15, reactive xyloglucan epitopes and LM1, reactive extensin epitope of *V. vinifera* top (I-1) and fourth (I-4) internodes after six weeks growth in complete nutrient medium (control) and in the absence of nitrogen (–N), phosphorus (–P) and sulfur (–S). Samples were also stained with Calcofluor white to reveal anatomical details. LM15 and LM1 signals are shown in green. Arrows highlight regions where altered LM15 pattern labeling occurs. No label localized on the CW was observed when primary antibodies were omitted from control sections (Supplementary Fig 4.1). Images were taken under the same exposition time for all treatments. Xy = Xylem; Ph = Phloem; Cp = Cortical parenchyma. Bar scale = 20 µm.

Concerning responses triggered by the absence of nutrients,–N and –P cuttings showed increased LM15-labelling in the I-1 phloem CW, while in the I-4 the effect was observed only in result of the former stress, and extended to cortical parenchyma cells (Fig. 4.6; Table 4.3). Under mineral stress an LM15 localization was observed in the walls of I-4 internode cortical parenchyma, as suggested by the increased labelling observed at some cell junctions and center of the adhesion plan (Fig. 4.7). Extensins were labelled with low intensity and

independent of the stress imposed in the top internodes. In I-4, LM1, a specific antibody for EXT, was detected only in xylem vessels and showed less intense signal in response to the absence of phosphorus and nitrogen, although with a less pronounced response in the later (Fig. 4.6; Table 4.3; Supplementary Fig. 4.1).

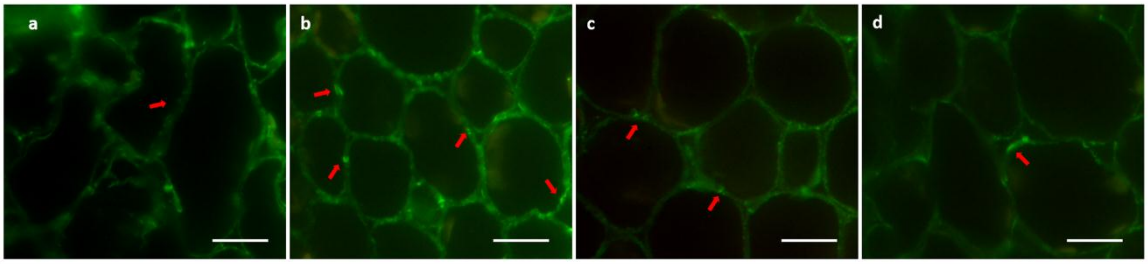

Fig. 4.7 In situ localization of the LM15 epitope in the cortical parenchyma of *V. vinifera* fourth (I-4) internode after six weeks growth in complete nutrient medium 8a) and in the absence of nitrogen (b), phosphorus (c) and sulfur (d). Arrows point to regions with increase accumulation of LM15 showing an uneven coating of XyG in the CW. Bar scale = 20 µm.

4.4. Discussion

Plant growth and development respond to environmental variation, influencing the plant phenotype. Due to its involvement in essential metabolic pathways, nitrogen (N), phosphorus (P) and sulfur (S) have a marked effect on plant growth and productivity.

The analysis of plant model systems in controlled experimental conditions provide useful tools to assess nutrient deficiency situations. The first indication of effects from N, P and S deficiency on *V. vinifera* cuttings was acquired through the confirmation that grapevine growth was affected by the mineral depletion. The lower number of internodes observed for each mineral stress condition (Fig. 4.1), supports the primary role of these major nutrients in plant development and metabolism and agrees with previous reports (Wu et al. 2003; Tschoep et al. 2009). The reduction of the number of internodes along with increased length of I-4 observed in shoots developed under –N was also observed by Triplett et al. (1981) in *Phaseolus*. Likewise, the observed alterations in xylem vessel area and form under –N (Table 4.2) corresponds with previous reports. Nitrogen effects on xylem morphology have been suggested to result from changes in cell elongation and expansion (Cooke et al. 2003; Pitre et al. 2010; Plavcová et al. 2012). We

observed that longer internodes were formed under –N conditions together with an increase in pectins with low methyl-esterification but a significant decrease in the potential of those pectins to form calcium bridges in young expanding internodes (Table 4.3). This combination could promote the activity of pectolytic enzymes, reducing of the molecular weight of pectic polymers and leading to expansion (Xiao et al., 2014). The alteration of grapevine cell morphology was also observed in callus tissues in response to nitrogen and phosphorus deficiency (Fernandes et al. 2016).

The impairment of cellulose deposition in organized tissues which was more pronounced in older internodes (Fig. 4.2; Table 4.3) and agrees with previous observations in dedifferentiated material (Fernandes et al. 2013). However, cellulose, although present in low concentration, provides mechanical strength for load bearing (Tenhaken 2015). In view of the importance of the CW for survival and adaption to environmental constrains, plants are equipped with compensatory alternative mechanisms to reinforce their CWs when the biosynthesis or deposition of a given component is impaired (Pilling and Höfte 2003; Wolf et al. 2012). Our results agree with such assumption.

The increased pectin amounts with a lower degree of esterification and the higher proportion of accessible arabinose-rich chains disclosed under –N and –P (Fig. 4.5; Table 4.3) are in agreement with our previously, observations in *V. vinifera* callus tissues (Fernandes et al. 2013), where an alteration in the degree of methyl-esterification occurred in response to nitrogen stress. This modification may occur localized to specific cells types and specific domains within the pectic chain, and is often developmentally regulated (Albersheim et al. 2010). PAM1 binds to long unesterified stretches of HG (regions of 30 contiguous unesterified HG) in a conformational dependent manner (Willats et al. 1999). PAM1 label was detected on the cell corners (Fig. 4.4). The occurrence of PAM1 epitopes within the CW junctions indicates that these HG domains have a role associated with cell adhesion at cell junctions (Willats at al. 2001). Pectins can serve as mechanical tethers between cellulose microfibrils (Park and Cosgrove, 2012; Peaucelle et al 2012; Wang et al 2012). Within the pectic family, RGs-I are highly heterogeneous and rich in neutral side chains (Caffall and Mohnen 2009). The increased accumulation of 1,5-arabinan epitopes in the CW of recently and later

formed internodes (Fig. 4.5; Table 4.3) can reflect a compensatory mechanism to cope with lower cellulose content. Apparently, in I-1, RG-I is more branched compered to I-4 that have a more linearized arabinan. *Arabidopsis* cellulose synthase mutant (*MUR10/CesA7*) showed an increase in pectic arabinan content in response to the impaired cellulose biosynthesis (Bosca et al. 2006). Likewise, under water deficit, Harholt et al. (2010) observed that RG-I arabinosyl side chains could work as plasticizers in CWs that undergo large physical remodeling to, in this way, reinforce their structure. CWs from callus growing under nitrogen and phosphorus depletion were also richer in tightly-attached arabinose-containing polysaccharides (Fernandes et al. 2013).

Pectin de-esterification can generate junction zones created by ordered, side-by-side associations of specific sequences of GalA linked through electrostatic and ionic bonding of carboxyl groups in the presence of calcium. In that situation pectin gelation occurs (Jarvis 1984) according to the well-known 'egg-box' model (Morris et al. 1982). Therefore, the observed increase of pectic chains linked by calcium ions in I-4 CWs developing under –N, revealed by higher 2F4 labelling (Liners et al. 1989), suggests additional CW stiffening (Michelli 2001) and reduced CW extensibility (Pelletier et al. 2010), which could explain the lower xylem vessel area observed under this condition (Table 4.2).

Hemicelluloses play an important role in the wall and as major class in dicots, XyG, can influence its characteristics. Also under nitrogen deficiency, the significant increase in the amounts of XyG detected in the CW can be explained as a mechanism to reinforce the CW, via biosynthesis of new material or the establishment of new linkages (Pilling and Hofte 2003; Wolf et al. 2012). The *Arabidopsis* XyG-deficient mutant (*xxt1/xxt2*) showed more extensible CWs than wild-type, supporting the reinforcing role for XyG (Park and Cosgrove 2012). XyG was observed in different region in I-1 and I-4. In both internodes XyG was present in the phloem and in some cells of the xylem, as observed by Marcus et al. (2008). In addition to the presence of XyG in the vascular bundle, in I-4, this polysaccharide was also present in the parenchyma cells (Fig. 4.6). Moreover, in I-4, the distribution of LM15 labelling is not contiguous along the wall with some preferred points of accumulation, especially under –N (Fig. 4.7). These observations suggest that XyG distribution is developmental regulated. Cellulose

microfibrils are not evenly coated with XyG but occurring in distinct CW domains and its structure can change during wall growth (Marcus et al. 2008). According to Ordaz-Ortiz et al. (2009), the localization pattern of the LM15 epitope may reflect the former edge of cell adhesion planes/intercellular space. The labelling pattern observed here may also be related to the "biomechanical hotspots" theory proposed by Park and Cosgrove (2012; 2015), where increased detection of XyG in some regions may be the result of the closely intertwine with cellulose at limited sites.

The lower amount of extensins incorporated in the wall observed resulting from growth under –N and –P conditions (Fig. 4.6; Table 4.3) can also contribute to compromise the CW structure. These hydroxyproline-rich glycoproteins are essential for cell plate formation as revealed by *Arabidopsis* mutant impaired in *AtEXT3* transcription (Hall and Cannon 2002) and it has been suggested that orderly assembly of pectins in the cell plate may involve covalent extensin-pectin cross-links (Nuñez et al. 2009; Qi et al. 1995). The fact that no changes in extensin amounts had been detected under –S may contribute for attenuating the effect caused, comparing to the other stress conditions.

Together our results support the assumption that grapevine organized tissues submitted to individual mineral stresses are impaired in specific CW components and suffer a reorganization of their deposition, in particular for pectin methyl-esterification and XyG degree and pattern, promoting a compensatory stiffening of the wall. The nutrient stress do not affected evenly all plant tissues. Mature internodes (I-4) showed a more pronounced reduction in cellulose and therefore an associated increase in Ca^{2+}-linked pectins and XyGs. Confirming a similar mechanism observed in callus tissues (Fernandes et al., 2013), our results highlight that *V. vinifera* used different strategies to overcome the adverse effects that mineral stress imposed at the CW level, depending on the severity perceived and its biological role. Due to its vital role on plant metabolism nitrogen affects more dramatically the CW.

Acknowledgements

The research was funded by Fundação para a Ciência e a Tecnologia (FCT) to CBAA (PestOE/AGR/UI0240/2011) and LEAF (Linking Landscape, Environment, Agriculture and Food) and Grant SFRH/BD/64047/2009 to JCF. The authors are pleased to acknowledge Prof. Leonor Morais and Vera Inácio for the assistance in the fixation procedures, Eng. Teresa Quilhó for her help in the preparation of cross-sections and Prof. Wanda Viegas for the use of the Leitz Laborlux S Fluorescence Microscope.

References

Albersheim P, Darvill A, Roberts K, Sederoff R, Staehelin A (2010) Plant cell walls: from chemistry to biology. Garland Science, New York.

Brashline L, Li S, Gu Y (2014) The trafficking of the cellulose synthase complex in higher plants. Ann Bot (Lond) 114: 1059–1067. doi: 10.1093/aob/mcu040.

Bosca S, Barton CJ, Taylor NG, Ryden P, Neumetzler L, Pauly M, Roberts K, Seifert GJ (2006) Interactions between MUR10/CesA7 dependent secondary cellulose biosynthesis and primary cell wall structure. Plant Physiol 142:1353–1363. doi: http://dx.doi.org/10.1104/pp.106.087700.

Braidwood L, Breuer C, Sugimoto K (2014) My body is a cage: mechanisms and modulation of plant cell growth. New Phytol 201:388–402. doi: 10.1111/nph.12473.

Caffall KH, Mohnen D (2009) The structure, function, and biosynthesis of plant cell wall pectic polysaccharides. Carbohydr Res 344:1879–1900. doi: 10.1016/j.carres.2009.05.021.

Cannon MC, Terneus K, Hall Q, Tan L, Wang Y, Wegenhart BL, Chen L, Lamport DT, Chen Y, Kieliszewski MJ (2008) Self-assembly of the plant cell wall requires an extensin scaffold. Proc Natl Acad Sci USA 105:2226–2231. doi: 10.1073/pnas.0711980105.

Cavalier DM, Lerouxel O, Neumetzler L, Yamauchi K, Reinecke A, Freshour G, Zabotina OA, Hahn MG, Burgert I, Pauly M, Raikhel NV, Keegstra K (2008) Disruption of two *Arabidopsis thaliana* xylosyltransferase genes results in plants

deficient in xyloglucan, a major primary cell wall component. Plant Cell 20:1519–1537. doi: 10.1105/tpc.108.059873.

Coimbra S, Almeida J, Junqueira V, Costa ML, Pereira LG (2007) Arabinogalactan proteins as molecular markers in Arabidopsis thaliana sexual reproduction. J Exp Bot 58:4027-35. doi: 10.1093/jxb/erm259.

Coito JL, Rocheta M, Carvalho L, Amâncio S (2012) Microarray-based uncovering reference genes for quantitative real time PCR in grapevine under abiotic stress. BMC Res Notes 5:220. doi: 10.1186/1756-0500-5-220.

Cooke JEK, Brown KA, Wu R, Davis JM (2003) Gene expression associated with N-induced shifts in resource allocation in poplar. Plant Cell Environ 26:757–770. doi: 10.1046/j.1365-3040.2003.01012.x.

Cosgrove DJ and Jarvis MC (2012) Comparative structure and biomechanics of plant primary and secondary cell walls. Front Plant Sci 3:204. doi: 10.3389/fpls.2012.00204

Cosgrove DJ (2005) Growth of the plant cell wall. Nat Rev Mol Cell Biol 6:850–861.

Cosgrove DJ (2000) Expansive growth of plant cell walls. Plant Physiol Biochem 38:109–24. doi:10.1016/S0981-9428(00)00164-9.

Fernandes JC, García-Angulo P, Goulao LF, Acebes JL, Amâncio S (2013) Mineral stress affects the cell wall composition of grapevine (*Vitis vinifera* L.) callus. Plant Sci 205-206:111–120. doi: 10.1016/j.plantsci.2013.01.013.

Hall Q, Cannon MC (2002) The cell wall hydroxyproline-rich glycoprotein RSH is essential for normal embryo development in *Arabidopsis*. Plant Cell 14:1161–1172. doi: http://dx.doi.org/10.1105/tpc.010477.

Harholt J, Suttangkakul A, Vibe Scheller H (2010) Biosynthesis of pectin. Plant Physiol 153:384–395. doi: 10.1104/pp.110.156588.

Hijazi M, Velasquez SM, Jamet E, Estevez JM, Albenne C (2014) An update on post-translational modifications of hydroxyproline-rich glycoproteins: toward a model highlighting their contribution to plant cell wall architecture. Front Plant Sci 5:395. doi: 10.3389/fpls.2014.00395.

Jarvis MC (1984) Structure and properties of pectin gels in plant cell walls. Plant Cell Environ 7:153–164. doi: 10.1111/1365-3040.ep11614586.

Knight H, Knight MR (2011) Abiotic stress signaling pathways: specificity and cross-talk. Trends Plant Sci 6:262–267. doi:10.1016/S1360-1385(01)01946-X.

Knox JP (2008) Revealing the structural and functional diversity of plant cell walls. Curr Opin Plant Biol 11:308–313. doi:10.1016/j.pbi.2008.03.001.

Knox JP (1992) Cell-adhesion, cell-separation and plant morphogenesis. Plant J 2:137–141.

Lamport DT, Kieliszewski MJ, Chen Y, Cannon MC (2011) Role of the extensin superfamily in primary cell wall architecture. Plant Physiol 156:11–19. doi: 10.1104/pp.110.169011.

Lee KJD, Marcus SE, Knox JP (2011) Cell wall biology: perspectives from cell wall imaging. Mol Plant 4:212–219. doi:http://dx.doi.org/10.1093/mp/ssq075.

Liners F, Letesson JJ, Didembourg C, Van Cutsem P (1989) Monoclonal Antibodies against Pectin: Recognition of a Conformation Induced by Calcium. Plant Physiol 91:1419–1424. doi: http://dx.doi.org/10.1104/pp.91.4.1419.

Lionetti V, Raiola A, Camardella L, Giovane A, Obel N, Pauly M, Favaron F, Cervone F, Bellincampi D (2007) Overexpression of pectin methyl-esterase inhibitors in *Arabidopsis* restricts fungal infection by Botrytis cinerea. Plant Physiol 143:1871–1880. doi: http://dx.doi.org/10.1104/pp.106.

Liu H, Ma Y, Chen N, Guo S, Liu H, Guo X, Chong K, Xu Y (2014) Overexpression of stress-inducible OsBURP16, the beta-subunit of polygalacturonase 1, decreases pectin contents and cell adhesion, and increases abiotic stress sensitivity in rice. Plant Cell Environ 37:1144–1158. doi: 10.1111/pce.12223.

Marcus SE, Verhertbruggen Y, Hervé C, Ordaz–Ortiz JJ, Farkas V, Pedersen HL, Willats WGT, Knox JP (2008) Pectic homogalacturonan masks abundant sets of xyloglucan epitopes in plant cell walls. BMC Plant Biol 8:60. doi: 10.1186/1471-2229-8-60.

Michelli F (2001) Pectin methylesterases: cell wall enzymes with important roles in plant physiology. Trends Plant Sci 6:414–419. doi:10.1016/S1360-1385(01)02045-3.

Moller I, Marcus SE, Haeger A, Verhertbruggen Y, Verhoef R, Schols H, Mikklesen JD, Knox JP, Willats W (2008) High-throughput screening of monoclonal antibodies against plant cell wall glycans by hierarchial clustering of their carbohydrate microarray binding profiles. Glycoconjug J 25:37–48. doi: 10.1007/s10719-007-9059-7.

Morris ER, Powell DA, Gidley MJ, Rees DA (1982) Conformations and interactions of pectins: I. Polymorphism between gel and solid states of calcium polygalacturonate. J Mol Biol 1982 155:507–516. doi:10.1016/0022-2836(82)90484-3.

Muszyńska A, Jarocka K, Kurczynska EU (2014) Plasma membrane and cell wall properties of an aspen hybrid (*Populus tremula* × *tremuloides*) parenchyma cells under the influence of salt stress. Acta Physiol Plant 36:1155–1165. doi: 10.1007/s11738-014-1490-3.

Nic-Can G, Hernández-Castellano S, Kú-González A, Loyola-Vargas VM, De-la-Peña C (2013) An efficient immunodetection method for histone modifications in plants. Plant Methods 9:47. doi: 10.1186/1746-4811-9-47.

Nuñez A, Fishman ML, Fortis LL, Cooke PH, Hotchkiss ATJ (2009) Identification of extensin protein associated with sugar beet pectin. J Agric Food Chem 57:10951–10958. doi: 10.1021/jf902162t.

Ordaz-Ortiz JJ, Marcus SE, Knox JP (2009) Cell wall microstructure analysis implicates hemicellulose polysaccharides in cell adhesion in tomato fruit pericarp parenchyma. Mol Plant 2:910–921. doi: 10.1093/mp/ssp049.

Park YB, Cosgrove DJ (2015) Xyloglucan and its interactions with other components of the growing cell wall. Plant Cell Physiol 56:180–94. doi: 10.1093/pcp/pcu204.

Park YB, Cosgrove DJ (2012) A revised architecture of primary cell walls based on biomechanical changes induced by substrate-specific endoglucanases. Plant Physiol 158:1933–1943. doi: 10.1104/pp.111.192880.

Pattathil S, Avci U, Baldwin D, Swennes AG, McGill JA, Popper Z, Bootten T, Albert A, Davis RH, Chennareddy C, Dong R, O'Shea B, Rossi R, Leoff C, Freshour G, Narra R, O'Neil M, York WS, Hahn MG. (2010) A comprehensive

toolkit of plant cell wall glycan-directed monoclonal antibodies. Plant Physiol 153:514–525. doi: 10.1104/pp.109.151985.

Peaucelle A, Braybrook S, Hofte H (2012) Cell wall mechanics and growth control in plants: the role of pectins revisited. Front Plant Sci 3:121. doi: 10.3389/fpls.2012.00121.

Peaucelle A, Louvet R, Johansen JN, Hofte H, Laufs P, Pelloux J, Mouille G (2008) *Arabidopsis* phyllotaxis is controlled by the methyl-esterification status of cell-wall pectins. Curr Biol 18:1943–1948. doi: 10.1016/j.cub.2008.10.065.

Pelletier S, Orden J, Wolf S, Vissenberg K, Delacourt J, Ndong YA, Pelloux J, Bischoff V, Urbain A, Mouille G, Lemonnier G, Renou JP, Hofte H (2010) A role for pectin de-methylesterification in a developmentally regulated growth acceleration in dark-grown *Arabidopsis* hypocotyls. New Phytol 188:726–739. doi: 10.1111/j.1469-8137.2010.03409.x.

Pelloux J, Rusterucci C, Mellerowicz EJ (2007) New insights into pectin methyl-esterase structure and function. Trends Plant Sci 12:267–277. doi: http://dx.doi.org/10.1016/j.tplants.2007.04.001.

Pilling E, Höfte H (2003) Feedback from the wall. Curr Opin Plant Biol 6:611–616. doi:10.1016/j.pbi.2003.09.004.

Pitre FE, Lafarguette F, Boyle B, Pavy N, Caron S, Dallaire N, Poulin PL, Ouellet M, Morency MJ, Wiebe N, Ly Lim E, Urbain A, Mouille G, Cooke JE, Mackay JJ (2010) High nitrogen fertilization and tension wood induction have overlapping effects on wood formation in poplar but invoke largely distinct molecular pathways. Tree Physiol 30:1273–89. doi: 10.1093/treephys/tpq073.

Plavcová L, Hacke UG, Almeida-Rodriguez AM, Li E, Douglas CJ (2012) Gene expression patterns underlying changes in xylem structure and function in response to increased nitrogen availability in hybrid poplar. Plant Cell Environ 36:186–199. doi: 10.1111/j.1365-3040.2012.02566.x.

Popper ZA, Fry SC (2008) Xyloglucan−pectin linkages are formed intraprotoplasmically, contribute to wall-assembly, and remain stable in the cell wall. Planta 227:781–794. Doi: 10.1007/s00425-007-0656-2.

Qi XY, Behrens BX, West PR, Mort AJ (1995) Solubilization and partial characterization of extensin fragments from cell walls of cotton suspension-cultures, evidence for a covalent cross-link between extensin and pectin. Plant Physiol 108:1691–1701. doi: 10.1104/pp.108.4.1691.

Ralet MC, Tranquet O, Poulain D, Moïs A, Guillon F (2010) Monoclonal antibodies to rhamnogalacturonan I backbone. Planta. 231:1373–1383. doi: 10.1007/s00425-010-1116-y.

Ringli C (2010) The hydroxyproline-rich glycoprotein domain of the *Arabidopsis* LRX1 requires Tyr for function but not for insolubilization in the cell wall. Plant J 63:662–669. doi: 10.1111/j.1365-313X.2010.04270.x.

Scheller HV; Ulvskov P (2010) Hemicelluloses. Ann Rev Plant Biol 61:263–289. doi: 10.1146/annurev-arplant-042809-112315.

Showalter AM (1993) Structure and function of plant cell wall proteins. Plant Cell 5:9–23. doi: http://dx.doi.org/10.1105/tpc.5.1.9.

Smallwood M, Martin H, Knox JP (1995) An epitope of rice threonine- and hydroxyproline-rich glycoprotein is common to cell wall and hydrophobic plasma membrane glycoproteins. Planta 196:510–522. Doi: 10.1007/BF00203651.

Tenhaken T (2015) Cell wall remodeling under abiotic stress. Front Plant Sci 5:771. doi: 10.3389/fpls.2014.00771.

Thompson DS (2005) How do cell walls regulate plant growth? J Exp Bot 56:2275–2285. doi: 10.1093/jxb/eri247.

Tschoep H, Gibon Y, Carillo P, Armengaud P, Szecowka M, Nunes–Nesi A, Fernie AR, Koehl K, Stitt M (2009) Adjustment of growth and central metabolism to a mild but sustained nitrogen limitation in *Arabidopsis*. Plant Cell Environ 32:300–318. doi: 10.1111/j.1365-3040.2008.01921.x.

Triplett EW, Heitholt JJ, Evensen KB, Blevins DG. (1981) Increase in internode length of *Phaseolus lunatus L.* caused by inoculation with a nitrate reductase-deficient strain of *Rhizobium* sp. Plant Physiol 67:1–4.

Velasquez SM, Salgado Salter J, Petersen BL, Estevez JM (2012) Recent advances on the post-translational modifications of EXTs and their roles in plant cell walls. Front Plant Sci 3:93. doi: 10.3389/fpls.2012.00093.

Velasquez SM, Ricardi MM, Dorosz JG, Fernandez PV, Nadra AD, Pol-Fachin L, Egelund J, Gille S, Harholt J, Ciancia M, Verli H, Pauly M, Bacic A, Olsen CE, Ulvskov P, Petersen BL,

Wang T, Zabotina O, Hong M (2012) Pectin-cellulose interactions in the *Arabidopsis* primary cell wall from two-dimensional magic-angle-spinning solid-state nuclear magnetic resonance. Biochemistry 51:9846–9856. doi: 10.1021/bi3015532.

Willats WGT, Orfila C, Limberg G, Buchholt HC, van Alebeek GJWM, Voragen AGJ, Marcus SE, Christensen TMIE, Mikkelsen JD, Murray BS, Knox JP (2001) Modulation of the degree and pattern of methyl-esterification of pectic homogalacturonan in plant cell walls. Implications for pectin methyl esterase action, matrix properties, and cell adhesion. J Biol Chem 276:19404–19413. doi: 10.1074/jbc.M011242200.

Willats WG, Gilmartin PM, Mikkelsen JD, Knox JP (1999) Cell wall antibodies without immunization: generation and use of de-esterified homogalacturonan block-specific antibodies from a naive phage display library. Plant J 18:57–65. doi: 10.1046/j.1365-313X.1999.00427.x.

Wolf S, Hematy K, Hoefte H (2012) Growth control and cell wall signaling in plants. Ann Rev Plant Biol 63:381–407. doi: 10.1146/annurev-arplant-042811-105449.

Wu P, Ma L, Hou X, Wang M, Wu Y, Liu F, Deng XW (2003) Phosphate starvation triggers distinct alterations of genome expression in *Arabidopsis* roots and leaves. Plant Physiol 132:1260–1271. doi: http://dx.doi.org/10.1104/pp.103.021022.

Xiao C, Somerville C, Anderson CT (2014) POLYGALACTURONASE INVOLVED IN EXPANSION1 functions in cell elongation and flower development in *Arabidopsis*. Plant Cell 26:1018–35. doi: 10.1105/tpc.114.123968.

Zabotina OA, Avci U, Cavalier D, Pattathil S, Chou YH, Eberhard S, Danhof L, Keegstra K, Hahn MG (2012) Mutations in multiple XXT genes of *Arabidopsis* reveal the complexity of xyloglucan biosynthesis. Plant Physiol 159:1367–84. doi: 10.1104/pp.112.198119.

Zykwinska A, Gaillard C, Buléon A, Pontoire B, Garnier C, Thibault JF, Ralet MC (2007) Assessment of in vitro binding of isolated pectic domains to cellulose by adsorption isotherms, electron microscopy and X-ray diffraction methods. Biomacromolecule: 8:223–232. doi: 10.1021/bm060292h.

Chapter 5

Relating water deficiency to berry texture, skin cell wall composition and expression of remodeling genes in two *Vitis vinifera* L. varieties

Fernandes JC[1], Cobb F[1,3], Tracana S[1], Costa GJ[1], Valente I[1], Goulao LF[2], Amâncio S[1]

[1] DRAT/LEAF, Instituto Superior de Agronomia, Universidade de Lisboa, Tapada da Ajuda, 1349-017 Lisbon, Portugal.

[2] BioTrop, Instituto de Investigação Científica Tropical (IICT, IP), Pólo Mendes Ferrão - Tapada da Ajuda, 1349-017 Lisbon, Portugal.

[3] Present address: Enotria Winecellars, London, UK

Published in Jornal of Agricultural and Food Chemistry (2015, 63:3951-61 doi: 10.1021/jf505169z)

5. Relating water deficiency to berry texture, skin cell wall composition and expression of remodeling genes in two *Vitis vinifera* L. varieties

Fernandes JC, Cobb F, Tracana S, Costa GJ, Valente I, Goulao LF, Amâncio S

Abstract

Cell wall (CW) is a dynamic structure that responds to stress. Water shortage (WS) impacts grapevine berry composition and its sensorial quality. In the present work berry texture, skin CW composition and expression of remodeling genes were investigated in two *V. vinifera* varieties, Touriga Nacional (TN) and Trincadeira (TR) under two water regimes, Full Irrigation (FI) and No Irrigation (NI). The global results allowed an evident separation between both varieties and the water treatments. WS resulted in increased anthocyanin contents in both varieties, reduced amounts in cellulose and lignin at maturation but an increase in arabinose-containing polysaccharides more tightly bound to the CW, in TR. In response to WS the majority of the CW related genes were down-regulated in a variety dependent pattern. The results support the assumption that WS affects grape berries by stiffening the CW through alteration in pectin structure, supporting its involvement in responses to environmental conditions.

Keywords: *Cell wall, gene expression, texture, V. vinifera, water stress*

Abbreviations

Act	Actin;
ºBrix	Total soluble solids;
CDTA	Cyclohexane–trans-1.2–diamine–N,N,N′,N′–tetraacetic acid sodium salt;
CW	Cell wall;
EXPA	Expansins;
GC	Gas Chromatography;
FI	Full Irrigation;
N	Newton;
NI	No Irrigation;
PCA	Principal Component Analysis;
PGs	Polygalacturonases;
PMEs	Pectin Methylesterases;
PMEIs	Pectin Methylesterases Inhibitors;
qPCR	real-time PCR;
TIF	Translation initiation factor eIF-3 subunit 4;
RGI	Rhamnogalacturonan-I;
TN	Touriga Nacional;
TR	Trincadeira;
XTH	Xyloglucan endotransglycosylase/hydrolase.

5.1. Introduction

Grapevine (*Vitis vinifera* L.) is one of the most important crops worldwide. About 80% of grapes cultivated are used in winemaking (Kammerer et al. 2004) but this species is also used to produce table grapes and raisins. Grapevines can be successfully grown in a range of different climates and management conditions, whose practices have been adapted to cope to each particular environment aiming at improved yields with adequate quality of the final product. Global climate changes are exacerbating problems associated with water deficit and high evapotranspiration rates that are likely to affect berry development, yield and ultimately wine quality. Much of the grape berry sensory characteristics, health benefits and quality for wine making are due to the presence of acids, anthocyanins, tannins and other phenolic compounds generally located in their skin cells (Pinelo et al. 2005; Montealegre et al. 2006) and whose accumulation is also dependent on the growing climatic conditions. Phenolic compounds are known to interact with the plant cell wall (CW) polysaccharides, so a role in polyphenol accessibility has been proposed (Ortega-Regules et al. 2008a).

For those reasons, understanding the CW changes that occur in grape skins during the berry development and softening has considerable importance in enology (Rolle et al. 2012).

Grape berries follow three distinct phases of development during their double sigmoidal growth curve. The phase I is due to cell division and enlargement and is followed by a phase II characterized by absence of changes in berry weight and volume, ending with the onset of ripening (veraison). After this lag phase a second growth phase (phase III) occurs in which is observed an increase in size of the central mesocarp cells, resulting from cell expansion within the berry. The ripening represents the last third of berry development, where softening and expansion occurs simultaneously, and is accompanied with sugar accumulation and water influx (Nunan et al. 1998). Both expansion and softening of the berry are modulated by modifications of its CW that include synthesis, disassembly and rearrangements of linkages between its components (Brummell 2006). CW remodeling provides flexibility to cell expansion directly altering the texture and indirectly, flavor and aromas (Dunlevy et al. 2009) Post-veraison corresponds to the stage where most of skin CW modifications occur although depending on

grape variety or abiotic conditions (Letaief et al. 2008). Some authors report a decrease in CW material accompanied by a thinning of the CW skins throughout berry maturation (Ortega-Regules et al. 2008b) but others report that the amount of CW polysaccharides remains constant although some modifications were observed at the pectic fraction level (Vicens et al. 2009).

The mesocarp CW of the grapes is composed of approximately 90% by weight of polysaccharides and up to 10% of proteins, in a structure that is typical of a Type-I CW model (Carpita and Gibeaut 1993) where cellulose and polygalacturonans account for 30-40% (Nunan et al. 1997; Vidal 2001). In the exocarp, polysaccharides account for 50% of the CW material (Lecas and Brilouet 1994) of which 30% are glycosyl-residues with composition similar to mesocarp walls (Saulnier and Brillouet 1989; Nunan et al. 1997) while 20% are pectins, mostly methyl esterified (Nunan et al. 1997). The remaining part is composed by insoluble proanthocyanidins, structural proteins (Lecas and Brilouet 1994) and lignin (Bindon et al. 2010).

Along berry development, a decrease in the molecular masses of both pectic and hemicellulosic polysaccharides and a reduction amount in cellulose and total hemicelluloses is observed at veraison and proceed throughout the subsequent phases (Yakushiji et al. 2001). In the pectic fraction the total amount and neutral and acid sugars temporally increase from before veraison to veraison, decreasing rapidly in post veraison (Salacci and Morrison 1990; Yakushiji et al. 2001). Conversely, the neutral sugar content of the hemicellulosic fraction decreases from before veraison to veraison. During veraison, the neutral sugar composition of each fraction changes little (Yakushiji et al. 2001). This result discloses a pattern of temporal modifications in grape berry softening from before veraison to veraison (Yakushiji et al. 2001).

Water is one of the most valued resources on the planet and understanding the impact of water deficit on grape development is vital. Mechanisms to cope with drought such as stomata control or extensive root systems developed by grapevine have been recognized (Chaves et al. 2003). It is well documented that water stress affects the variation in sugar and phenolic contents (Matthews and Nuzzo 2007; Deluc et al. 2011; Zarrouk et al. 2012). Although to lower extent than shoot organs, berry growth is sensitive to water deficits, being arrested (Dai et al.

2011), mainly at the mesocarp level, so that the seed and skin mass account more significantly to berry weight (Greenspan et al. 1994; Roby and Matthews 2004), leading to an irreversible reduction in berry size (Poni et al. 1994; Ojeda et al. 2001) often with thicker exocarps.

Under water deficit conditions occurring either before or post-veraison, the anthocyanin content in the grape skin increases in a cultivar-dependent pattern (Castellarin et al. 2007; Intrigliolo and Castel 2011). In ripening Cabernet Sauvignon grapes, water deficit leads to an increase in sugar accumulation only if imposed before veraison (Castellarin et al. 2007) while in the red cultivar Shiraz water deficit applied at post-veraison lead to a reduction in sugar concentration and an increase in phenolic compounds content, except for anthocyanins (Petrie et al. 2004). Despite that, a moderate water stress may increase the extractability of the anthocyanins into wine (Koundouras et al. 2009), therefore establishing a balanced water regime is vital to attain a quality wine.

Functional genomic resources for *V. vinifera* have proliferated rapidly in the last years after genome sequencing (Jaillon et al. 2007; Velasco et al. 2007) and such information has paved the way for large-scale studies of gene expression profiling during berry development. CW metabolism related genes were over-represented in gene clusters with significant differential expression in several development stages (Terrier et al. 2005; Waters et al. 2005;Deluc et al. 2007; Grimplet et al. 2007; Blazquez et al. 2012; Dal Santo et al. 2013).

In grapes, differences in CW composition and transcriptome (Venturini et al. 2013) were described between red wine varieties, advising investigating the behavior of different genetic backgrounds to understand physiological events and agronomic performances.

The goal of this research was to investigate the effect of non-irrigation versus irrigation practices on grape quality parameters, with emphasis on the berry skin CW in two Portuguese grape varieties, Touriga Nacional (TN) and Trincadeira (TR). Our hypothesis was to verify if the changes in berry composition due to water shortage were related with remodeling of skin CWs. For that purpose, berry yield, chemical characteristics and mechanical properties as well as skin CW composition and expression of key candidate genes associated with berry

development and ripening, were examined at two developmental stages, veraison and full maturation.

5.2. Materials and methods

5.2.1. Experimental vineyard and plant material

The study was conducted in 2012, on a vineyard located at the Centro Experimental de Pegões, Portugal (38°39'1"N; 8°38'42"W). The climate in the vineyard is Mediterranean with atlantic influence, summers with hot days and fresh nights and mild winters (Supplementary Fig. 5.1; 5.2). The soil is derived from podzols, with a sandy surface layer (0.6 – 1.0 m) and clay at 1 m depth. Mixed clones of Touriga Nacional and Trincadeira were established in 2002, both varieties grafted on 1103 Paulsen rootstock. The plants spaced 2.5 m between rows and 1 m within rows were trained on vertical trellis and uniformly pruned on a bilateral Royat Cordon, circa 12 buds per vine. Two irrigation regimes were considered: rain fed, non irrigation (NI) and full irrigation in which water was supplied according to the evapotranspiration (100% ETc) (FI, control). ETc was estimated from the reference evapotranspiration (ET0), obtained in an automatic weather station located within the experimental vineyard as described in Lopes et al. (2011). Irrigation water was applied with drip emitters (4.0 L h-1 for FI) two per vine, positioned 30 cm from the vine trunk and began on 29 June. Relative soil humidity in the soil profile was measured with a Diviner 2000TM capacitance probe (Sentek Environmental Technologies, Stepney, Australia) in vertical tubes at increments of 0.1 m from soil surface to a depth of 1.0 m (Santos et al. 2007) and assessed at plant level by predawn leaf water potential on the preselected plants as described by Scholander et al. (1965). Three plants in each treatment and plot were preselected for analysis for a total of six plants per water regime and variety. At veraison (50% colored berries) on 27 July for TR and 10 August for TN and full maturation the berries were pooled per water regime and variety and development stages (Supplementary Fig. 5.2). Berries were kept frozen from arrival from the field until further analyses.

5.2.2. Grape berry composition

Three samples of 100 berries were used for berry composition analysis per treatment and variety. After detaching the pedicels and acquired the sample fresh weight, must volume, pH, total soluble solids (TSS in °Brix) and total acidity, skin anthocyanin content and total phenol index were assessed.

The must pH was measured with a calibrated pH meter at room temperature. TSS were quantified using an Atago Brix pocket refractometer. Total acidity was measured via titration with sodium hydroxide, and expressed in g dm^{-3} of tartaric acid. Color density is given as the sum of absorbances in 1 cm pathway at 420, 520 and 620 nm (Dallas and Laureano 1994). For extracted anthocyanin content the skins were treated by the method of Carbonneau and Champagnol (1993). The skins were suspended in 96% ethanol buffered with tartaric acid solution (pH 3.6) and after 24 hours of maceration at 37°C the solution was centrifuged at 5000 g, 10 min for: 1) the calculation of extracted anthocyanin concentration was quantified by the method of Ribéreau-Gayon and Stonestreet (1965) with the absorbances obtained at 520 nm converted from a standard curve prepared with malvidin 3-glucoside; 2) estimation of total phenol by the absorbance in 1 cm pathway at 280 nm (Ribéreau-Gayon 1970).

5.2.3. Texture analyses

Two compression tests were employed to address texture attributes. Skin firmness was measured using a penetration test carried out on the detached skin of 50 mature berries trapped between two perforated acrylic plates. Measurements were made using a TA-XT Texture Analyser (Stable Micro Systems Ltd, UK) equipped with a HDP/90 platform and a cylinder flat probe of 2 mm Ø (ref.:P/2), using a 5 kg load cell (Walker et al. 2001). Tests were performed at 1 mm s^{-1} and berry skin breaking force is expressed in Newton (N). Berry texture analysis was carried out in 50 uniform mature berries. Measurements were made using a TA-XT Texture Analyser (Stable Micro Systems Ltd, UK) equipped with a HDP/90 platform and compression platens of 75 mm Ø, using a 5 kg load cell. The force to deform 10% of the berry equatorial diameter was expressed in Newton (N) (Rolle et al. 2011).

5.2.4. Cell Wall analysis

5.2.4.1. Cell wall extraction

Ten grams of fresh skins were lyophilized and homogenized in liquid nitrogen and the cell wall extracted according to the method described by Talmadge et al. (1973) as per Fernandes et al. (2013).

5.2.4.2. Cellulose and lignin quantification

Cellulose was quantified by the Updegraff (1969) method, using the hydrolytic conditions described by Saeman et al. (1963) and quantifying the released glucose by the anthrone method (Dische 1962). Klason lignin was determined using the method described by Hatfield et al. (1994). The results are expressed as µg per mg of CW.

5.2.4.3. Cell wall fractionation and monosaccharide quantification

The fractionation of berry skin CW at maturation followed the method by Selvendran and O'Neill (1987) with minor modifications as in Fernandes et al. (2013). Total sugars and uronic acids were determined using the phenol–sulphuric acid assay and the m–hydroxydiphenyl assay (Blumenkrantz and Asboe-Hansen 1973), respectively. Glucose and galacturonic acid were the corresponding standards. Neutral sugars were quantified by Gas Chromatography (GC) according to Albersheim et al. (1967) with minor adaptations (Fernandes et al. 2013) using a Supelco SP–2330 30m x 0.25mm x 0.20µm Capillary Column in a Varian 450-GC fitted with flame–ionization detector. The temperature program consisted of 210 °C (6 min hold) increased to 230 at 20 °C/min (25 min hold). Helium (2ml min^{-1}) was used as the carrier gas. Pure rhamnose, fucose, arabinose, xylose, mannose, galactose and glucose were used as monosaccharide standards and inositol as internal standard. For data acquisition the Galaxie Chromatography Software (Agilent, USA) was used.

5.2.5. Quantification of gene expression

5.2.5.1. RNA extraction and cDNA synthesis

Total RNA was extracted from *V. vinifera* berries using the Spectrum Plant Total RNA Kit (Sigma-Aldrich) with some modifications. Samples were ground in liquid nitrogen and 400 mg of the material was split into two Eppendorf tubes, and 900 µl lysis buffer was added per tube (Fasoli et al. 2012). After centrifugation (10 min) the combined supernatants were filtered using the necessary number of filtration columns. 750 µl of binding solution was added to each filtrate and passed through a single binding column. The RNA was then eluted using milliQ water. RNA samples were further treated with RNase-free DNase I (Qiagen) according to the manufacturer protocol and quantification was carried out in a Synergy HT Multiplate Reader, with Gene5 software, using a Take3™ Multi-Volume Plate (Bio-Tek Instruments Inc. Winooski, USA). For reverse transcription, the RevertAid reverse transcriptase priming with oligo-d(T) kit was used (Thermo Scientific) according to the manufacturer's recommendations.

5.2.5.2. Quantification of gene expression by quantitative PCR (RT-qPCR)

For each *V. vinifera* cDNA sequence retrieved from public data bases (Genoscope 12X (http://www.genoscope.cns.fr/spip/)), a set of specific primers (Supplementary Table 5.1) were designed and used to amplify grapevine skin cDNA resulting from the transcription of 2 µg of total RNA, using conventional PCR. When amplification confirmed the expression, the transcripts were quantified by real-time PCR (qPCR), performed in 20 µL reaction volumes composed of cDNA derived from 2 µg RNA, 0.5 µM gene-specific primers (Supplementary Table 5.1) and SsoFast™ EvaGreen® Supermixes (Bio-Rad, Hercules, CA) using a iQ5 Real-Time Thermal Cycler (BioRad, Hercules, CA). Reaction conditions for cycling were: 95°C for 3 min followed by 40 cycles at 95°C for 10 sec, 61°C for 25 sec and 72°C for 30 sec. Melting curves were generated in each case to confirm the amplification of single products and absence of primer dimerization. Each analysis was performed in triplicate reactions, each in three biological replicates (n=9, in which each replicate is the average of 3 technical measurements). The corresponding quantification cycles (Cq) obtained by the

iQ5 optical system software (Bio-Rad, Hercules, CA) were exported to a MS Excel spreadsheet (Microsoft Inc.) for quantification. Cq values of each gene of interest were normalized with respect to actin (Act) and translation initiation factor eIF-3 subunit 4 (TIF) Cqs (Coito et al. 2012). Relative gene expression values in NI conditions are presented in heat maps, performed using the MeV software (Saeed et al. 2003), as log_2 fold-change values in relation to control conditions (FI).

5.2.6. Statistical and Principal Component analysis

All data are presented as mean values ± standard deviation (SD) of at least three biological replicates in each assay. The results were statistically evaluated by variance analysis (ANOVA) and post hoc Bonferroni test with a $p<0.01$ significance level to compare the meaning of each effect with the SigmaPlot (Systat Software Inc.) statistical package. The Pearson correlation coefficient was calculated to disclose correlations between texture and skin composition values.

Data from 50 individual attributes measured at maturation were standardized and a pair-wised correlation matrix was calculated and subjected to eigenvalue decomposition to identify orthogonal components of the original matrix and generate a Principal Component Analysis (PCA) bi-plot, using the NTsys-PC version 2.20e software package (Rohlf 2008). The weight of each character in sample separation was determined by calculating eigenvectors using the mean values of each treatment (Supplementary Table 5.3).

5.3. Results

5.3.1. Composition of grape berries

A first indication of the effect of stress imposition (rain fed, Non Irrigation (NI) compared with Full Irrigation (FI), control) (Supplementary Fig. 5.1) on the *V. vinifera* berries was gained through the measurement of berry composition. NI treatment decreased berry weight and must volume in all cases and increased TSS at maturity in both varieties, as shown in Table 5.1, .although more

pronounced in TN at veraison and in TR at maturation. At veraison under water deficit total acidity was significantly different between varieties. However TR was delayed comparing to TN in either sugar increase or acid decrease (Table 5.1).

Table 5.1 Berry composition parameters (mean ± standard deviation) measured at Veraison and Maturation for Touriga Nacional (TN) and Trincadeira (TR), under Fully Irrigated (FI) and Non Irrigated (NI) conditions. Lower case letter indicates significant differences between treatments, capital letter indicates significant differences between stages and asterisk indicates significant differences between varieties, at $p<0.01$ significance.

			Berry Weight (g) per 100 berries	Must Volume (ml) per 100 berries	pH	Total soluble solids	Total acidity *(g l^{-1} of Ta)*
Veraison	**TN**	**FI**	126.83^{aA}±5.95	78.83^{a}±8.89	3.02^{A}±0.16	13.33^{A}*±0.51	13.00^{A}±1.88
		NI	78.60^{A}*±0.0	39.33^{A}*±3.06	3.11^{A}±0.13	12.67^{A}*±0.12	11.55^{A}*±0.91
	TR	**FI**	125.93^{A}±12.17	80.33^{A}±11.93	3.00^{A}±0.21	11.30^{A}±0.70	13.90^{aA}±2.13
		NI	105.33^{A}±6.35	61.00^{A}±4.36	2.87^{A}±0.08	10.53^{A}±0.90	17.50^{A}±0.74
Maturation	**TN**	**FI**	143.10^{a}*±4.88	92.83^{a}*±2.36	4.16±0.07	22.20^{a}*±0.26	2.70±0.15
		NI	113.28±11.93	64.00±11.03	4.29±0.06	20.23±0.84	2.55±0.26
	TR	**FI**	217.60^{a}±11.46	134.33^{a}±11.02	4.20±0.11	20.60^{a}±0.60	3.05±0.23
		NI	132.87±4.54	83.67±6.66	4.32±0.45	19.33±0.45	2.95±0.31

Furthermore we observed that in TN water shortage (TN-NI) induced anthocyanin accumulation while in TR higher anthocyanin content was observed at maturity in the absence of water shortage (Fig. 5.1A). The total phenol index followed the same pattern except for a slight increase at veraison in TR-NI (Fig. 5.1B). The color is one of the most important characteristics for a wine. At maturation water shortage induces a more intense color in the berry skin, which was more intense in TN berries (Fig. 5.1C).

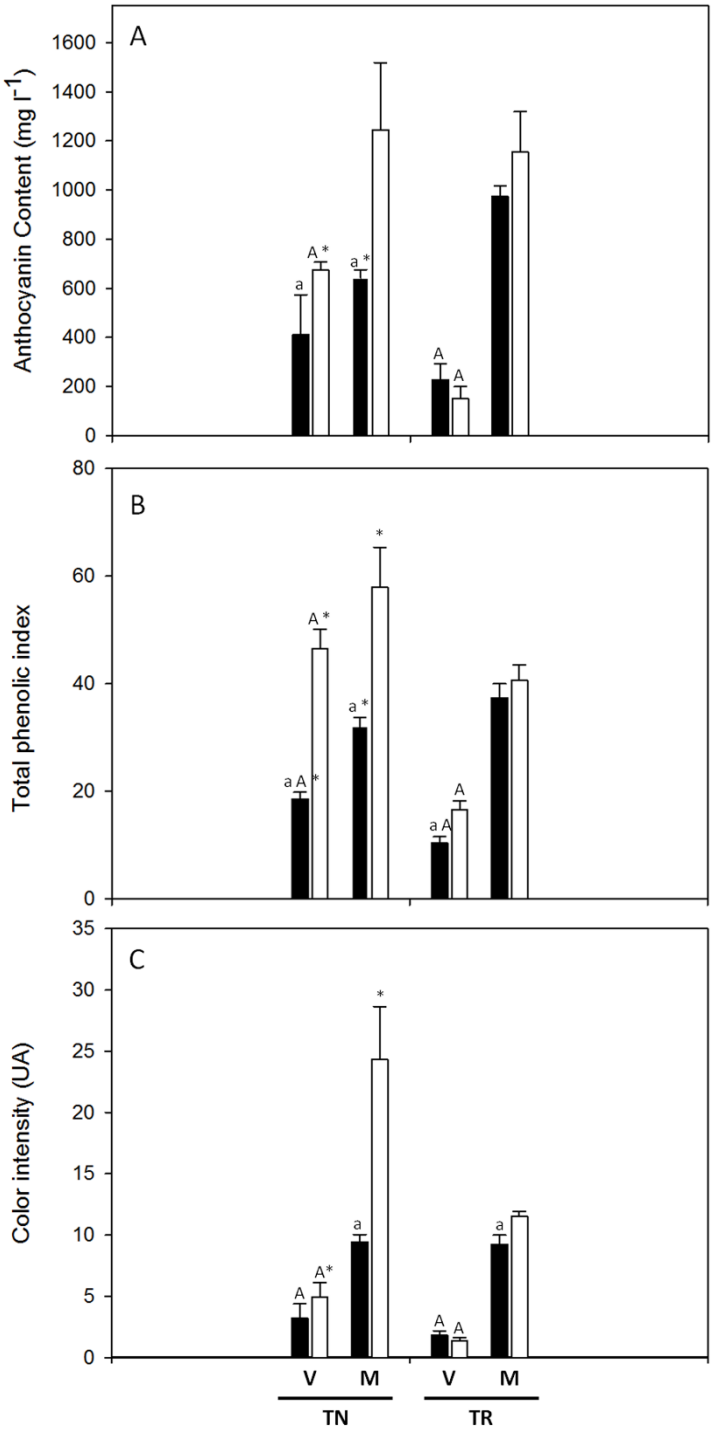

Fig. 5.1 (A) Anthocyanin content and (B) Total phenols and (C) Color intensity of Touriga Nacional (TN) and Trincadeira (TR) berries at Veraison (V) and Maturation (M) grown in Full Irrigation (FI, black bars) or Non Irrigation (NI, white bars). Bars represent means ±SD of three samples of 100 berries. Lower case letter indicates significant differences between treatments, capital letter indicates significant differences between stages and asterisk indicate significant differences between varieties, at $p<0.01$ significance.

5.3.2. Cellulose and lignin content

The cellulose content of TN berry skins was not affected by the water regime, either in veraison or in maturation. However in TR a statistically significant decrease was observed in NI between veraison and maturation and, at maturation, between control and NI (Fig. 5.2A). Following the same pattern, lignin decreased in TR-NI at maturation (Fig. 5.2B).

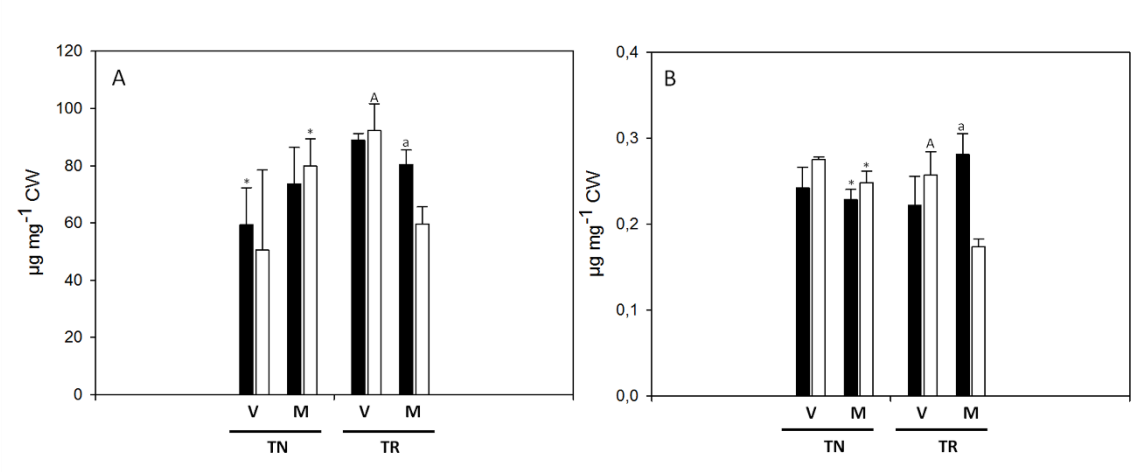

Fig. 5.2 (A) Cellulose content and (B) lignin contend of Touriga Nacional (TN) and Trincadeira (TR) berry skin CW at Veraison (V) and Maturation (M) grown in Full Irrigation (FI, black bars) or Non Irrigation (NI, white bars). Bars represent means of three samples ±SD. Lower case letters indicate significant differences between treatments, capital letters indicate significant differences between stages and asterisk indicate significant differences between varieties, at p<0.01 significance.

5.3.3. Berry texture

Alterations in berry firmness can be addressed by measuring changes in compression while skin break force is given by the force rendered in penetration tests. In TN-NI a higher force for berry deformation was necessary while skin break force and energy were higher in TR-NI, decreasing from veraison to the maturation as expected (Table 5.2). The Young modulus (E_{sk}) that represents the material resistance to axial deformation had the same trend as skin break force, revealing a decrease in the springiness of TR-NI berry skins (Table 5.2). Our results suggest that these specific properties may be influenced by the amount of phenolic compounds (Supplementary Table 5.2).

The Pearson correlation between the berry texture attributes and CW composition showed significant negative correlations between skin break force

and skin break energy with anthocyanin and total phenol contents. Noticeably, cellulose content was found to be positively correlated to the force needed to break the skin while lignin correlated to the energy applied to achieve rupture.

Table 5.2 Berry compression, Skin break force, Skin break energy and Young's modulus for elasticity parameters (mean ± standard deviation) of Touriga Nacional (TN) and Trincadeira (TR) berries at Veraison (V) and Maturation (M) grown in Full Irrigation (FI) or Non Irrigation (NI). Lower case letters indicate significant differences between treatments, capital letters indicate significant differences between stages and asterisk indicate significant differences between varieties, at $p<0.01$ significance.

			Berry Firmness (N)	Skin break force (N)	Skin break energy (mJ)	Young's modulus for elasticity (N mm^{-1})
Veraison	TN	FI	2.07^{a*}±0.62	4.75^{a}±0.65	3.82^{a}±1.1	2.85±0.62
		NI	4.46*±0.71	3.40*±0.73	2.14^{A*}±0.79	2.87*±0.82
	TR	FI	3.54±0.39	5.08^{a}±0.79	4.85^{aA}±1.26	3.11^{aA}±0.83
		NI	2.99±0.42	7.17^{A}±0.84	6.05^{A}±1.63	5.2^{A}±0.98
Maturation	TN	FI	1.03^{a*}±0.67	4.83±0.78	3.58±0.9	2.7^{a*}±0.43
		NI	4.19*±0.37	4.50±0.75	3.58*±0.96	3.25*±0.64
	TR	FI	3.10±0.36	3.54^{a}±0.60	3.73^{a}±0.99	1.93^{a}±0.37
		NI	2.49±0.46	4.97±0.60	4.85±0.91	2.51±0.31

5.3.4. Sugar composition in CW fractions

Since major differences in cellulose and lignin between irrigation practices and varieties were observed at maturation stage, only this stage was considered for berry skin CW fractionation. CDTA extracts polysaccharides that are less bound to the CW. The more tightly bound CW polysaccharides are extracted by increasing KOH molarity. The majority of polysaccharides were extracted in the alkaline fractions, particularly the 6M KOH, with the exception of TR-FI. Considering the responses of the varieties to the irrigation regimes, in TN-NI weakly bound polysaccharides showed to be more extractable than under full

water availability. In TR-NI more polysaccharides were extracted in the 6M KOH fraction suggesting a more tight binding to the CW (Fig. 5.3).

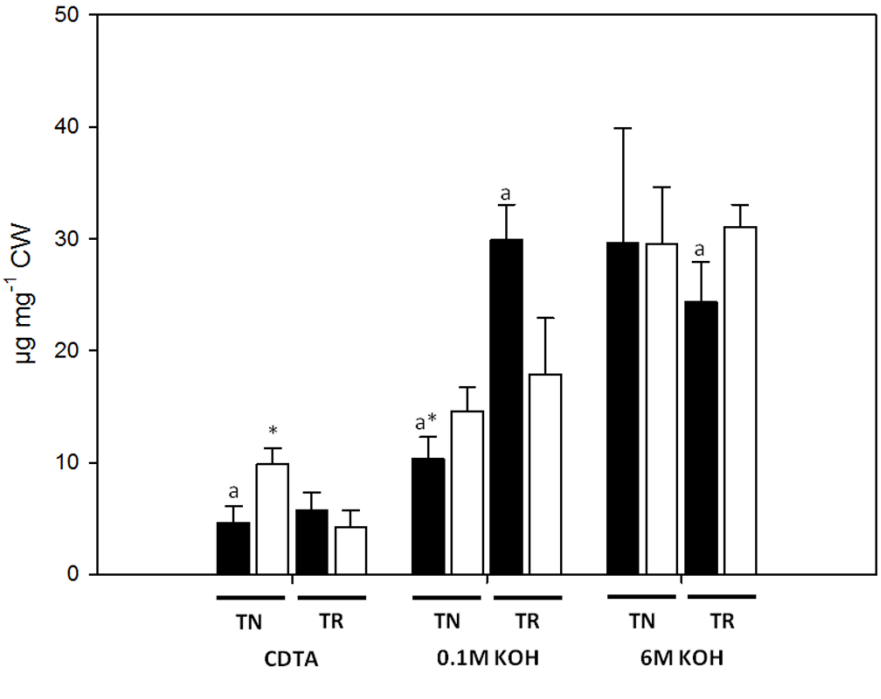

Fig. 5.3 Total sugar quantification in CW fraction obtained from Touriga Nacional (TN) and Trincadeira (TR) berry skin CW at Maturation (M) grown in Full Irrigation (FI, black bars) or Non Irrigation (NI, white bars). Units are µg of glucose equivalentes mg^{-1} CW. Bars represent means of three samples ±SD. Lower case letters indicate significant differences between treatments, and asterisk indicate significant differences between varieties, at p<0.01 significance.

The majority of uronic acids (reflecting the pectin content) were extracted in the CDTA and 0.1M KOH fractions, with higher amounts in the latter (Fig. 5.4A, B). No differences were observed between treatments or varieties. The analysis of the CW fractions by GC showed that the most abundant neutral monosaccharide present in all fractions was arabinose, followed by glucose, xylose and galactose. The arabinose-, xylose- and glucose-containing polysaccharides was in all cases higher in TR in all alkaline treatments although in 0.1M KOH fraction, TR-NI samples showed decreased arabinose-containing polysaccharides when compared to the control (Fig. 5.4B), which were shifted to the strong alkaline fraction (Fig. 5.4C). For TN-NI, the 6M KOH fraction, showed a small but significant increase of arabinose-containing polysaccharides. The majority of xylose-containing polysaccharides were putatively tightly bounded to the CW

since they only could be extracted by strong alkaline conditions. Conversely to TN, TR-NI was richer in xyloglucan polysaccharides (Fig. 5.4C).

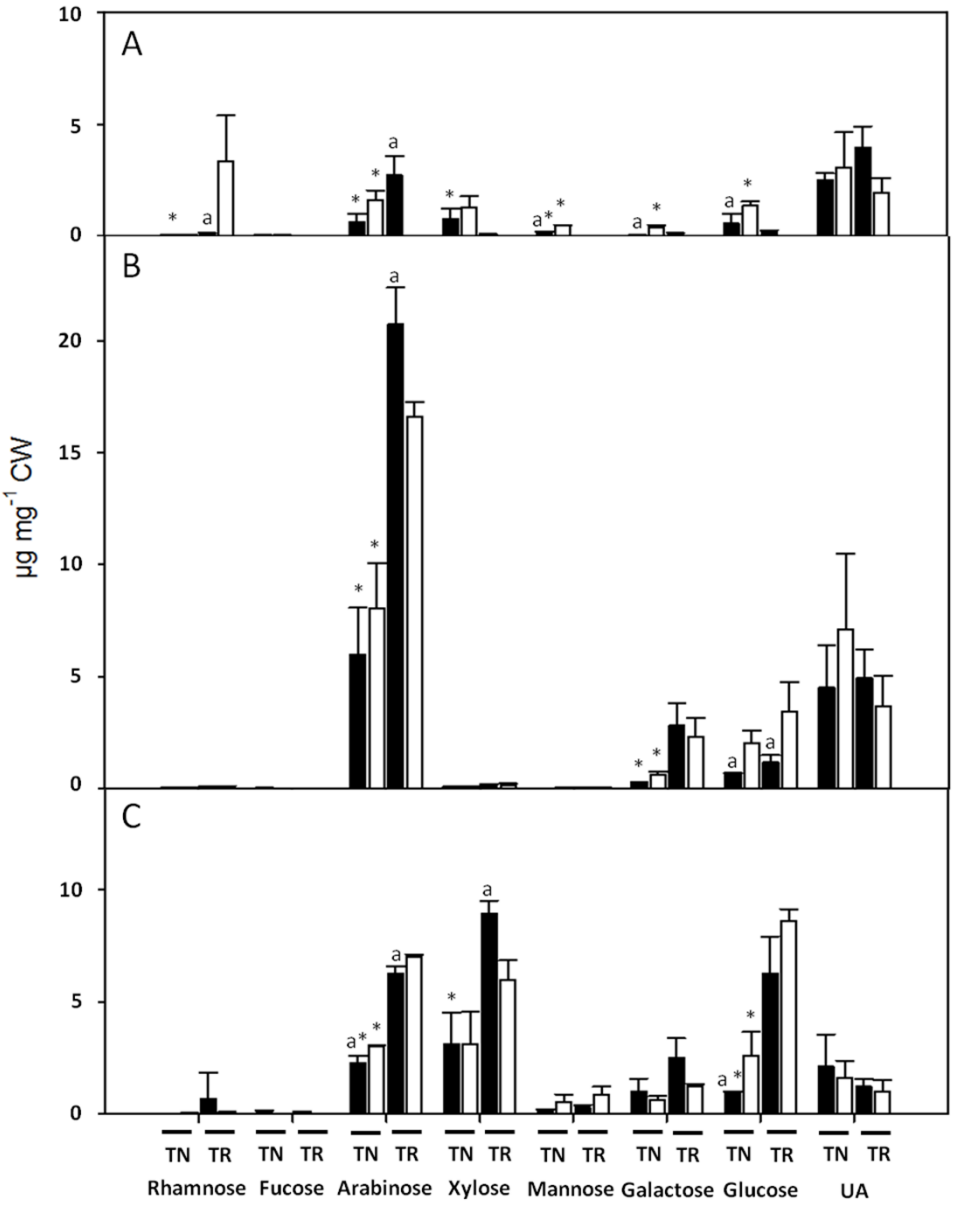

Fig. 5.4 Monosaccharide composition of berry skin CW (A) CDTA-soluble fraction, (B) 0.1M KOH-soluble fraction and (C) 6M KOH-soluble fraction obtained by GC analysis and Uronic acids levels measured by the m-hydroxydiphenyl assay in Touriga Nacional (TN) and Trincadeira (TR) berries at Maturation grown in Full Irrigation (FI, black bars) or Non Irrigation (NI, white bars). Units are µg of each monosaccharide and galacturonic acid equivalents for uronic acids (UA) mg^{-1} CW. Bars represent means of three samples ±SD. Lower case letters indicate significant differences between treatments, and asterisk indicate significant differences between varieties, at p<0.01 significance.

5.3.5. Changes in the expression of selected key genes involved in modification of the berry CW

One way to assess the effect of a stress on a given metabolic event is to understand the transcription of related genes. Fig. 5.5 shows that water depletion gave rise to different gene expression patterns some activated at veraison and others at maturation. As compared to TR, TN had more responsive genes, most of them down-regulated after water deficit in the two varieties. The expression of XTH genes was severely down-regulated at veraison in both varieties, with the exception of VvXTH14 in TN. Conversely, at maturation, members of this family were not affected by the water shortage.

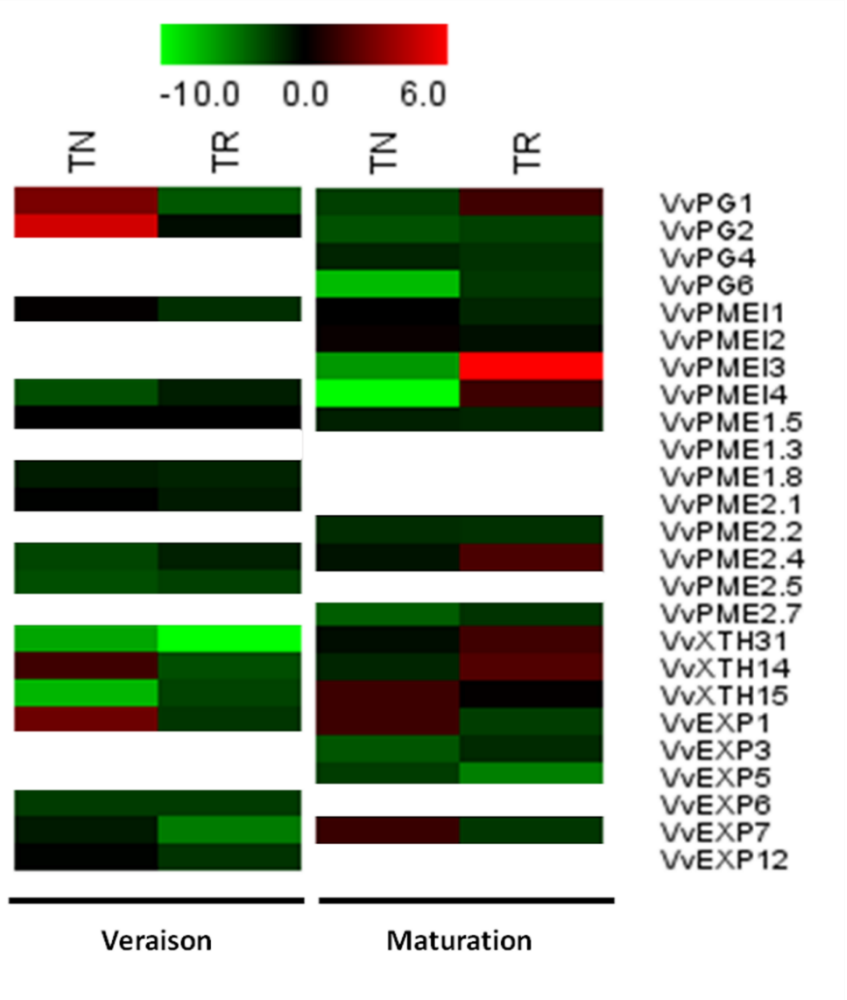

Fig. 5.5 Heat-map of transcriptional responses to water shortage of CW modifying genes in TN and TR varieties at veraison and maturity. Color scale from green to red indicates log2 NI/FI expression ratio from 10-fold repression to 6-fold over transcript.

At veraison both PGs investigated were up-regulated in TN while VvPG1 in TR showed a 3 fold down-regulation compared to the control. In maturation the majority of PGs were repressed, including VvPG6 which had a 7 fold repression compared to the control (Fig. 5.5). The majority of EXPA gene expression had a similar down-regulation at veraison. EXPA genes were more repressed at maturation (Fig. 5.5). The expression of PME genes unraveled a higher number of members showing down-regulation under water scarcity in both TN and TR. As in the case of EXPA, these genes were more repressed at maturation. Interestingly, under water shortage, PMEI gene expression showed to be generally not affected at veraison. At maturation in TN two genes were down-regulated (VvPMEI3 and VvPMEI4) but the same VvPMEI3 in TR was up-regulated with a fold change of 6 (Fig. 5.5).

5.3.6. Data integration

To obtain a global representation of all data collected at maturation, samples were graphically plotted in a reduced number of axis after multivariate analysis (Principal Component Analysis; PCA). Principal components 1 and 2 (PC1 and PC2) in combination explain 58.8% of the total variation and could separate the samples according to the variety and water regime they were submitted. Replicates were generally closely clustered, demonstrating the accuracy of the analyses performed and the true biological basis of the measured dissimilarities. The results shown in Fig. 5.6 reveal that PC1 clearly differentiates between varieties while PC2 separates the samples according to the treatments. According to the resultant eigenvectors calculated using the average values of the triplicates (Supplementary Table 5.3), the variables that contributed more to PC1 separation were the higher amounts of arabinose- and galactose-containing polysaccharides extracted in the 0.1M KOH fraction and xylose-containing polysaccharides collected in both alkaline solutions, and the lower relative transcription of VvPMEI1, VvPMEI2, VvXTH31 and VvXTH15 in the TR variety. PC2 separation was mainly explained by lower amounts of glucose-containing polymers extracted by 0.1M KOH solutions, by mannose- and fucose-containing polysaccharides present in the 6M KOH solution under FI regime and by the lower

relative expression of two polygalacturonase genes, VvPG2 and VvPG4 in the control.

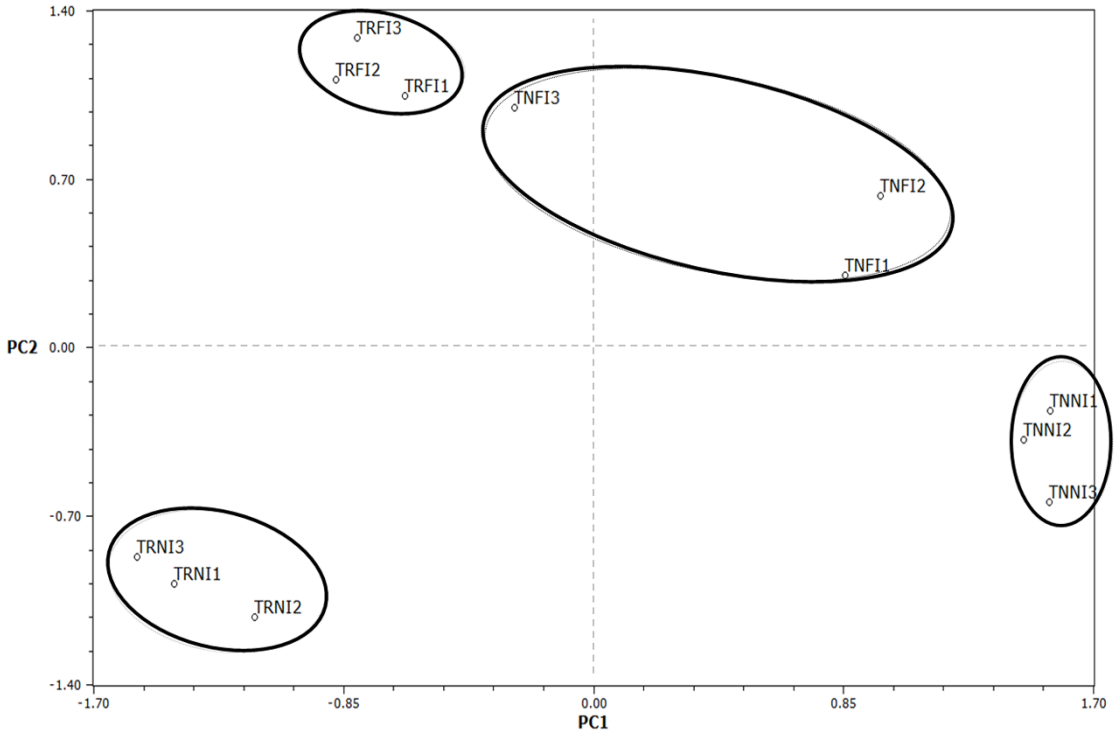

Fig. 5.6 Principal component analysis (PCA) from 50 individual attributes measured at maturation. PC1 and PC2 explain respectively 35.3% and 25.6% of the total variation.

5.4. Discussion

Water deficit during *Vitis vinifera* L. growth, like other abiotic stresses, is known to decrease growth and yield (Chaves et al. 2007; 2010; Flexas et al. 2010), impacting berry physical and chemical composition (Zsófi et al. 2014), and ultimately, influencing the sensorial quality of the final product (Bucchetti et al. 2011). In this work, we assessed the influence of non-irrigation in comparison with water full conditions in berry characteristics, CW composition, and gene expression of two widespread Portuguese winegrape varieties, Touriga Nacional and Trincadeira, growing under Mediterranean conditions with atlantic influence, to which some grapevines varieties are better adapted than others (Schultz and Stoll 2010). The clear effects exerted by water deficit on berry characteristics (Table 5.1) confirm previous results showing that water deficiency results in an increase in anthocyanin concentration (Olle et al. 2011), and in total phenols (Fig 5.1) (Castellarin et al. 2007). It is unsure whether the increase in total polyphenol

content is purely due to the fluctuations in anthocyanin content or by the increase of other phenolic compounds including flavanols and proanthocyanidins (Castellarin et al. 2007). Moreover, the variety-specific amount of anthocyanin observed is also in agreement with previous studies (Mazza 1995). The global CW results allowed an evident separation of both varieties and the imposed water regimes, as illustrated by the PCA plots (Fig. 5.6). The separation in the two first components is mainly explained by the amount of monosaccharides extracted in distinct fractions, which suggest different polysaccharide linkages, and by CW-related gene expression (Supplementary Table 5.3).

Among the effects on CW, the alterations mostly associated with changes in composition and architecture are the berry texture characteristics. Texture analysis is a rapid and low-cost analytical technique that can be applied in viticulture and enology as a routine tool for monitoring grape quality (Rolle et al. 2012). In our research, texture measurements were conducted with the objective of comparing the changes in mechanical properties of the berry and berry skin between the two cultivars under the water regimes imposed during grape development. Therefore, and since the assays were conducted with frozen/thawed grapes, the measurements do not describe fresh berries values but clearly indicate that under our conditions the higher skin break force measured in TR-NI berries (Table 5.2) seems to be variety dependent, since TN break force was not affected by the water regime. Conversely, in TN-NI compression tests higher forces were needed to attain the same berry deformation (Table 5.2). The increased in berry skin break force in TR-NI was also observed in stressed Mondeuse, Becuét, and Fumin grapes obtained during on-vine drying (Rolle et al. 2009; 2010). Recent observations by Zsófi et al. (2014) in Kékfrankos grapes growing in greenhouse conditions, suggest that skin break force increase significantly as a result of water deficit. Conversely, berry firmness measured as berry deformation by the compression test was decreased in TN-NI. As a whole, the skin break force and skin break energy correlated negatively with the amounts of berry secondary metabolites but positively with cellulose and lignin contents, respectively (Supplementary Table 5.2). This suggests that the lower cellulose and lignin content verified after water deficiency contributes, although in different dimensions to the alteration in the skin mechanical

properties. The responses obtained so far corroborate the dependence on the variety and the environmental conditions (Rolle et al. 2011; Rio Segade et al. 2011). However, and taking advantage of aftermost results with fresh berries from an experimental water regime similar but not equivalent to the one reported here, for fully clarification the presented results might be confirmed with fresh berries from the cultivars and under the same experimental set up as applied in the present study.

Aiming at gaining a further insight on the basis of water deficit on polysaccharide differences, general CW composition was investigated in all samples. In this work TR-NI showed reduced amounts in cellulose and lignin at maturation (Fig. 5.2) which was accompanied by a marked reduction in berry size (Table 5.1). In Muscat Gordo Blanco variety, Nunan et al. (1998) found that cellulose remained unaltered during ripening putting forward the assumption that the decrease in TR may be a genotype-specific response to water availability. Conversely, the increased break force may be caused by CW polysaccharides besides cellulose since this polymer serves as a scaffold for the binding of other CW components (Lerouxel et al. 2006). The shift of arabinose-containing polysaccharides from the 0.1M KOH to 6M fraction in TR-NI (Fig. 5.4) may indicate that rhamnogalacturonan-I (RGI) arabinosyl residues became more tightly bound into CW with water shortage. The presence of RGI decorated with arabinose rich side chains in water deficient conditions can work as CW plasticizers (Harholt et al. 2010). Under water shortage arabinose- and also galactose- rich polymers are known to retain relatively longer mobility than other CW polymers filling the cavities created upon physical rearrangement of the CW (Tang et al. 1999). The unusually high arabinan content (approximately 38 mol %) observed in the resurrection plant *Myrothamnus flabellifolius* (Moore et al. 2006) further suggests arabinose role for plants coping with water scarcity. Changes in pectin, break energy and Young modulus (E_{sk}) showed similar patterns to break force, again with a variety dependent behavior, skins becoming less elastic in the absence of water. From the correlation of E_{sk} values with total phenols content (Supplementary Table 5.2), it can be inferred that the stiffening of the CW may contribute to the extractability of the phenolic compounds, as observed by Rolle

et al. 2011) As referred by other authors Torchio et al. (2010) and Zsófi et al. (2014) an increase in elasticity was observed from veraison to ripening.

Gene expression of key candidate genes was considered to be differential when above a $\log_2$ +/- 2-fold change relative to the control and showed that all gene families investigated possess members that respond to water shortage (Fig. 5.5). This complementary approach provided evidence that, although with a general pattern of down-regulation, responsive individual genes within each family were different depending on the stages. Exceptions were VvPG1 and VvPG2 at veraison in TN and VvPMEI3 at maturation in TR that are up regulated, both indicating changes in the pectic network of the CWs, which suggests different patterns of expression depending of the development stage, in accordance with Deluc et al. (2007) findings. According to PCA, concerning gene expression, the observed differences between varieties are putatively associated with differences in the inhibition of pectin methylesterification and in the expression of members of the xyloglucan endotransglycosylase/hydrolase (XTH) family. Pectins are embedded within the cellulose/hemicellulose network, forming a hydrophilic gel that impose mechanical features to the wall such as regulation of the hydration status or defining the porosity and stiffness of the wall (Peaucelle et al. 2012). PME activity can alter the degree and pattern of methyl esterification (Jolie et al. 2010) and therefore, change the biophysical properties of the CW. Under water scarcity the PME expression decreased, as also observed for some members in Sangiovese grapes (Zoccatelli et al. 2013). The maintenance in the degree of methyl esterification of pectins, as observed by Zoccatelli et al. (2013) in Sangiovese grapes, may lead in our case to the preservation of the CW structure, especially in TR, which is further supported by the penetration tests. At the biochemical level, the activity of PMEs is also regulated by PMEIs. Grimplet et al. (2007) reported modifications in the expression of a PMEI member, with downregulation at maturation, which is in agreement with the pattern observed in this work in TN. Conversely in TR its expression is upregulated, which contributes to the variety separation observed in the PCA analysis (Fig. 5.6) This PME activity may change the pectin methyesterification degree. Changes in the degree of pectin methylation seem to be genotype-specific in *Vitis*, decreasing as ripening progresses in some cultivars like Cabernet Sauvignon, Merlot and Monastrell,

while it hardly changes in Syrah (Ortega-Regules et al. 2008). This observation is in accordance with the differences found between TN and TR. Fifteen to 25% of the hemicelluloses present in dicot primary CW are constituted by xyloglucans (Carpita and Gibeaut 1993). The xyloglucans frame can be modified by XTHs which can potentially have two distinct catalytic activities, namely transglycosylase (XET), or hydrolase (XEH) (Fry et al. 1992; Nishitani 1992; Rose et al. 2002). These activities have been associated with the fruit softening that occurs during Phase III of berry development and largely modulate CW loosening (Nunan et al. 1998). In the present study, the lowest VvXTH expression was observed at veraison, mainly in TR in result of water shortage. The low activity suggested by the down-regulation of XTH genes may lead to maintenance of the CW structure under water shortage. On the other hand, Deluc et al. (2007) observed that XTH gene expression declined significantly along berry development.

The effect of distinct water regimes on gene expression was mainly due to the transcript abundance of polygalacturonases (PGs), which are CW-localized enzymes that cleave stretches of unesterified GalA residues and weaken the middle lamella (Brummell and Harpster 2001). PG activity is known to accompany fruit ripening (Cabanne et al. 2001). The up-regulation of PG at veraison and subsequent down-regulation at maturation is in agreement with Grimplet et al. (2007) under water deficit. In the pectin fraction of the grape mesocarp, both polysaccharide amounts and the neutral and acidic sugars of the water soluble fraction, temporally increase from before veraison to veraison stages, decreasing rapidly thereafter (Silacci and Morrison 1990; Yakushiji et al. 2001). The maintenance of the pectin level in response to water shortage, especially in the 6M KOH fraction may be partially explained by the low transcription levels of PMEs and PGs strengthening the CW and increasing the force necessary to break the skin. In the mesocarp, pectin and xyloglucan solubilization seems to occur at later stages of ripening while depolymerization events occur at earlier stages (reviewed by Goulao et al. (2012)).

Expansins (EXPA) play also an important role in CW loosening phenomenon via non-enzymatic mechanisms (Sampedro and Cosgrove 2005). Under water shortage most expansin genes decreased expression during berry development,

as observed by Grimplet et al. (2007). Studies in post-harvest Corvina withering berries, which can be considered as a water stress condition (Dal Santo et al. 2013) demonstrated the alteration in expression of several expansin genes, namely the downregulation of VvEXPA1, VvEXPA14 and VvEXPA19 during withering. Some authors propose that expansins are associated to pectin turnover, probably by regulating the contact between pectins and pectin-degrading enzymes (Jolie et al. 2010). Brummell et al. (1999) suggests the relation between different networks: the disassembly of the hemicellulosic network by expansin may be necessary for modifications in the pectins promoting physical accessibility of pectin substrates to PGs enzymes. From our results it is possible to forward the hypothesis that water depletion has an indirect impact on pectins through the process proposed by Brummell et al. (1999).

In summary, the overall results suggest differences in pectin metabolism between varieties in response to distinct water availability during growth under field conditions, and support its involvement in distinct responses to environmental conditions. Water shortage affects grape berries by stiffening the CW, probably through alteration in PGs expression and pectin structure, in a way that significantly depends on the variety. Contrasting softening behaviors during ripening differs sufficiently between genotypes to allow discrimination regarding technological differences that can influence oenological practices.

Acknowledgements

The research was funded by Fundação para a Ciência e Tecnologia (FCT): project PTDC/AGR-GPL/099624/2008, the PhD research grant SFRH/BD/64047/2009 to JCF and CBAA PestOE/AGR/UI0240/2011. This work also benefited from European project KBBE InnoVine (ref. 311775) and the European COST Action FA1106 “QualityFruit”. The field work was performed at PORVID Experimental Station (Pegões, PT) and the authors thank the president of its executive board, Prof. Antero Martins. The authors also like to acknowledge Prof. Isabel Sousa and Prof. Margarida Moldão for excellent discussions on biophysical and chromatography experiments.

References

Albersheim P, Nevins DJ, English PD, Karr AA (1967) method for the analysis of sugars in plant cell-wall polysaccharides by gas-liquid chromatography. Carbohyd Res 5:340-345.

Bindon KA, Smith PA, Kennedy JA (2010) Interaction between grape-derived proanthocyanidins and cell wall material. Effect on proanthocyanidin composition and molecular mass. J Agr Food Chem 58:2520-2528.

Blazquez MA, Lijavetzky D, Carbonell-Bejerano P Grimplet J, Bravo G, Flores P, Fenoll J, Hellín P, Oliveros JC, Martínez-Zapater JM (2012) Berry flesh and skin ripening features in *vitis vinifera* as assessed by transcriptional profiling. Plos One 7:e39547.

Blumenkrantz N, Asboe-Hansen G (1973) New method for quantitative determination of uronic acids. Anal Biochem 54:484-9.

Brummell DA (2006) Cell wall disassembly in ripening fruit. Funct Plant Biol 33:103.

Brummell DA, Harpster MH (2001) Cell wall metabolism in fruit softening and quality and its manipulation in transgenic plants. Plant Mol Biol 47:311-40.

Bucchetti B, Matthews MA, Falginella L, Peterlunger E, Castellarin SD (2011) Effect of water deficit on Merlot grape tannins and anthocyanins across four seasons Sci Hortic 128:297–305

Cabanne C, Doneche B (2001) Changes in polygalacturonase activity and calcium content during ripening of grape berries. Am J Enol Viticult 52:331-335.

Carbonneau A, Champagnol F (1993) Nouveaux systemes de culture integré du vignoble. In Programme AIR.

Carpita NC, Gibeaut DM (1993) Structural models of primary-cell walls in flowering plants - Consistency of molecular-structure with the physical-properties of the walls during growth. Plant J 3:1-30.

Chaves MM, Maroco JP, Pereira JS (2003) Understanding plant responses to drought - from genes to the whole plant. Funct Plant Biol 30:239-264

Chaves MM, Santos TP, Souza CR, Ortuño MF, Rodrigues ML, Lopes CM, Maroco JP, Pereira JS (2007) Deficit irrigation in grapevine improves water-use efficiency while controlling vigour and production quality. Ann Appl Biol 150:237-252.

Chaves MM, Zarrouk O, Francisco R, Costa JM, Santos T, Regalado AP, Rodrigues ML, Lopes CM (2010) Grapevine under deficit irrigation: hints from physiological and molecular data. Ann Botany 105:661-676.

Castellarin SD, Matthews MA, Di Gaspero G, Gambetta GA (2007) Water deficits accelerate ripening and induce changes in gene expression regulating flavonoid biosynthesis in grape berries. Planta 227:101-12.

Coito JL, Rocheta M, Carvalho L, Amâncio S (2012) Microarray-based uncovering reference genes for quantitative real time PCR in grapevine under abiotic stress. BMC Research Notes 5:220.

Dai ZW, Ollat N, Gomes E, Decroocq S, Tandonnet JP, Bordenave L, Pieri P, Hilbert G, Kappel C, van Leeuwen C, Vivin P, Delrot S (2011) Ecophysiological, genetic, and molecular causes of variation in grape berry weight and composition: a review. Am J Enol Viticult 62:413-425.

Dal Santo S, Vannozzi A, Tornielli GB, Fasoli M, Venturini L, Pezzotti M, Zenoni S (2013) Genome-wide analysis of the expansin gene superfamily reveals grapevine-specific structural and functional characteristics. Plos One 8.

Dallas C, Laureano O (1994) Effects of pH, sulphur dioxide, alcohol content, temperature and storage time on colour composition of a young Portuguese red table wine. J Sci Food Agr 65:477-485.

Deluc LG, Grimplet J, Wheatley MD, Tillett RL, Quilici DR, Osborne C, Schooley DA, Schlauch KA, Cushman JC, Cramer GR (2007) Transcriptomic and metabolite analyses of Cabernet Sauvignon grape berry development. BMC Genomics 8:429.

Deluc LG, Decendit A, Papastamoulis Y, Mérillon J-M, Cushman JC, Cramer GR (2011) Water deficit increases stilbene metabolism in Cabernet Sauvignon Berries. J Agr Food Chem 59:289-297.

Dunlevy JD, Kalua CM, Keyzers RA, Boss PK (2009) The production of flavour & aroma compounds in grape berries A.K. Roubelakis-Angelakis (Ed.), Grapevine Molecular Physiology & Biotechnology, Springer, Dordrecht, pp. 293–340

Dische Z (1962) General color reactions. In Carbohydrate chemistry, Whistler, R. L. W., M. L., Ed. Academic: New York, pp 477–512.

Fasoli M, Dal Santo S, Zenoni S, Tornielli GB, Farina L, Zamboni A, Porceddu A, Venturini L, Bicego M, Murino V, Ferrarini A, Delledonne M, Pezzotti M (2012) The grapevine expression atlas reveals a deep transcriptome shift driving the entire plant into a maturation program. Plant Cell 24:3489-3505.

Fernandes JC García-Angulo P, Goulao LF, Acebes JL, Amâncio S (2013) Mineral stress affects the cell wall composition of grapevine (*Vitis vinifera* L.) callus. Plant Science 205-206:111-120.

Flexas J, Galmés J, Gallé A, Gulías J, Pou A, Ribas-Carbo M, Tomàs M Medrano H (2010) Improving water use efficiency in grapevines: potential physiological targets for biotechnological improvement. Aust J Grape Wine Res 16:106-121.

Fry SC, Smith RC, Renwick KF, Martin DJ, Hodge SK Matthews KJ (1992) Xyloglucan endotransglycosylase, a new wall-loosening enzyme-activity from plants. Biochem J 282:821-828.

Goulao LF, Fernandes JC, Lopes P, Amâncio S (2012) Tackling the Cell Wall of the Grape Berry. In The biochemistry of the grape berry, Gerós, H. C., M. M.; Delrot, S., Ed. Bentham Science Publishers, pp 172-193.

Greenspan MD, Shackel KA, Matthews MA (1994) Developmental-changes in the diurnal water-budget of the grape berry exposed to water deficits. Plant Cell Environ 17:811-820.

Grimplet J, Deluc LG, Tillett RL, Wheatley MD, Schlauch KA, Cramer GR, Cushman JC (2007) Tissue-specific mRNA expression profiling in grape berry tissues. BMC Genomics 8:187.

Harholt J, Suttangkakul A, Scheller HV (2010) Biosynthesis of pectin. Plant Physiol 153:384-395.

Hatfield RD, Jung HJG, Ralph J, Buxton DR, Weimer PJA (1994) Comparison of the insoluble residues produced by the klason lignin and acid detergent lignin procedures. J Sci Food Agr 65:51-58.

Intrigliolo DS, Castel JR (2011) Interactive effects of deficit irrigation and shoot and cluster thinning on grapevine cv. Tempranillo. Water relations, vine performance and berry and wine composition. Irrigation Sci 29:443-454.

Jaillon O, Aury JM, Noel B, Policriti A, Clepet C, Casagrande A, Choisne N, Aubourg S, Vitulo N, Jubin C, Vezzi A, Legeai F, Hugueney P, Dasilva C, Horner D, et al. (2007) The grapevine genome sequence suggests ancestral hexaploidization in major angiosperm phyla. Nature 449:463-U5.

Jolie RP, Duvetter T, Van Loey A.M, Hendrickx ME (2010) Pectin methylesterase and its proteinaceous inhibitor: a review. Carbohyd Res 345:2583-2595.

Kammerer D, Claus A, Carle R, Schieber A (2004) Polyphenol screening of pomace from red and white grape varieties (*Vitis vinifera* L.) by HPLC-DAD-MS/MS. J Agr Food Chem 52:4360-4367.

Koundouras S, Hatzidimitriou E, Karamolegkou M, Dimopoulou E, Kallithraka S, Tsialtas,JT, Zioziou E, Nikolaou N, Kotseridis Y (2009) Irrigation and rootstock effects on the phenolic concentration and aroma potential of *Vitis vinifera* L. cv. Cabernet Sauvignon grapes. J Agr Food Chem 57:7805-7813.

Lecas M, Brillouet JM (1994) Cell-Wall composition of grape berry skins. Phytochemistry 35:1241-1243.

Lerouxel O, Cavalier DM, Liepman AH, Keegstra K (2006) Biosynthesis of plant cell wall polysaccharides — a complex process. Curr Opin Plant Biol 9:621-630.

Letaief H, Rolle L, Gerbi V (2008) Mechanical behavior of winegrapes under compression tests. Am J Enol Viticult 59:323-329.

Lopes CM, Santos TP, Monteiro A, Rodrigues ML, Costa JM, Chaves MM (2011) Combining cover cropping with deficit irrigation in a Mediterranean low vigor vineyard. Sci Hortic 129:603–612.

Matthews MA, Nuzzo V (2007) Berry size and yield paradigms on grapes and wines quality. Acta Hortic 754:423-435.

Mazza G (1995) Anthocyanins in grapes and grape products. Crit Rev Food Sci 35:341-371.

Montealegre RR, Peces RR, Vozmediano JLC, Gascuena JM, Romero EG (2006) Phenolic compounds in skins and seeds of ten grape *Vitis vinifera* varieties grown in a warm climate. J Food Compos Anal 19:687-693.

Moore JP, Nguema-Ona E, Chevalier L, Lindsey GG, Brandt WF Lerouge P, Farrant JM, Driouich A (2006) Response of the leaf cell wall to desiccation in the resurrection plant Myrothamnus flabellifolius. Plant Physiol 141:651-662.

Nishitani KT, Tominaga R (1992) Endo-xyloglucan transferase, a novel class of glycosyltransferase that catalyses transfer of a segment of xyloglucan molecule to another xyloglucan molecule. J Biol Chem 267:21058–21064.

Nunan KJ, Sims IM, Bacic A, Robinson SP, Fincher GB (1997) Isolation and characterization of cell walls from the mesocarp of mature grape berries (*Vitis vinifera*). Planta 203:93-100.

Nunan KJ, Sims IM, Bacic A, Robinson SP, Fincher GB (1998) Changes in cell wall composition during ripening of grape berries. Plant Physiol 118:783-792.

Ojeda H, Deloire A (2001) Carbonneau, A. Influence of water deficits on grape berry growth. Vitis 40:141-145.

Olle D, Guiraud JL, Souquet JM, Terrier N, Ageorges A, Cheynier V, Verries C (2011) Effect of pre- and post-veraison water deficit on proanthocyanidin and anthocyanin accumulation during Shiraz berry development. Aust J Grape Wine Res 17:90-100.

Ortega-Regules A, Romero-Cascales I, Ros Garcia JM, Bautista-Ortin AB, Lopez-Roca JM, Fernandez-Fernandez JI, Gomez- Plaza E (2008a) Anthocyanins and tannins in four grape varieties (*Vitis vinifera* L.) - Evolution of their content and extractability. J Int Sci Vigne Vin 42:147-156.

Ortega-Regules A, Ros-García JM, Bautista-Ortín AB, López-Roca JM, Gómez-Plaza E (2008b) Changes in skin cell wall composition during the maturation of four premium wine grape varieties. J Sci Food Agric 2008, 88:420–428

Peaucelle A, Braybrook S, Höfte H (2012) Cell wall mechanics and growth control in plants: the role of pectins revisited. Front Plant Sci 3:121. doi: 10.3389/fpls.2012.00121.

Petrie PR, Cooley NM, Clingeleffer PR (2004) The effect of post-veraison water deficit on yield components and maturation of irrigated Shiraz (*Vitis vinifera* L.) in the current and following season. Aust J Grape Wine Res 10:203-215.

Pinelo M, Del Fabbro P, Manzocco L, Nunez MJ, Nicoli MC (2005) Optimization of continuous phenol extraction from *Vitis vinifera* byproducts. Food Chem 92:109-117.

Poni S, Lakso A, Turner J, Melious R (1994) Interactions of crop levels and late season water stress on growth and physiology of field-grown Concord grapevines. Am J Enol Viticult 45:252-258.

Ribereau-Gayon P, Stonestreet E (1965) Le dosage des anthocyanes dans le vin rouge. Bull Soc Chim 9:2649-2652.

Ribéreau-Gayon P (1970) Le dosage des composés phénoliques totaux dans les vins rouges. Chimie. Analitique 52:627-631.

Río Segade S, Vázquez ES, Orriols I, Giacosa S, Rolle L (2011) Possible use of texture characteristics of winegrapes as markers for zoning and their relationship with anthocyanin extractability index. Int J Food Sci Technol 46:386–394

Roby G, Matthews MA (2004) Relative proportions of seed, skin and flesh, in ripe berries from Cabernet Sauvignon grapevines grown in a vineyard either well irrigated or under water deficit. Aust J Grape Wine Res 10:74-82.

Rohlf FJ (2008) NTSYSpc: Numerical Taxonomy System, ver. 2.20. Exeter Publishing, Ltd: Setauket, NY

Rolle L, Torchio F, Zeppa G, Gerbi V (2009) Relationship between skin break force and anthocyanin extractability at different ripening stages. Am J Enol Viticult 60:93-97.

Rolle L, Torchio F, Cagnasso E, Gerbi V (2010) Evolution of mechanical variables of winegrapes for icewine production during on-vine drying. Ital J Food Sci 22:143-149.

Rolle L, Giacosa S, Gerbi V, Novello V (2011) Comparative study of texture properties, color characteristics, and chemical composition of ten white table-grape varieties. Am J Enol Vitic 62:49-56.

Rolle L, Río Segade S, Torchio F, Giacosa S, Cagnasso E, Marengo F, Gerbi V (2011) Influence of grape density and harvest date on changes in phenolic composition, phenol extractability indices, and instrumental texture properties during ripening. J Agric Food Chem 59:8796−8805

Rolle L, Gerbi V, Schneider A, Spanna F, Río Segade S (2011) Varietal Relationship between Instrumental Skin Hardness and Climate for Grapevines (*Vitis vinifera* L.). J Agric Food Chem 59:10624–10634

Rolle L, Torchio F, Ferrandino A, Guidoni S (2012) Influence of wine-grape skin hardness on the kinetics of anthocyanin extraction. Int J Food Prop 15:249-261.

Rolle L, Siret R, Río Segade S, Maury C, Gerbi V, Jourjon F (2012) Instrumental Texture Analysis Parameters as Markers of Table-Grape and Winegrape Quality: A Review. Am J Enol Vitic 63:11-28.

Rose JKC, Braam J, Fry SC, Nishitani K (2002) The XTH family of enzymes involved in xyloglucan endotransglucosylation and endohydrolysis: Current perspectives and a new unifying nomenclature. Plant Cell Physiol 43:1421-1435.

Saeed AI, Sharov V, White J, Li J, Liang W, Bhagabati N, Braisted J, Klapa M, Currier T, Thiagarajan M, Sturn A, Snuffin M, Rezantsev A, Popov D, Ryltsov A, Kostukovich E, Borisovsky I, Liu Z, Vinsavich A, Trush V, Quackenbush J (2003) TM4: A free, open-source system for microarray data management and analysis. Biotechniques 34:374.

Saeman JF, Moore WE, Millet MA (1963) Sugar units present. Hydrolysis and quantitativepaper chromatography. In CarbohydrateChemistry, Vol. 3, Cellulose, Whistler, R. L., Ed. Academic Press: New York, pp 54–69.

Santos TP, Lopes,CM, Lucília R. M, de Souza CR, Ricardo-da-Silva JM, Maroco JP, Pereira JS, Manuela CM (2007) Effects of deficit irrigation strategies on cluster microclimate for improving fruit composition of Moscatel field-grown grapevines. Sci Hortic 112:321.

Saulnier L, Brillouet JM (1989) An arabinogalactan protein from the pulp of grape berries. Carbohyd Res 188:137-144.

Scholander P, Hammel H, Brandstreet E, Hemmingsen E (1965) Sap pressure in vascular plants. Science 148:339-346.

Schultz HR, Stoll M (2010) Some critical issues in environmental physiology of grapevines: future challenges and current limitations. Aust J Grape Wine Res 16:4-24.

Selvendran RR, Oneill MA (1987) Isolation and analysis of cell-walls from plant-material. Method Biochem Anal 32:25-153.

Silacci M.W, Morrison JC (1990) Changes in pectin content of cabernet-sauvignon grape berries during maturation. Am J Enol Viticult 41:111-115.

Tang HR, Belton PS, Ng A, Ryden P (1999) C-13 MAS NMR studies of the effects of hydration on the cell walls of potatoes and Chinese water chestnuts. J Agr Food Chem 47:510-517.

Talmadge KW, Keegstra K, Bauer WD, Albersheim P (1973) The structure of plant cell walls: I. The macromolecular components of the walls of suspension-cultured sycamore cells with a detailed analysis of the pectic polysaccharides. Plant Physiol 51:158-173.

Terrier N, Glissant D, Grimplet J, Barrieu F, Abbal P, Couture C, Ageorges A, Atanassova R, Leon C, Renaudin JP, Dedaldecham, F, Romieu C, Delrot S, Hamdi S (2005) Isogene specific oligo arrays reveal multifaceted changes in gene expression during grape berry (*Vitis vinifera* L.) development. Planta 222:832-847.

Torchio F, Cagnasso E, Gerbi V, Rolle L (2010) Mechanical properties, phenolic composition and extractability indices of Barbera grapes of different soluble solids contents from several growing areas. Analytica chimica acta 660:183-189.

Updegraff DM (1969) Semimicro determination of cellulose inbiological materials. Anal Biochem 32:420-424.

Velasco R, Zharkikh A, Troggio M, Cartwright DA, Cestaro A, Pruss D, Pindo M, FitzGerald LM, Vezzulli S, Reid J, Malacarne G, Iliev, D.; Coppola, G.; Wardell B,

Micheletti D, Macalma T, et al. (2007) A High quality draft consensus sequence of the genome of a heterozygous grapevine variety. Plos One 2.

Venturini L, Ferrarini A, Zenoni S, Tornielli GB, Fasoli M, Dal Santo S, Minio A, Buson G, Tononi P, Zago ED, Zamperin G, Bellin D, Pezzotti M, Delledonne M (2013) De novo transcriptome characterization of *Vitis vinifera* cv. Corvina unveils varietal diversity. BMC Genomics 14:41.

Vicens A, Fournand D, Williams P, Sidhoum L, Moutounet M Doco T (2009) Changes in polysaccharide and protein composition of cell walls in grape berry skin (Cv. Shiraz) during ripening and over-ripening. J Agr Food Chem 57:2955-2960.

Vidal S (2001) Polysaccharides from grape berry cell walls. Part I: tissue distribution and structural characterization of the pectic polysaccharides. Carbohyd Polym 45:315-323.

Walker TL, Morris JR, Threlfall RT, Main GL, Lamikanra O, Leong S (2001) Density separation, storage, shelf life and sensory evaluation of 'Fry' muscadine grapes. HortScience 36:941-945.

Waters DLE, Holton TA, Ablett EM, Lee LS, Henry RJ (2005) cDNA microarray analysis of developing grape (*Vitis vinifera* cv. Shiraz) berry skin. Funct Integr Genomic 5:40-58.

Yakushiji H, Sakurai N, Morinaga K (2001) Changes in cell-wall polysaccharides from the mesocarp of grape berries during veraison. Physiol Plantarum 111:188-195.

Zarrouk O, Francisco R, Pinto-Marijuan M, Brossa R, Santos RR, Pinheiro C, Costa JM, Lopes C, Chaves MM (2012) Impact of irrigation regime on berry development and flavonoids composition in Aragonez (Syn. Tempranillo) grapevine. Agr Water Manage 114:18-29.

Zoccatelli G, Zenoni S, Savoi S, Dal Santo S, Tononi P, Zandonà V, Dal Cin A, Guantieri V, Pezzotti M, Tornielli GB (2013) Skin pectin metabolism during the postharvest dehydration of berries from three distinct grapevine cultivars. Aust J Grape Wine Res 19:171-179.

Zsófi Z, Villangó S, Pálfi Z, Tóth E, Bálo B (2014) Texture characteristics of the grape berry skin and seed (*Vitis vinifera* L. cv. Kékfrankos) under postveraison water deficit. Sci Hortic 172:176-182.

Chapter 6

Final Considerations

6. Final considerations

Plant model systems analyzed in controlled experimental conditions are useful tools to assess stress conditions. *V. vinifera* callus cultures, as a homogeneous and dedifferentiated system, provides an elegant and useful tool to access the effect of abiotic stresses. Since the goal was to understand Cell Wall (CW) responses to an induced stimulus, this system reduced the impact of possible interference with other concomitant effects. However, plant differentiated tissues, namely shoots, are also required as a more complex experimental system since the organization of polymers in the CW is a key-factor for tissue organization.

Abiotic stress in plants refers to conditions that are unfavorable for growth. Mineral stress and drought which are likely to affect the plant development, yield and ultimately the quality of economic products, are included in these forms of stress. To investigate the effect of mineral stress, N, P and S were withdrawn from *V. vinifera* callus and shoots growing substrates. Water stress on berry skin CW was studied in non-irrigated versus irrigated plants.

The first indication of the effects exerted by N, P and S deficiency on *V. vinifera* was acquired through the confirmation that grapevine growth was affected by the mineral depletion. *V. vinifera* callus growth, under mineral stress, was drastically reduced to levels significantly lower than the control after six weeks (chapters 2 and 3). Using *V. vinifera* cuttings, a reduction of the number of internodes along with an increase in internode length in –N was observed (chapter 4). Water deficit also affected berry growth in both the studied varieties (chapter 5).

Our goal to address changes in CW composition triggered by abiotic stress was firstly investigated by Fourier–Transformed Infrared Spectroscopy (FT-IR) in callus tissues. The overall results suggest changes in all of the main CW components in response to mineral deficiency. Modifications in the biosynthesis or rearrangements of cellulose microfibers, matrix linked glycans, pectin biochemistry and in the amounts of structural proteins were among the most striking indications provided by this technique. A more detailed biochemical analysis of the stressed response revealed a significant reduction in cellulose content under –N and –P (chapter 2). Under water stress the same reduction was observed in Trincadeira (TR) berries at maturation (Fig. 6.1a). On the other hand, this treatment increased the levels of arabinose which was tightly bounded to CW

in callus (chapter 2), shoots (chapter 4) and berry skin (chapter 5) and may indicate increased substitution by arabinosyl residues in the rhamnogalacturonan–I (RGI) side chains of pectic polysaccharides. RGI arabinosyl side chains can work as plasticizers in CWs that undergo large physical remodeling under abiotic stresses (Harholt et al. 2010). The same was confirmed by LM13 labeling, a monoclonal antibody that specifically recognises linear (1-5)-α-L-arabinans, in *V. vinifera* cuttings under mineral stress, supporting the results obtained using biochemical methods (Fig. 6.1b). The observed decrease in cellulose and increase in arabinan may be a general response to abiotic stresses, although a genotype-specific response may occur under water shortage (Fig. 1) as observed by Rolle et al. (2011) and Río Segade et al. (2011).

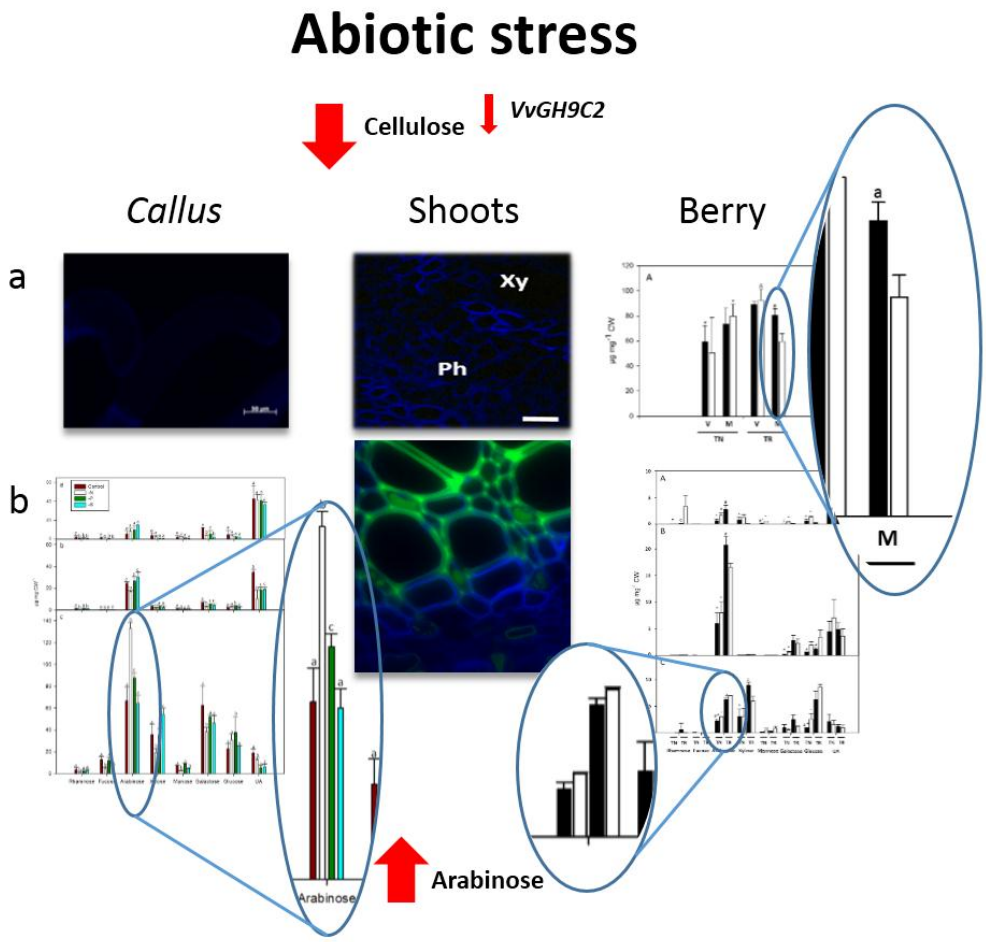

Fig. 6.1 *V. vinifera* general response to abiotic stress in callus, shoots and grape berry. Abiotic stress caused a a) Cellulose reduction under –N and –P and TR berrys due to the down-regulated of *VvGH9C2* and b) increase in Arabinose tightly bonded to CW.

Lower cellulose levels led us to investigate the gene expression of the cellulose synthase (CesA) gene family. The majority of these genes showed an increased transcript accumulation, which conflicts with the observed reduction in cellulose content. Nevertheless, CesA activity is known to be insufficient to produce cellulose, requiring the combined action with members from other families, such as the classes C of the glycosyl hydrolase family 9 (GH9) (Urbanowicz et al. 2007). The involvement in regulation of the degree of cellulose crystallinity by GH9C's, was recently prooved (Glass et al. 2015). In callus under mineral stress *VvGH9C2*, was severely down-regulated under –N and –S (chapter 3).

Due to the importance of the CW for survival and environment adaptation, plants are equipped with compensatory mechanisms to reinforce their CWs when the biosynthesis or deposition of a given component is impaired (Wolf et al. 2012). CWs growing under mineral deficiency, particularly –N, respond to low levels of cellulose by reducing their degree of pectin methyl esterification. This de-esterification occurs in long stretches of the homogalacturonan (HG), indicated by PAM1 labeling, and in this way promotes the formation of calcium bridges, in "egg–box" structures (Pelloux et al. 2007) observed with 2F4 antibody (Fig. 6.2a). It was proposed that, under abiotic stress, this pattern of de-esterification reinforces the CW conferring additional stiffening and absence of alterations in CW elastic deformation (Micheli 2001) (chapter 3 and 4). The lower global degree and pattern of methyl-esterification observed under some mineral starvation conditions cannot be directly explained by the pectin methylesterase (PME) gene expression levels. The majority of PME genes were down-regulated, both in callus and berry skins. The observed up-regulated PMEI genes may regulate the activity of PMEs. The exception is the basic PME which acts upon the HG chain in a linear way promoting the formation of Ca^{2+}-linked gel structures and thereby stiffening and reducing CW extensibility (Micheli 2001). Protein extracts of –N and –P callus increased the plastic deformations in cucumber hypocotyl. This may be derived from the ability of the proteins to promote irreversible modifications in the physical properties due to mechanical, non-enzymatic effects (Hohl and Schopfer 1992) (Fig. 6.2b) (chapter 3). Xyloglucan (XyG) may play an important role in the wall and influence its characteristics. Under nitrogen deficiency, an increase in the amounts of XyG in the shoot CWs was observed.

This increase can be explained as a CW reinforcement mechanism, via biosynthesis of new material or establishment of new linkages (chapter 4). The most drastic effects, both in callus and cuttings was always observed in –N, probably due to the vital role of nitrogen in plant metabolism. This result supports the primary role of these major nutrients in plant development and metabolism (Wu et al. 2003;Tschoep et al. 2009).

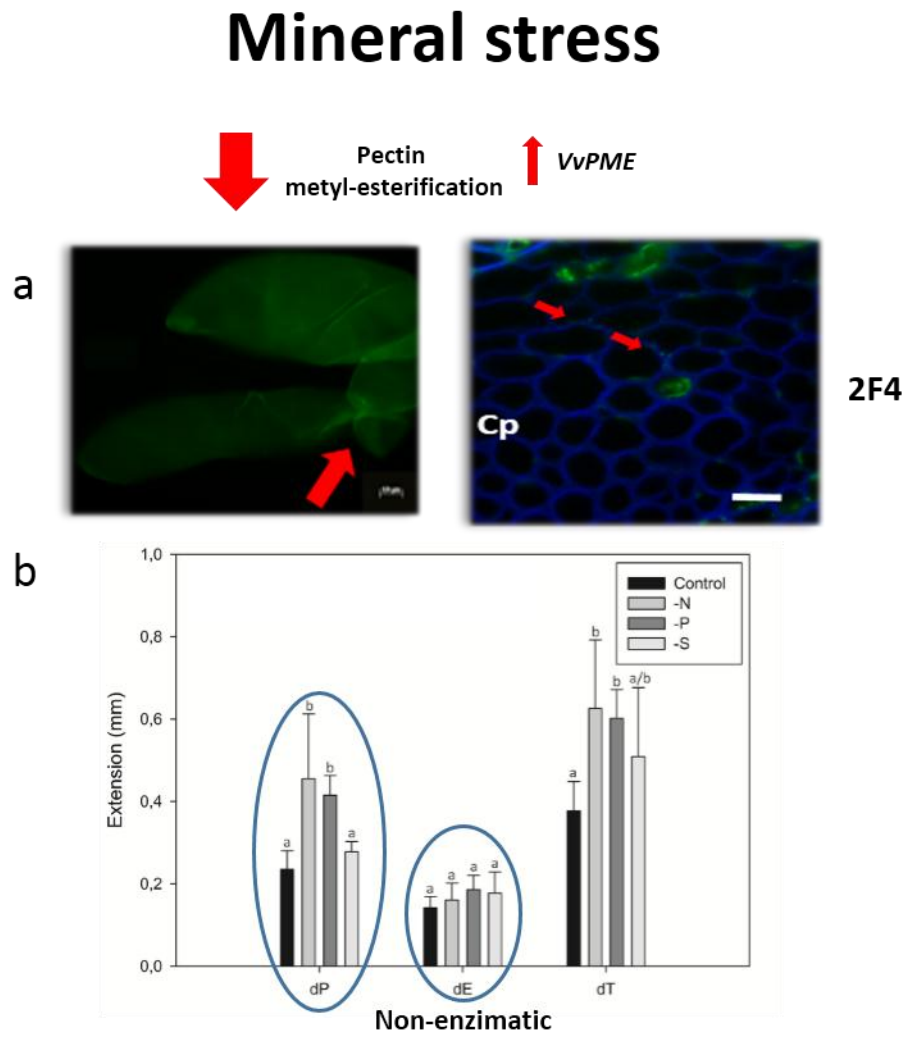

Fig. 6.2 *V. vinifera* response to mineral stress in callus and shoots. a) Reductions in the degree of methyl-esterification in callus and shoots, probably due to the increase in the basic PME expression levels. b) Plastic deformation, induced by protein saline extracts of –N and –P callus, increased under mineral stress.

Global climate changes are intensifying problems like water deficit that affect berry development. Under water deficit, along with the reduction in cellulose and increase in arabinose, texture measurements conducted on berry and berry skin

revealed a higher skin break force measured in TR suggesting that skin break force increase significantly as a result of water deficit but in a variety depend manner (Torchio et al. 2010; Zsófi et al. 2014). This may be the result of down-regulation of xyloglucan transglycosylase/hydrolases (XTH) and polygalacturonases (PG) (Fig. 3) (chapter 5).

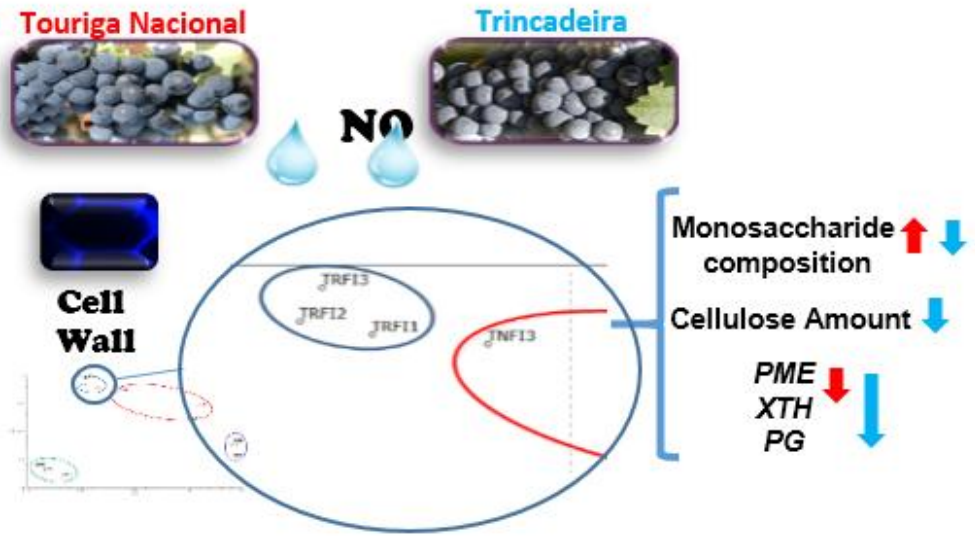

Fig. 6.3 *V. vinifera* Cv Touriga Nacional (Red) and Trincadeira (Blue) berries respond to water by reducing cellulose and increase arabinose and skin break force. Was also observed a reduction in PME, XTH and PG transcription.

6.1. Conclusions

In summary, *V. vinifera* experimental models (callus, shoots and berries) submitted to abiotic stress conditions, namely individual mineral or water stresses (berries) are impaired in specific CW components, in particular cellulose. To overcome this, *V. vinifera* CW suffers a reorganization on deposition of several components, in particular the degree and pattern of pectin methyl-esterification, arabinan and XyG, promoting a compensatory stiffening of the wall. The nutrient stress did not affect evenly all plant tissues with mature internodes showing more pronounced responses. Depending on mineral stresses the impact on the CW is different, with nitrogen leading to more pronounced responses, supporting the primary role of this major nutrient in plant development and metabolism. Water shortage affects grape berries by stiffening the CW, probably through alteration

in PGs, XTH and PME expression and pectin structure in a variety dependent way.

The results described within this thesis highlight the different strategies employed by *V. vinifera* tissues and organs to overcome the adverse effects induced by abiotic stress conditions on the CW composition, structure and remodeling according to the affected biological pathways and the severity perceived. In this work, the responses concerning changes in individual polymers described in other woody species were confirmed in an integrated way using complementary models and experimental approaches. When collectively analysed in the light of recently proposed hypothesis for CW architecture and remodeling processes, association of complementary or compensatory events could be hypothesized. To the best of our knowledge, we present for the first time gene expression results of CW biosynthesis and remodeling enzyme families in the same materials that were comprehensively analysed at biochemical and rearrangement point of view.

References

Glass M, Barkwill S, Unda F, Mansfield SD (2015) Endo-β-1,4-glucanases impact plant cell wall development by influencing cellulose crystallization. J Integr Plant Biol 57:396-410. doi: 10.1111/jipb.12353.

Harholt J, Suttangkakul A, Vibe Scheller H (2010) Biosynthesis of pectin. Plant Physiol 153:384–395

Hohl M, Schopfer P (1992) Physical extensibility of maize coleoptile cell walls: apparent plastic extensibility is due to elastic hysteresis. Planta 187:498-504. doi: 10.1007/BF00199968

Micheli F (2001) Pectin methylesterases: cell wall enzymes with important roles in plant physiology. Trends Plant Sci 6:414-419. doi: 10.1016/S1360-1385(01)02045-3

Pelloux J, Rustérucci C, Mellerowicz EJ (2007) New insights into pectin methylesterase structure and function. Trends Plant Sci 12:267-277. doi: 10.1016/j.tplants.2007.04.001

Río Segade S, Vázquez ES, Orriols I, Giacosa S, Rolle L (2011) Possible use of texture characteristics of winegrapes as markers for zoning and their relationship with anthocyanin extractability index. Int J Food Sci Technol 46:386–394

Rolle L, Giacosa S, Gerbi V, Novello V (2011) Comparative study of texture properties, color characteristics, and chemical composition of ten white table-grape varieties. Am J Enol Vitic 62:49-56.

Torchio F, Cagnasso E, Gerbi V, Rolle L (2010) Mechanical properties, phenolic composition and extractability indices of Barbera grapes of different soluble solids contents from several growing areas. Analytica Chimica Acta 660:183-189.

Tschoep H, Gibon Y, Carillo P, Armengaud P, Szecowka M, Nunes–Nesi A, Fernie AR, Koehl K, Stitt M (2009) Adjustment of growth and central metabolism to a mild but sustained nitrogen limitation in *Arabidopsis*. Plant Cell Environ 32:300–318

Urbanowicz BR, Catalá C, Irwin D, Wilson DB, Ripoll DR, Rose JKC (2007b) A tomato endo-*β*-1,4-glucanase, SlCel9C1, represents a distinct subclass with a new family of carbohydrate binding modules (CBM49). J Biol Chem 282**:**12066–12074. doi: 10.1074/jbc.M607925200

Wolf S, Mravec J, Greiner S, Mouille G, Höfte H (2012) Plant cell wall homeostasis is mediated by brassinosteroid feedback signaling. Curr Biol 22:1732-7. doi: 10.1016/j.cub.2012.07.036.

Wu P, Ma L, Hou X, Wang M, Wu Y, Liu F, Deng XW (2003) Phosphate starvation triggers distinct alterations of genome expression in *Arabidopsis* roots and leaves. Plant Physiol 132:1260-1271

Zsófi Z, Villangó S, Pálfi Z, Tóth E, Bálo B (2014) Texture characteristics of the grape berry skin and seed (*Vitis vinifera* L. cv. Kékfrankos) under postveraison water deficit. Scientia Horticulturae 172:176-182.

Supplementary Material

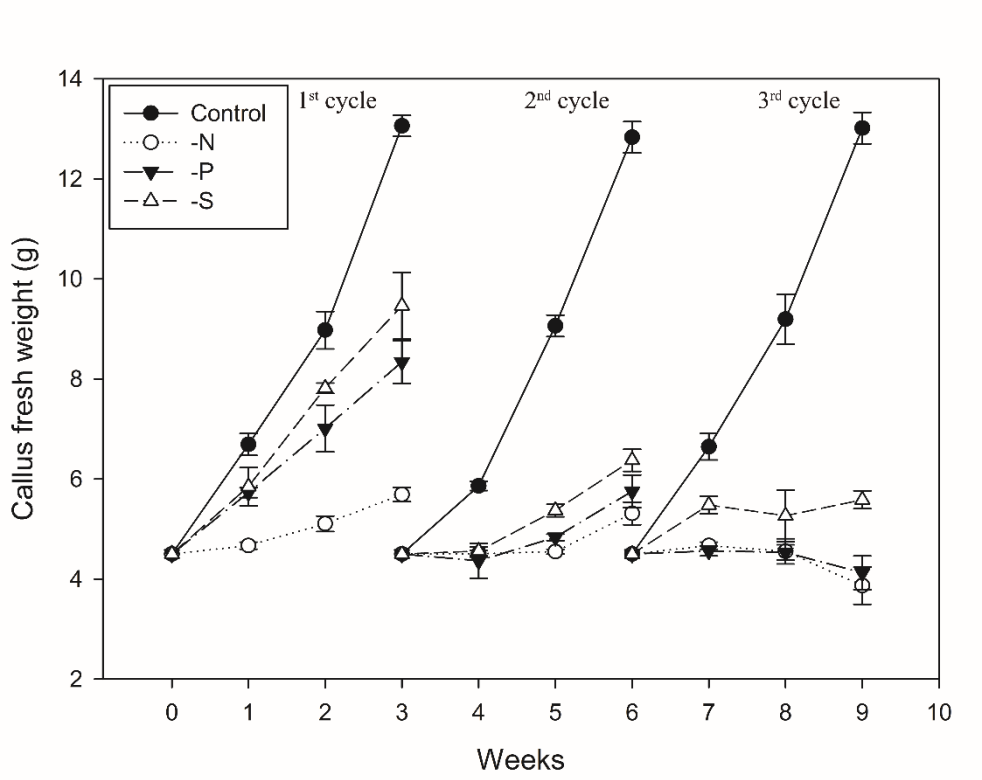

Supplementary Fig. 3.1 Fresh weight of *V. vinifera* callus growing under nitrogen deficient (-N), phosphorus deficient (-P), sulfur deficient (-S) and with full nutrients (Control) for three, 6 and 9 weeks. Each point represents the mean of the fresh weight values of callus from 5 petri dishes ± SD.

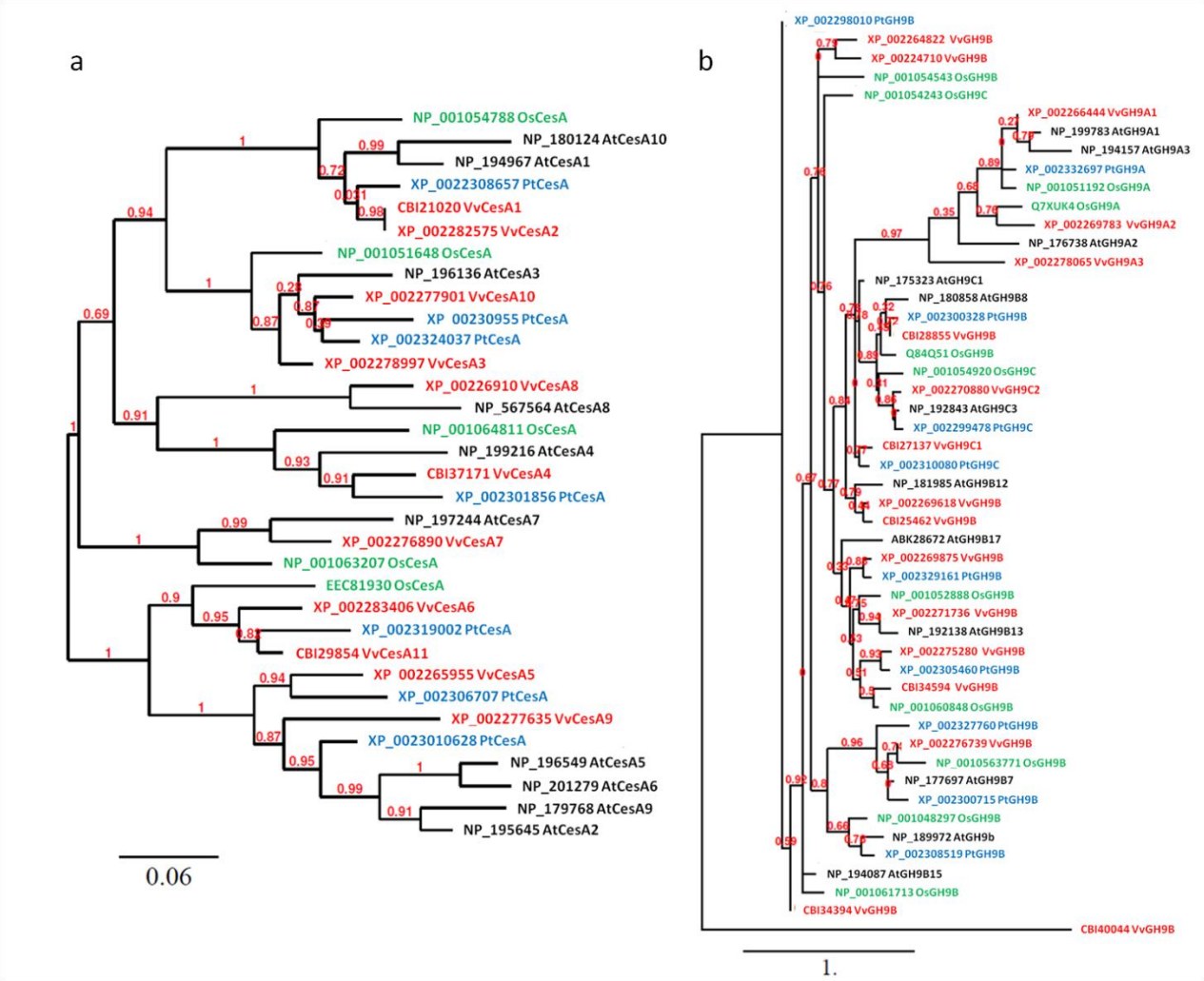

Supplementary Fig. 3.2 Phylogenetic dendrogram of a) cellulose synthase (CesA) genes b) β-1,4-endo-glucanase (GH9) with *V. vinifera* family members (red) and representative members of *A. thaliana* (black), *O. sativa* (green) and *Populus* (blue) protein families.

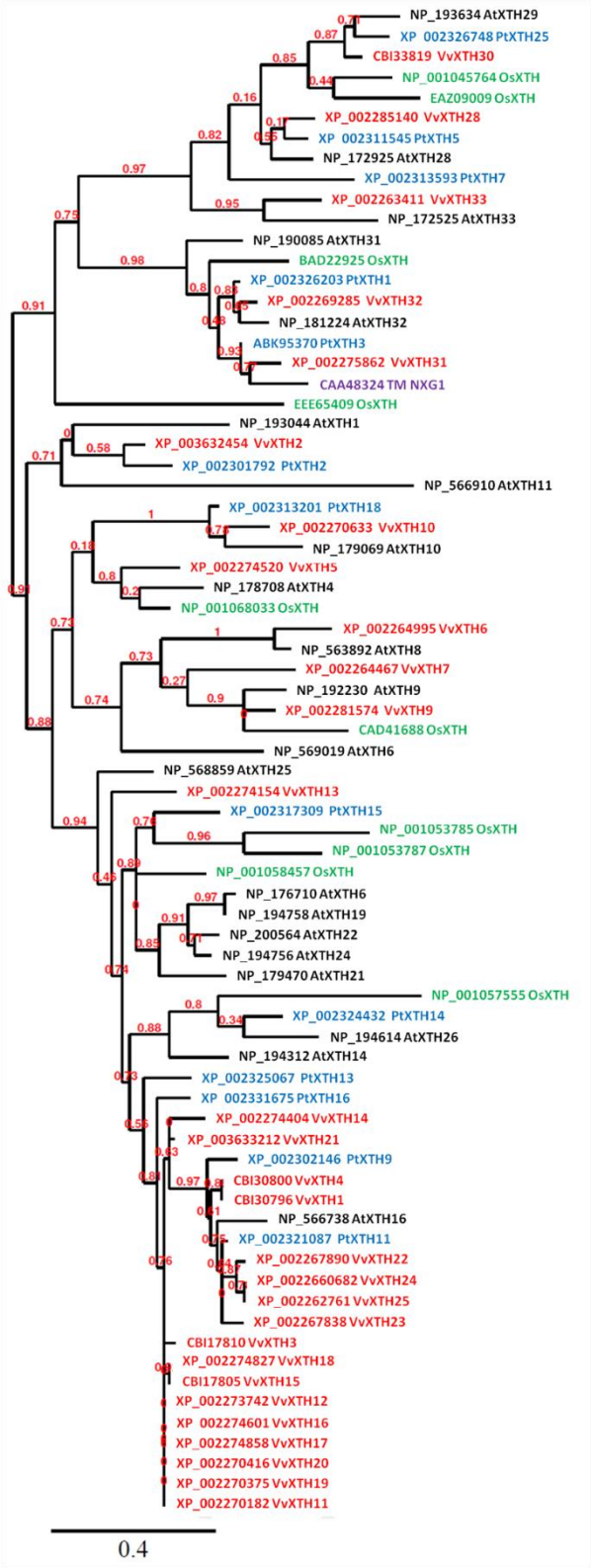

Supplementary Fig. 3.3 Phylogenetic dendrogram of xyloglucan endotransglycosylases/hydrolases (XTHs) with *V. vinifera* family members (red) and representative members of *A. thaliana* (black), *O. sativa* (green) and *Populus* (blue) protein families

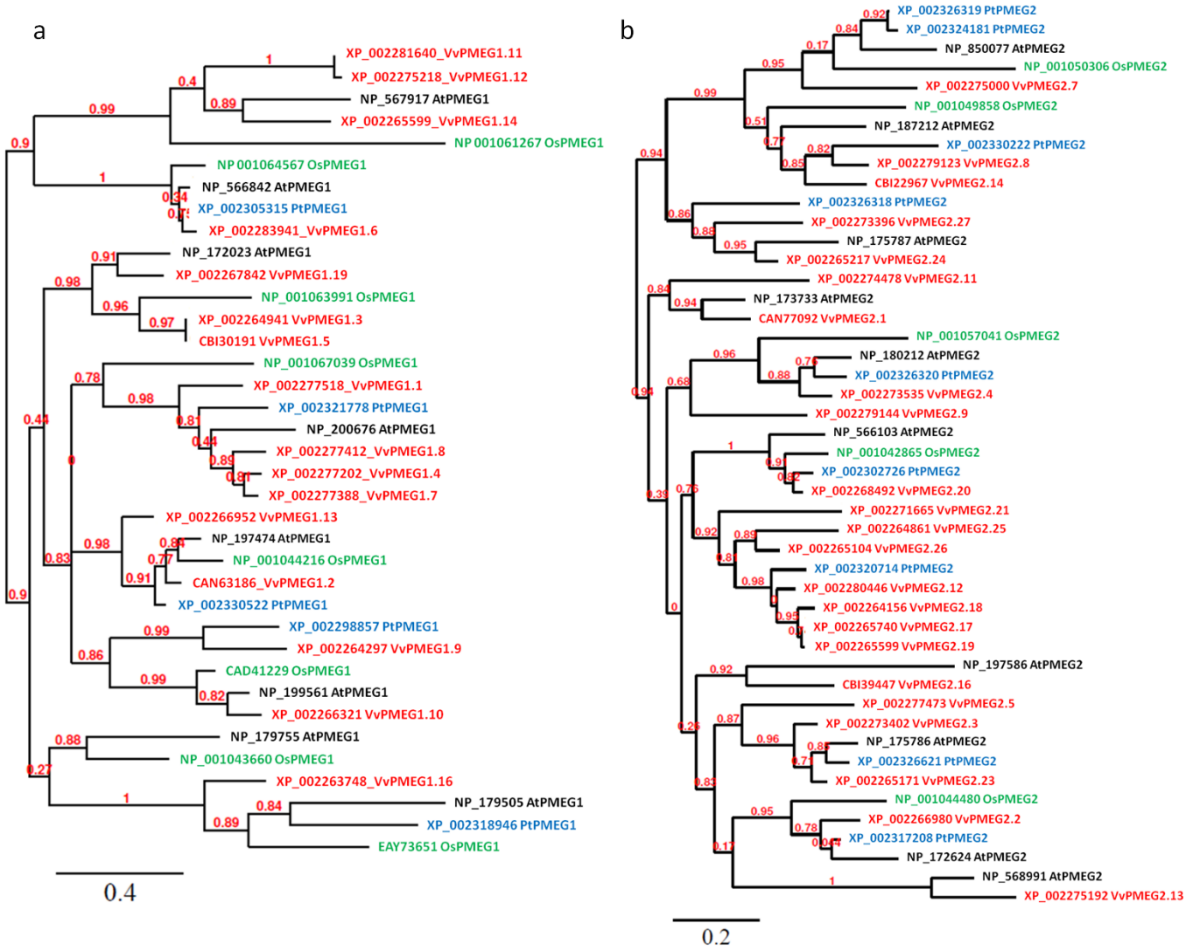

Supplementary Fig. 3.4 Phylogenetic dendrogram of pectin methyl esterase (PME) a) from Group 1 b) from Group 2 with *V. vinifera* family members (red) and representative members of *A. thaliana* (black), *O. sativa* (green) and *Populus* (blue) protein families

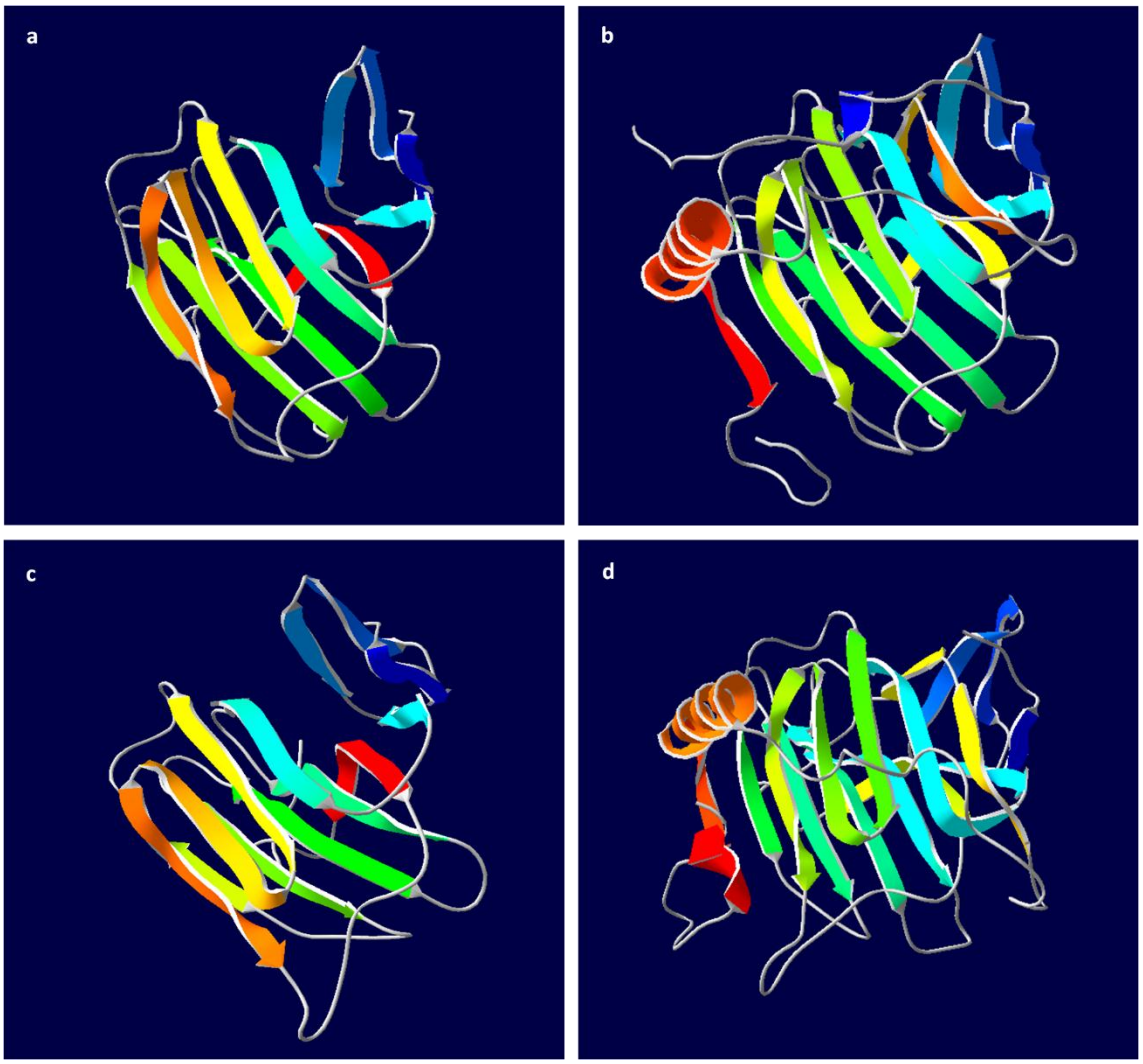

Supplementary Fig. 3.5 Representation of the 3D structure of a) VvXTH31, b) Tm-NXG1, c) VvXTH7 and d) AtXTH8

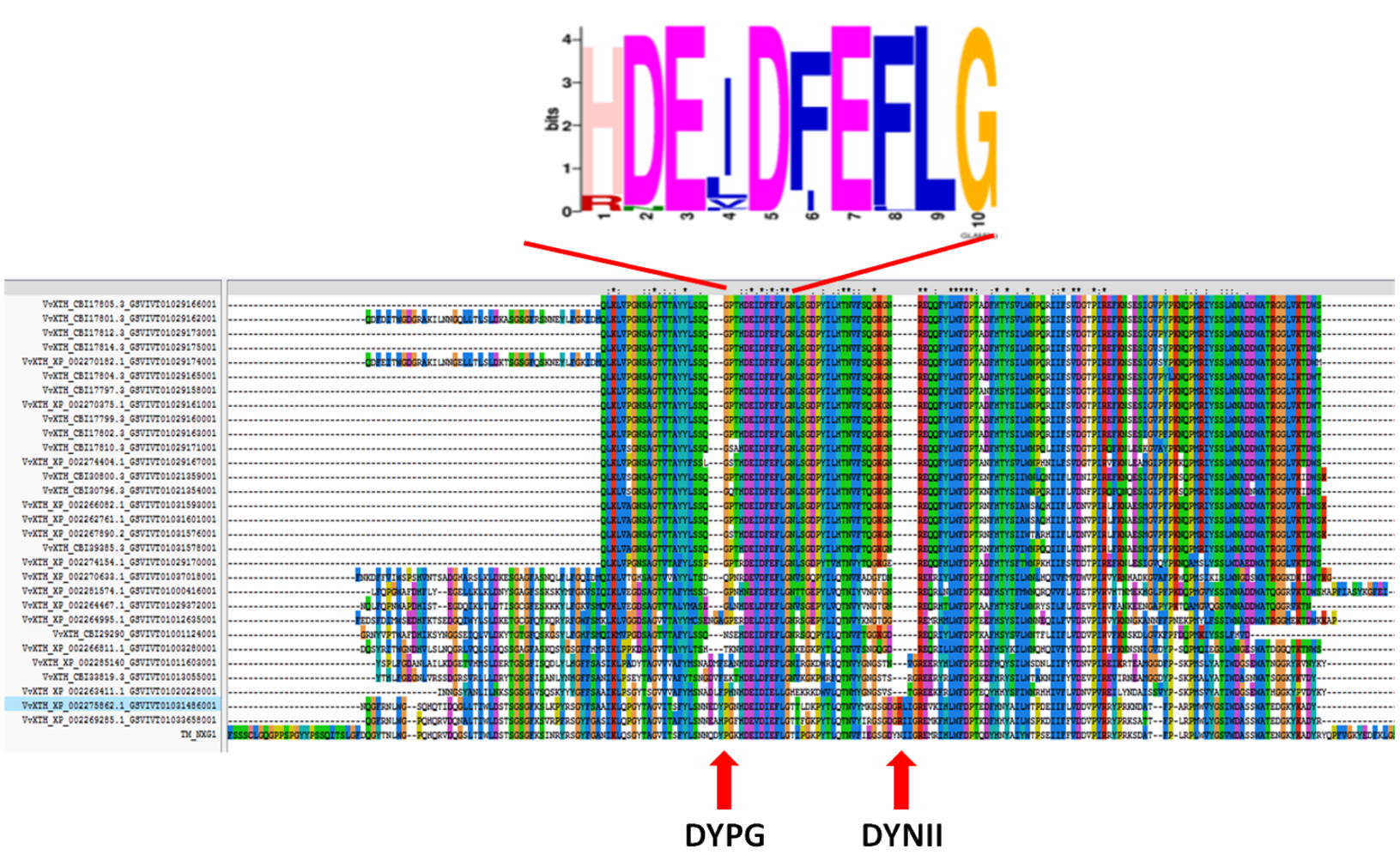

Supplementary Fig. 3.6 Multiple protein alignment of *V. vinifera* and *Tropaeolum majus* XTH. In the top, is the sequence logo for the conserved catalytic motif common to all XTH designed using WebLogo 3. Highlighted with arrows are the insertions characteristic of the hydrolytic activity

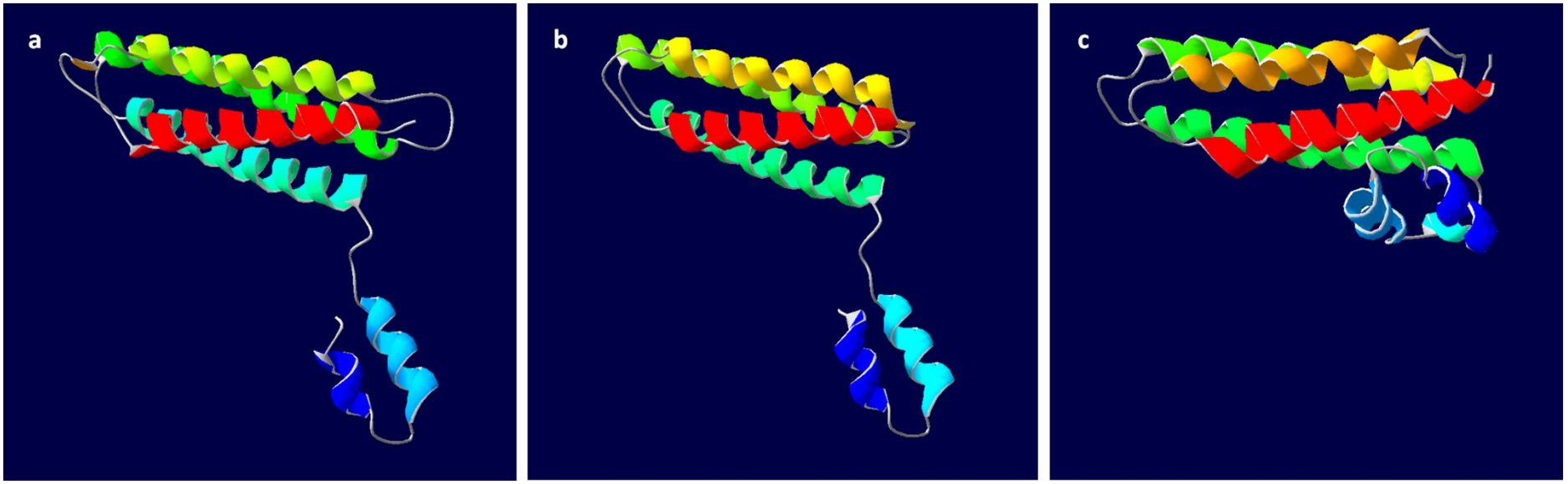

Supplementary Fig. 3.7 Representation of the 3D structure of a) VvPMEI, b) AtPMEI and c) Nt-CIT

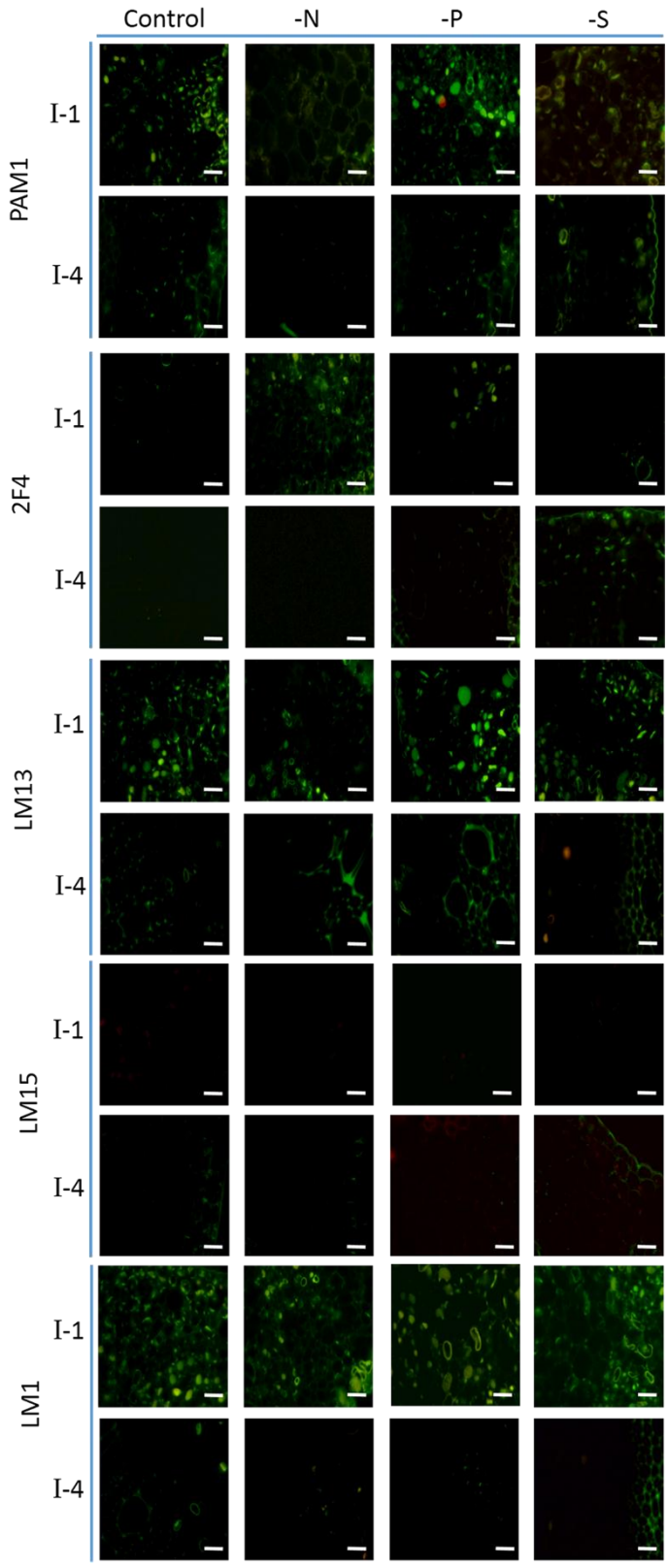

Supplementary Fig. 4.2 Negative control of *V. vinifera* top (I-1) and forth (I-4) internodes after six weeks growth in complete nutrient medium (control) and in the absence of nitrogen (–N), phosphorus (–P) and sulfur (–S), acquired under the same conditions described in the Material and Methods: Immunolocalization analysis subsection but in which the respective primary antibody was omitted. Images were taken under the same exposition time for all treatments. The number of pixels quantified was subtracted from the images obtained with the respective primary antibody hybridizations. Values are given in Table 2. Bar scale represents 20 µm.

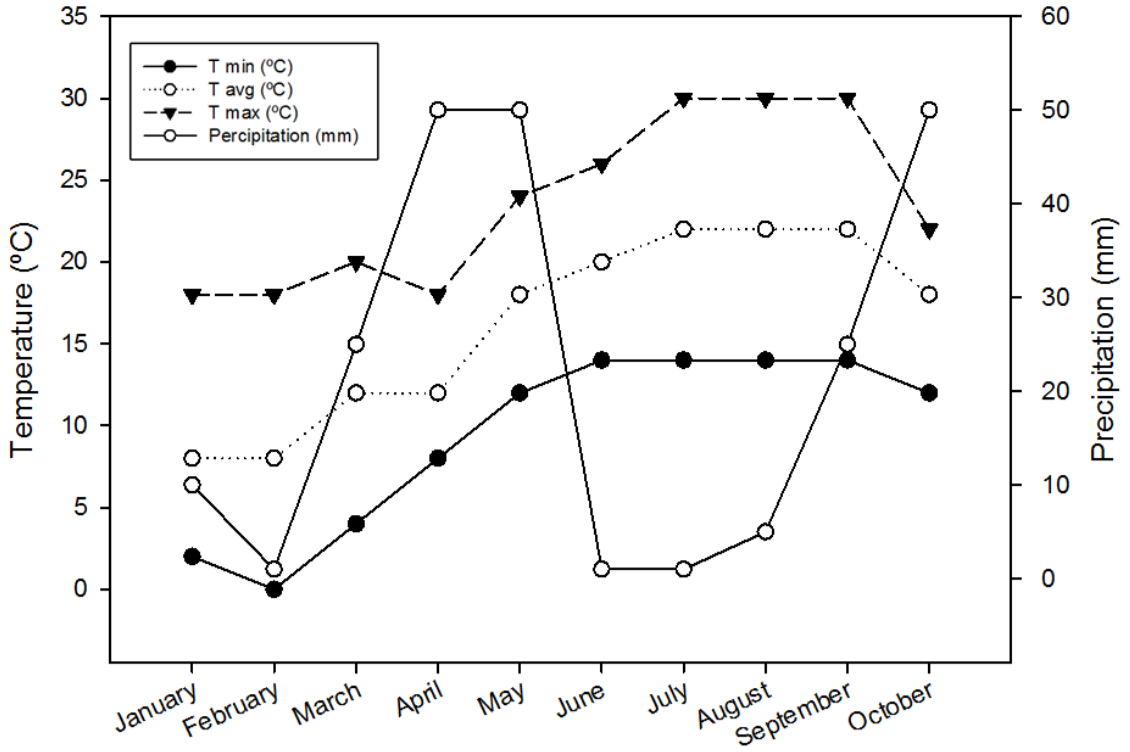

Supplementary Fig. 5.1 Monthly maximum (max), Average (avg) and Minimum (min) temperatures and the total monthly precipitation at the vineyard throughout 2012.

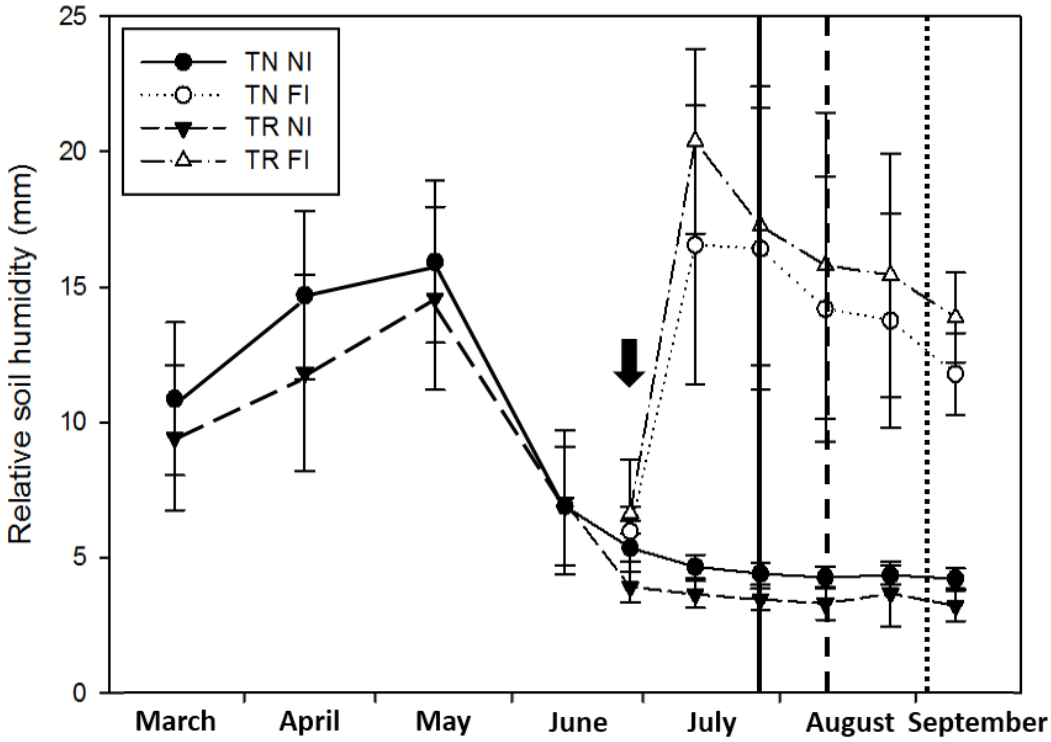

Supplementary Fig. 5.2 The average soil humidity at different dates of the growing season for the different treatments and varieties. The solid bar represent the veraison of TR (——), the veraison of TN is represented by (– –) and the Maturation date is represented by (– – –). The arrow stand as the beginning of the irrigation on FI.

Supplementary Table 3.1 List of primers used for RT-qPCR

Accession number (NCBI)	ID attributed[1]	Primer sequence	Product length
XM_002282539 (XP_002282575)	VvCesA1F VvCesA1R	AAA GCA CAG AAG ACG CCA GAA G CAC TGT GGC CTA AGA ACA CCT G	112
XM_002277677 (XP_002277713)	VvCesA2F VvCesA2R	AAA GGA TCT GCA CCC ATC AAT C ACC ACC TCC ATA CCC ATA CCA C	118
XM_002278961 (XP_002278997)	VvCesA3F VvCesA3R	CGA GGG GAG GAT ACA AAC TAC G ATA GAA AGA CGC TCG GGT GAA G	116
FN596502 (CBI37171)	VvCesA4F VvCesA4R	TTA TGT CCA GTT CCC ACA GAG G CCC ATC TAG GCC TTT CAT GTT G	103
XM_002265919 (XP_002265955)	VvCesA5F VvCesA5R	GTT CAT TGT CCC CGA GAT TAG C CTG CTC ATT TCT CCA CCA GTC A	133
XM_002283370 (XP_002283406)	VvCesA6F VvCesA6R	TGG TAT GGG TAT GGT GGT GGT C GAT GAA TTT GCC TGT GAG CAA G	136
XM_002276854 (XP_002276890)	VvCesA7F VvCesA7F	GTG CAC CCT TAT CCA GTG TCT G CAG GGT CAT TGT AGT CGT CAG C	139
XM_002269574 (XP_002269610)	VvCesA8F VvCesA8R	TGG ATA TAT GGG TCG GTC ACT G AAC CTG GTG AAG ACG ATC AGA C	142
XM_002277599 (XP_002277635)	VvCesA9F VvCesA9R	TTA ATA GTG CCC CCA TTT ACG G TTC CAT GCC ACA CTT CCA TAT C	140
XM_002277865 (XP_002277901)	VvCesA10F VvCesA10R	GTC ACA GCC ATT CCA CTT CTT G AAT ATA CCC GTG GCA AAG ATG G	143
XM_002266408 (XP_002266444)	VvGH9A1F VvGH9A1R	GTC TGG ACG GTC GGA TCT ATT C AGT TAT CAG GAG GAG CGT GAG G	109
XM_002269747 (XP_002269783)	VvGH9A2F VvGH9A2R	CTA CTT GGT GGG CTA TGG AAC C GAG GAT TTG GGT TGC GAC TAT C	131
XM_002278029 (XP_002278065)	VvGH9A3F VvGH9A3R	GCT ATC CAA TCC ATG TTC ACC A TCA TGT TGG TCT GGT CCT CCT A	151
XM_002277141 (XP_002277177)	VvGH9C1F VvGH9C1R	AAT GCT GTA CTC AAA TGC CCA G AAA TCC CTC CAC ACA TCC TCT G	134
XM_002270844 (XP_002270880)	VvGH9C2F VvGH9C2R	TTA CCC AAC CAA AAT CAG CTC C GTA AGT GTT CCC CTT GGC TTT C	119
XM_002285104 (XP_002285140)	VvXTH1F VvXTH1R	GAA CCC ACT TCC AAG GAT TCA G GTG CCT TTT GTT GAG TGG AGT C	130
FN594964 (CBI17804)	VvXTH2F VvXTH2R	ACG GCC CTG CTA ATC TCT GTA G GAG TAT CTT AGC ACG CCC ATC C	108
FN594964 (CBI17810)	VvXTH3F VvXTH3R	TGT TGC ATA CCC AAAGAA CCA G AGC TCT TGG CTC CAG TCT GTC T	108
FN595770 (XP_002274520)	VvXTH4F VvXTH4R	TAC ATG GGC TTT TGA CCA CAT C CTG AAG TGG CCG AAC AAG TAA G	120
FN595992 (CBI30800)	VvXTH5F VvXTH5R	TCT TCT CAA GGC CCA ACA CAC G TGC TGC TCT CTA TTC CCT TTC C	119
FN594964 (CBI17814)	VvXTH6F VvXTH6R	ATG CAC TAC CAC CAC CAT TTG G CCC TGT ATC AGC GCA GTA GTT G	117
XM_002264431 (XP_002264467)	VvXTH7F VvXTH7R	GGC TTT GAG ATT GAT GCT TGT G CCT ATT GAG CCC ACT CAT CCT C	117
XM_002264959 (XP_002264995)	VvXTH8F VvXTH8R	GAT TCC CAG AAG ATG GAT TTC G CCC ATG GAC TCA ATG AAC ACT C	115
XM_002281538 (XP_002281574)	VvXTH9F VvXTH9R	ATG CAC TAC CAC CAC CAT TTG CTG AAG TGG CAC ACA TCC TGA G	128
	VvXTH10F	ATT CCT GTT TGG GCA GAT TGA C	130

XM_002270597 (XP_002270633)	VvXTH10R	ATT TCC CAG GAA CTC AAA GTC G	
XM_002270146 (XP_002270182)	VvXTH11F VvXTH11R	TGC TGA CTG AAC CTT CTT CTC G GGA AGT AGT TTT GAG CGT GGA A	135
FN594964 (CBI17812)	VvXTH12F VvXTH12R	GAA ATT CTG CTG GCA CTG TCA C ATA TAG GGG TCC CCA CTG AGG T	106
XM_002274118 (XP_002274154)	VvXTH13F VvXTH13R	TCA CCG CCT TCT ACT TAT CTT C TCT CTT TCA CCC TTC CCT TGA G	130
XM_002274368 (XP_002274404)	VvXTH14F VvXTH14R	ATG CAG ATG ACT GGG CTA CAA G GAG TCC AGC TCA TGT TTC ATC C	117
FN594964 (CBI17805)	VvXTH15F VvXTH15R	CGC ATT CAA TGG CTT CTC CTT C GCC ATC ACC CCA AGT GAT ATC C	132
FN595992 (CBI30796)	VvXTH16F VvXTH16R	GCC TGT GGA ATG CTG ATA ACT G GCT TTT TGC GTC TAG TCC GTA G	137
FN594964 (CBI17802)	VvXTH17F VvXTH17R	GAA CCA GCC CAT GAG GAT ATA C GTA GGA GGC TGT GAA AGG TGC T	111
FN594964 (CBI17801)	VvXTH18F VvXTH18R	AAT CCA TTG GTG TTC CAT ACC C CTC TTG GCT CCA GTC TGT CTT G	120
XM_002270339 (XP_002270375)	VvXTH19F VvXTH19R	CAG CGC ATA ATC TTC TCT GTG G ATC CTC ATG GGC TGG TTC TTT G	100
FN594964 (CBI17799)	VvXTH20F VvXTH20R	GAG AAT GAA ATG GGT GCA GAA G TCT CCT TTA GGA TGT GGT GGT G	115
FN594964 (CBI17797)	VvXTH21F VvXTH21R	TTC CAC AAG CCA AGA GAG AAT G TGG GCAT AGA TTC CAT TCC TTC	149
XM_002267854 (XP_002267890)	VvXTH22F VvXTH22R	CAC CCT TCA CAG CAT ACT ACC G TGA ACC CAT CTC AGC CTT CTT C	129
FN596745 (CBI39385)	VvXTH23F VvXTH23R	CAC TTG TTT GGG TGC TTA AGA G CAA CTG TTT GAA GAG TGG CTG A	114
XM_002266046 (XP_002266082)	VvXTH24F VvXTH24R	GGT GTC CCT CCT GAG TGT AAG C ATC AAG CCC ATA ATG GAG AGG A	122
XM_002262725 (XP_002262761)	VvXTH25F VvXTH25R	AAA CTT CAG AGC CAG CAC TTC C TGA ACC CAT CTC AGC CTT CTT C	105
XM_002275826 (XP_002275862)	VvXTH31F VvXTH31R	GCC TTA TAC CCT GCA GAC CAA C GAT CTC ATC TGG GGT CCA TAG G	142
XM_002269249 (XP_002269285)	VvXTH32F VvXTH32R	CCG TAC TGC CCA CAA TAA TTA C CCA TCT CAA GAC ACC CCA AAA	106
XM_002272843 (XP_002272879)	VvEXP1F VvEXP1R	AGC CTG TCT TCC AAC ACA TTG C GAG TGG CCA TTG ATG GTA AAC C	120
XM_002283109 (XP_002283145)	VvEXP3F VvEXP3R	GGA TGG AGA AGT TGT GGC AGT G CTG CTG GTT GTC ACC TCA AAA G	137
XM_002269967 (XP_002270003)	VvEXP4F VvEXP4R	GGT CAG AAC TGG CAT CTC AAT G TGC TTG CCT TCA AAA GTC TGT C	140
AM442310 (CAN82746)	VvEXP5F VvEXP5R	CAA GCA ATG TCT CGC AAC T GCC ACA TTG TTC GAC ACT AC	130
XM_002283494 (XP_002283530)	VvEXP6F VvEXP6R	AGC GTA AAA GGG TCG AAG ACA G CGA TGT TCC AGG ATG TTG ATG T	145
XM_002273247 (XP_002273283)	VvEXP8F VvEXP8R	TGC TGG AGA AGT CTC TAA GG GCT CTG GCC GTT CAG GTA TT	115
XM_002266589 (XP_002266625)	VvEXP11F VvEXP11R	CCT TTC TTA CCC TGG TTC ATG C CGT AGC CCT GGC TGT AGA GAT T	150
XM_002280264 (XP_002280300)	VvEXP14F VvEXP14R	GCT AAT TGG CAC CCG CAT G ATC TAA AAA GCT TGG AGG GC	130
	VvEXP17F	CAA ACT TGC TTA ATG GTG TAT	150

XM_002284822 (XP_002284858)	VvEXP17R	CCA GAA TCT ACA CTA AAC TAA	
XM_002285855 (XP_002285891)	VvEXP19F VvEXP19R	CCT TCT CTA GCT CAG TAC AG GGG CGG GCT GCT TCA TTA AA	125
XM_002282205 (XP_002282241)	VvEXP20F VvEXP20R	CGC TCA TGC CAC TTT TTA TGG CAC TCA CTG CTG CTG TGT TGA C	114
XM_002277166 (XP_002277202)	VvPME1.4F VvPME1.4R	ACT GGC GGC AAC ACT TTC TTA G AGG GTG GAT GTT ATT GGA CCA C	117
XM_002281604 (XP_002281640)	VvPME1.11F VvPME1.11R	GAT GGG TAA AAC GGT AAT TAC G ATG AAC CCA TCA CCA CTC ACA C	100
XM_002273391 (XP_002273427)	VvPME1.17F VvPME1.17R	AAA TCA GAA CAC TGG CAT CTC C CAT GGA CGA CCC AGA TAA TTC A	102
XM_002266285 (XP_002266321)	VvPME1.18F VvPME1.18R	ACA AGA CAC TCT CTG CGA CGA C GAG TGC AGT TCG CAG TCT TTG T	120
XM_002267806 (XP_002267842)	VvPME1.19F VvPME1.19R	TGC TAC ATC CAG GGT TCC ATT G GAT CCT ACT GGC ACT GGG TTA G	120
XM_002273360 (XP_002273396)	VvPME1.20F VvPME1.20R	CTG GCC AGC AGA ACA CTA TCA C GAG CTC AAG TCT GCT GAC GGT A	106
XM_002266944 (XP_002266980)	VvPME2.2F VvPME2.2R	TGC ACA CAC CAA CAG ACA ATT C GCT TGTT TAT CCA TGG GCT TTC	129
XM_002273499 (XP_002273535)	VvPME2.4F VvPME2.4R	GAA TGG AAA TGA AGG CTT GGA C CTT CCA TCA CAT GAT ACC CTT G	108
XM_002277437 (XP_002277473)	VvPME2.5F VvPME2.5R	TGC CCT CTC CAC CCT CTA CTA C GAA AGG CCC CAC TGT GTA TTT C	133
XM_002274964 (XP_002275000)	VvPME2.7F VvPME2.7R	ATC AGA CAC AAG GCA CAG AGT C GAG CCA TGA ACT AGG GGA AAA C	143
XM_002274442 (XP_002274478)	VvPME2.11F VvPME2.11R	AAG GAA AGA GTG AAG TGG CCT GG CAG GAG AGA AGG GAA CAC CAC T	126
XM_002280410 (XP_002280446)	VvPME2.12F VvPME2.12R	TCC AAA GCT CGG TGA AGA CAT A GGC AAA GTT ACC ACT CCA TTC C	128
XM_002279087 (XP_002279123)	VvPME2.14F VvPME2.14R	TCG TCC TCT TCG GCT ACT GAT G TCG CTG AAG TCA GGC TGT TTA C	127
XM_002268456 (XP_002268492)	VvPME2.20F VvPME2.20R	CCA TGA CTT GCA GAC GTT GTT G CTT CGA TTG AAC TCC GAA TGT G	101

Supplementary Table 3.2 Number of pixels present in callus in each individual mineral stress (–N, –P and –S) and Control using Calcofluor, 2F4 and PAM1 epitopes. Data are presented as mean ± SD of 50 measurements. Different letters indicate significant differences at $p<0.05$.

	Control	**–N**	**–P**	**–S**
Calcofluor	$60.47^{a} \pm 4.19$	$33.91^{b} \pm 4.90$	$42.47^{c} \pm 4.20$	$57.22^{a} \pm 2.87$
2F4	$23.47^{a} \pm 4,99$	$41.83^{d} \pm 7.71$	$28.13^{b} \pm 3.53$	$34.88^{c} \pm 4.11$
PAM1	$29.31^{c} \pm 2.92$	$16.72^{a} \pm 2.51$	$23.69^{b} \pm 3.35$	$16.11^{a} \pm 1.66$

Supplementary Table 3.3 Differentially expressed genes transcribed in callus under mineral stress imposition relative to control. Data are expressed in log_2. Color scale is given when fold change of 2 was observed.

	Gene expression relative to the control (log_2 fold change)		
	–N	**–P**	**–S**
VvCesA1	1.82±0.22	-0.01±0.12	2.17±0.12
VvCesA2	1.27±0.87	0.14±0.15	2.02±0.25
VvCesA3	2.76±3.16	-0.89±0.63	2.15±0.19
VvCesA4	-0.87±0.89	-0.56±0.60	-0.13±0.83
VvCesA5	1.11±0.24	-1.55±0.11	-0.26±0.33
VvCesA6	0.84±0.39	-0.14±0.59	-3.01±1.94
VvCesA8	0.72±0.41	2.68±0.48	-1.40±0.39
VvCesA10	0.92±0.09	-0.60±0.50	-0.41±0.38
VvGH9A1	-0.15±0.15	-0.64±0.15	-1.48±0.16
VvGH9A2	1.98±0.10	-0.09±0.07	-0.86±0.28
VvGH9C2	-4.45±0.23	-0.83±0.45	-5.25±0.99
VvEXP1	-1.25±0.17	0.03±0.04	-0.62±0.37
VvEXP3	-0.40±0.15	-0.441±0.12	-1.22±0.13
VvEXP4	-0.37±0.06	0.03±0.04	0.23±0.07
VvEXP5	-0.10±0.21	-1.02±0.17	-2.21±0.54
VvEXP6	-3.08±1.15	-5.54±0.35	2.01±0.84
VvEXP8	1.46±0.16	0.49±0.31	1.34±0.85
VvEXP11	-2.45±0.60	-5.54±0.25	-1.46±4.01
VvEXP14	-1.52±0.15	-0.63±0.24	0.56±0.11
VvEXP17	0.60±0.04	-1.34±0.15	1.29±0.16
VvEXP19	0.58±0.93	-0.64±0.46	-3.64±0.35
VvEXP20	-1.58±0.53	1.86±0.41	-2.01±0.49
VvXTH2	-0.68±0.54	-2.34±0.08	-1.38±0.16
VvXTH3	0.10±0.01	-0.97±0.54	-1.38±1.11
VvXTH4	1.22±0.38	3.37±0.33	2.70±0.77
VvXTH8	0.07±0.23	0.003±0.08	2.17±0.73
VvXTH10	1.59±0.30	0.34±0.38	0.54±0.36
VvXTH12	0.38±0.24	0.25±0.38	-0.44±0.08
VvXTH14	-3.54±0.59	-2.73±2.25	-1.42±0.98
VvXTH15	-0.61±0.26	-2.01±0.49	-0.94±0.60
VvXTH31	-3.71±0.30	0.63±0.18	-1.54±0.20
VvXTH32	-4.44±0.32	-3.89±0.30	-3.67±0.03
VvPMEI2	2.88±0.26	3.50±0.03	1.30±0.20
VvPMEI3	1.45±0.20	2.03±0.11	0.41±0.04
VvPMEI4	0.79±0.11	2.08±0.13	0.68±0.27
VvPMEI5	-1.88±0.21	1.59±0.03	2.45±0.19
VvPME 1.4	-4.98±0.56	2.09±0.25	6.32±0.12
VvPME 1.11	-1.30±0.20	2.45±0.25	3.61±0.45
VvPME 1.17	-2.49±0.23	-4.57±0.23	-2.26±0.13
VvPME 1.18	-1.16±0.18	-3.73±0.45	-1.00±0.35
VvPME 1.19	-1.77±0.74	-2.34±0.11	-4.07±0.51
VvPME 1.20	-0.59±0.29	-1.06±0.31	0.33±0.31
VvPME 2.2	-0.80±0.30	0.12±0.43	1.39±0.13
VvPME 2.4	-1.48±0.06	-0.57±0.39	-0.81±0.25
VvPME 2.5	-0.67±0.21	-1.11±0.38	0.33±0.22
VvPME 2.7	-2.50±0.18	-1.03±0.15	-0.33±0.35
VvPME 2.11	-0.77±0.34	1.07±0.45	-2.48±0.20
VvPME 2.12	-0.84±0.30	0.07±0.43	0.84±0.11
VvPME 2.14	-0.82±0.34	-3.07±0.27	-2.21±0.12
VvPME 2.20	-2.16±0.18	-2.56±0.17	-1.003±0.35

Supplementary Table 4.1 Concentrations of elements present in the external solution given to control and each individual mineral stress (–N, –P and –S) *V. vinifera* cuttings.

	Control	**–N**	**–P**	**–S**
$Ca(NO_3)_2$ $4H_2O$	1.5 mM		1.5 mM	1.5 mM
$CaCl_2$ $2H_2O$		1.5 mM		
KNO_3	0.5 mM		0.5 mM	0.5 mM
K_2SO_4		0.25 mM	0.25 mM	
$MgSO_4$ $7H_2O$	0.5 mM	0.5 mM	0.5 mM	
$MgCl_2$ $6H_2O$				0.5 mM
$(NH4)_2SO_4$	0.05 mM		0.05 mM	
NH_4Cl_2				0.5 mM
KH_2PO_4	0.1 mM	0.1 mM		0.1 mM
NaCl	0.03 mM	0.03 mM	0.03 mM	0.03 mM
$CaSO_4$ $7H_2O$	0.17 µM	0.17 µM	0.17 µM	
$(NH_4)_6Mo_7O_2$ $4H_2O$	0.018 µM	0.018 µM	0.018 µM	0.018 µM
Na_2CrO_4	0.192 µM	0.192 µM	0.192 µM	0.192 µM
NH_4VO_3	0.2 µM	0.2 µM	0.2 µM	0.2 µM
$NiSO_4$ $7H_2O$	0.182 µM	0.182 µM	0.182 µM	
$CuSO_4$ $5H_2O$	0.316 µM	0.316 µM	0.316 µM	
$CuCl_2$ $2H_2O$				0.316 µM
H_2SO_4	81 µM	81 µM	81 µM	
H_3BO_3	46 µM	46 µM	46 µM	
$MnCl_2$ $4H_2O$	9.14 µM	9.14 µM	9.14 µM	
$ZnSO_4$ $7H_2O$	765 µM	765 µM	765 µM	
$ZnCl_2$				765 µM
Fe Citrate	4.9 µM	4.9 µM	4.9 µM	4.9 µM

Supplementary Table 5.1 List of primers used for RT-qPCR

Accession number (NCBI)	ID attributed[1]	Primer sequence	Product length
XM_003632610 (XP_003632658)	VvPG1F VvPG1R	TCA AAG CCG TGA GAC TGA GAA C TCC AAG CTT TCT TGA ATG CCT C	147
XR_077675 (CBI34471)	VvPG2F VvPG2R	TGC AGA TGG TGT TCA TGA TGT G TTC AAT GAG ATT CGG CCT AGT G	122
XM_002266305 (XP_002266341)	VvPG4F VvPG4R	GTT CCA ACT TCG CCG TGT ATT C TTG ACC CCC TCC GAG TAT TTT G	100
XM_002277203 (XP_002277239)	VvPG6F VvPG6R	AGA AGC TTT TGA GAG GGC AAT C AAC AGC ATC TTG GTC AAG GAA C	143
XM_002274368 (XP_002274404)	VvXTH14F VvXTH14R	ATG CAG ATG ACT GGG CTA CAA G GAG TCC AGC TCA TGT TTC ATC C	117
FN594964 (CBI17805)	VvXTH15F VvXTH15R	CGC ATT CAA TGG CTT CTC CTT C GCC ATC ACC CCA AGT GAT ATC C	132
XM_002275826 (XP_002275862)	VvXTH31F VvXTH31R	GCC TTA TAC CCT GCA GAC CAA C GAT CTC ATC TGG GGT CCA TAG G	142
XM_002272843 (XP_002272879)	VvEXP1F VvEXP1R	AGC CTG TCT TCC AAC ACA TTG C GAG TGG CCA TTG ATG GTA AAC C	120
XM_002283109 (XP_002283145)	VvEXP3F VvEXP3R	GGA TGG AGA AGT TGT GGC AGT G CTG CTG GTT GTC ACC TCA AAA G	137
AM442310 (CAN82746)	VvEXP5F VvEXP5R	CAA GCA ATG TCT CGC AAC T GCC ACA TTG TTC GAC ACT AC	130
XM_002283494 (XP_002283530)	VvEXP6F VvEXP6R	AGC GTA AAA GGG TCG AAG ACA G CGA TGT TCC AGG ATG TTG ATG T	145
XM_002276529 (XP_002276565)	VvEXP7F VvEXP7R	TCC TCT CCA ACA CTT CGA CCT C GAT TCC TCC TTT CTT CGC ACA T	115
XM_002266207 (XP_002266243)	VvEXP12F VvEXP12R	CTC TAC CTC CTG GCA TAT CG TCC TTT GTG CCT GGC AGA AC	150
XM_002264905 (XP_002264941)	VvPME1.3F VvPME1.3R	GGT GAC CTT GAA CTG GCC TTT C GCC TCT GGG ATG CTC TAT CAG T	103
XM_002265563 (XP_002265599)	VvPME1.15F VvPME1.15R	CCA AAG CTC GGT CAA GAC ATA C CCA ACC AGC CGA GTT TAT TAG G	103
XM_002277376 (XP_002277412)	VvPME1.8F VvPME1.8R	GTT CGG CAG AAC CAT CAA GAA C AAG TCT CCT CCG CCA CTT TTA C	115
	VvPME2.2F	TGC ACA CAC CAA CAG ACA ATT C	129

XM_002266944 (XP_002266980)	VvPME2.2R	GCT TGTT TAT CCA TGG GCT TTC	
XM_002273499 (XP_002273535)	VvPME2.4F VvPME2.4R	GAA TGG AAA TGA AGG CTT GGA C CTT CCA TCA CAT GAT ACC CTT G	108
XM_002277437 (XP_002277473)	VvPME2.5F VvPME2.5R	TGC CCT CTC CAC CCT CTA CTA C GAA AGG CCC CAC TGT GTA TTT C	133
XM_002274964 (XP_002275000)	VvPME2.7F VvPME2.7R	ATC AGA CAC AAG GCA CAG AGT C GAG CCA TGA ACT AGG GGA AAA C	143

Supplementary Table 5.2 Pearson correlation values between berry texture parameter and berry CW components. * $p<0.05$ significance; ** $p<0.01$ significance.

	Anthocyanins	Total phenols	Cellulose	Lignin
Berry Firmness	0.026	0.251	0.070	0.138
Skin break force	-0.517**	-0.563**	0.423*	0.202
Skin break energy	-0.631**	-0.641**	0.020	0.432*
Young's modulus for elasticity	0.214	0.413*	0.133	0.257

Supplementary Table 5.3 Eigenvectors for each PC calculated using the average values of triplicates. * stand as the most contributing traits for sample separation in each PCA.

	PC		
	1	**2**	**3**
Anthocyanin	0.8308	2.6917	2.5458
Total phenols	-1.5473	1.6506	3.0352
Cellulose	-0.7978	-3.0011	2.2475
Lignin	0.4829	-3.2269	2.0312
Total sugars_CDTA	-2.0164	0.0649	3.2355
Total sugars 0.1KOH	4.1999	-0.9957	1.2307
Total sugars 6KOH	-2.6898	2.9110	-1.2405
CDTA Rhamnose	1.7384	3.3421	-1.3514
CDTA Fucose	-2.1891	-2.7154	1.9790
CDTA Arabinose	1.6122	-2.5720	2.4207
CDTA Xylose	-4.1708	-0.3832	1.5367
CDTA Mannose	-3.3547	0.3568	2.4614
CDTA Galactose	-2.1677	0.2332	3.1698
CDTA Glucose	-3.5621	-0.3205	2.2846
CDTA UA	1.6108	-2.7932	2.2085
0.1KOH Rhamnose	4.4243	0.2559	-1.0599
0.1KOH Fucose	-1.5318	-2.0724	-2.8174
0.1KOH Arabinos	4.6051*	0.2248	0.3967
0.1KOH Xylose	4.5305*	-0.1579	-0.7663
0.1KOH Mannose	2.8534	3.0535	-0.5386
0.1KOH Galactose	4.5948*	0.4854	0.2463
0.1KOH Glucose	1.1472	3.8143*	0.2091

0.1KOH UA	-2.2696	-0.6255	3.0817
6KOH Rhamnose	3.7586	-2.0668	0.9469
6KOH Fucose	1.5489	-3.5899*	-0.8798
6KOH Arabinose	4.2642	1.5524	-0.1050
6KOH Xylose	4.5527*	-0.6980	0.2873
6KOH Mannose	1.1824	3.7740*	0.4982
6KOH Galactose	4.0914	-1.8609	0.0462
6KOH Glucose	3.9127	2.1193	-0.0763
6KOH UA	-3.7728	-2.1543	-0.7254
VvPG1	-1.3209	-3.2044	-1.8276
VvPG2	0.3941	-3.4950*	-1.6360
VvPG4	0.6781	3.8863*	0.3105
VvPG6	-3.8282	-2.2262	-0.1106
VvPMEI1	4.5622*	-0.6737	0.2420
VvPMEI2	4.6163*	0.1655	0.3385
VvPMEI3	-1.3323	1.2728	-3.2404
VvPMEI4	-0.6390	-1.1712	-3.3949
VvXTH31	-4.6243*	-0.2786	-0.1692
VvXTH14	-2.9349	0.0762	-2.7823
VvXTH15	-4.4274*	-0.5222	0.9669
VvEXP1	3.3324	-1.2719	2.2160
VvEXP3	-1.9565	-3.0138	-1.7537
VvEXP5	3.4600	-2.6060	-0.3115
VvEXP7	2.8624	-1.4707	2.4906
VvPME2.2	2.7181	-2.9057	-1.2137
VvPME2.4	-2.5059	1.4680	-2.7123
VvPME2.7	-0.0176	-3.1832	-2.1209
VvPME1.5	3.1365	-2.6500	-1.0881

Supplementary Table 5.4 Differentially expressed genes transcribed in berries under water shortage imposition with respect to berries grown under complete water supply, at veraison and maturation. Data are expressed in log_2. Color scale is given when fold change of 2 was observed. Capital letter indicates significant differences between stages and asterisk indicates significant differences between varieties, at $p<0.01$ significance.

	Veraison		Maturation	
	TN	**TR**	**TN**	**TR**
VvPG1	2.91^{*A}±0.91	-3.43^{A}±0.22	-2.47*±0.13	1.51±0.15
VvPG2	4.95^{*A}±2.52	-0.49^{A}±0.09	-3.21*±0.15	-2.53±0.10
VvPG4	0	0	-1.43±1.03	-1.95±0.58
VvPG6	0	0	-7.33*±0.44	-2.19±0.57
VvPMEI1	0.09±0.39	-1.83±0.30	-0.03±0.73	-1.45±0.99
VvPMEI2	0	0	0.25±0.08	-0.62±0.29
VvPMEI3	0	0	-5.99*±0.53	6.19±0.01
VvPMEI4	-3.06^{*A}±0.32	-1.20±0.47	-9.89*±0.63	1.47±0.13
VvPME1.5	0	0	-1.27±0.63	-1.47±0.47
VvPME1.3	0.66±0.63	0.46±0.23	0	0
VvPME1.8	-1.09±0.30	-1.38±0.52	0	0
VvPME2.1	-0.09±0.30	-1.05±0.30	0	0
VvPME2.2	0	0	-1.74±0.28	-1.88±0.14
VvPME2.4	-2.73^{*A}±0.54	-1.26^{A}±0.12	-0.77*±0.54	1.76±0.57
VvPME2.5	-3.08±0.09	-2.51±0.17	0	0
VvPME2.7	0	0	-3.67*±0.09	-2±0.68
VvXTH31	-6.54^{*A}±1.77	-10.28^{A}±0.63	-0.51*±0.11	1.51±0.15
VvXTH14	1.50^{*A}±0.06	-3.07^{A}±0.11	-1.48*±0.57	1.95±0.17
VvXTH15	-7.16^{*A}±0.14	-2.65^{A}±0.22	1.43*±0.36	0.09±0.48
VvEXP1	2.57*±0.40	-2.10±0.44	1.45*±0.07	-2.33±0.46
VvEXP3	0	0	-3.35*±0.32	-1.67±0.20
VvEXP5	0	0	-2.38*±0.32	-4.99±0.45
VvEXP6	-2.32±0.38	-2.33±0.59	0	0
VvEXP7	-1.02*±0.32	-4.83^{A}±1.05	1.36*±0.74	-2.15±0.44
VvEXP12	-0.12*±0.30	-2.01±0.32	0	0